Universidad de Huelva

Departamento de Ingeniería Química, Química Física y Ciencias de los Materiales

Binder design for low temperature asphalt mixes

Memoria para optar al grado de doctor
presentada por:

Avido Yuliestyan

Fecha de lectura: 2 de noviembre de 2017

Bajo la dirección de los doctores:

Pedro Partal López

Moisés García Morales

Huelva, 2017

UNIVERSITY OF HUELVA

Department of Chemical Engineering, Physical Chemistry and Material Science

BINDER DESIGN FOR LOW TEMPERATURE ASPHALT MIXES

a doctoral thesis submitted to fulfill the requirements for the degree of

DOCTOR OF PHILOSOPHY

by

Avido Yuliestyan

Supervisors:

Dr. Pedro Partal López

Dr. Moisés García Morales

Huelva, 2017

DISEÑO DE LIGANTES PARA MEZCLAS BITUMINOSAS DE BAJA TEMPERATURA

Memoria presentada por Avido Yuliestyan para aspirar al Grado de Doctor con Mención Internacional por la Universidad de Huelva.

Avido Yuliestyan

La presente Tesis ha sido realizada en el Departamento de Ingeniería Química, Química Física y Ciencias de los Materiales de la Universidad de Huelva bajo la dirección del Dr. Pedro Partal López y Dr. Moisés García Morales, los cuales autorizan su presentación:

Dr. Pedro Partal López Dr. Moisés García Morales

Huelva, 2017

AUTORIZACIÓN PARA LA DEFENSA DE LA TESIS DOCTORAL EMITIDA POR EL DIRECTOR Y EL TUTOR Y POR LA COMISIÓN ACADÉMICA DEL PROGRAMA DE DOCTORADO

DATOS DEL DOCTORANDO:

Apellidos y nombre: Yuliestyan, Avido	NIF/NIE/Pasaporte: Y2662915N	Nacionalidad: Indonesio
Dirección a efectos de notificaciones: Calle San Sebastian, 7, 4º G, Huelva		
Teléfono: 677078469	EMAIL: avido.yuliestyan@diq.uhu.es	

DATOS DE LA TESIS DOCTORAL:

Título: Diseño de ligantes para mezclas bituminosas de baja temperatura
Programa Oficial de Doctorado al que se adscribe y órgano responsable: Ciencia Y Tecnología Industrial Y Ambiental
Línea de investigación a la que se adscribe y órgano responsable: Ingeniería De Procesos Y Productos Químicos
Rama de Conocimiento **(marcar casilla):** ☐ Arte y Humanidades ☐ Ciencias ☐ Ciencias de la Salud ☐Ciencias Sociales y Jurídicas ☐ Ingeniería y Arquitectura

A CUMPLIMENTAR POR EL DIRECTOR Y POR EL TUTOR DE LA TESIS DOCTORAL: (en caso de que el Director y Tutor sean la misma persona, no es necesario cumplimentar los campos relativos al Tutor ni se precisa la firma de éste).

Director/es:	**Tutor/es:**
Dr./Dra.: Pedro Partal López Dr./Dra.: Moisés García Morales Dr./Dra.:	Dr./Dra.: Pedro Partal López Dr./Dra.: Dr./Dra.:
como Director/Tutor de la Tesis Doctoral antes indicada **AUTORIZA** LA DEFENSA DE LA MISMA.	

En Huelva a, ... de ..... de .....

Firma del/los Director/es de la Tesis Doctoral

Fdo.: Fdo.: Fdo.:

Firma del/los Tutor/es de la Tesis Doctoral

Fdo.: Fdo.: Fdo.:

A CUMPLIMENTAR POR LA COMISIÓN ACADÉMICA DEL PROGRAMA DE DOCTORADO:

Cumplidos los criterios de calidad aprobados para este Programa de Doctorado por el Comité de Dirección de la Escuela de Doctorado de la Universidad de Huelva y una vez valorada la Tesis Doctoral presentada por el Doctorando y haber incorporado éste las modificaciones y/o cambios que esta Comisión Académica le pudiera haber indicado, **se AUTORIZA** en reunión de fecha _____ **LA DEFENSA** de la misma.

En Huelva a, ... de ..... de .....

Firma y sello del Presidente de la Comisión Académica

Fdo. .....

Acknowledgment

Piece-by-piece of every single ideas, inspirations and supports were bonded, constructed and transformed into words, sentences, paragraphs and finally a book, this Doctoral Thesis.

First, I would like to express my very great gratitude and thanks to my supervisors, Dr. Pedro Partal López and Dr. Moisés García Morales, for giving me this opportunity to work in complex fluid group. They have continuously supported me with their time, knowledge, motivation and understanding from the beginning until the end of the journey over the last three years. Their guidance has assisted me in finding a way for every problematic situation.

Assistances and discussion provided by Dr. Antonio Abad Cuadri, who have shared his technical expertise and thought regarding bituminous product experimental works were greatly appreciated which would also extend to Dr. Claudia Roman and Dr. Francisco Ortega Bravo. I would also thank to Dr. Latchmi Raghunanan and Dr. Harshal Santan for their insightful conversation about chemistry. In addition, I have to sincerely thank to all colleagues in complex fluid lab, Adrian, Anjum, Antonio, Isa, Espe, Rocio and all the professors and members.

I wish to acknowledge the financial support and technical training provided by European Union through Marie Curie Initial Training Network (ITN) action, FP7-PEOPLE-2013-ITN under grant agreement 607524. My thanks to Dr. Gordon Airey, Dr. Davide Lo Presti, Mr. Paul Marsac and Dr. Maria del Carmen Rubio Gamez for organizing this SUP&RITN project and to all ESRs and ER (Helena, Ana, Miguel, Simona,

Jose, Giacomo, Fernando, Natalia, Emina, Paraic, Luca, James, Stefanie, Sara, and Joao) for every memorable moment.

To all colleagues in REPSOL asphalt group (Dr. Virginia Carrera, Ms. Veronica Contreras, Mr. Franscisco Guisado and Mr. Emilio Moreno) for all experience and collaboration. To all researcher in the laboratory of materials for transport infrastructure (MIT) at IFSTTAR (Dr. Thomas Gabet, Mr. Paul Marsac, Dr. Vincent Gaudefroy and Dr. Emmanuel Chailleux), I would like to thank for your collaboration and fruitful discussion. I would also like to extend my thanks to the technicians in Repsol and IFSTTAR for their help in offering me the resources in running the experiment.

I wish to thank my parents, Bapak Yunani and Ibu Siwi Subektyastuti, and my sister Devina Yudhistiarta (dan keluarga), for their support and encouragement throughout my study. My extended thanks to Papa Sulistyo and Mama Tri Daya Rini, Mbak Lionidya Marhaera, Mas Ahmad Faisal, Livannia Marseila and Gusti Satria Putra.

Finally, my sincere thanks go to my beloved family, my wife, Lisendra Marbelia, and my daughter, Karla Alesha Yuliestyan, for their continuous understanding, love and support.

Table of content

Chapter 1

Introduction

1.1 Background

Sustainable development is highly encouraged in many sectors including transport infrastructure (Ortiz et al. 2009). Increasing population around the world has forced society to accommodate the needs of transportation, for example, by constructing the new road infrastructures while maintaining the existing with embedded constraint for preserving sustainability. The limiting parameter enforces researcher to innovate and develop novel materials and technology for road paving, which is not only functional but also less harmful to the environment.

Roads are constructed by compacting aggregates, previously coated with binder. Binder contribution is only about 5%, but still is extensively investigated due to its unique stiff-flexible natural characteristics (viscoelastic) within the mix. Due to geographical feature, binder selection shall consider its temperature-related performance. For instance, in extremely high temperature regions, road incapability to resist load may results in permanent deformation, whilst road suffers thermal crack in cold regions (Zanzotto et al. 2000). Those would lead to shorten its service life. Alternatively, the addition of polymer, with a technical term of polymer modified bitumen (PMB), can improve the viscoelastic properties, so that binder becomes more elastic and able to dissipate energy at high and low temperature, respectively (Zhu et al. 2014). One among many challenges within PMB research is the proper selection of the type of polymer according to the required properties in such a way that yields mild enough operating conditions during production, or emulsification (further process), while simultaneously maintains its good performance upon service. For these purpose, Ethylene vinyl acetate, a synthetic copolymer, is perceived as a very potential bitumen modifier, besides its lower price. The presence of pendant group, in this case

is vinyl acetate, offers a broad range of morphologies associated to its melting point and melt flow index, that may satisfy the aforementioned expectations.

Conventionally, a binder is processed at 160-190 °C in order to improve its flowability, by the introduction of heat. Such method, known as hot mix asphalt (HMA) technology, raises some negative concerns that are not only defective for environment but also harmful for the worker. Those are associated to the higher amount of toxic substances emitted (Gaudefroy et al. 2010) and a great energy consumed by the machinery for heating both aggregate and binder. With such background, reduced-temperature technologies, which are classified into a) warm mix asphalt – WMA (120-140 °C), b) half-warm mix asphalt – HWMA (<100 °C) and c) cold mix asphalt – CMA (ambient), are vastly explored in the last decades. WMA and HWMA mostly employ foaming process and/or chemical additives (Rubio et al. 2012). For CMA, the binder is either a cutback bitumen or bitumen emulsion. The arisen issue for cutback bitumen is the potential air pollution caused by the evaporation of the solvent (light hydrocarbon fraction) that is initially used to lower the binder viscosity. For this reason, bitumen emulsion, a dispersion of bitumen in aqueous phase in the presence of emulsifying agents, is preferred.

Interestingly, organic based emulsifying agents, especially derived from renewable sources, have also gained interest. Lignin, a waste product of pulp industry, presents a great potential due to its hydroxyl (-OH) functional group and highly reactive aromatic ring (Laurichesse and Avérous 2014). Under alkaline environment, the existence of $-O^-$ (naturally present) and $-SO_3^-$ (derived from the production process) functional groups lead to trigger its surface activity by negative ion formation, thereby being useful as anionic emulsifier (Norgren and Edlund 2014). However, mineral aggregates

with positive surface charge are less common than those with negative charge (Mallawarachchi et al. 2016; Ronald and Luis 2016). For that reason, bitumen emulsion market is dominantly cationic type (Read and Whiteoak 2003). Fortunately, lignin aromatic structure can be used as a potential building block for the attachment of protonatable functional units (Windeisen and Wegener 2016), eligible for being positively charged in acidic environment (cationic emulsifier).

Another important material is reclaimed asphalt pavement (RAP). In the past, its potential reutilization was not considered and always ended up landfilled. When sustainability became a concern, recycling of RAP was perceived environmentally and economically attractive, due to the reduction in both virgin aggregate and binder consumption (Birgisdóttir et al. 2006; Thives and Ghisi 2017). When dealing with RAP, numerous challenges yet arise, especially when reduced-temperature technologies are involved, for instance, size homogeneity and the requirement to adopt either "white" (RAP binder being initially stripped down) or "black" aggregates assumption. In addition, RAP binder blending degree with fresh binder remains also unclear at lower temperature as compared to conventional HMA method. This fact limits its use in road paving, hence, further research on RAP recycling is needed.

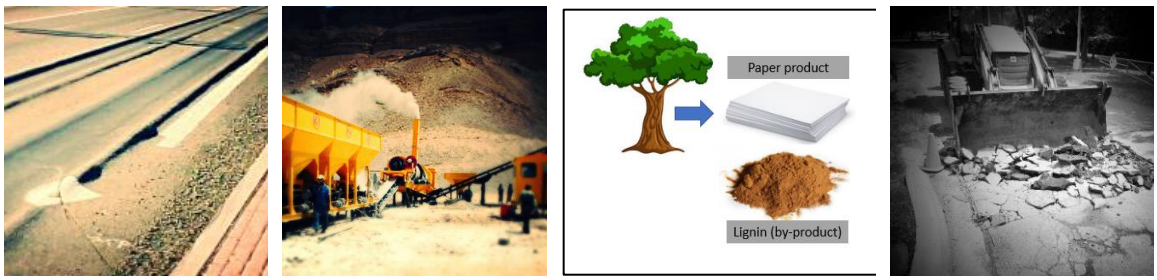

(a) (b) (c) (d)

Figure 1. 1 Some issues; (a) permanent deformation, (b) high energy consumption and toxic compound release, (c) lignin, waste of pulp industry and (d) aged asphalt mixture

Overall, the challenges are to overcome issues depicted in Figure 1.1 with a general expectation to reduce negative impact to environment by 1) maximizing recycling and reusing (with modification) material initially considered less valuable, and 2) using less harmful technology, without sacrificing the road performance. By the end, this thesis aims to offer solution to those mentioned challenges, by designing binder (material) as well as processing technology (reduced temperature) that includes the design of a polymer modified bitumen able to be manufactured and applied at lower temperature, lignin based cationic emulsifier, bitumen emulsion, and asphalt mixes with the possibility of 100% RAP inclusion. Therefore, the combination between the proposed product and process might expectedly contribute to reach the goals with respect to sustainability.

1.2 Objectives

The main goal of this research is to formulate sustainable improved materials and processing technologies, implemented for road paving application, which are in-line with "Sustainable Pavement and Railways Initial Training Network" European research project's goal: investigation of promising sustainable technologies, respectively for road pavement and railways. This general objective can be subdivided as follows:

- To design an improved-performance polymer modified binder which does not cause excessive energy consumption during its preparation and can be potentially used as a precursor for other products, such as emulsified polymer modified bitumens.

- To synthesize lignin based cationic emulsifier, via chemical modification with amine functional groups and to optimize their use, initially, on a silicone oil-in-water emulsion prototype.
- To use the optimum formula in the formulation of bitumen emulsions where their physical and rheological properties meet the standards and to evaluate the influence of lignin based emulsifier on the final emulsion residue.
- To use previously optimized lignin amine bitumen emulsion in the preparation of reduced temperature asphalt mixes containing 100% RAP as aggregate and to evaluate their performance.

The detailed experimental methodology that allows those goals to be reached are presented in Chapter 4 (Results) for each corresponding topic.

1.3 Structure

The structure of this Doctoral Thesis is organized into five chapters.

Introduction consists of an overview of this current research, a background and problem statement as a stepping stone for this research initiation, a set objectives in response to the stated problem and a thesis structure information.

Literature Review evaluates the basic concepts and fundamentals relevant to this current research, reviewing the bitumen, PMB, bitumen emulsion, lignin, and asphalt mixes.

Materials and Methods describes the material used and general methodology followed for the preparation of PMB, lignin-based cationic emulsifier, bitumen

emulsion, and reduced-temperature asphalt mixes and the characterization method for their physical, chemical, and thermal properties.

Results contains the main part of this thesis manuscript, a collection of results obtained and published in high-impact peer-reviewed scientific journals during the entire doctoral program. This section is divided into polymer modified bitumen (Subchapters 4.1 & 4.2); lignin based emulsifiers and emulsions (Subchapters 4.3, 4.4, 4.5, and 4.6); and reduced-temperature asphalt mixes (Subchapters 4.5 & 4.6). Subchapter 4.1 evaluates EVA co-polymer melting point and its Melt-Flow-Index (MFI) on PMB medium-high temperature performance by means of morphology, thermal, viscous flow and viscoelastic properties. With the same polymer considered in Subchapter 4.1, low temperature rheological assessment is presented in Subchapter 4.2. Then, in Subchapter 4.3, a selected PMB, is emulsified under mild operating conditions, and the resulting PMB emulsion is studied based on droplet formation, surface properties and its flow behavior. Subchapter 4.4 deals with the modification of a waste product of pulp plant, a Kraft lignin, into a cationic emulsifier, providing stability and desired flow characteristics in silicone oil in water emulsion prototypes. The optimum parameters obtained in Subchapter 4.4, including reaction route, reagent ratio, type of amine, emulsifier concentration, pH of aqueous phase and bitumen to water ratio, are used as a basis of information for manufacturing bitumen emulsion. Finally, in Subchapters 4.5 and 4.6, using the same lignin based emulsifier and emulsion formulation, the performance of asphalt mixes, fabricated with reduced-temperature technique and maximum recycling (100% RAP), are evaluated according to standard design method used for hot mix asphalt.

Conclusion collects the most outstanding outcomes derived from this research.

Chapter 2

Literature Review

2.1 Bitumen

2.1.1 Definitions and uses of bituminous binder

Bitumen is defined in *Oxford English Reference Dictionary* as a mixture of hydrocarbons derived from petroleum naturally or by distillation and used for road surfacing and roofing (Read and Whiteoak 2003). 'Bitumen' in Europe, or known as binder, has a North American term equivalent, that is called 'asphalt'. As a point of clarification, the term 'asphalt' will always be used for a mixture of bitumen and aggregates in thesis book, as referred to in Europe.

Bitumen is multifunctional. About 250 applications have been listed in Eurobitume application description 2013, that takes vital roles in several sectors including agriculture, buildings, hydraulics and erosion control, industrial, paving and railways. Referring to Eurobitume 2015 bitumen consumption report, the application for road paving and roofing takes up to 91.3 % of European bituminous market with a total of 11871 metric tonnes, thanks to bitumen major advantageous properties of adhesiveness and water proofing characteristics.

2.1.2 Source, manufacturing and type of bituminous binder

Referring to its availability in nature, bitumen may readily be used directly from the resources in the form of 'pitch lake' and 'rock asphalt'. Pitch lake is a surface deposit of natural bitumen which possesses highly viscous characteristic as a consequence of the penetrated silt and clay, whilst rock asphalt is eventually a bitumen impregnated rock. Apart from those, the majority of bitumen is processed through fractionation of crude oil.

Crude oil at 350 °C enters the atmospheric distillation column and is separated into fractions based on different boiling point interval range of the hydrocarbon components. The lightest fractions are collected from top-mid section of the column and vice versa. Bitumen, with a high molecular weight and a high boiling point, will be accumulated at the bottom of column as part of a heavy fraction hydrocarbon. The final process includes re-feeding this stream into vacuum process at about 0.1 bar and a slightly higher working temperature which is equivalent to 500 °C in atmospheric condition (Speight 1999). This process allows for further separation of bitumen from other lighter compounds. The bottom product output, known as straight-run bitumen, varies its hardness depending on the adapted process and crude oil sources.

With regards to their application, various bituminous products can be categorized into:

- **Paving grade bitumens** are meant for its stiff yet flexible characteristic. Mostly, straight run bitumen requires blending process to match certain specified grade criteria based on physical properties such as penetration, rheology, etc. Note that the criteria are different from one region to another.
- **Cutback or fluxed bitumen**, is another class of bituminous product that encloses solvent to improve bitumen flowability and so workability. 'Cutback' uses volatile solvent derived from naphta and kerosene fraction and 'fluxed' uses non-volatile solvent (Read and Whiteoak 2003). The time required for solvent removal, that is eventually related to solvent volatility, qualifies cutback bitumen into rapid, medium and slow curing. As recently reported by (Król et al. 2016), the trend into a greener product inspires the use of fatty acid

methyl ester (FAME) derived from vegetable oil as solvent especially when working with hard binder (as in RAP binder),.

- **Oxidized bitumen** is mostly used for water proofing purpose. The process, known as air blown method, involve soft bitumen being partially oxidized at temperature between 200 and 275 °C in order to make it harder (Lesueur 2009). This type of bitumen is not advised for paving application, as it is prone to cracking.
- **Bitumen with additives** employs various chemical substances, such as sulfur, amines, etc. to overcome specific problems. For antistripping, amines (amidoamine and polyamine), hydrated lime and organometallic could be used. Polyphosphoric acid (PPA), by itself or combined with polymer, may enhance binder stiffness through chemical reaction with bitumen (Masson 2008). Other additives used to improve bitumen properties, including its uses and drawbacks, are summarized in Table 2.1

Table 2. 1 Bitumen additives, its uses and drawbacks

	Additives	**Advantages**	**Disadvantages**
Extender (Wen et al. 2001)	Sulphur	• Improved storage stability • Good high-temperature properties	• Only applicable for unsaturated polymer modifiers, like SBS • High sensitivity to oxidative aging and dynamic shear • Hydrogen sulfide released • Poor recyclability

Antioxidants	Carbamates (lead, zinc) Carbon black Hydrated lime Phenols Amines	• Reduced oxidation	• High cost
Hydrophobic clay minerals	Montmorillonite Kaolinite	• Improved storage stability • Good rutting resistance • Increased aging resistance	• Limited improvement in low-temperature properties, ductility, and elastic recovery • Hard to be ideally exfoliated
Functionalization	Amino Carboxylic acid Maleic anhydride Methacrylic acid Glycidyl methacrylate	• Improved compatibility	• Uncontrollability in some cases • High cost

- **Polymer modified bitumen** deals with mechanical durability for extreme environmental and traffic conditions which will be later described in Subchapter 2.2.
- **Bitumen emulsion**, a bitumen dispersed in aqueous medium. This type of product is mostly used for road maintenance purpose, yet also functional for asphalt mixes. Bitumen emulsion has gained interest due to lower working temperature, especially when problems associated to high temperature process are concerned. Details on this topic are given in Subchapter 2.3.

2.1.3 Bitumen composition and structure

As mentioned earlier, bitumen internal chemical composition and microstructure rely on the refining process and crude oils source. Crude oil consists of hydrocarbon

components that are generally described as paraffinic, naphtenic or aromatic and non-hydrocarbon components (sulfur, nitrogen or oxygen) in the form of heterocyclic compound. The elemental analysis (Goodrich et al. 1986), in Table 2.2, identifies that bitumen consists of 90-95% hydrocarbon.

Table 2. 2 Bitumen elemental analysis results

Component	**Fraction (%)**
Hydrogen	9.8 - 10.8
Carbon	80.2 - 84.3
Oxygen	0.4 - 1.0
Sulfur	0.9 - 6.6
Nitrogen	0.2 - 1.2

Those elements construct abundant types of chemical compounds, over a wide range of structure, molecular weight and polarity. Some steps to ease bitumen composition understanding is by fractioning it into groups of components, by means of solvent extraction, adsorption, chromatography, and molecular distillation in-conjunction with the aforementioned techniques. Among them, chromatography is the most extended tool for determining bitumen composition.

Initially, dissolution of bitumen in linear n-alkanes yields an insoluble fraction, termed asphaltenes, with solid characteristics. The remaining soluble compounds, which constitute the so-called maltenes, are physically separated by filtration. Maltenes can be further classified into some fractions by various chromatography techniques (Masson et al. 2001). For bitumen, thin layer chromatography coupled with flame ionization detection (TLC-FID) offer a faster and cheaper analysis (Ecker 2001). In principle, maltenes, from bitumen solubilized in a solvent, travel over a quartz rod

coated by an adsorbent of silica. Depending on the interaction between mobile and stationary phase, the different fractions locate at different positions along the rod, and their relative content is quantified from the ion formed after combustion process in FID device. Using this technique, bitumen components are commonly classified into four fractions, saturates, aromatics, resins and asphaltenes (Speight 1999). In that sequence, each fraction has molecular weight, aromaticity, heteroatomic content and polarity properties, in an increasing order (Polacco et al. 2015). It is worth noting that chromatography is commonly coupled with rheological characterization in order to associate SARA fractions to sol/gel behavior.

Asphaltenes are easily identified since it is the only bitumen fraction that is insoluble in n-heptane and become soluble in toluene. Asphaltenes are constituted by polycyclic aromatics, polar group, and a metal complex. Regarding its complex structure, asphaltenes are agglomerates of condensed aromatics of 4 to 10 rings with side chains that form graphite-like stacks of some planar sheet interconnected by pi-pi bonds or other secondary intermolecular forces. Vanadium and Nickel may be present in some crude oil source. Asphaltenes have the smallest H/C ratio between 0.98 and 1.56. Despite many researchers agree that molecular weight is about 2000 and higher, it is still subject of debate due to the resin interchangeable fraction which peptizes asphaltenes. The polar characteristic is commonly hypothesized based on its insolubility in organic solvent, n-heptane. This polarity may be originated from the presence of nitrogen and oxygen element, although its percentage may be considerably low. Tg of asphaltenes is reported at about 70 °C, observed from the peak in the heat capacity first derivative using MDSC technique (Masson and Polomark 2001).

Resins have a molecular structure which resembles asphaltenes fractions with lower MW, less aromaticity, and polarity, but soluble in n-heptane. It is constituted by polar aromatic with a MW of 1100, the amount of fused aromatic between 2 and 4, and H/C oscillates between 1.38 and 1.69. The proportion of resin to asphaltenes governs its physical characteristic either considered as sol or gel.

Aromatics mainly constituted of naphthene aromatic since it covers a range of asphalt molecules with more regular aliphatic like structure and shape, where condensed rings are sporadic or even totally absent. The molecular weight is of 800 approximately.

Saturates have the simplest chemical structures which are aliphatic and naphthenic hydrocarbons with a molecular weight of 600 having H/C ratio of 2 or higher. The characteristic is a non-polar, without heteroatoms content, and dominated by different homologues of alkanes: n-alkane, iso-alkane and cyclo-alkanes.

Those saturates, aromatics, resins, and asphaltenes fractions govern the total bitumen chemical structure. Despite many other models proposed, thus far, the two models below have been mostly used to describe bitumen structure:

a) Colloidal model,describes bitumen as a colloid system of dispersed large and complex hydrocarbons with solid characteristic (asphaltenes) peptized by polar resins on maltenes liquid-like continuous phase, of aromatics and saturates (Nellensteyn 1923). Gel structure may be formed if the amount of resins available for peptizising is not high enough such that attraction forces among the asphaltenes cores is counterbalanced, Figure 2.1a (Pfeiffer and Saal 1939). Such theory may be supported by atomic force microscopy (AFM), that illustrates hypothetical asphaltenes, shown as bee-like structures (Loeber et al. 1996), dispersed in the matrix.

Another author (Jäger et al. 2004) supports that hypothesis, based on the absence of bee-like structures in maltene fraction, where asphaltenes were previously separated using solvent. In contradictory, a different interpretation was offered by (Masson et al. 2006) suggesting that bee-like structure has no correlation with asphaltenes, instead, higher metallic content, of Vanadium, and Nickel, is proposed to be responsible for that. However, it again remains controversial, since the association between the trace metals and the asphaltene fraction due to polarity makes it difficult for anyone to differentiate the effects from either the asphaltenes or the metal content (Yu et al. 2014).

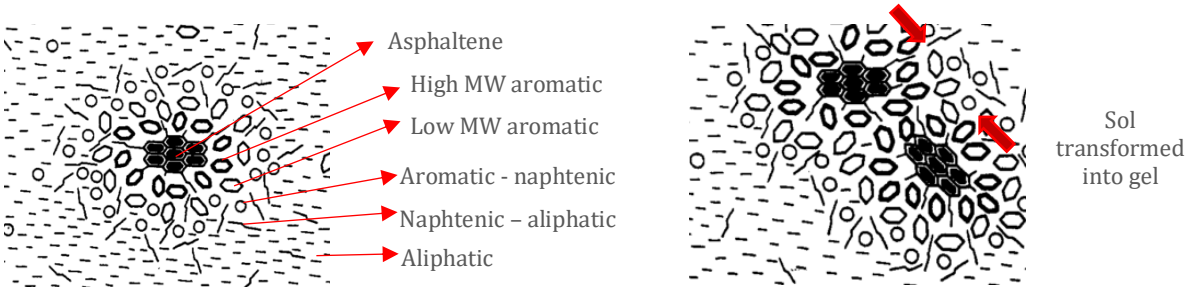

(a)

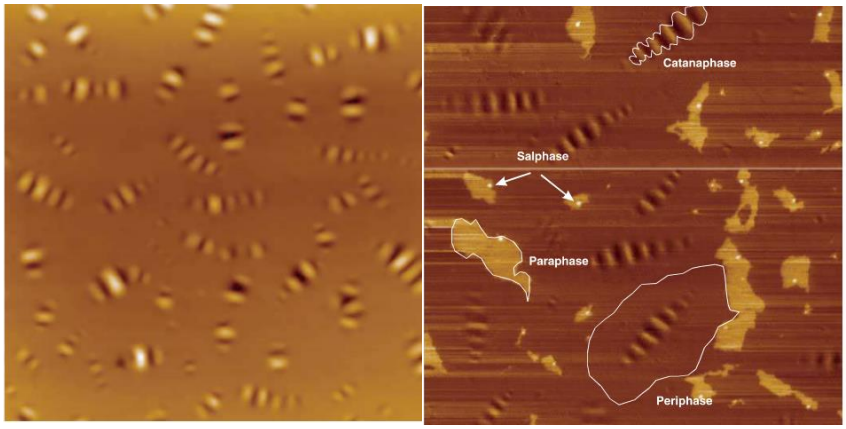

(b)

Figure 2. 1 a) Schematic representation of biphasic model and its possibility to form gel structure and b) Topographic AFM image (15 x 15 µm)

b) Simple homogenous fluid (or dispersed polar fluid, DPF) model criticizes the previous model since there does not exist experimental proof which evidently provides distinction between dispersing and dispersed phase (Petersen et al. 1994). Redelius, 2004, explores bitumen solubility using Hansen parameter involving up to 50 types of solvents. The results suggest that the difference in solubility parameters between asphaltenes and maltenes is not high enough for asphaltenes to be considered insoluble and are in fact in a single phase with maltenes. Recently, using AFM technique combined with differential scanning calorimetry (DSC), several laboratories under RILEM technical committee conducted round robin tests which was published in 2013 (Soenen et al. 2013), concluding that bee-like structure gradually disappears after reaching certain temperature, and are believed to be the melting temperature of wax crystallite fraction, as observed by endothermic melting enthalpy at the same temperature (Figure 2.2).

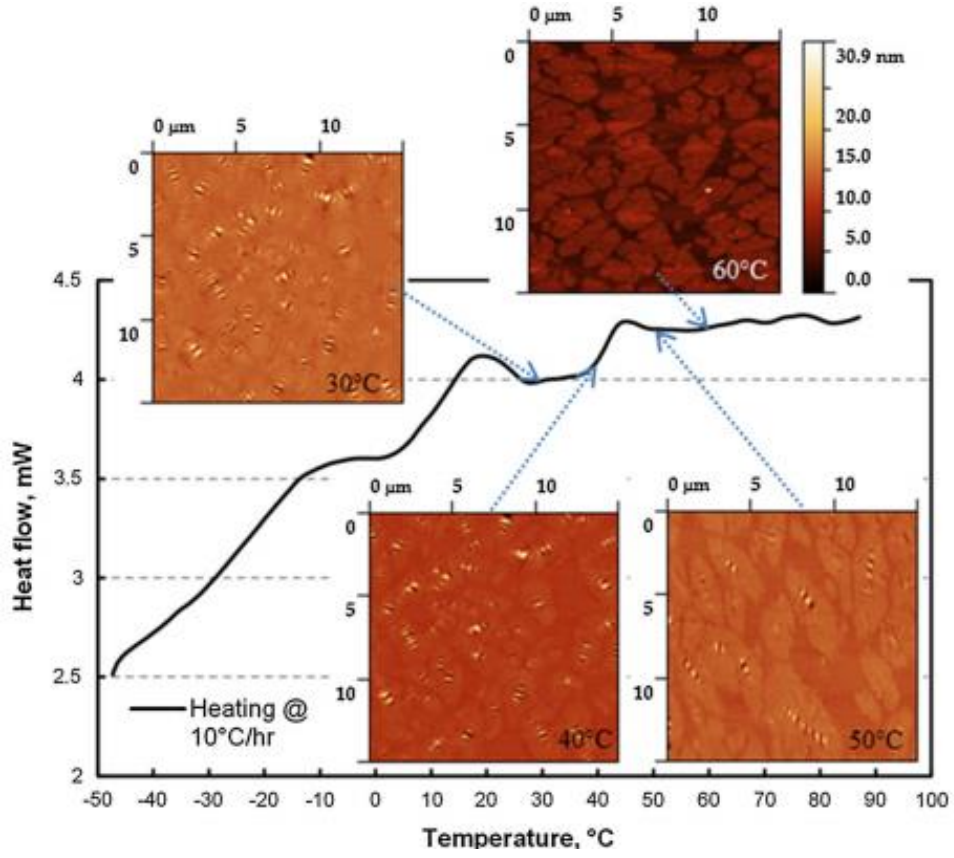

Figure 2. 2 Topographic AFM image (15 x 15 μm) combined with DSC thermogram (Soenen et al. 2013)

2.1.4 Bitumen properties and the relation with constituents

In Europe, for preliminary identification of 'hard – soft' characteristic, bitumen manufacturer labels their product based on physical (technological) properties derived from penetration test at 25 °C ($Pen_{25°C}$) and ring-and-ball softening point (SP) test. In performance grading system, the rheological behavior of bitumen is more emphasized and, basically, relies on dynamic shear rheometry (DSR) for the determination of bitumen high temperature threshold, bitumen viscosity by rotational viscometry, low temperature properties by bending beam rheometer. A rheological characterization will be briefly described in Subchapter 2.6.

Bitumen is a brittle elastic material in the vicinity of its glass transition temperature, has viscoelastic behavior at ambient temperature, but becomes a thick liquid (flow) when heated. So, its physical properties vary significantly with temperature. Moreover, they strongly depend on crude sources. For example, its glass transition temperature can fall in the range between -40 and 5 °C due to a broad range of bitumen chemical compositions (Read and Whiteoak 2003).

Bitumen physical properties are thought to be originated from each (SARA) fraction. Asphaltenes are believed to be responsible for a higher value of viscosity. Asphaltenes, which at ambient temperature form plate-like sheets held by inter and intramolecular bonding, lose their conformations, alter their size and shape and finally disrupt as the temperature further increase (hence, viscosity decreases). In addition, complex structures in bitumen, especially those containing high crystalline fractions, have shown failure to follow time-temperature superposition principle when Black

diagram (modulus vs phase angle) is plotted (Lesueur 1996). Another study (Soenen and Redelius 2014) investigates the influence of polyaromatic structures, through UV-Vis and FTIR spectroscopy, on the dynamic rheological properties. It shows that larger polyaromatic structures seem to govern the elastic behavior at long loading times, low frequency or high temperatures. In fact, bitumen physical properties are derived from its chemistry based on molecular interactions, such as dispersive, polar, hydrogen and π-π bonding, and molecular weight distribution (Redelius and Soenen 2015).

Due to weathering, thermal properties of bitumen have a crucial role on its performance. Modulated differential scanning calorimetry technique (Masson and Polomark 2001), an advanced version of standard DSC (in Subchapter 3.3.1.4), can be used for thermal characterization. Based on non-reversing heat flow, steric hardening is more pronounced on oxidized bitumen, observed by crystallization of high molecular weight saturates and the formation of a mesophase constituted by resin and asphaltenes fractions. These fractions were reported to exhibit time evolution of their properties, due to thermal hysteresis, what suggests the characterization to be performed after material is fully annealed (Masson et al. 2002).

2.2 Polymer modified bitumen (PMB)

2.2.1 Definitions and uses of PMB

Polymer modified bitumen is a class of bituminous product in which polymer is homogenously dispersed by high mechanical shearing at temperature above the melting points of each constituents. The addition of polymer aims to improve binder viscoelastic properties featuring proper rigidity, elasticity, ductility and durability that expectedly increase road service life. For regions experiencing extreme weathering,

those features are sometimes hard to be fulfilled by using straight run bitumen only, hence may be benefitted by addition of PMB instead. Polymers offer a large variety of properties. For instance, blending stiff semicrystalline polymers with bitumen may solve rutting resistance issues during summer. A blend of bitumen with a rubbery polymer may better dissipate energy at low temperature during winter than an unmodified bitumen. A complementary use of polymers may be able to also improve noise reduction (Bueno et al. 2014).

2.2.2 Brief overview of polymer

The word 'polymers', rooted from *Greek*, consists of *poly-* and *meros,* meaning *many/much* and *part,* respectively. It is commonly understood as macromolecules composed of repeating units, connected by covalent bonds, that form various structures (Ravve 2012). The simplest structure is linear sequence of monomers (Figure 2.3a). When monomers appear attached to the backbone, branch type polymer exists (Figure 2.3b). From branch precursor, many other types, such as star, comb, ladder, semi-ladder, may be formed. The interconnection between branches results in the formation of network structures (Figure 2.3c), either planar or three-dimensional networks (Ravve 2012).

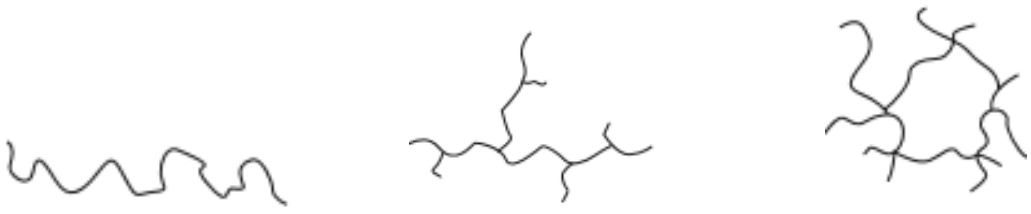

(a) (b) (c)

Figure 2. 3 Some examples of polymer structure (Ravve 2012)

Based on the source, the polymer can be categorized into two; natural and synthetic (from crude oil). Natural polymers include polysaccharides (starch, cellulose, chitin, alginate, etc.), polyamides (in animal or vegetal proteins), polyisoprenes (in natural rubber), polynucleotide (DNA and RNA of all living organism), and lignin. Natural substance sometimes needs to deal with the certainty of chemical compositions that may raise properties-related concerns. Instead, synthetic polymer compositions are relatively controllable, depending on the reaction mechanism, type of monomers and ability for crosslinking, that can be classified as follows:

- Reaction mechanism, **step-growth polymer** reacts in discreet step whilst **chain-growth polymer** propagates through the inclusion of monomer to the active site located at the chain ends.
- Type of monomer, polymer may contain one (**homopolymer**), two or more type of repeating units (**copolymer**). Depending on the order, copolymer may be in **alternate** (ABABAB) or **random** position (ABAABB). If a group-sequence appeared in the back bone, **block-copolymer** (AAABBB) exists, while if it attached as a branch of the main chain, a term of **graft-copolymer** is used.
- Ability to form crosslink or gelation, polymer that once crosslinked by covalent bonds shows irreversible state from melt to solid, is **thermosetting polymer**. Oppositely, **thermoplastic polymers** can never undergo gelation, and transition from molten to solid state is a reversible process upon decreasing temperature due to polymer chains crystallization and entanglement network formation.

2.2.3 Typically used polymer modifiers

For road paving materials, both natural and synthetic polymers have been reported successful to modify bitumen properties. A natural rubber polyisoprene can be used as a modifier building unit, and if combined with epoxy group, is able to cope with poor wet grip properties and poor weather resistance issues (Al-Mansob et al. 2014). Lignin, in the blend with bitumen, exhibit antioxidant properties as observed by low carbonyl content, commonly used for aging identification (Thomas 2005). This particular material has gained many interests lately, to be used as precursor for advanced materials. Subchapter 2.4 will be dedicated to lignin, which within this research will be investigated for cationic emulsifier synthesis.

On the other hand, the first use of synthetic polymer is dated back in 1954, in which thermoplastic styrene-butadiene-styrene (SBS) was used to improve bitumen thermal susceptibility and cracking resistance. Such success originated a vast PMB research which underlined the use of thermoplastic polymers, either elastomer or plastomer, for bitumen physical modification. Elastomer, e.g. SBS, has found superior performance when dealing with both extreme high and low temperature, thus widening bitumen in-service temperature span. SBS combines stiffness and flexibility characteristics, derived from the parent rigid polystyrene and flexible polybutadiene blocks, respectively (Lu and Isacsson 2000; Fawcett and McNally 2001; Robinson 2004; Navarro et al. 2005; Collins et al. 2006). The second typically used polymers are thermoplastic plastomers (polyolefins), known for extending high in-service temperature limit of bitumen (Lu et al. 1999; Panda and Mazumdar 1999; González et al. 2002; Airey 2002a; Polacco et al. 2005; Pérez-Lepe et al. 2006), and being relatively lower-priced commodity. Alternatively, chemical bonding by using reactive polymers

can help overcome storage stability issues derived from the use of traditional thermoplastics. In general, the recent studies on PMB yet aim to exploit polymer properties whilst simultaneously minimizing the negative impact (Zhu et al. 2014). A list of polymers for bitumen modification, with their advantages and disadvantages, is summarized in Table 2.3.

Table 2. 3 Several types of bitumen modifiers (Bahia et al. 1998; Zhu et al. 2014)

Type of modifiers	**Examples**	**Advantages***	**Disadvantages***
Polymers – plastomers	Polyethylene Polypropylene	• Good high-temperature properties • Relatively low cost	• Limited improvement in elasticity • Phase separation
	Ethylene vinyl acetate Ethylene butyl acrylate	• Relatively good storage stability • High resistance to rutting	• Limited improvement in elastic recovery • Limited enhancement in low-temperature properties
Polymer – thermoplastic elastomer	Styrene-butadiene-styrene (SBS) Styrene-isoprene-styrene (SIS)	• Increased stiffness • Reduced temperature sensitivity • Improved elastic response	• Compatibility problems in some bitumen • Low resistance to heat, oxidation, and ultraviolet • Relatively high cost
	Styrene-ethylene/butylene styrene (SEBS)	• High resistance to heat, oxidation, and ultraviolet	• Storage instability problems • Relatively reduced elasticity • High cost
Reactive polymer	Ethylene-based polymer w/ epoxy ring Isocyanate based polymer; polyethylene/ polypropylene glycol + isocyanate (MDI)	• Improved compatibility • Enhanced high-temperature properties	• Limited improvement in low-temperature properties • Gelation problems

The workability issues of PMBs, in which the addition of polymer yields drawback concerning highly viscous behavior, are rarely discussed in the literature. Moreover, these drawbacks are further exacerbated if the attempt for lowering manufacturing temperature is encouraged. Rossi et al., (2013) aims to address this issue by proposing a ternary blend composed of polymer/wax/bitumen, with expectation to combine stiffness benefit and workability, from polymer and wax, respectively.

2.2.4 PMB properties

PMB is expected to resemble the positive influence from its parent polymer, despite the fact that the blend final properties are affected by the interaction of the constituents. On the polymer side, its physical structure, related to amorphous and crystalline phases, determines its thermal properties such as glass transition (Tg) and melting temperature (Tm). Tg is a transition state when amorphous phase no longer exhibits mobility as temperature is further decreased. Its value is usually taken as the middle between starting and ending point of the phenomenon. This (second order) transition manifests an alteration in its stiffness, specific volume, heat content, thermal conductivity, refractive index, and dielectric loss (Ravve 2012). Tm is a solid to liquid (first order) phase transition, due to the loss of regularity in crystalline phase with increasing temperature. Both Tg and Tm are very useful for estimating PMBs lowest and highest threshold service temperature, respectively. At temperature higher than Tm, polymer melt flow is affected by intermolecular interaction which can be quantified in terms of Melt-Flow-Index (MFI). Thus, understanding the state of polymer may be useful for the prediction of the overall PMB properties, despite that polymer interaction toward bitumen may be more influential.

Enhanced binder properties are not straightforwardly obtained merely by polymer addition. The microstructure in the binder requires to be majorly occupied by a certain morphology, refer the formation of polymeric three-dimensional network as a consequence of polymer swelling by some bituminous fraction (Polacco et al. 2015). Each fraction interacts differently toward the polymer which in turn to be influenced by polymer type, concentration, processing condition during mixing, etc. Thus, no guarantee on certain value of those parameters can be sealed to obtain such morphology. Low degree of swelling results the polymer simply being dispersed with limited improved properties and unstable system. A very compatible system is neither good, meaning that negligible polymer influence on mechanical performance can be exerted despite providing stability. Storage stability is another problem that may become a handicap for workability and may lead to performance consistency due to inhomogeneity of polymer distribution. The evaluation is commonly done by vertical 'tube test' stored at 180 °C to imitate non-stirred storing. If the system is not stable enough, PMB segregates into asphaltenes rich phase (ARP) on the bottom and the remaining polymer rich phase (PRP) on the top. To proof any instability, technological, rheological and morphology (microscopy, mainly) tests are performed on PRP and ARP. A study on SBS-bitumen interaction (Lu and Isacsson 1997) reported that a more stable system is favored when the ratio of asphaltenes over aromatic fractions is low. Besides, linearity in structure and less concentration of polymer prone to finer dispersion that also lead to positive influence on stability. In the case of EVA-bitumen, the above concentration effect is also amplified (González et al. 2004; Bulatović et al. 2013). Moreover, that may also be attributed to polar functional unit in the polymer which may associate themselves or with asphaltenes, together with resin as dispersant for asphaltenes in aromatic-aliphatic medium (Fawcett and Mcnally 2001).

Furthermore, a third component, such as sulfur and maleic anhydride functional group, may be introduced with the idea to improve intra and intermolecular interaction (Polacco et al. 2015). Even though, a highly soluble polymer in bitumen results in limited contribution to the improved physical properties (Redelius 2004). Finally, biphasic form, with coexistence of polymer-rich phase (swollen by migration of some bituminous fractions) and asphaltene-rich phase in microscale metastable is the one eventually desired (Polacco et al. 2006). Thus, searching the ideal zone providing stability is preferably addressed only if accompanied by the presence of morphology giving rise to physical properties.

2.3 Bitumen emulsion

2.3.1 Definition, uses and manufacture of bitumen emulsion

Colloid system includes suspensions, emulsions, suspoemulsions (mixtures of suspensions and emulsions), foams, etc. For road paving application, emulsion and foam of bitumen are of particular interests, since workability of mixes prepared using both system can be conducted at a lower temperature than conventional HMA. This subchapter will be dedicated to bitumen emulsion. Table 2.4 summarizes the types of bitumen emulsions application, that requires specific destabilization mechanism (emulsion breaking rate) associated to each specific purpose.

Table 2. 4 Several types of bitumen emulsion application

Application	Purpose	Emulsion required	Procedure
Chip seal	Improve surface profile and for small maintenance	Rapid set	Spraying warm bitumen followed by placement of aggregate, either for single or multiple layer and finally compacted
Tack coat	Tack between layer	Rapid set	Spraying on the surface
Prime coat	Preparation on the first granular base to protect by waterproofing the underlying base and hardening the layer	Slow set, with fluxant if necessary	Spraying on the surface
Slurry seal and microsurfacing	Improve surface profile, ie. skid resistance	Controlled set	Mixing aggregate with water, cement (for breaking initiation) and lastly the emulsions
Asphalt mixture	To be used in structural layer	Various type	In subchapter 2.5.2 asphalt mixing technology

For each application, the emulsion recipe can be tuned by setting the type of emulsifier used, bitumen content, and additives during the manufacturing process.

The emulsification is the dispersion of hot molten bituminous droplet by high mechanical shearing into continuous aqueous phase in the presence of emulsifier. The mixing apparatus can be rotor-stator, colloid mill, or static in-line mixer (high pressure), either in batch or semi-continuous process depending on the production scale. No matter which rotating device is used, basically, bitumen is forcefully pushed

in radial direction through static aperture by the rotating part, to undergo fluid breakage that leads to droplet formation. If bitumen is too hard (e.g. very low penetration bitumen, PMB, etc.), emulsification requires to be conducted at high temperature (possibly > 100 °C) for viscosity reduction, that is in conflict with the evaporation of water. Thus, for such case, pressurized vessels have to be used in order to suppress water loss.

2.3.2 Thermodynamic approach

Thermodynamic approach attempts to explain the fundamentals of emulsification based on energetic balance between internal and external work of the system using the 2nd law of thermodynamics.

$$\Delta G^{form} = \Delta A \cdot \gamma_{12} - T \cdot \Delta S^{conf}$$

During emulsification, bitumen with surface area A_1, in its liquid state, is dispersed into aqueous phase by the introduction of external mechanical energy to form droplets with surface overall area A_2. The change in free energy is made from two contributions: (i) a surface energy term (positive) that is equal to $\Delta A \cdot \gamma_{12}$ (where $\Delta A = A_2 - A_1 > 0$); and (ii) an entropy of dispersions term which is also positive (since the production of a large number of droplets is accompanied by an increase in configurational entropy) which is equal to $T \cdot \Delta S^{conf}$. In most cases $\Delta A \cdot \gamma_{12} \gg T \cdot \Delta S^{conf}$, which means that ΔG^{form} is positive; that is, the formation of emulsions is non-spontaneous (Tadros 2014). A dispersed phase with positive free energy is thermodynamically unstable and the consequence of that energy balance is destabilization by coalescence. Hence, the manufacture of emulsions of two immiscible

liquids requires a third component, namely emulsifier, that induces the stability by reducing γ_{12}.

2.3.3 Stabilization, wettability and destabilization of bitumen emulsions

The fundamentals of stabilization of emulsions are based on the theory of interparticle interactions, of a) hard-sphere, b) electrostatic (soft), c) steric and d) Van-der-Waals interaction (Tadros 2011, 2014). The schematic models relating the energy evolution with the distance of two interacting particles are presented in Table 2.5.

Table 2.5 Type of force, origin and equation applied, summarized from Tadros 2011

Interaction type	Origin	Equation
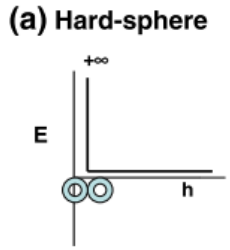	Two identical sphere with r radius separated by core-core distance less than 2r or else touch each other	N/A
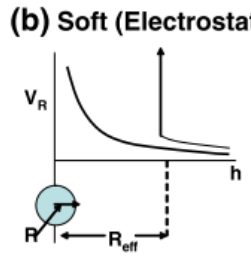	By interaction of similarly charged counter-ion in the diffuse (double layer) surrounding charged surface layer	$G_E = \frac{4\pi\varepsilon_r\varepsilon_o R^2 \psi_o^2 \exp-(\kappa h)}{2R + h}$ Function of permittivity (ε_T, ε_0), radius (R), distance (h), double layer extension (κ) and surface potential (ψ_0)

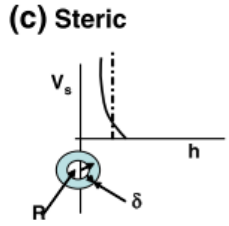	By compressed or overlapped molecule or polymeric chain surrounding the particle	$G_s=G_{mix}+G_{el}$ G_{mix} is contribution of osmotic pressure increase caused by unfavorable mixing $\frac{G_{mix}}{kT}=\left(\frac{2V_2^2}{V_1}\right)\nu_2^2\left(\frac{1}{2}-\chi\right)\left(\delta-\frac{h}{2}\right)^2\left(3R+2\delta+\frac{h}{2}\right)$ Function of temperature (T), radius (R), distance (h), interaction coefficient (χ), molar volume of molecule and solvent (V), number of molecule per unit area (v) G_{el} is energy term by entropic change due to compressed layer $\frac{G_{el}}{kT}=2\nu_2\ln\left[\frac{\Omega(h)}{\Omega(\infty)}\right]=2\nu_2 R_{el}(h)$ R is geometric function due to segment density distribution
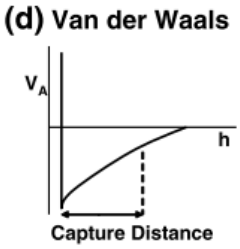	By either dipole-dipole (Keesom), dipole – induced dipole (Debye) or London dispersion force	$G_A=-\frac{A_{11(2)}\,R}{12\,h}$ Function of Hamaker constant particle 1 in the medium 2 ($A_{11(2)}$), radius and distance

According to interaction type a), b) or c), the energy values (positive) increase abruptly at a certain distance point when two particles approach each other, that is interpreted as repulsive force. On the other hand, naturally, two particles are attracted by Van-der-Waals forces in such close proximity, assigned by negative energy value. Obviously, each of force contributes to the total energy of the entire colloid system that governs the emulsion stability. As bitumen emulsion is commonly stabilized using emulsifier (either ionic, non-ionic, or polymer), the relevant interaction can be of b-d

for ionic (DLVO principle), c-d for non-ionic or polymer, or b-c-d for polyelectrolyte emulsion. To avoid droplet coalescence, the net energy requires a positive value, providing ample repulsive force to keep particles apart. If a electrostatically stable system is desired, surface potential (ψ_0) that contribute to G_E can be manipulated by selecting a certain type of emulsifier. For steric stabilized system, number of molecule per unit area (v), molar volume of molecule (V) and interaction coefficient (χ) are parametres which affect G_{mix}, and G_s.

Moreover, in a bitumen emulsion, the selection of emulsifier is not always related to stabilization, but that depends also on the rate of destabilization, associated to final emulsion application. For charged bitumen emulsion, this destabilization rate is evaluated in terms of a breaking test consisting in measuring the quantity of a specific filler needed for droplet breakage to occur (EN 13808, for cationic type emulsion using filler Sikaisol). According to this, the emulsion is classified into rapid, medium, and slow setting. That (experimentally controlled) breaking index value depends on bitumen content, aqueous phase composition, and droplet size distribution, as well as external parameters including environmental conditions, spray apparatus, and breaking agents (Read and Whiteoak 2003).

The initial step of breaking begins with wetting of bitumen emulsion onto aggregate surface. Wetting properties may affect emulsion distribution quality on the surface. Wettability can be assessed by measuring the contact angle through the Sessile drop method, which can be used to further calculate work of adhesion between the phases. Dispersive and polar components of the surface free energy (SFE) for solid and liquid phases can be also separated by application of the two-component Owens-Wendt method. A study by (Ziyani et al. 2016) suggests that wettability is significantly

affected by aggregates rugosity, as well as its surface interaction with bitumen emulsion Once aggregate surface wetted, this physical interaction continues to finally cause emulsion breaking either with or without reactive destabilization, as depicted in Figure 2.4.

In non-reactive solid-liquid dispersions, such as latex or non-ionic emulsions, reactive destabilization does not occur, and the curing is rather governed by the evaporation kinetic. The removal of water causes droplets in close proximity, followed by coalescence,that yields transformation of flocs into a film at the final stage. On the other hand, the positively charged groups(-RH^+) originated upon dissociation of a strong acid in water medium in cationic emulsions may interact with alkaline aggregates leaving functional group uncharged. In this way, lack of repulsive force cause droplet contraction, followed by destabilization of emulsion to form gelation. Besides that, flocculation can be also induced by electrolyte addition to neutralize electrostatic force (Boucard et al. 2015).

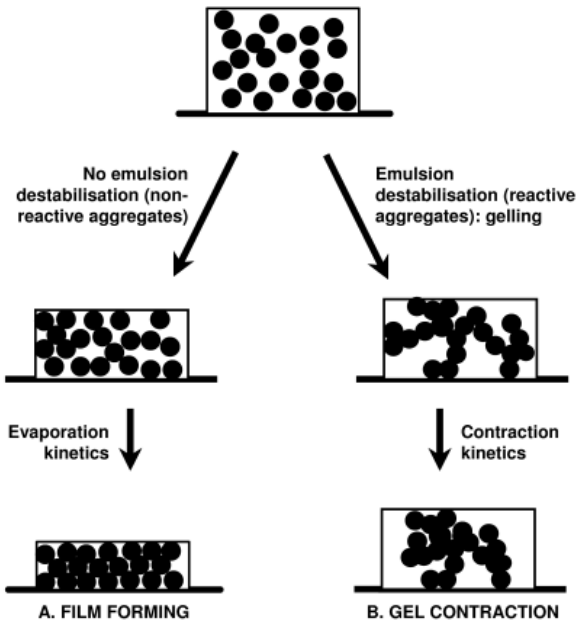

Figure 2.4 Two possible breaking scenarios (Lesueur and Potti 2004)

Thereby, stabilization, wettability and destabilization depend on the type of emulsifier used, that are summarized in Table 2.6:

Table 2. 6 Type of emulsifier (Tadros 2014)

Type of emulsifier	**Charges**	**Typical functional group (character)**
Anionic	Negative	• Carboxylate • Sulfates • Sulfonates • Phosphates
Cationic	Positive	Amines
Amphoteric	Negative and positive	Combined both functional group of cationic and anionic with isoelectric point at which both opposite ion presence (around intermediate pH)
Nonionic	Without charges	Ethoxylate

2.3.4 Flowability

Another important property of bitumen emulsions is their ability to flow, governed by viscosity. Less viscous emulsions are required for the penetration into narrow channeling cavity, whilst others aim to avoid drainage due to inclination by using fairly more viscous ones.

Viscosity is ruled by the nature of bituminous dispersed phase (internal properties – deformability, concentration, size distribution), continuous phase rheology and the type of droplet-droplet physical interaction (Barnes 1994). For bitumen emulsion, the standardized method to characterize viscosity (EN 12846) consists in measuring the time required for emptying a certain volume of bitumen emulsion in standardized geometry through a fixed orifice size. This method is very practical and, in fact,

represents the high-shear limiting viscosity η_∞ of the emulsions. However, it may not be accurate for instance in soil stabilization application for which long loading times(or low shear rates) may be required (Lesueur et al. 2003). In this sense, a complete characterization of their steady viscous flow behavior, covering low to high shear-rate dependence, as that shown in Subchapter 2.6, constitutes a better approach.

2.4 Lignin

2.4.1 Lignin definition and chemical structure

Lignocellulosic biomass is composed of complex carbohydrates (cellulose and hemicellulose) and complex aromatics (lignin and tannin). Lignin stands for the most abundant source of aromatic biopolymer from renewable sources. The evolution of biomass-based polymer development depends also on the improved technologies associated with papermaking, wood processing, textile and lately biorefinery. During the isolation process, the breakdown of lignocellulosic material results in considerable change in its chemical structure (Pandey and Kim 2011; Radotić and Mićić 2016).

Lignocellulosic biomass is composed of 35-83% of cellulose, 0-30% of hemicellulose and 1-43% of lignin (in dry weight percentage). In its early development, lignin is amorphous that consists of unordered connected phenylpropane units. The oxidative cracking abolishes those connecting linkages, lignin rings, alkyl-aryl ether linkage and other bonds within lignin (Pandey and Kim 2011). Further, the amount of phenylpropane units is predicted to be about 12, that is recognized as a highly branched macromolecule with aliphatic, phenolic, carboxylic, carbonyl and methoxy groups. The phenylpropane units could be categorized into three monolignol

precursor where p-hydroxyphenyl (H), guaiacyl (G), and syringyl (S) are from coumaryl, coniferyl and sinapyl alcohol, respectively (in Figure 2.6). Depending on the wood species, the percentage of monolignol varies, for instance, harwood lignin consists of G and S units with some traces of H units whilst in softwood lignin the G-unit is mostly present with a low level of H-units. This lignin source difference affects broadly lignin molecular weight.

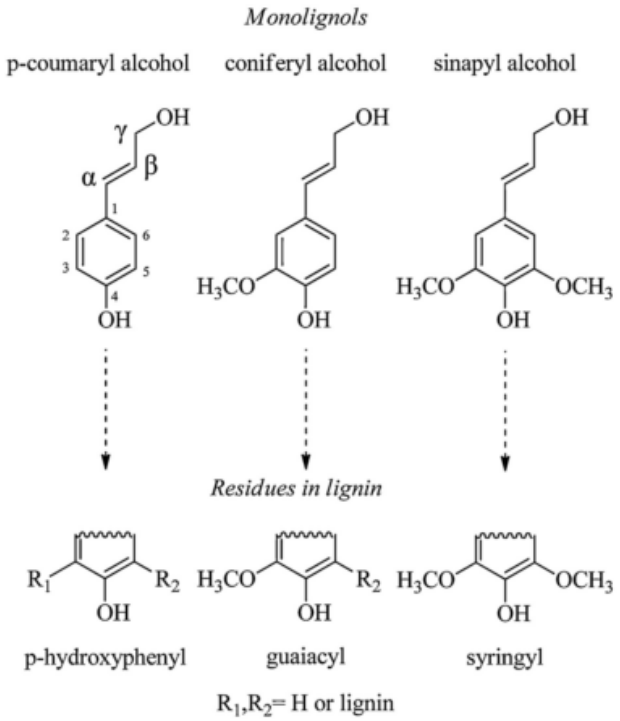

Figure 2. 5 Three main monomers and their corresponding form in lignin polymer, extracted from (Laurichesse and Avérous 2014)

The differing chemical compositions, associated to lignin species, affect their physical properties. For instance, lignin glass transition temperature may range from 100 to 170 °C, being the highest with increasing molar mass (Irvine 1985). Not only that, degradation temperature (Td) depends also on lignin composition. For instance, the different quantity of oxygen-based functional groups results in different thermal stability which broadens the Td range. The decomposition occurs as a result of

consecutive processes that begin with dehydration in the hydroxyl group at about 150 °C, followed by rupturing of aryl-ether linkage, aliphatic side chain, C-C between phenyl propylene unit and lastly with the total volatilization at about 700 °C. Besides chemical composition, other influencing parameters include isolation method, absorbed water, molecular weight and thermal history.

2.4.2 Lignin isolation

As mentioned earlier, the isolation method of lignin from wood is a very crucial parameter which determines its final chemical structure, as well as derived physical properties. Several extraction methods, of physical, chemical, biochemical or combinations, widely used in the pulp industry to yield the various type of lignin, are summarized in Table 2.7.,

Table 2.7 Some lignin isolation technology (Laurichesse and Avérous 2014; Radotić and Mićić 2016)

Isolation technology	Process description	Lignin obtained*
Via preceding extraction of pulp	First to obtain pulp by extraction of milled wood chip with 1st cyclohexane/ethanol and 2nd toluene ethanol, or using pressurized water. Second, isolation by enzymatic or acid hydrolysis	In enzymatic process, non-removable carbohydrate exists, but higher recovery (65-80%) In acid hydrolysis, no non-removable carbohydrate, but lower recover (40-60%) and more phenolic hydroxyl its native (from altered aryl ether linkage)

With ionic liquids	A purification step by using low volatile ionic liquids (ie. 1-butyl-3-methylimiazolium methyl sulfate) on lignin obtained from sodium hydroxide or organosolv process.	With lower neutral sugar as compared to classical method
Brauns native lignin	By percolating milled lignin (100-150 mesh) with 95% ethanol for 8-10 days, followed by evaporating the filtrate	Low lignin yield obtained (8%)
Kraft lignin (sulfate)	By degrading and dissolving lignin in Na_2S and NaOH and cooking at temperature between 155 and 180 °C depending on wood source (hard/softwood)	Potentially with trace of sulfur typically less than 1-2% More hydroxyl group due to aryl ether linkage alteration.
Lignosulfonate (sulfite)	By cooking wood chips in solution containing Na_2SO_3 at 175 °C. Reaction can be performed in acidic, neutral or alkaline	Contain sulfonate groups
Soda cooking	By hydrolysis of annual plant and specific method for precipitation method using mineral acids	Chemically unmodified lignin having silicate and nitrogen content

*It is noteworthy that lignin structure is always partially altered from its native form

Among those, sulfur lignin, referring to Kraft lignin and lignosulfonate, is majorly produced (as a by-product), with Kraft pulping process in cellulose pulp plant worldwide domination of approximately 85% (Carvajal et al. 2016). In that sense, modification, if necessary, is driven toward the use of Kraft lignin.

2.4.3 Lignin modification by amination

There are two general ways to value-add lignin: (i) by lignin depolymerization or fragmenting lignin into smaller units such as vanillin, hydroxylated aromatics, etc.(Pandey and Kim 2011); and (ii) by modification, either substituting the existing hydroxyl groups or introducing new functional groups, through halogenation, amination, nitration, alkylation, etc. Within the scope of this project, lignin is perceived as a potential precursor building block for the preparation of cationic emulsifiers. Native lignin, which contains both hydroxyl and sulfonate groups, can be solubilized in aqueous alkaline medium at high enough pH values (Norgren and Edlund 2014). However, the absence of protonatable functional units leaves lignin insoluble in acidic medium. Thus, modification by amination, in this particular case, is of interest due to conjugate acid formation in the amines group, which accepts H^+ ion from a donor strong acid (Liu et al. 2013; Du et al. 2014).

Amination is based on Mannich reaction that can be done under either acidic or alkaline condition. The Mannich reaction (Mannich and Krösche 1912) is an organic reaction used to convert a primary or secondary amine, a non-enolizable (aldehyde) and an enolizable carbonyl compound into an aminomethylated product, also known as a Mannich base. As an example, in the acidic medium, the enolizable carbonyl compound gets protonated to form an enol intermediate. The non-enolizable carbonyl compound, also gets protonated, reacts with the amine to form an iminium ion. The enol intermediate then attacks the iminium ion which after deprotonation provides the final Mannich base product. (Mannich and Krösche 1912; Li 2006)

Overall reaction:

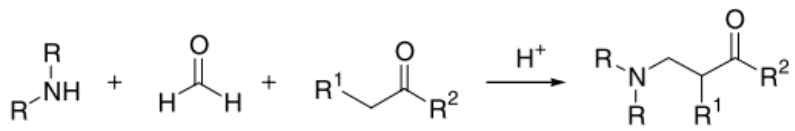

Intermediate Immonium ion:

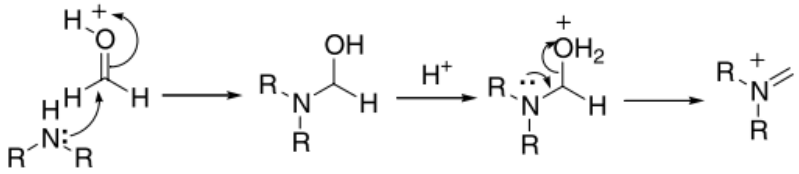

Enolation:

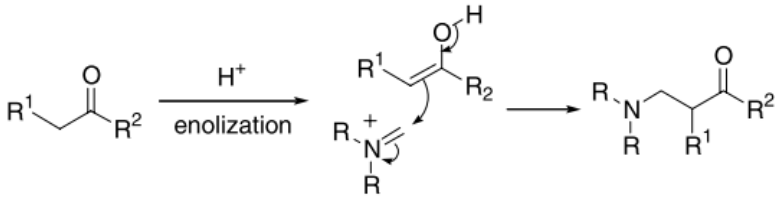

Figure 2. 6 Mannich reaction procedure (Li 2006)

Detail on Mannich reaction, either following acidic or alkaline route can refer to introduction and experimental section in Subchapter 4.4, or 4.6. The resulting modified lignin is very hydrophilic, possesses high molecular mass and is perceived as a polycationic compound in acidic medium, with high charge density with potential application in cationic bitumen emulsions.

2.5 Asphalt mixes

2.5.1 Definition and classification

Road pavement can be classified into flexible (asphalt mixture) and rigid (cement concrete), which differ in modulus magnitude and flexibility. In contrast to rigid pavements, where the structural capacity is only dependent on the concrete slab (surface), in a flexible pavement the load is transmitted downwards. Thus, the bearing capacity requirement is in descending order towards the deeper layer. From the top to the bottom, a flexible bituminous pavement typically consists of surface, base, and sub-grade course. Sometimes further partition may apply, if necessary (Figure 2. 7). The first two layers are asphalt mixtures which are available in various types depending on their functionality, for instance dense graded (for general use), stone mastic asphalt (for high resistance to deformation and durable surface layer), open graded (for improved drainage surface layer), etc.

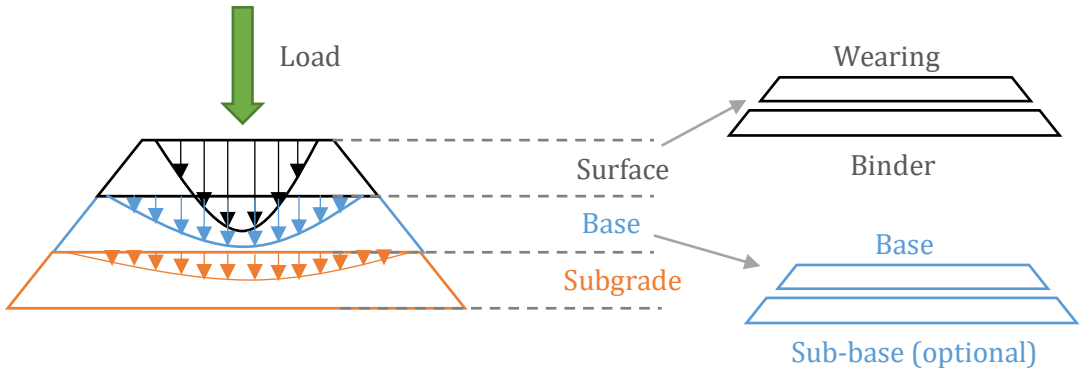

Figure 2. 7 Schematic of road pavement structural layer

The two main constituents of flexible asphalt mixes are aggregate and bituminous binder. The standard manufacture of asphalt mixture consists in mixing hot aggregate and liquid bituminous binder (for coating purpose), followed by lay-down compaction.

The composition and selection of each component depends on the final use of the pavement, with the aim to fulfill specific criteria, such as resistance to deformation, fatigue failure, low temperature cracking, moisture, and skid. Similar to that, French road authority (Delorme et al. 2007) standardize a four test level, associated to EN-13108-1, to ensure the on-spec criteria for each type of asphalt mixes, loading and intended use, summarized in Table 2.8:

Table 2.8 French test level and its standardized parameter

Level	**EN-13108-1**	**Test**	**Standardized parameter ***
Level 0	General + empirical	Without test	N/A
Level 1		Gyratory and water resistance	• Void percentage range at certain number of gyration • Ratio of indirect tensile strength value of wet (pretreated by immersing in water) over dry specimen
Level 2		Wheel tracking	• Rut depth after certain number of cycles
Level 3	General + Fundamental	Stiffness modulus	• Stiffness value at 15 °C and 10 Hz
Level 4		Fatigue	• Fatigue specification (ε_6) at 10 °C and 25 Hz

* Further detail on each type and its corresponding value refer to document (Delorme et al. 2007)

The need to conduct tests at each level increases as the required quality does. For instance, asphalt mixes dedicated to road with low volume and load may only need to satisfy criteria at level 1.

2.5.2 Reduced-temperature mixing technology

Among the construction methods available, hot mix technology is the most extended and accepted current practice. The introduction of heat into aggregate allows the moisture to release, whilst in bitumen side, it permits the viscosity reduction, lower than that recommended by American Association of State Highway and Transportation Officials at 3 Pas, for better workability during compaction. However, technical issues regarding long bitumen exposure to heat may cause a premature oxidation that reduces the coating ability and potentially the service life, besides its negative environmental and energy-consuming issues previously mentioned. Thus, reduce-temperature technologies are introduced as seen in Figure 2.8

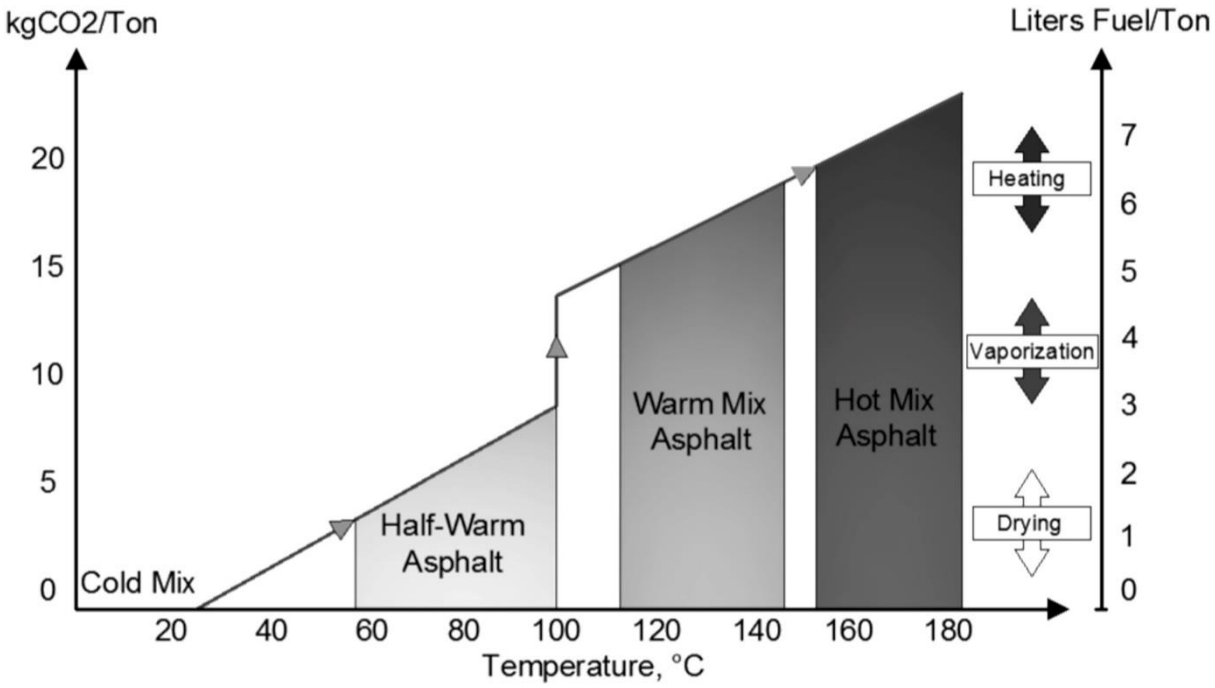

Figure 2. 8 Classification by temperature range, temperatures and fuel usage are approximations (cited from (D'Angelo et al. 2008))

Workability performance is driven by type of gradation and binder viscosity (so its hardness and temperature). If a hard binder is required (e.g. for high modulus), low manufacturing temperatures yield undesirable compactability problems. In that

sense, adaptation by a) the use of additives such as fluxant, wax, etc., and/or b) new processes such as physical foaming (Van de Ven et al. 2007), chemical foaming with zeolite (Barthel et al. 2004), polyurethane (Izquierdo et al. 2012) and finally in the form of bitumen emulsion (Needham 1996; Ronald and Luis 2016) are required. Reduced temperature mixes are not free of issues. For instance, the release of light hydrocarbons to the atmosphere still becomes an important environmental concern for cutback bitumen. Curing process for solvent removal is also problematic especially when dense graded mixture is selected, thus highly time consuming (Needham 1996). Improper curing is a root of performance issues in CMA. Theoretically, reduced-temperature mixes can be applied for any type of asphalt mixture on every structural layer as long as design criteria, such as coating, void percentage, moisture resistance, etc., can be fulfilled.

2.5.3 Reclaimed asphalt pavement (RAP)

In the past, old asphalt mixture ended up landfilled. In 1970, when bitumen price increased, the use of reclaimed asphalt pavement, referred to as RAP, in order to partially replace virgin material started to be investigated. The reduction of virgin material is advantageous in both economic and environmental sense. Moreover, aged binder from roofing (shingles), with higher percentage of bitumen, may also be used as an alternative to RAP binder, (Zhao et al. 2016). Basically, RAP is an old asphalt mixture that is milled into small size 'aggregate'. Due to various mechanical processes which involve different types of machine and intensity, RAP homogeneity is uncertain. In addition, the gradation assumption based on black aggregate (without removing RAP binder) can be misleading from the initial design especially when high mixing temperature is adapted, and a fully blended binder (between RAP and rejuvenator)

expected. Alternatively, the gradation can refer to 'cleaned' aggregates in which aged binder is previously stripped down using solvent, so called white aggregate assumption. When reduced temperature mixing is applied, RAP gradation is difficult to design as the assumption becomes more complicated together with binder degree of blending.

Specifications regarding reclaimed asphalts are described in EN 13108-8. As in the specification EN 13808-8, the authorized RAP contents are 10% and up to 20%, for surface and base courses, respectively. Study reported that the use of 30% RAP in the mix presents almost equivalent performance on fatigue resistance, rutting, moisture susceptibility and stiffness modulus as compared to a well-controlled design asphalt mixture containing all virgin materials (Maupin et al. 2008; Apeagyei et al. 2013). Moreover, the presence of aged binder in RAP, which is harder than fresh bitumen, might be seen as beneficial for improving mechanical properties with respect rutting performance. However, it is noteworthy that low temperature region performance is more prone to failure due to lack of flexibility. To deal with this, rejuvenating agents are normally added to revive aged binder into a new binder with the expected properties. A study by (Zaumanis et al. 2014b) reported several types of rejuvenator, originated from waste vegetable oil, waste vegetable grease, organic oil, distilled tall oil and aromatic extract. In HMA research, one of the most challenging goals regarding RAP use is to be able to predict the quantity of fresh bitumen to be added having into account the high degree of partial blending expected at the temperatures involved (Zaumanis et al. 2014a). Partial blending has been reported to range from 70 to 96% when the formulation of asphalt mixture was altered from 25% RAP and bitumen PG70-28 to 35% RAP and bitumen PG 58-28. Partial blending is favoured for bitumens with lower viscosity, due to enhanced diffusion at the same corresponding

temperature (Oliver 1974). Thus, above increase partial blending is based on using softer bitumen (PG 58-28) rather than increasing the RAP percentage (to 35 %). By combining blending chart, the estimated degree of blending and the expected blend properties, a blending design has been proposed for hot mixes (Lo Presti et al. 2016). For reduced temperature technology, instead, estimations on partial blending can be quite more complicated.

2.6 Rheology for bituminous product

The science of rheology is the branch of physics that studies flow and deformation of matter. Rheology is very useful for understanding the behavior of complex materials, such as bituminous products in the present research. In road engineering, rheological characterizations are considered mandatory. In fact, standardized rheological tests are used for bitumen performance grading.

Rheological properties, relations between stress and strain/strain rate, of complex materials differ from those derived from the classical theory of elasticity and hydrodynamics. Both stress and deformation are better represented in the form of a tensor of nine components (based on three dimension of x,y and z). Further detail on this is described elsewhere (Barnes 2000; Morrison 2001). The characterization of such properties is based on either shear or extensional deformation.

One useful deformation mode to determine the properties of a material is simple shear, defined as a top plane moving in x direction parallel to a stationary bottom plane, separated by several increments in y direction, depicted in Figure 2.9. The shear stress, calculated as the force applied per parallel area unit (τ=F/A), moves the plane with velocity (Vx). As the velocity only acts on x direction, no other velocities in y and

z direction are considered. The velocity gradient in y direction (dVx/dy), which is expressed as deformation in x relative to y direction, per time increment, ((dx/dy)/dt), is termed shear rate ($\dot{\gamma}$). Viscosity (η), is an intrinsic material propertie calculed as the ratio of shear stress applied and consequent shear rate observed (□=τ/$\dot{\gamma}$), which is defined as resistance to flow. When viscosity is independent of shear rate, material is classified as Newtonian; otherwise, the material is designated as Non-Newtonian. Bituminous products (bitumen, PMB and bitumen emulsion) may exhibit Newtonian or Non-Newtonian behavior, depending on the morphology, pressure, temperature, etc. Viscosity is commonly characterized by using rotational shear rheometry. In road paving, viscosity has been used, for instance, to predict binder rutting behavior at 60 °C, workability at 135°C, flow of bitumen emulsion at 30 °C, etc.

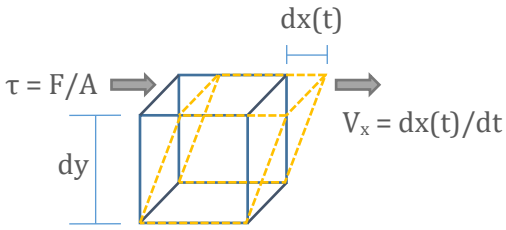

Figure 2. 9 Simple shear schematic

Different rheological models (the most common ones shown in Table 2. 9) are used to describe the steady shear viscous flow behavior of bituminous products. Power law (or Ostwald-de-Waele) model is the simplest one, and is characterized by a linear shear-rate dependence of viscosity in double-log plot. Most bituminous products exhibit a decrease in viscosity with increasing shear rate (termed “shear-thinning” behavior), that can be represented by this simple model. Some products, for instance low viscosity bitumen emulsions, may present both Non-Newtonian and Newtonian response at low-intermediate and high shear rate regions, respectively. Sisko model

is, then, introduced to adapt to the region uncovered by power law model, which is accounted for by a third parameter, the so-called "high shear limiting viscosity", η_∞. Finally, another viscosity plateau (coined "zero shear limiting viscosity", η_0) which stands for almost unaltered sample behavior, may also be expected at very low shear rates. In such a case, the use of the Cross model is required.

Table 2. 9 Steady shear viscous flow behavior rheological models

Model*	Equation	Fitting parameter
Power law	$\eta = k \cdot \dot{\gamma}^{(n-1)}$	k is consistency index n is power law index if n = 1 (Newtonian), else (Non-Newtonian), which 0 < n < 1 (shear thinning), and n > 1 (shear thickening)
Sisko	$\eta = \eta_\infty + k \cdot \dot{\gamma}^{(n-1)}$	η_∞ is high shear limiting viscosity
Cross	$\eta = \eta_\infty + \frac{\eta_0 + \eta_\infty}{1 + \lambda \cdot \dot{\gamma}^{(p)}}$	η_0 is low shear limiting (zero shear viscosity) p (<1)

* other models shall be found elsewhere (Barnes 2000; Morrison 2001)

Linear viscoelasticity is another fundamental aspect of bituminous materials that is necessary. As mentioned earlier, when in-service, bitumen behavior is neither that for a complete solid nor a viscous liquid, but something in between, refer to viscoelastic. For example, when bitumen is subjected to constant strain, the response is an instantaneous stress increase, followed by a decrease with time until reaching stress plateau or close to zero in the case of very soft bitumen (liquid dominant). On the other hand, holding the deformation on bitumen with a certain stress leads to an immediate strain deformation to some degree at the early stage, in which the speed to attain maximum strain decrease, with time. If this stress is released, the strain recovery will

neither be expected as solid or liquid, as seen in Table 2.10. In small amplitude oscillatory shear test of bitumen, the sinusoidal stress response is delayed and is not in phase with strain applied (as in pure elastic solid at 0°), neither completely out of phase (as in pure viscous fluid at 90°) but is somewhere in between these extremes. It also applied on the other way around.

Table 2.10 Tests to determine viscoelastic properties

Test	Description	Properties
Stress relaxation	By deforming material to a certain maintained strain, the stress evolution is recorded as function of time 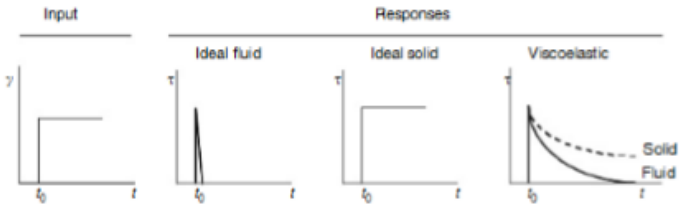	Relaxation modulus $G(t) = \frac{\tau(t)}{\gamma_0}$
Creep tests	By applying certain stress for certain time, the strain evolution is recorded 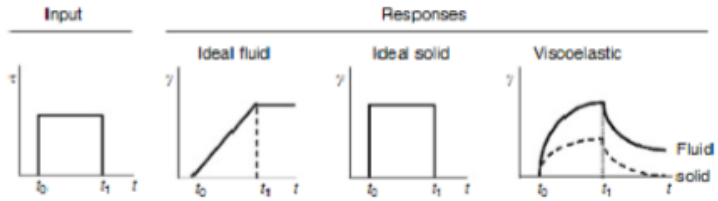	Creep compliance $J(t) = \frac{\gamma(t)}{\tau_0}$ $J(t) = \frac{\gamma_0}{\tau_0} + \frac{\dot{\gamma}(t)}{\tau_0} t$
Dynamic mechanical analysis using small amplitude oscillatory shear (SAOS)	By applying oscillatory stress or strain at certain frequency, the strain or stress response is evaluated Example: Apply: $\gamma(t) = \gamma_0 \cdot \sin(\omega \cdot t)$ Response: $\tau(t) = \tau_0 \cdot \sin(\omega \cdot t + \delta)$ or $\tau(t) = \tau_0 \cdot \cos\delta \cdot \sin(\omega \cdot t) + \tau_0 \cdot \sin\delta \cdot \cos(\omega \cdot t)$ or $\tau(t) = G' \cdot \gamma_0 \cdot \sin(\omega \cdot t) + G'' \cdot \gamma_0 \cdot \cos(\omega \cdot t)$ And vice versa.	Complex modulus $\lvert G* \rvert = \frac{\tau_0}{\gamma_0}$ Elastic and viscous moduli $G' = \lvert G* \rvert \cdot cos\delta$ $G'' = \lvert G* \rvert \cdot sin\delta$ Loss tangent $tan\delta = \frac{G''}{G'}$

It should be noted that such experimental tests and their corresponding viscoelastic properties summarized in Table 2.10 are within its linearity without the dependence on the magnitude of the stress nor strain applied.

Based on the above tests, further information can be gathered variating the tested parameter dependence, such as time, frequency, amplitude and temperature. Detailed information on the characterization procedures performed in the present research can be found in Subchapter 3.3

Moreover, when representing time (or frequency) dependence of the viscoelastic functions above, it is impractical to perform tests covering a very large range of the independent variable. Alternatively, as viscoelastic materials are time (or frequency) and temperature dependent, the above functions obtained at different temperatures over a fixed frequency experimental window (which can be practically operated by the rheometer) can, sometimes, be superposed into a single "mastercurve" by multiplying time (or frequency) by a factor whose value inversely depends on temperature. Hence, curves are shifted horizontally with respect to a certain reference data set as seen in Figure 2.10.

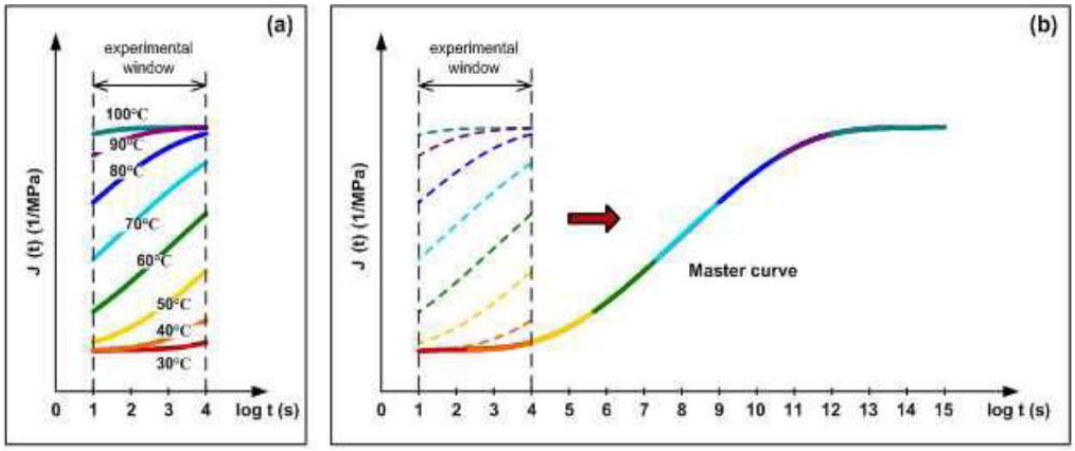

Figure 2. 10 Time temperature superposition scheme. a) Set of data obtained within experimental window for each temperature and b) master curve constructed.

The shift factor, a_T, is commonly described by either Arrhenius or William-Landel-Ferry (WLF) equations (Dealy and Larson 2006), in Table 2.11

Table 2.11 Shift factor dependence with temperature

Shift factor dependence	**Equations**	**Information**
Arrhenius	$a_T(T) = exp\left[\frac{Ea}{R}\left(\frac{1}{T} - \frac{1}{T_0}\right)\right]$	Ea = activation energy R = universal gas constant C_1 and C_2 = empirical constants T and T_0 = temperature and reference temperature (in Kelvin unit)
WLF*	$a_T(T) = \frac{-C_1(T - T_0)}{[C_2 + (T - T_0)]}$	

*WLF can be derived from Doolittle equation relating viscosity and free volume (as a function of temperature)

For bituminous material, construction of complete master curve does not always lead to a smooth profile, meaning that some data points are not superposed, to indicate different microstructure on that corresponding temperature or cannot be considered thermorheological simple. For clarification, sometimes moduli data is presented against phase angle, so called Black diagram, to avoid misleading information due to shifting procedure. The origin of disjoint curve implies the breakdown of superposition that usually associated to the presence of high wax content, asphaltenes structuring or polymer modification (Lesueur 1996)

Chapter 3

Materials and Methods

3.1 Materials

3.1.1 Bitumen

For studying the influence of polymer modification on the performance of modified binders, two types of paving grade bitumen samples supplied by Repsol S.A (Spain), having penetration interval of 70/100 and 160/220 with its respective softening point at 43-51 and 35-43 °C, were used. The feedstock of fractionation which yields bitumen as a by-product may vary significantly in composition. Therefore, in order to avoid any discrepancies on the results, bitumens used always came from the same batch.

3.1.2 Polymer modifiers: EVA, SBS, and Sasobit

One of the goals of this research is to investigate the influence of low melting point polymer addition, **ethylene-vinyl-acetate (EVA)**, on binder performance. For that purpose, different types of EVA, all of them under the commercial name of Alcudia, from Repsol S.A. (Spain), were selected. Varying vinyl acetate (VA) content between 7 and 33 wt.%, and Melt Flow Index (MFI) between 2 and 800 g/10 minutes (190 °C; 2.16 kg), were studied. EVA is a copolymer of ethylene and vinyl acetate monomers in which varying proportions of each monomer may provide tailored characteristics in terms of melting point, crystallinity and melt viscous flow, mainly. EVA is categorized as a thermoplastic plastomer, because its melt properties are reversibly established upon heating from the semicrystalline solid state. As a benchmark, two commonly used bitumen modifiers, of SBS and wax (Sasobit) were opted. The chemical structure of EVA and SBS are shown in Figure 3. 1.

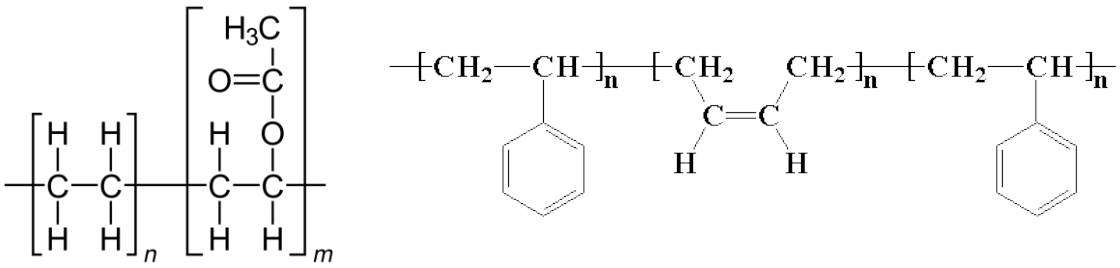

a) b)

Figure 3. 1 Chemical structure of a) EVA and b) SBS

3.1.3 Lignin

Lignin used in this study is derived from Kraft process, known as Kraft or alkali lignin. It is a water-insoluble brown powder with a molar mass of about 10000 g/mol. To be applied as a cationic emulsifier, lignin molecule requires functionalization, by attaching groups that can be protonated in acidic medium, providing positive charge distributed on their structure. Modification for such requirement is commonly performed through the Mannich reaction, procedure which requires formaldehyde and amine groups as reagents to form immonium ion or aminomethanol, under acidic or alkaline environment, respectively. These ions act as precursors of further reactions with lignin. A non-commercial Kraft lignin with a molecular mass of about 3000 g/mol obtained from *Instituto Nacional de Investigación y Tecnología Agraria y Alimentaria, INIA, (*Spain), and a commercial lignin obtained from Sigma Aldrich (Spain) were used and compared.

3.1.4 Amines

Amines are ammonia derivatives where hydrogen atoms are substituted by alkyl or aryl groups. In this work, alkyl amines, from Sigma Aldrich (Spain), are used as reagent for modifying lignin structure. In general, classification of amines (also applied to alkyl

amines) are categorized into primary, secondary and tertiary amines which explain the number of H atom substituents (ie. by alkyl) attached to N atom. For example, a secondary amine, such as dimethylamine, contains two organic alkyls (methyl groups) attached to an N atom, whilst a remaining H atom is still present. Moreover, an amine molecule can contain more than one N atom, so giving rise to higher functionality (protonation ability). For example, the molecule of diethylenetriamine presents two end-capped primary amines additionally to an intramolecular secondary amine. Several amines used in this Thesis are listed in Table 3.1

Table 3. 1 Amines used as reagent for modifying lignin

Amines	**Molar mass, g/mol**	**Chemical structure**
Dimethylamine (DMA)	45.08	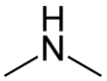
Diethylenetriamine (DETA)	103.17	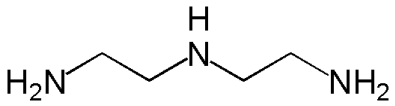
Tetraethylene pentamine (TEPA)	189.30	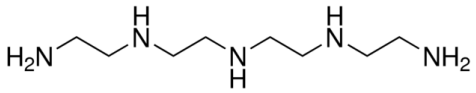
Polyethyleneimine (PEI)	~800	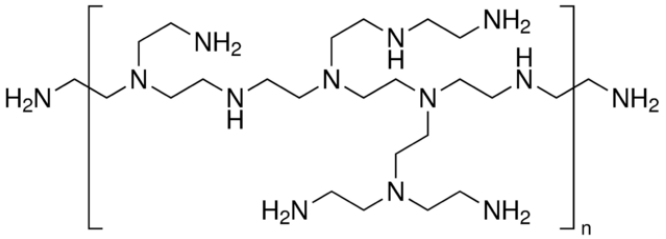

3.1.5 Silicone oil

As the development of lignin derived cationic emulsifier is aimed to produce bitumen emulsion, silicone oil is used in subchapter 4.4 in order to avoid the lengthy procedure of heating bitumen required to condition its viscosity as the oil phase for emulsification. Emulsion prototypes were prepared using silicone oil (polydimethylsiloxane) FS 100, from Esquim SA (Spain), with a viscosity of 100 mPa·s at ambient temperature, so that emulsification could be performed close to ambient temperature. Justification for opting FS 100 is to imitate the recommended bitumen viscosity prior to emulsification, that is < 200 mPa·s (Read and Whiteoak 2003).

3.2 Processing

3.2.1 Preparation of polymer modified bitumen

The general procedure for polymer modified bitumen preparation is by physical dispersion of the polymer into bitumen in their liquid (molten) state. Initially, bitumen was at 150 °C (temperature well above its melting point) inside an oven, until it became a liquid with low viscosity. Solid polymer pellets were slowly dropped into the hot bitumen in the presence of mild stirring to assist the melting process. Once all the polymer was incorporated, a higher mechanical energy was introduced in the form of severe shearing, using a rotor-stator apparatus, so that polymer will finally form microdroplets (Figure 3.2). A homogenous polymer-bitumen mix was immediately poured onto aluminium foil to form a thin layer, and cooled down to ambient temperature, aiming to avoid polymer-bitumen segregation. Detailed information on the specific procedure used shall be included in the experimental section on each subchapter in Results.

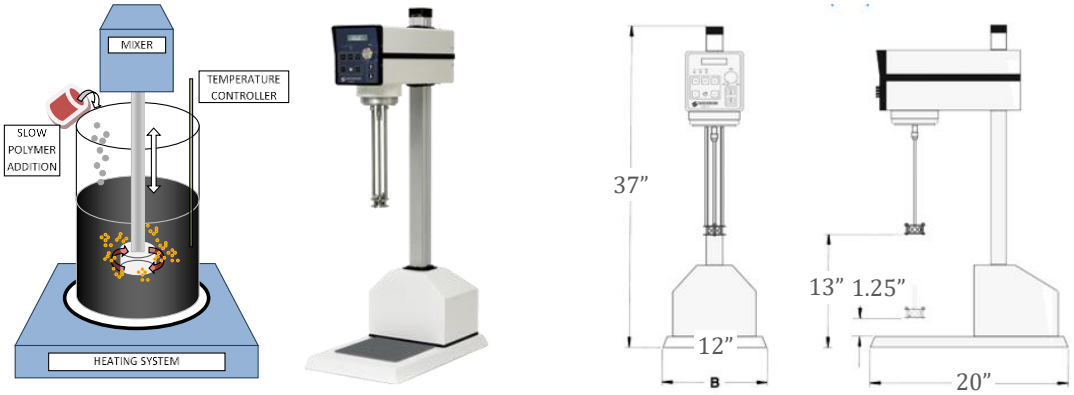

(a) (b)

Figure 3. 2 a) Processing for polymer modified bitumen apparatus using Silverson L5M and b) Detailed geometry

3.2.2 Preparation of cationic emulsifier

The cationic emulsifier was obtained via the Mannich reaction procedure. Kraft lignin was initially dissolved into alkaline aqueous solution in the presence of stirring to assist the process. The solution was placed into a rounded bottom flask with three necks providing circulating water condenser line, temperature controller line, and reagent addition line. Then, tetraethylene pentamine (it proved to be the optimum amine) was poured into the above solution before adding diluted formaldehyde drop-wise. The stirring speed, temperature and time of reaction were controlled. For water phase preparation of the emulsion, the pH of the solution was adjusted by addition the proper dose of hydrochloric acid. Further details shall be given in the experimental section of subchapters 4.4 - 4.6.

3.2.3 Preparation of bitumen emulsion

The processing of bitumen emulsion could be divided into two types with regards to the nature of bitumen phase, either bitumen with or without polymer modification. Neat bitumen (bitumen without polymer modification) was always processed at a temperature higher than its softening point (this facilitates flowability) but below 100 °C (it prevents excessive evaporation upon contact with water phase, such that allows the use of an open system). On the other hand, for bitumen containing a polymer, particularly the one with a melting temperature higher than 100 °C, it was necessary to conduct emulsification in a closed system involving air pressurization in order to suppress water evaporation. Several types of rotor-stator apparatus were utilized, in either batch or continuous process, to disperse bituminous droplets into water phase containing an emulsifier. Schematics of these two processes are presented in Figure 3. 3.

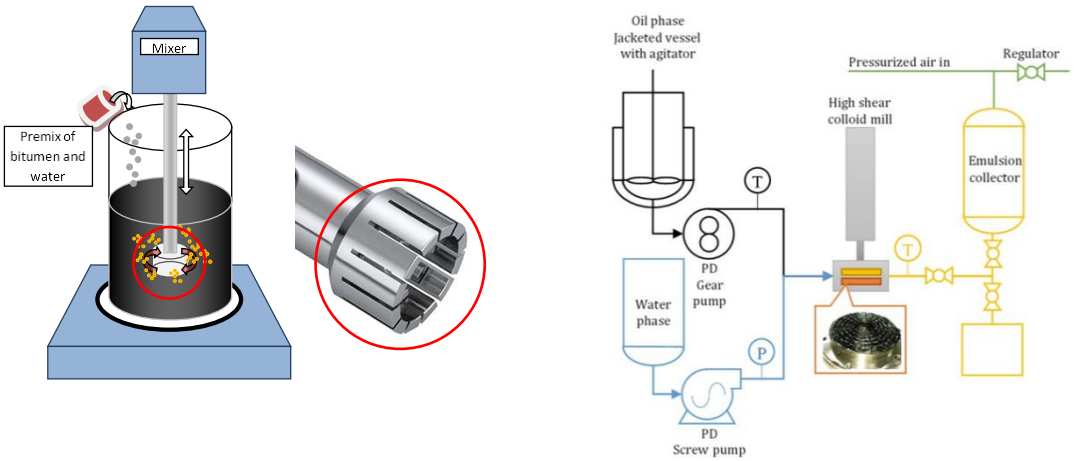

(a) (b)

Figure 3. 3 Emulsion processing device a) batch mechanism using Ultraturrax with S25N-25F dispersing element and b) Home-made semi-continuous laboratory pilot plant

The details on the processing parameter values, consisting of pressure and temperature, device used, emulsification time and procedures can be found in the experimental section of Subchapters 4.3 - 4.6.

3.2.4 Preparation of asphalt mixes

The preparation of asphalt mix specimens consists of mixing and compaction steps. As mentioned earlier, the preparation procedure is classified based on temperature, referred to as HMA, WMA, HWMA and CMA (in decreasing order of working temperature). Depending on the type of layer (or final purpose), the aggregate size used must follow specific gradation curve as per regional standard. As this work was developed in Spain and France, the design applied to each local authority is considered, for instance, mixes known as AC 16 and BBSG-10 in Subchapters 4.5 and 4.6, respectively.

In the preparation of HWMA specimens, aggregates were initially heated inside the oven at 110 °C for 3 hours, before entering the mixer. The mixing itself is divided into two stages, the first 30 s of mixing without bituminous binder allows to homogenously distribute the aggregates. Afterward, a little quantity of water, to moisturize aggregate surface, is poured into mixer followed by bitumen emulsion at 60 °C, stage that lasts 2 minutes. The loose coated aggregate temperature is controlled in oven at 80 °C for 30 minutes before compaction either using gyratory or roller compactor. Similar steps are applied for WMA and CMA, though with different working temperature. Further details shall be provided in Subchapter 4.5. The compacted specimens are subjected to 3 days maturing inside an oven at 50 °C.

When RAP is used, gradation curve is estimated by initially splitting RAP into several fractions and then recomposed it. If white (fresh) aggregate assumption is used, aged binder is separated from the aggregates prior to sieve test to provide gradation curve of each fraction. Conversely, a direct sieve test on each fraction can be performed, if the recomposing employs black (aged) aggregate assumption.

3.3 Experimental characterization

3.3.1 Characterization for bitumen, PMB, and emulsion residue

3.3.1.1 Technological tests: Penetration test and ring & ball softening point test

Two technological tests for initial assessment of bitumen properties includes penetration and softening point tests, authorized in European standard EN 1426:2007 and 1427:2007, respectively. **Penetration test** predicts the hardness of bitumen at 25 °C by measuring the depth of a standard needle penetrating bitumen with the load of 100 gr for 5 sec. **Softening point test** informs about the bitumen thermal susceptibility, providing an estimated temperature for the onset of "melting" (in this case, this term is not accurate, as bitumen is an amorphous material). This test, which is carried out by immersing the sample into a heating water medium at a controlled rate of 5 °C/min and controlled agitation of 100 rpm, monitors the temperature when a standardized steel ball, set on the bitumen sample, penetrates the softened bitumen by gravity until it touches a plate set below. The apparatuses are presented in Figure 3. 4

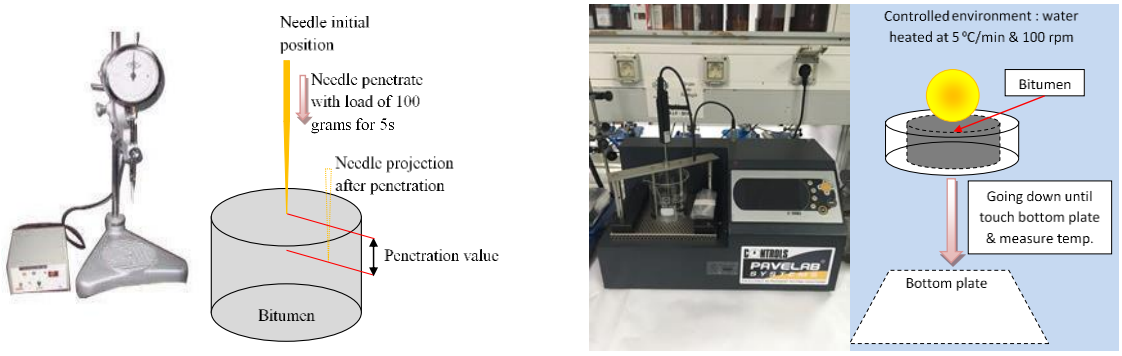

a) b)

Figure 3. 4 Apparatus and schematic principle of a) penetration and b) ring & ball softening point tests

3.3.1.2 Microstructural analysis: Optical microscopy

The microstructures of PMBs, silicone oil/water emulsions and bitumen/water emulsions residues were observed at ambient temperature through the optical microscope Olympus BX51 (Japan). Sample preparation is performed on the standard slide, of 76 mm x 26 mm, by introducing a mild heating, slightly above the corresponding softening point of the sample, in order to form a thin film which allows light to pass through. The transmitted image is then captured by a photo camera Olympus Camera 5050 (Japan).

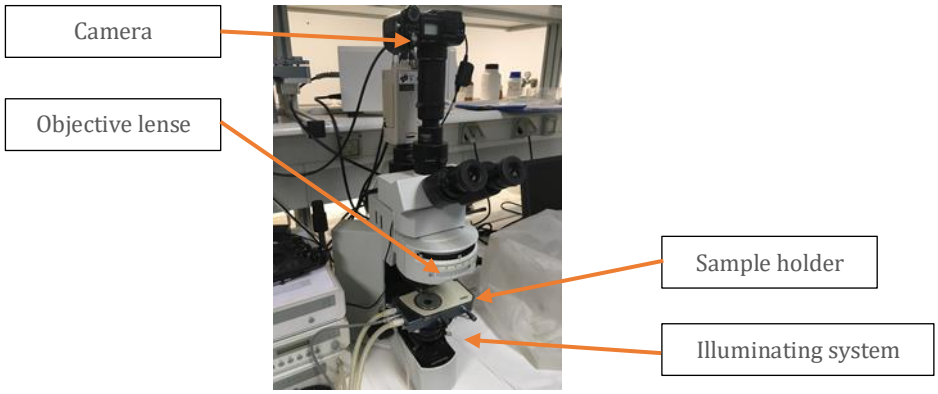

Figure 3. 5 Optical microscope Olympus BX51

3.3.1.3 Rheological characterization: Viscous flow tests and Temperature and Frequency sweeps

Viscous flow tests were performed under steady rotational shear within a specified shear rate range. Physica 301 controlled stress rheometer (by Anton Paar, Austria) was employed using serrated plate-plate 25 mm diameter geometry, with 1 mm gap between plates. Two test temperatures, of 60 and 135 °C, are selected to resemble the maximum expected pavement in-service temperature in warm climates and binder workability at compaction, respectively. For the purpose of maintaining fixed temperature, the rheometer is equipped with electrical heating system and air convection chamber. It is noteworthy that the interval range over which the shearstress steps were applied were within the minimum/maximum torque range specified by the rheometer supplier.

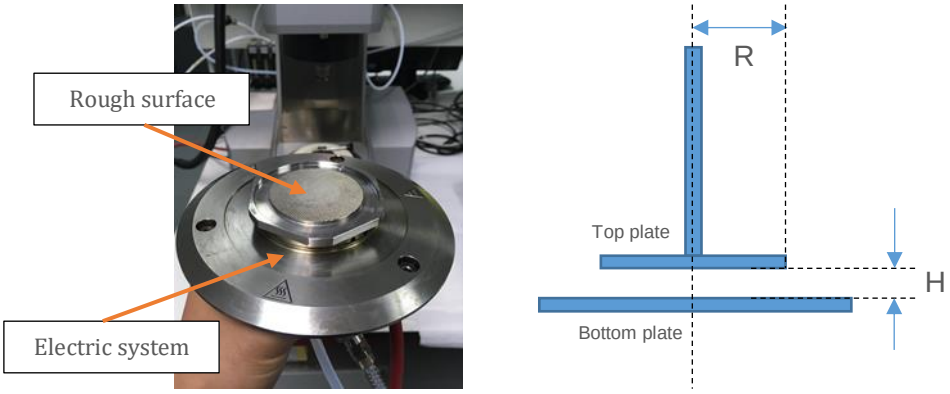

Figure 3. 6 a) Bottom plate of Anton Paar Physica 301 and b) schematic plate-plate geometry

For **temperature sweep tests**, dynamic "sinusoidal" stress oscillation, with constant amplitude and frequency, is applied to a bitumen sample whilst it is heated at a rate of 1 °C/min, from 30 to 100 °C. The test was performed using the Rheostress 600 controlled stress rheometer (by HAAKE, Germany), with 20 mm ϕ serrated plate-plate geometry. The sample was heated from both bottom and top in such a way that

temperature gradients are removed or, at least, minimized. The frequency and shear stress applied are fixed at 10 rad/s and 100 Pa (within linear viscoelastic regime). The determination of LVE is performed using stress sweep method where the limit for stress dependency is noticed from the evolution of G' and G''. Figure 3. 7 depicts the apparatus and the geometry used.

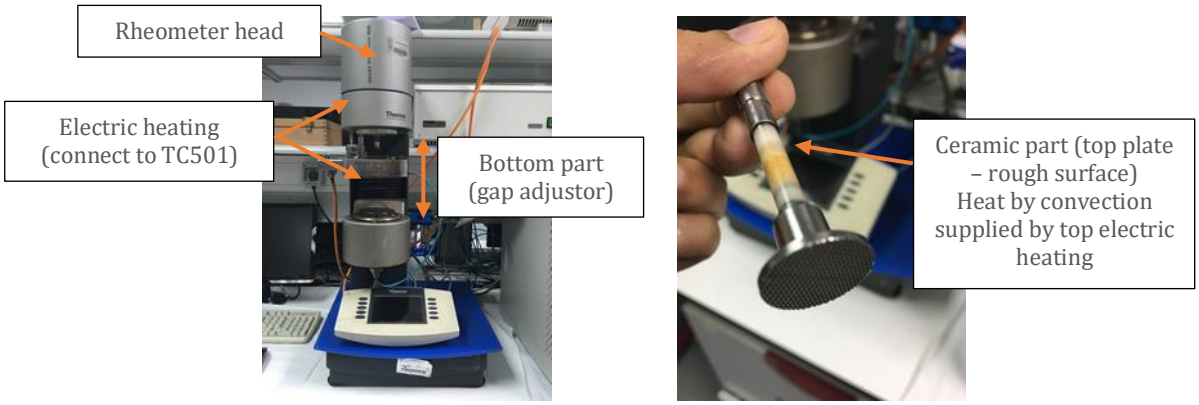

a) b)

Figure 3. 7 Oscillatory shear temperature sweep test using a) HAAKE Rheostress 600 b) Serrated plate-plate 20 mm diameter geometry with ceramic shaft for thermal isolation.

Similar to temperature sweeps, **frequency sweep tests** were also conducted in oscillation mode, but at selected fixed temperatures. Within this research, the test is used to construct a master curve, by implementing time-temperature superposition principle of five frequency sweep data set at a various temperature, of -30, -20, -10, 0 and 10 °C, for binder low in-service temperature evaluation. The stress applied is fixed at a value between 5000 - 10000 Pa (always below LVE limit) and the frequency gradually decreased from 100 to 1 rad/s in logarithmic scale for each set. The test is performed in torsional mode on parallelepiped specimens, previously done by compression-molding, using Anton Paar Physica 301 with the solid rectangular fixture (SRF). To maintain the low temperature, cold N_2 has is blown inside the CTD 600 convection chamber. The chamber temperature is controlled by coupling a

temperature controller (TC30) and evaporation unit (EVU10), which provides a controlled gas flow rate by evaporation of liquid N_2. It is worth mentioning that for each temperature, **stress sweeps** were always performed, not only to guarantee the LVE limit but also used to determine strain at breakage beyond LVE.

The strain breakage test was performed in the similar setup by extending stress sweep interval range beyond LVE limit up to the point where material could no longer sustain the applied load, indicated by an abrupt drop in the moduli value. Example of broken specimen is shown in Figure 3. 8 a. Limit determination and specific measuring geometry as in Figure 3. 8 b, shall refer to standard ASTM D5279-99, D 4065, and DIN 53445.

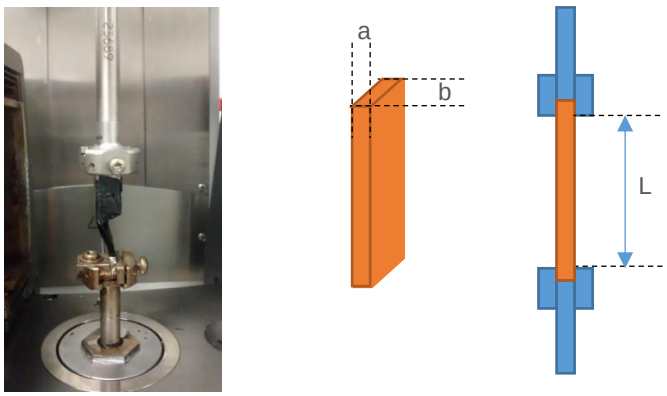

a) b)

Figure 3. 8 Low temperature oscillatory instrument a) example of broken sample after strain breakage test, and b) schematic of SRF geometry as per ASTM D5279-99, D 4065, and DIN 53445

3.3.1.4 Thermal analysis: modulated differential scanning calorimetry (MDSC) and thermogravimetric analysis (TGA)

Modulated differential scanning calorimetry (MDSC) is an advanced version of standard DSC where heat flow can be deconvoluted, by modulating mode (a sinusoidal term is added to the standard linear heating signal), to dissociate an overlapped material response into reversing and non-reversing thermal event. Similar as in DSC, materials are subjected to heating/cooling ramps for observing any endothermic and exothermic peaks, peculiarity from the baseline. Material heat evolution is obtained after subtracting the signal corresponding to the reference (empty) pan, schematically represented in Figure 3. 9 a.

In this research, three scans of heating – cooling – heating were conducted for every run, with a TA Instrument Q100 apparatus. The first heating aims to erase the thermal history the material might have experienced prior to its characterization. The next cooling, followed by heating, were ramped at 5 °C/min with amplitude of modulation fixed at ±0.5 °C and oscillation period of 60s, in the presence of N_2 purge gas.

A second type of thermal analysis was based on mass changes monitored as temperature is raised at constant heating rate. This type of tests, known as thermogravimetric analysis (TGA), was carried out using Q50 Analyzer by TA Instruments (Figure 3. 9 b). At a constant heating rate of 10 °C/min, from 30 to 600 °C, material decomposition was observed through sample mass variation with temperature.

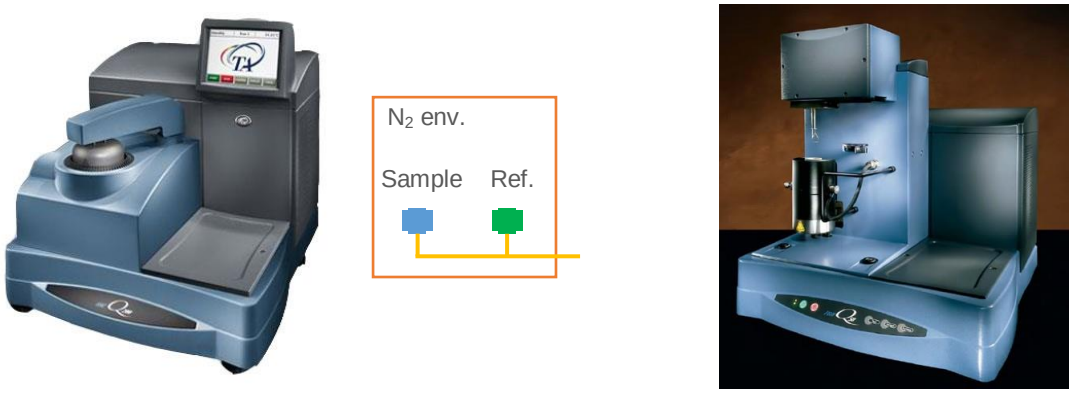

a) b)

Figure 3. 9 Thermal analysis instruments a) (Modulated) differential scanning calorimetry Q100 TA Instruments apparatus and b) Thermogravimetry Q50 TA Instruments apparatus

3.3.2 Characterization for Cationic emulsifier

3.3.2.1 Filtration test

This test was conducted to estimate the solubility of the Kraft lignin upon functionalization, as a function of the pH of the aqueous phase. Solution at ambient temperature was poured into vacuum filtration set up, consisting of feeder, filter paper of either 7-9 or 45 µm, vacuum chamber and ejector, shown in Figure 3. 10. Filtrate containing the soluble MKL was collected in the chamber whilst filter cake of insoluble MKL were retained in the filter paper.

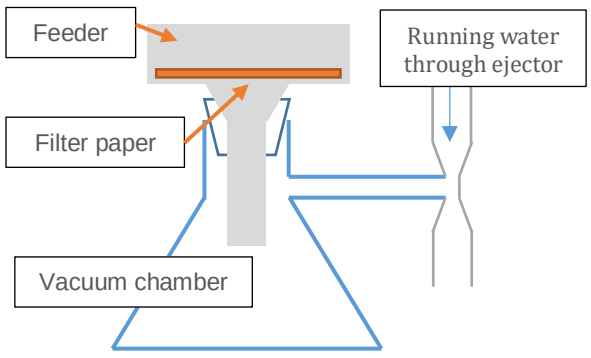

Figure 3. 10 Vacuum filtration set up

3.3.2.2 Microstructural analysis: Fourier transform infrared (FT-IR) spectroscopy

The functionalization (attachment of amine groups) of the Kraft lignin was verified through Fourier transform infrared (FTIR) spectroscopy, obtained using JASCO FT/IR 4200 in Figure 3. 11 a. The spectra, in a wavenumber interval range of 400-4000 $cm^{-1}$and at 4 cm^{-1} resolution, were obtained in transmission mode. A disk sample (in Figure 3. 11 b), blend of lignin and KBr, was prepared by compaction using a hydraulic press at 5 bar for at least 5 minutes, and then the sample was placed onto disk holder inside FT/IR device.

a) b)

Figure 3. 11 Infrared apparatus using JASCO FT/IR 4200 and disk sample

3.3.3 Characterization for Bitumen emulsion

3.3.3.1 Water content and breaking index test

Water content using drying balance and breaking index tests comply with EN standards 16849 and 13075-1, respectively. Parameters derived by these technical tests, of bitumen content and breaking index, are used to specify the class of bitumen emulsion as well as for its particular application, listed in Annex of EN 13808.

Water content using drying balance works by evaporating water contained in a bitumen emulsion in a controlled heating mode and continuously measuring the mass of the remaining bitumen up to a constant value reached. A sample of 3 g of bitumen is poured into drying cups, followed by covering it with glass fiber filter to avoid any bitumen splash/removal that can affect final bitumen content.

Breaking index value was determined by pouring siliceous filler, at a controlled mass rate, into 100 g of cationic bitumen emulsion in the presence of mixing until breakage occurred, which was evidenced by the formation of semisolid ball of emulsion-filler blend. From the quantity of filler required until breakage, the index is then calculated using the equation mentioned in EN 13075-1.

3.3.3.2 Physical analysis for droplet size distribution and zeta potential

Droplet size distribution of bitumen emulsion was characterized by laser diffraction method using Malvern Master Sizer 2000 (UK) in Figure 3.12. Dilution of concentrated bitumen emulsion was performed in dispersing chamber with stirring at 1500 rpm and pumping recirculation by the addition of distilled water. The refractive indices for bitumen and water were set at 1.61 and 1.33, respectively.

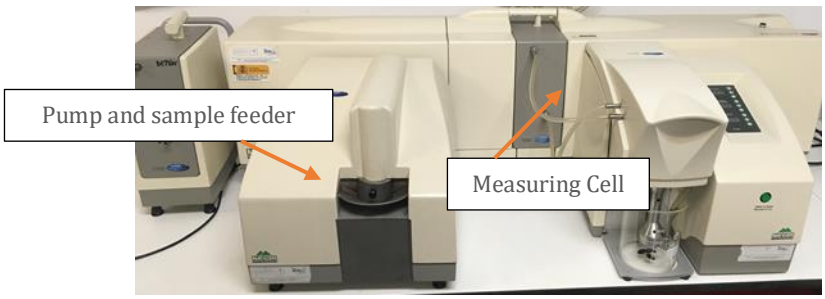

Figure 3. 12 Droplet size and droplet size measurement apparatus based on laser diffraction in Malvern mastersizer 2000

Zeta potential tests, performed using Malvern Zetasizer (UK), allowed surface charges to be inferred by measuring droplet electrophoretic mobility. DTS 1070, a U-folded capillary zeta cell, was filled with sample by injection using syringe. Measurement was performed for three replicates.

3.3.3.3 Rheological characterization: viscous flow test and frequency sweep

Viscous flow tests on emulsions were performed under steady rotational shear using corrugated cup-bob geometry in Anton Paar Physica 301. This geometry was chosen for various reason: first, to gain sensitivity with a material of low viscosity; second, to minimize water evaporation, since evaporation occurs on the top of the sample, hence does not affect shearing area and measurement; third, wall slip issue was also eliminated by the use of a corrugated shearing surface. The measurements were developed according to protocols stated in ISO 3219 for this geometry.

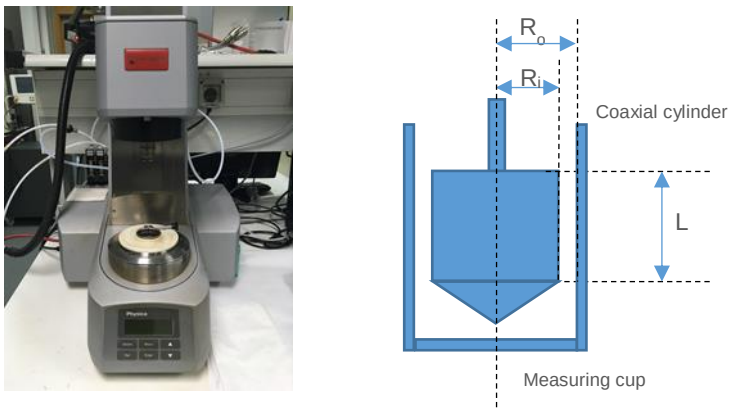

a) b)

Figure 3. 13 a) Steady flow curve test using Physica 301 measured with coaxial cylinder and b) schematic coaxial cylinder geometry as per ISO 3219

Viscoelasticity of emulsion were observed via frequency sweep method within its linear viscoelastic region. Test were conducted using the same rheometer, Physica 301, with different accessories, a parallel plate with diameter of 50 mm and a cap.

3.3.4 Characterization for asphalt mixes (according to French standard)

The preparation and characterization of asphalt mix refer to French standard. Asphalt mixes components, aggregate gradation and binder content, are proposed by the designer based on gyratory performance. Once finalized, the prepared specimens are subjected to a sequencial assesment procedure that includes empirical and fundamental tests.

3.3.4.1 Empirical tests

Empirical tests consist of two levels: a) level 1 for assuring compaction performance and water sensitivity, observed through gyratory test and Duriez strength compression test, respectively and b) level 2 for permanent deformation evaluation using large wheel tracking device, as summarized in Table 3. 2

Table 3. 2 French empirical tests

Gyratory compaction	**Duriez compression**	**Wheel tracking test**
NFP 98-252	NFP 98-251-1	EN 12697-22 or NFP 98-253-1
		
Parameter for evaluation		
The evolution of void percentage (V%) as a function of gyrations number	The ratio of compression strength between wet and dry specimen	The relative rut depth and its evolution at 1000, 3000, 10000 and 30000 cycles.
Operating input		
• 200 gyrations • 0.82 ° internal angle • 0.6 MPa vertical pressure	• 6 dry specimens at 18°C of 50% RH and 6 wet specimens (immersed at water bath) • Axial compression load, 1mm/s	• 100 mm thick parallelepiped • 1 Hz frequency • 60 °C temperature • 5 kN loads • 0.6 MPa smooth tire

3.3.4.2 Fundamental tests

Level 3 and 4, of stiffness modulus and fatigue life test in Table 3. 3, are considered as fundamental tests focusing on mechanical behavior of the asphalt mix specimen. Both tests are based on two-point bending on a trapezoidal specimen with dimension of 56 mm (bottom width), 25 mm (top width), 20mm (thickness) and 250 mm (height)

Table 3. 3 French fundamental tests

Stiffness modulus test	**Fatigue life test**
EN-12697-26 or NFP 98-260-2	EN 12697-24 or NFP 98-261-1
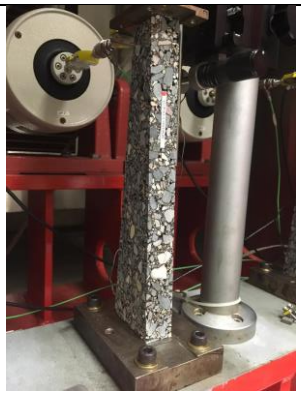	
Parameter for evaluation	
Master curve by applying time-temperature superposition principle and in particular modulus (E) at 15 °C 10 Hz	Recommended strain level at 1 million of cycle (ε6)
Operating input	
• Frequency sweep between 1 to 40 Hz • Temperature between -10 to 40 °C	• Strains levels between 80-150 µstrain • 10 °C temperature • 25 Hz frequency

Chapter 4

Results

4.1 Influence of polymer melting point and Melt Flow Index on the performance of ethylene-vinyl-acetate modified bitumen for reduced-temperature application

Published in :

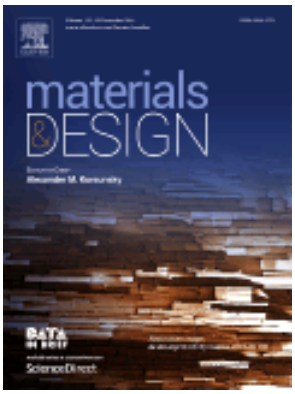

Materials & Design
Publishing Company : Elsevier B.V.
Editor in Chief : Alexander M. Korsunsky
Volume: 96, PP : 180-188
Year : 2016
ISSN : 0264-1275
DOI : 10.1016/j.matdes.2016.02.003

ABSTRACT

The paving industry is currently demanding polymer modified bitumens (PMBs) with enhanced in-service performance and low enough viscosity at lower application temperatures. With this aim, this study focuses on the use of ethylene vinyl acetate (EVA) copolymers with low melting temperatures and explores the effect on the desired properties of the vinyl acetate (VA) content and Melt Flow Index (MFI). To that end, binders were prepared from EVA copolymers having varying VA contents from 7 to 33 wt.%, and MFI from 2 to 800. A comprehensive characterization based on viscous flow curves, dynamic shear temperature sweeps, standardized technological tests, differential scanning calorimetry (DSC) and optical microscopy analysis was conducted on EVA-binders with 5 and 7.5 wt.% EVA. Low VA contents proved to endow bitumen with improved performance at medium-high in-service temperatures. Interestingly, binder viscosity at 135°C decreased with increasing the MFI, regardless the selected VA content. This means that tailored PMBs can be designed with both improved in-service performance at medium-high temperatures and reduced viscosity to facilitate polymer-bitumen mixing, mineral coating and asphalt mix laydown/compaction at lower temperatures.

4.1.1 Introduction

Bitumen, by-product from crude oil distillation, has been largely used as binder of mineral aggregates in road paving (Liang et al. 2015). Even though its content in the asphalt mixtures (composed of mineral aggregates and bitumen) never exceeds 5 wt.%, its contribution to the road performance is decisive (Cuadri et al. 2013b). In that sense, it is the only deformable component in the mixtures and actually constitutes their continuous matrix.

Consequently, the viscoelastic properties of bitumen, over a wide range of temperatures and loadings, are of special importance when predicting roads performance (Cuadri et al. 2013a). For certain applications, bitumen quality needs to be enhanced, commonly by its modification with polymers (Munera and Ossa 2014). Depending on the requirements demanded, a bitumen additive should improve the binder properties at the in-service temperature range expected (Zanzotto et al. 2000). Thus, in the warmest climate countries, it should withstand the traffic loads which cause the so-called permanent deformation at high temperature. Moreover, if harsh winters are expected, high flexibility at low temperature is certain to help mitigate thermal fracturing. In addition to that, a modifying agent of bitumen should also meet the following features: (a) easy to incorporate; (b) homogeneously dispersed during storage; and (c) low viscosity at the mix asphalt temperatures, which assures the correct coating of the arids and laydown/compaction operations.

Traditional asphalt mixtures, also termed as hot mix asphalt (HMA), have been always produced and applied at very high temperatures, never below 150 °C. Moreover, the use of polymer modified bitumens (PMBs) in HMA requires temperatures that

normally exceed 160°C and very frequently approaches 180-190 °C. Otherwise, the viscosity of a PMB is not low enough so that coating of aggregates and further operations are performed adequately. Concerns with the environment impact and the health consequences of exposure to asphalt fumes have resulted in a major effort to develop alternative paving practices (Qin et al. 2014). In this sense, reduced-temperature technologies represent a number of processes and additives that allow the production of asphalt mixes to be conducted at significantly lower temperatures than HMAs, reducing energy consumption and asphalt fumes emissions (Rubio et al. 2012; Cuadri et al. 2014; Airey and Thom 2015). So, whilst HMAs are produced and applied at temperatures never below 150°C, the more recent reduced-temperature technologies have been classified as follows: 100-140 °C, for warm mix asphalt (WMA); 60-100 °C, for half warm mix asphalt (HWMA); and 25-60 °C, for cold mix asphalt (CMA) (Rubio et al. 2012). With that purpose, novel additives and/or processes are required in order to achieve the desired lower viscosity at the mix production (Zaumanis 2010). For instance, the selection of low melting point polymers may provide an advantage if compared to traditional SBS-modified binders that normally require very high temperatures of mixing with the aggregates (Doyle et al. 2013). So, as far as warm climate countries are concerned, the success of WMA technologies involving PMBs relies on the development of binders with low viscosity in the 100-140°C temperature range which, instead, offer a high degree of modification at the highest in-service temperatures expected. Furthermore, for an even more substantial energy saving, the use of CMA technologies is also encouraged (Collins et al. 2006).

On this basis, excellent efforts have been so far done to study EVA (ethylene vinyl acetate)-modified bitumen in performance related concern. In this sense, they mainly focused on obtaining the optimum blending conditions (these are, mixing temperature, blending time and shear rate) for preparing EVA bituminous binders (Saboo 2015) or their morphology, thermal and rheological properties depending of the EVA copolymers characteristics and concentration (Airey 2002a; Zhu et al. 2014; Dekhli et al. 2015; Polacco et al. 2015). Other researchers reported the use of recycled EVA polymers as bitumen modifying agent (Garcia-Morales et al. 2004; García-Morales et al. 2007) and even the blend into ternary formulations with other polymer or clay (Sureshkumar et al. 2010; Markanday et al. 2010). Still, not so many in-depth investigations have been conducted on the potential of EVA as modifier in reduced-temperature technologies for asphalt roads.

The present paper explores the development of PMBs binders with enhanced in-service performance and low viscosity at reduced working temperatures. This objective is addressed through the use of EVA copolymers with melting temperatures substantially lower than other traditional polyolefins, which exhibit low viscosity at their molten state, but which impart a reinforcing effect on the bitumen matrix when they re-crystallize. With that purpose, a selection of PMBs derived from different EVA copolymers with varying vinyl acetate (VA) content and Melt Flow Index (MFI) value was studied. From their comprehensive characterization, it was proved that the optimal selection of VA content and MFI value may yield promising bituminous binders with the above desired properties.

4.1.2 Experimental

4.1.2.1 Materials

Two different types of neat bitumen supplied by Repsol S.A. (Spain), with penetration grades within the intervals 70/100 and 160/220 (EN 12591:2009), were used as base material for the modification.

Ethylene vinyl acetate (EVA) copolymers, also kindly donated by Repsol S.A. (Spain) under commercial names of Alcudia®, with different VA contents ranging 7 to 33 wt.%, and MFI between 2 and 800 were used as modifying agents (Table 4. 1. 1). VA contents relate to EVA melting point (Table 4. 1. 3) and the MFI is a measure of mass of polymer flowing under specific temperature and loading in a standard measuring device for 10 minutes. For EVA, the temperature is specifically set at 190 °C and the loading at 2.16 kg, according to ASTM D1238. For sake of clarity, these EVA copolymers will be identified attending both their VA and MFI values, e.g. EVA-VA7-MFI2 refers to a EVA with VA of 7 wt.% and MFI of 2 g/10min. Furthermore, a Styrene-Butadiene-Styrene (SBS) Calprene® C501 (Dynasol) and a wax Sasobit® (Salsol Wax) were selected as reference modifying agents, for sake of comparison.

Table 4. 1. 1 Penetration values and ring & ball softening temperatures for neat and modified bitumens with wax, SBS and EVA with varying VA content and MFI.

Neat bitumen	Modifying agent		Binder	
			Penetration (dmm)[a]	**R&B softening point (°C)[b]**
70/100	Unmodified		73	46
	SBS		45	63
	wax		57	58
	EVA Polymer		**EVA Binder**	
	VA (wt. %)	**MFI (g/10min)**	**Penetration (dmm)[a]**	**R&B softening point (°C)[b]**
	7	2	39	65
	18	2	40	69
		500	53	64
	28	7	44	60
		400	58	54
		800	58	51
	33	45	54	54
160/220	Unmodified		190	39
	7	2	99	61
	18	500	124	57
	28	400	135	44
	33	45	149	44

[a]According to EN 1426:2007.

[b]According to EN 1427:2007.

4.1.2.2 Bituminous sample preparation

EVA/bitumen blends (referred to as EVA-binders) and reference systems (SBS and wax modified bitumens) were processed with a Silverson L5M (Silverson Machines Ltd., U.K.) homogenizer equipped with a J.P. Selecta (Spain) controlled heating system. The processing protocol consisted in mixing neat bitumen with 5 or 7.5 wt.% EVA

polymer at 150°C in a cylindrical vessel (110 mm diameter and 130 mm height). Pre-blending of bitumen and EVA pellets was performed at 3500 rpm for 15 min, before the speed was increased up to a final value of 5000 rpm and maintained for 1 hour. Alternatively, other two binders were also prepared: (a) one with 1.5 wt.% wax following the same processing protocol and; (b) a 3 wt.% SBS modified bitumen processed at 180 °C, for 1 h and 6000 rpm. Immediately after mixing, all binders were poured on aluminium foil and cooled down to room temperature, in order to prevent polymer phase separation and, so, sample heterogeneity.

4.1.2.3 Tests and measurements

Two selected technological tests, penetration and ring-and-ball softening temperature, were performed on neat and modified binders according to EN 1426:2007 and EN 1427:2007 standards, respectively.

Two different rheological tests were carried out on bituminous binders: a) viscous flow measurements at 60 and 135 °C; and b) temperature sweep tests under oscillatory shear between 30 and 100 °C. Viscous flow curves were conducted in a controlled-stress rheometer Physica MCR-301 (Anton Paar, Austria) using plate-plate geometry (25 mm diameter and 1 mm gap). Measurements were performed by ranging shear stress from 1 to 1000 Pa and collecting the viscosity data every 2 minutes, once apparent viscosity had reached steady state values at the applied stress. On the other hand, temperature sweep tests in oscillatory shear, from 30 to 100 °C and using a continuous heating ramp of 1 °C/min, a frequency of 10 rad/s and a shear stress of 100 Pa (within the linear viscoelasticity, LVE, interval), were conducted in a controlled-stress rheometer RheoStress RS600 (Haake, Germany). Previously to temperature sweep tests, shear stress tests, at the same frequency and at selected

constant temperatures within the 30-100°C interval, were performed in order to determine the limit value below which the material moduli did not show any stress dependence. Plate-and-plate geometry (20 mm diameter and 1 mm gap) was selected for these measurements. In order to ensure accurate results, at least two replicates were conducted for every sample.

DSC was conducted with a TA Q-100 (TA Instrument, USA) to provide any relevant thermal event information for the different EVA copolymers and their corresponding bituminous binders. Samples of 5-10 mg were always subjected to the following testing procedure: (a) a first heating ramp from room temperature to 20 °C above its corresponding EVA melting point, in order to eliminate discrepancy in the molecular structure in response to a distinct thermal history; (b) cooling ramp, to -60 °C; and (c) a second heating ramp, to the same final temperature used for the first one. The heating/cooling rate was set at 5 °C/min, and N_2 was used as purge gas. The values of the melting temperatures were determined during the second heating ramps. Degree of crystallinity (χ_c) of each sample was calculated as follows:

$$\chi_C = \frac{\Delta H_C}{\Delta H_{100} \cdot C_{EVA}} \cdot 100 \qquad (4.1.1)$$

where ΔH_c and ΔH_{100} are the crystallization enthalpy obtained from integration peak in the cooling ramp and the melting enthalpy of 100 % crystalline polymer (Wunderlich 1976), respectively, and "C_{EVA}" represents the EVA weight fraction (0.05 or 0.075 in every case) in the bituminous binders.

Optical microscopy images, taken at room temperature, were used to study the morphology of the EVA modified binders. A LTS-350 Heating-Freezing Stage,

manufactured by Linkam Scientific Instruments (U.K.), coupled with a standard Olympus BX51 microscope equipped with a pair of crossed polarisers, by Olympus Optical (Japan), was employed to that purpose. Samples were prepared by using standard microscope slides (76 x 26 mm). Very thin layers of the modified binders were set on them and prepared at temperature above its corresponding softening temperature, allowing them to be in-placed, excluding too high temperature causing a microstructural change.

4.1.3 Results and discussion

4.1.3.1 Effect of Vinyl Acetate content

With the aim of evaluating the effect of EVA vinyl acetate concentration on the in-service performance and morphology of the resulting modified bitumens, a rheological, technological, calorimetric and microstructural characterization was conducted on bituminous binders prepared from EVA copolymers with different VA contents, at selected concentrations of 5 and 7.5 wt. % EVA.

The viscous flow curves, at 60 °C (usually considered as the maximum expectable temperature to be reached in a pavement exposed to ambient in warm climates), for the neat bitumens and their corresponding EVA-binders (5 and 7.5 wt.% EVA), as a function of VA content, are presented in Figure 4. 1. 1.

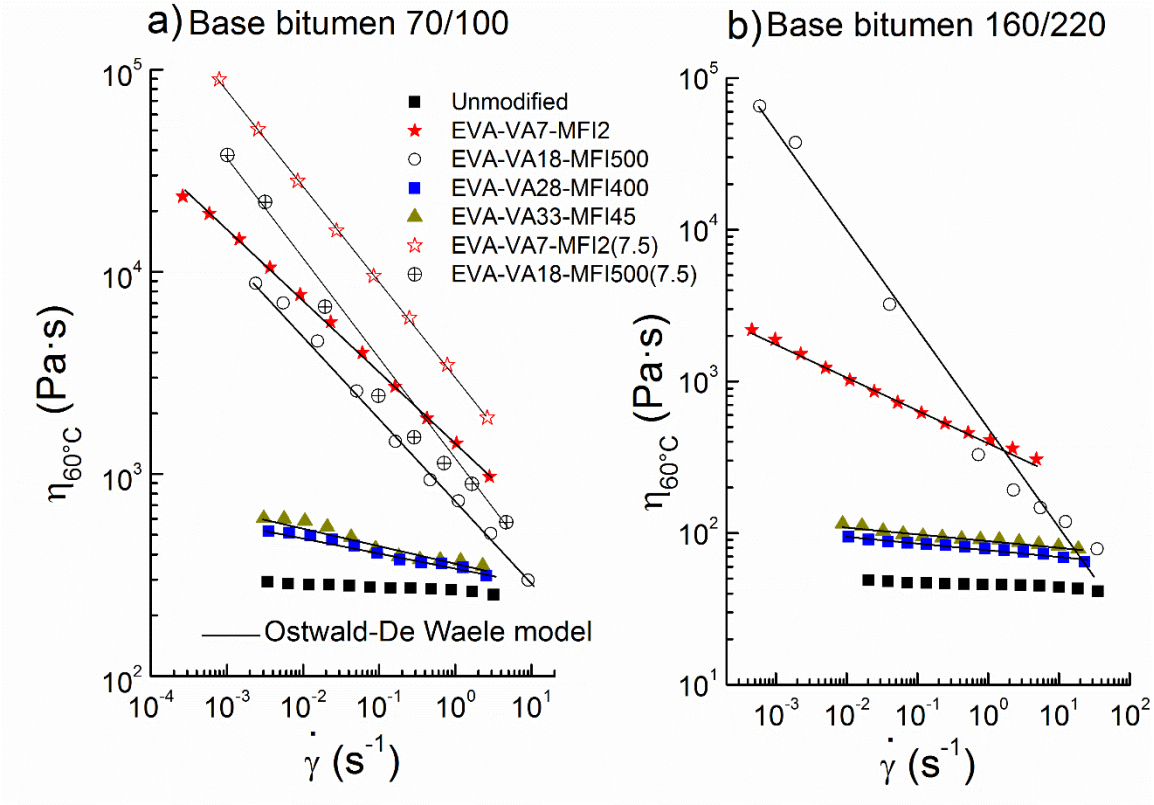

Figure 4. 1. 1 Viscous flow curves, at 60 °C, for EVA-binders prepared from (a) the base bitumen 70/100 and (b) the base bitumen 160/220, as a function of the vinyl acetate (VA) content and polymer concentration. Neat bitumens are included.

A Newtonian behaviour over the whole range of shear rates tested is exhibited by both neat bitumens. On the contrary, modification with EVA copolymers leads to a shear-thinning behaviour that can be characterized by the Ostwald-De Waele model fairly well:

$$\eta = k(\dot{\gamma})^{n-1} \qquad (4.1.2)$$

where “k” and “n” are the consistency and flow indexes, respectively.

Table 4. 1. 2 Fitting parameters of the Ostwald-De Waele model, at 60 °C, for the EVA-binders, as a function of VA content and polymer concentration.

Polymer concentration	EVA copolymer	Base bitumen 70/100		Base bitumen 160/220	
		k ($Pa.s^n$)	n	k ($Pa.s^n$)	n
5 wt. %	EVA-VA7-MFI2	1443.15	0.65	407.44	0.79
	EVA-VA18-MFI500	745.38	0.58	473.19	0.35
	EVA-VA28-MFI400	343.27	0.92	77.50	0.96
	EVA-VA33-MFI45	361.05	0.91	89.77	0.96
7.5 wt. %	EVA-VA7-MFI2	3025.01	0.53	n.p.	n.p.
	EVA-VA18-MFI500	1003.72	0.49	n.p.	n.p.

n.p. not performed

As can be seen in Table 4. 1. 2, much lower values of flow index, that is, more remarkable shear-thinning properties, are obtained for the EVA-binders having the lowest VA contents (7 and, mainly, 18 wt.%). On the contrary, EVA-binders with the highest VA contents (28 and 33 wt.%) present a much less pronounced shear-thinning behaviour, with flow index values (n) very close to 1, in the range of shear rates considered. On the other hand, a significant increase in the consistency index and, therefore, in the EVA-binder viscosity, is found as the VA content of the EVA copolymer decreases, which suggests enhanced properties for such EVA-binders at 60°C. For these EVA copolymers, their corresponding binders viscosities also increased when the EVA polymer concentration was raised from 5 to 7.5 wt.%, mainly for the EVA copolymer with the lowest VA content. In addition to that, an increase in polymer concentration does not significantly alter the values of flow index, showing the EVA-binders similar shear-thinning properties.

Likewise, Table 4. 1. 1 presents the values of penetration and ring & ball softening temperature tests. The addition of polymer to bitumen is well-known to decrease its penetration value and increases its softening temperature (Isacsson and Lu 1999; Airey 2002a; Sengoz et al. 2009), which was also corroborated on the EVA-binders studied. As expected from the previous viscosity results, the lowest penetrations and highest softening temperatures correspond to the binders prepared with EVA copolymers containing 7 and 18 wt.% VA. If compared to the corresponding neat bitumens, the addition of EVA-VA7 produced a decrease of about 50 % in their penetration values, as well as increases of 19 and 22 °C in their softening temperatures, for the base bitumen 70/100 and 160/220, respectively. It can be also noticed that, for the bitumen 70/100 EVA-binders, the parameter "k" of the Ostwald-De Waele model is in good agreement with the results of the technological tests (mainly, with binder penetration values). However, for the 160/220 neat bitumen, the highest consistency value corresponds to the modification with EVA-VA18, whilst the lowest penetration and highest softening temperature is found for EVA-VA7. However, Ostwald-De Waele model does not accurately described the flow behaviour of EVA-VA18, giving consistency index above the real one. Instead, if it is accepted that "k" represents binder viscosity at 1 s^{-1}, Figure 4. 1. 1b shows that there still exist a good correlation between rheological and technological results (i.e. EVA-VA18 shows a lower viscosity at 1 s^{-1} and is softer than binder EVA-VA7). On the whole, the results obtained from technological tests and viscosity curves indicate, in general terms, a larger degree of modification for bituminous binders prepared from EVA with 7 and 18 wt.% VA contents.

In addition to the viscous flow tests, Figure 4. 1. 2 shows the dynamic shear temperature sweeps for the neat bitumen 70/100 and their EVA-binders.

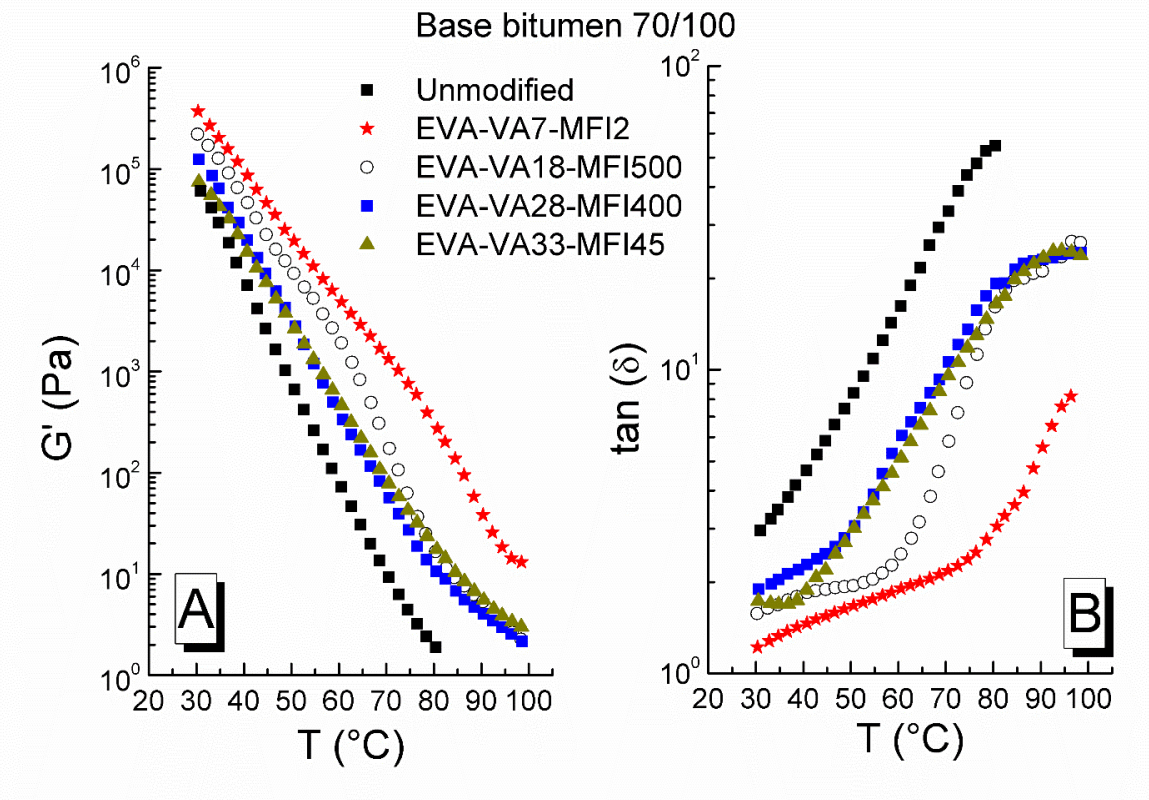

Figure 4. 1. 2 Evolution with temperature of the storage modulus and loss tangent for the EVA-binders prepared from base bitumen 70/100, as a function of the vinyl acetate (VA) content. Neat bitumen is included.

It can be seen that storage modulus (G') decreases with increasing testing temperature from 30 to 100 °C (Figure 4. 1. 2a). Among all the EVA-binders studied, the one containing EVA-VA7 presents significantly higher G' values in the medium-high temperature range (30-75 °C) than the others. This reveals a better resistance to permanent deformation at that temperature interval. In addition, an enhancement in the temperature susceptibility is also observed after modification with EVA-VA7, if compared to the base bitumen 70/100, as deduced from a decreased value of the average slope of G' (and also tan δ) vs. temperature, within the interval 30-75 °C. Interestingly, an abrupt variation of slope in G', starting at about 80 and 60 °C for the EVA-binders with 7 and 18 % VA content, respectively, can be clearly observed. With regard to the EVA copolymers containing 28 and 33 wt.% VA this behaviour in G'

vanishes. This fact was also observed for polymer gels based on EVA with different VA content and vegetable oils (Martin-Alfonso and Franco 2014). Furthermore, Figure 4. 1. 2b shows values of loss tangent (tan δ=G"/G') always higher than 1 in the entire temperature interval tested, which points out a prevailing viscous behaviour. In accordance with the previous viscous flow curves and technological results, addition of EVA containing low VA content (7 and 18 wt.%) yields an increase in storage modulus compared to the neat bitumen. Likewise, a decrease in VA content leads to lower values of loss tangent, which evidences improved elastic properties (enhanced performance) at medium-high in-service temperatures.

DSC runs and microstructural observations allowed shedding some light on these results. Figure 4. 1. 3 shows the thermograms corresponding to the second heating ramps for the EVA copolymers (Figure 4. 1. 3a) and their resultant EVA-binders (Figures 3b and 3c).

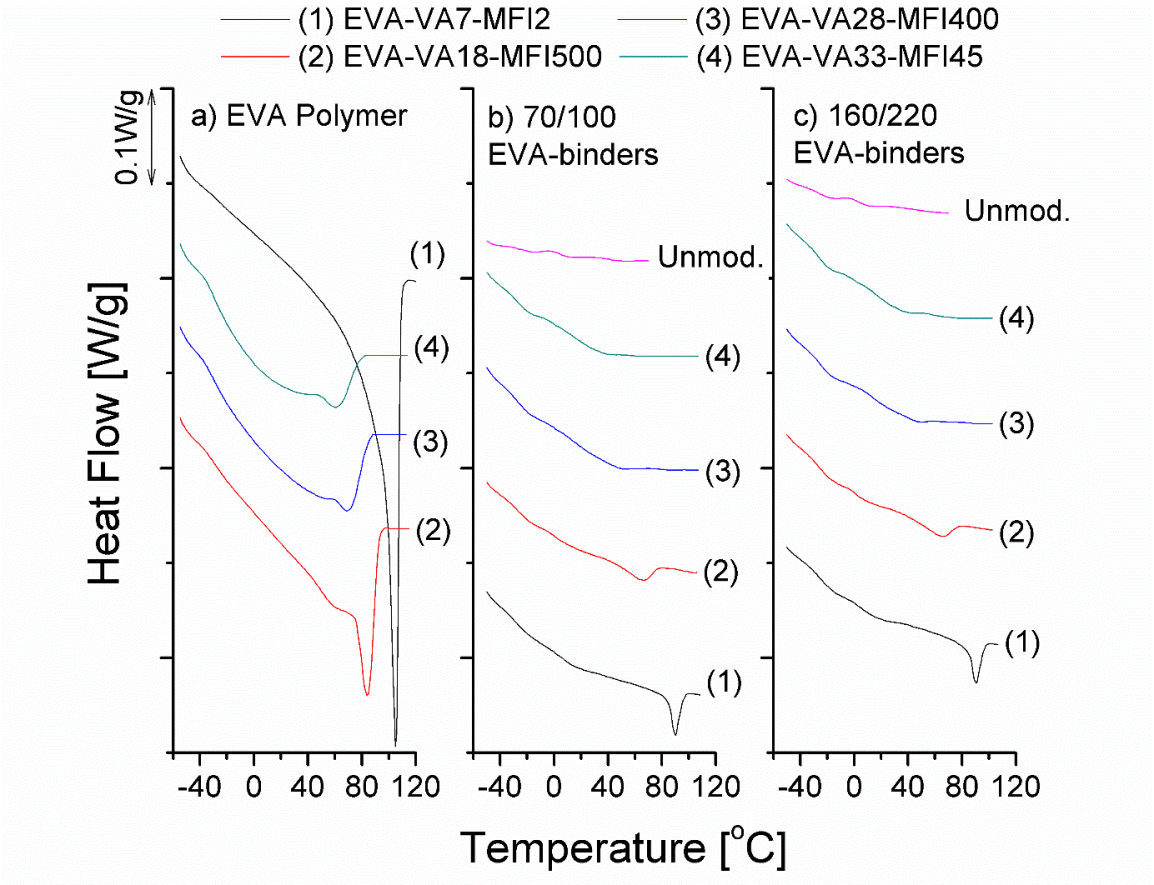

Figure 4. 1. 3 Heat flow curve for (a) neat EVA copolymers; (b) EVA-binders from bitumen 70/100; and (c) EVA-binders from bitumen 160/220.

The values of the melting temperature (T_m), crystallization enthalpy (ΔH_c) and crystallinity degree (χ_c) are shown in Table 4. 1. 3. Firstly, the DSC scans for some selected EVA copolymers (varying VA contents and MFI values) were studied. As can be observed in Figure 4. 1. 3a, they all display a broad shoulder followed by a unique endothermic event, which appears at temperature ranges typically found for this type of polyolefins (Stark and Jaunich 2011). It has been considered that the width of EVA melting peak can reflect the distribution of the lamellar thickness of its crystalline fraction (Somrang et al. 2004; Shi et al. 2008). Therefore, EVA-VA7 has the narrowest size distribution of crystallites (and highest melting temperature), followed by EVA-VA18, EVA-VA28 and EVA-VA33. In addition to that, the decrease in the crystallinity (please, see Table 4. 1. 3) can be explained based on the amount of total

non-crystallizable, intra-molecular defects (Somrang et al. 2004), such as acetate pendant groups. Thus, EVA copolymers with high VA content present a higher amount of pendant groups which partially hinder crystallization. In contrast, EVA copolymers with low VA content resemble the behaviour of LDPE.

Table 4. 1. 3 Melting temperatures (Tm), crystallization enthalpy (ΔHc) and crystallization degree (χc) for EVA copolymers and EVA-binders, as a function of the VA content and MFI.

EVA		EVA polymer data			EVA Binder data					
VA (wt.%)	MFI (g/10 min)	T_m (°C)	ΔH_c (J/g)	χ_c (%)	Neat bitumen 70/100			Neat bitumen 160/220		
					T_m (°C)	ΔH_c (J/g)	χ_c (%)	T_m (°C)	ΔH_c (J/g)	χ_c (%)
7	2	105.3	110.8	37.8	89.7	4.5	30.9	90.5	4.4	30.1
18	2	84.5	75.8	25.9	65.0	3.5	23.7	n.p.		
	500	84.1	76.5	26.1	64.7	3.3	22.7	64.9	3.1	21.3
28	7	69.5	51.7	17.6	n.m.			n.p.		
	400	68.8	51.5	17.6				n.m.		
	800	69.3	49.3	16.8						
33	45	60.7	36.7	12.5						

n.m. not measureable
n.p. not performed

Secondly, the DSC scans for the EVA-binders prepared from the two base bitumens 70/100 and 160/220 were studied in Figure 4. 1. 3b and 3c, respectively. As can be observed, the melting temperatures of EVA copolymers in the corresponding bituminous binders appear shifted to lower temperatures (Table 4. 1. 3). As a result, when EVA-VA7 is blended with the base bitumen 70/100, the melting temperature decreases from 105 °C, for pure EVA, to 90 °C, for its corresponding EVA-binder. For

the EVA-VA18, a reduction of 19 °C in the melting temperature is observed. Furthermore, the magnitude of this reduction is not affected by the hardness (or penetration) of the neat bitumen used (70/100 and 160/220). This fact can be explained on the basis of the swelling experienced by the polymer-rich phase by migration of compounds from the bitumen (Munera and Ossa 2014). The bitumen-rich phase is artificially enriched in asphaltenes by a "physical distillation" of the lighter species from the original bitumen (e.g. paraffinic and aromatic compounds). Thus, their inclusion in the polymer-rich phase prevents the formation of larger crystallites and, as observed for EVA-VA18, yields an eventual broader size distribution (or broader melting peak) (Fawcett and McNally 2000). In consequence, the decrease in the EVA melting points after its blending with bitumen would result from the presence of crystallites with smaller size. Moreover, for each EVA-binder, its addition to bitumen reduces the extent of crystallization of the polymer (Table 4.1.3) due either to migrated bitumen species hindering crystallization or even to a fraction of crystallizable molecules retained within the amorphous bitumen-rich phase (Fawcett and McNally 2000). Finally, the EVA melting events for the binders prepared with EVA-VA28 and EVA-VA33 cannot be observed on DSC thermograms.

Further microstructural considerations may be drawn from the optical microscopy images (Figure 4.1.4), taken at 25 °C, for neat bitumen 70/100 and their EVA-binders, as a function of VA content.

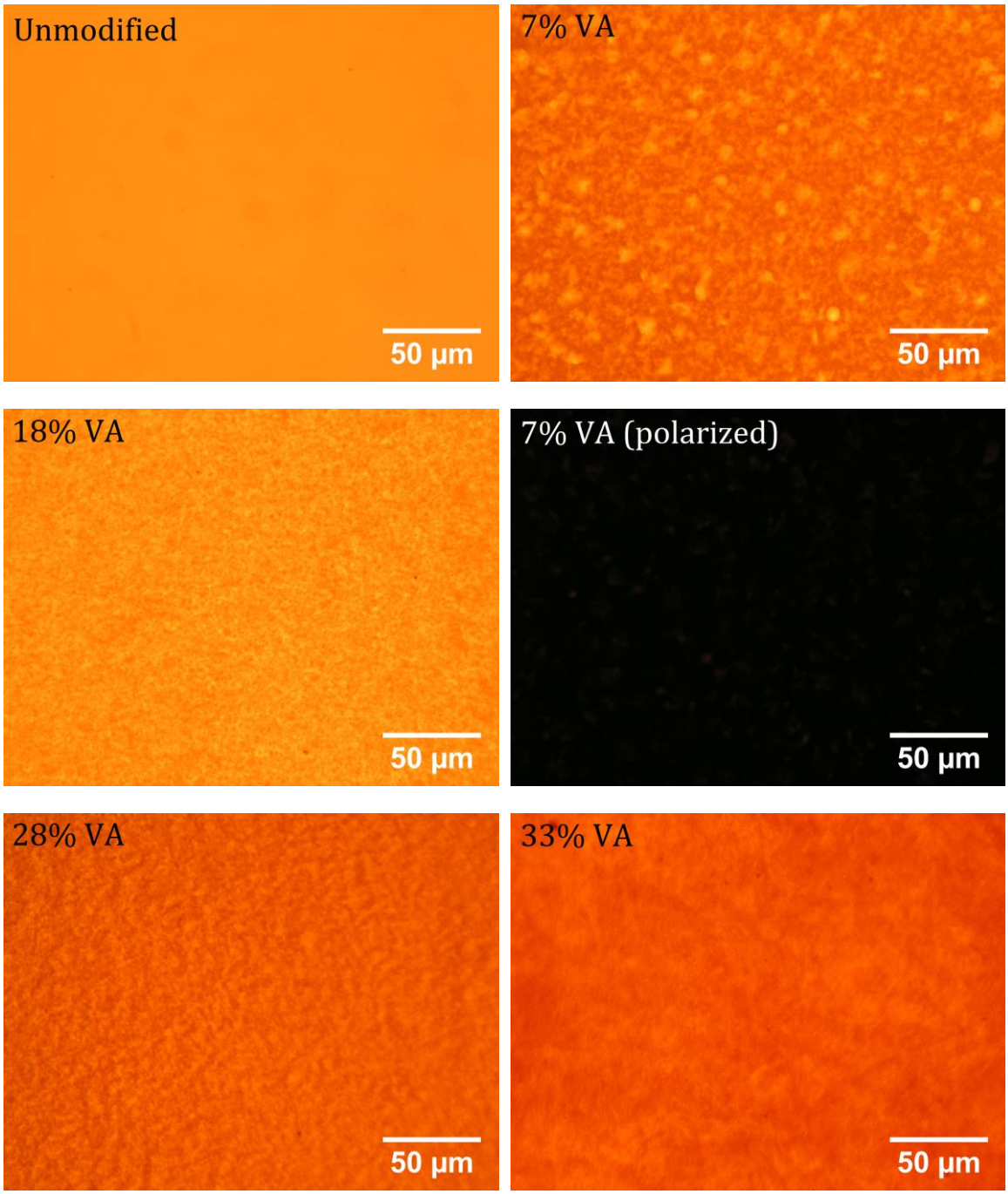

Figure 4. 1. 4 Optical microscopy images, at 25°C, for base bitumen 70/100 and their corresponding EVA-binders, as a function of the vinyl acetate (VA) content.

Compared to the neat bitumen, its modification with EVA copolymers yields a new morphology in the resulting binders, where two phases are clearly distinguished. The lightly toned regions were assigned to a polymer-rich phase, whereas the bitumen-rich phase appears as a darker background. As expected from previous DSC results,

the formation of a polymer-rich phase becomes more evident for EVA-binders prepared with polymer containing the lowest VA contents, mainly for the EVA-VA7 (Figure 4. 1. 4). Instead, high VA contents lead to a highly dispersed polymer phase and a very homogeneous binary blend at the micro-scale. The presence of crystals in the EVA-binder prepared with the EVA-VA7 copolymer was corroborated by a polarized light microscopy imagen, which is also included in the Figure 4. 1. 4.

Figure 4. 1. 2a demonstrates for EVA-binders with low VA contents (7 and 18 wt.%) a sudden decay in G' (or the end of the loss tangent plateau) as temperature approaches the EVA melting point determined by DSC scans. However, this evidence is hardly noticed in the EVA-binders prepared with 28 and 33 % VA content, which is in accordance with their poorer crystals contents. In consequence, their melting process results more evident from the abrupt increase observed in the tan δ curve (Figure 4. 1. 2b).

Consequently, uniformly distributed polymer-rich domains (optical microscopy observations) including larger and more crystals (DSC scans) exert a reinforcing effect on the bitumen-rich matrix that enhances rheological behaviour of the EVA-binders with the lowest VA contents, at temperature below EVA melting (ie. at medium-high in-service temperatures). Additionally, the observed sudden decrease in G' upon melting of the binder polymer-rich phase would facilitate its final application. In this sense, EVA-binder viscosity at 135 °C is of particular interest in evaluating its pumpability (between storage facilities and into the HMA manufacturing plant), mixability (mixing with and coating of aggregates in the HMA manufacturing plant) and workability (ease with which a HMA can be placed, worked by hand, and compacted) (Gudimettla, L.M., Cooley, L.A., Brown, E.R. 2003). According to the

standard AASHTO MP320, viscosity must be maintained below 3 Pa·s at 135°C for the binder to be adequately pumped, mixed with the mineral aggregates, and the resulting mix to be properly laid down and compacted (Silva et al. 2010). Figure 4. 1. 5 displays the viscosity flow curves for base bitumen 70/100 and their corresponding EVA-binders, as a function of VA content, at 135 °C.

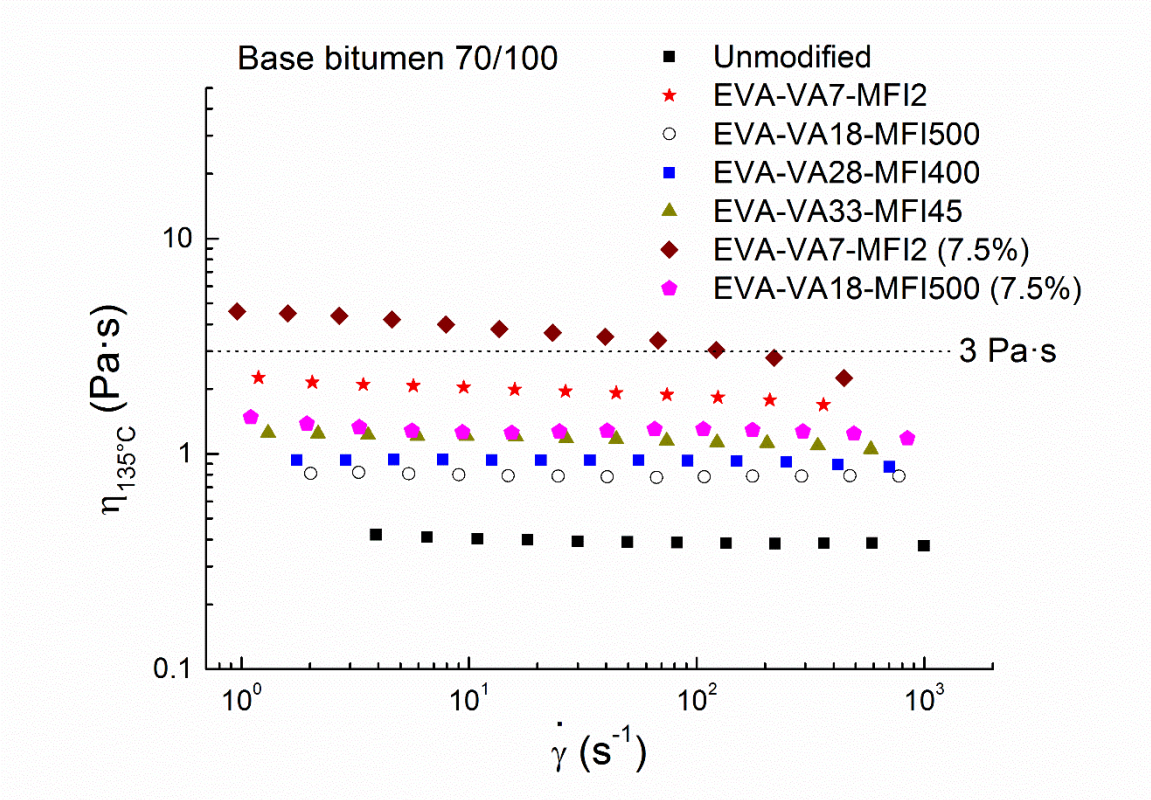

Figure 4. 1. 5 Viscous flow curves, at 135 °C, for base bitumen 70/100 and their corresponding EVA-binders, as a function of the vinyl acetate (VA) content and polymer concentration.

Despite the increases in viscosity (Figure 4. 1. 1) and elastic modules (Figure 4. 1. 2) found, all the 5 wt. % EVA-binders studied fulfil this specification. However, if the EVA-VA7-MFI2 copolymer is used, its corresponding EVA-binder exceeds this limit viscosity when the EVA polymer concentration is increased up to 7.5 wt.%. Interestingly, this fact is not observed for the EVA-VA18-MFI500 copolymer, since its 7.5 wt.% EVA-binder displays viscosity value lower than 3 Pa·s. Surprisingly, there

does not exist a good correlation between the VA content and the viscosity at this temperature (Figure 4.1.5), suggesting that VA content is not the only parameter controlling the binder viscous behaviour at temperatures well above the EVA copolymer melting point.

4.1.3.2 Effect of Melt Flow Index

Previous results suggest that additional EVA properties, other than the VA content, may also affect the binder's quality. In order to study the effect of MFI on the in-service performance and workability of EVA-binders containing 5 wt.% polymer, different EVA polymers with 18 and 28 % VA content and varying MFI values have been considered.

Table 4. 1. 3 displays the melting temperatures (T_m), crystallization enthalpy (ΔH_c) and crystallinity degree (χ_c) for EVA copolymers, and their corresponding EVA-binders prepared from neat bitumen 70/100, as a function of MFI values. It can be clearly observed that, for every type of EVA copolymer studied, varying MFI values do not produce significant differences in none of the three measured parameters. If further attention is paid to EVA-binders prepared from EVA-VA18, a very similar reduction in both EVA copolymer melting point and crystallinity degree is observed. Likewise, the optical microscopy images (results not shown) for the binders prepared with EVA copolymer having the same VA content but differing MFI values displayed very similar morphology in terms of size and distribution of their polymer-rich phases. Consequently, the swelling process experienced by the polymer-rich phase of the EVA-binders, which is the responsible for the decreases in T_m and χ_c values, depends only on the VA content. Finally, as expected, the EVA-binders prepared with the three different EVA-VA28s do not show any measurable endothermic peak on the DSC

thermograms.

In addition to this, the presence of a significant amount of crystals can be also corroborated by the dynamic shear temperature sweeps displayed in Figure 4. 1. 6, which shows the evolution with the temperature of complex shear modulus (|G*|) and tan δ for EVA-binders, as function of MFI values.

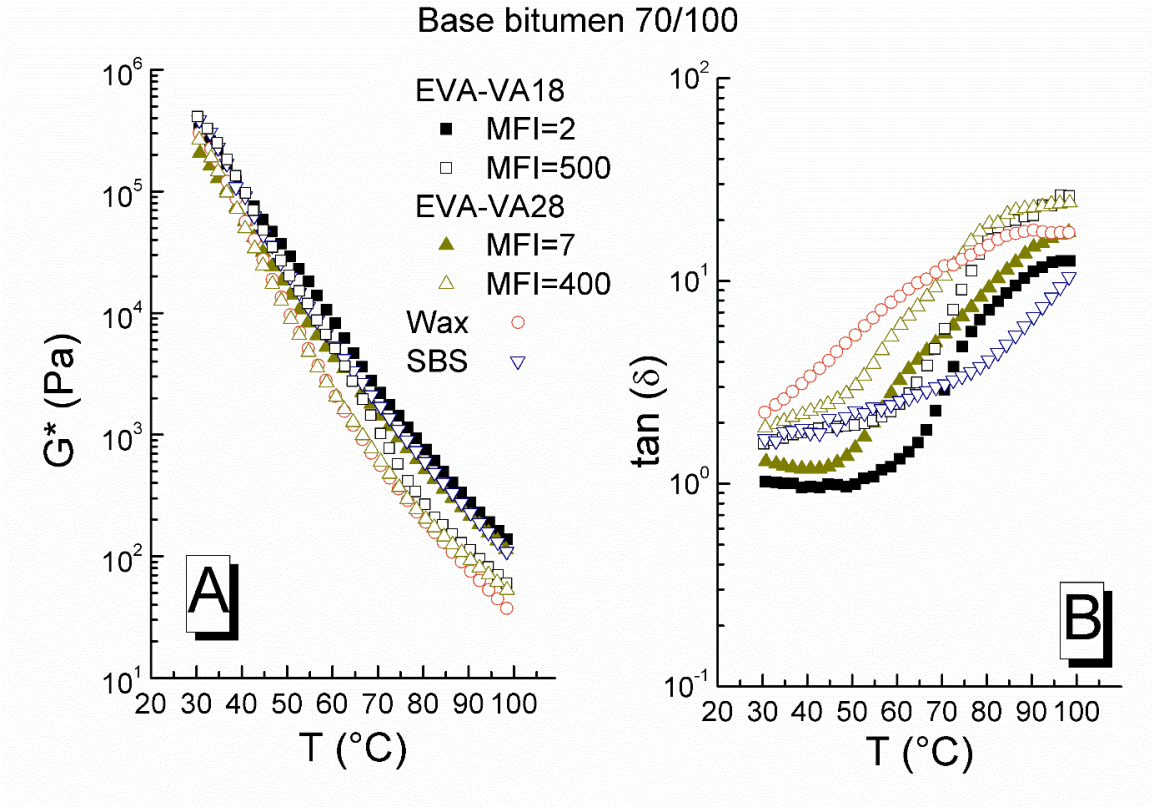

Figure 4. 1. 6 Evolution with temperature of (a) the complex modulus and (b) loss tangent for the 5 wt. % EVA-binders prepared with either EVA-VA18 or EVA-VA28 and neat bitumen 70/100, as a function of the Melt Flow Index value.

It can be seen that the EVA-VA18-MFI500 binder shows an abrupt decay in |G*| at about 60 °C (Figure 4. 1. 6a), similar to that found in G' (Figure 4. 1. 2a) when approaching the polymer-rich phase melting point. Interestingly, this event in |G*| does not occurred in the modified binders prepared with neither EVA-18-MFI2 nor EVA-VA28s. Furthermore, Figure 4.1.6b demonstrates lower values of the loss tangent, between 30 and 50 °C, imparted by the EVA copolymers with the lowest MFIs,

revealing an enhancement in the in-service elastic properties with respect to the viscous ones and leading to a highly structured binder for EVA-VA18-MFI2 with a trend to predominantly elastic response (being tan δ slightly below 1) between 30 and 50 °C. For sake of comparison, two modified binders, containing 3 wt.% SBS and 1.5 wt.% wax, respectively, have been included in Figure 4. 1. 6. If attention is paid to Figure 4. 1. 6a, the SBS modified bitumen presents values of the complex shear modulus very similar to that shown by the EVA-VA18-MFI500 binder at the medium-to-high in-service temperatures (30 to 60 °C), but much higher values at higher temperatures, at which its application is expected. In contrast, the wax modified binder shows |G*| values quite close to those exhibited by the bitumen modified with EVA-VA28-MFI400. On the whole, EVA modification imparts better elastic properties and improved thermal susceptibility (loss tangent much less temperature-dependent and with presence, in some cases, of a pronounced plateau up to about 60 °C) if compared to the wax. SBS modification also yields a plateau in tan δ up to even higher temperatures than EVA does, but with poorer elastic properties than the two EVA-binders with the lowest MFIs (e.g., 2 and 7).

On top of that, Figure 4. 1. 7 shows the viscosity flow curves, at 60 °C, for the EVA-binders prepared from the neat bitumen 70/100, as a function of the MFI values.

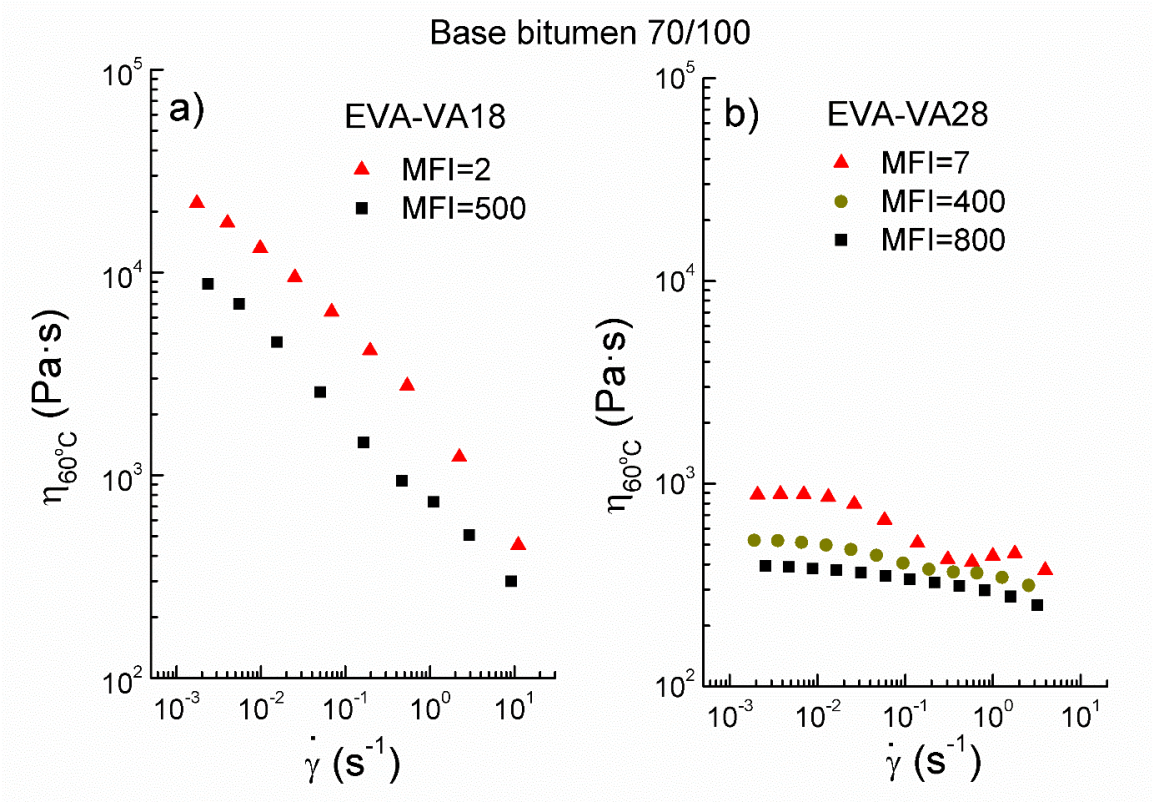

Figure 4. 1. 7 Viscous flow curves, at 60 °C, for the 5 wt. % EVA-binders prepared with either (a) EVA-VA18 or (b) EVA-VA28 and neat bitumen 70/100, as a function of the Melt Flow Index value.

For the both VA contents studied, the binder's viscosity always increased with decreasing MFI value, what is in accordance with the values of the complex shear modulus, at 60 °C, observed in Figure 4. 1. 6a. It has been reported (Ravve 2012) that EVA copolymer molecular weight and MFI values are inversely proportional, as the chain entanglement and the friction increase the viscosity of the EVA copolymer. Consequently, EVA copolymers with the same VA content but lower MFI values endow EVA-binders with increased viscosity. However, a significant reduction in the MFI value, from 500 to 2, did not modify its shear thinning behaviour, as deduced from their similar flow indexes (Figure 4.1.7a). Moreover, with a view to their application, Figure 4. 1. 8 presents the effect of MFI values on the EVA-binders viscosity at 135 °C.

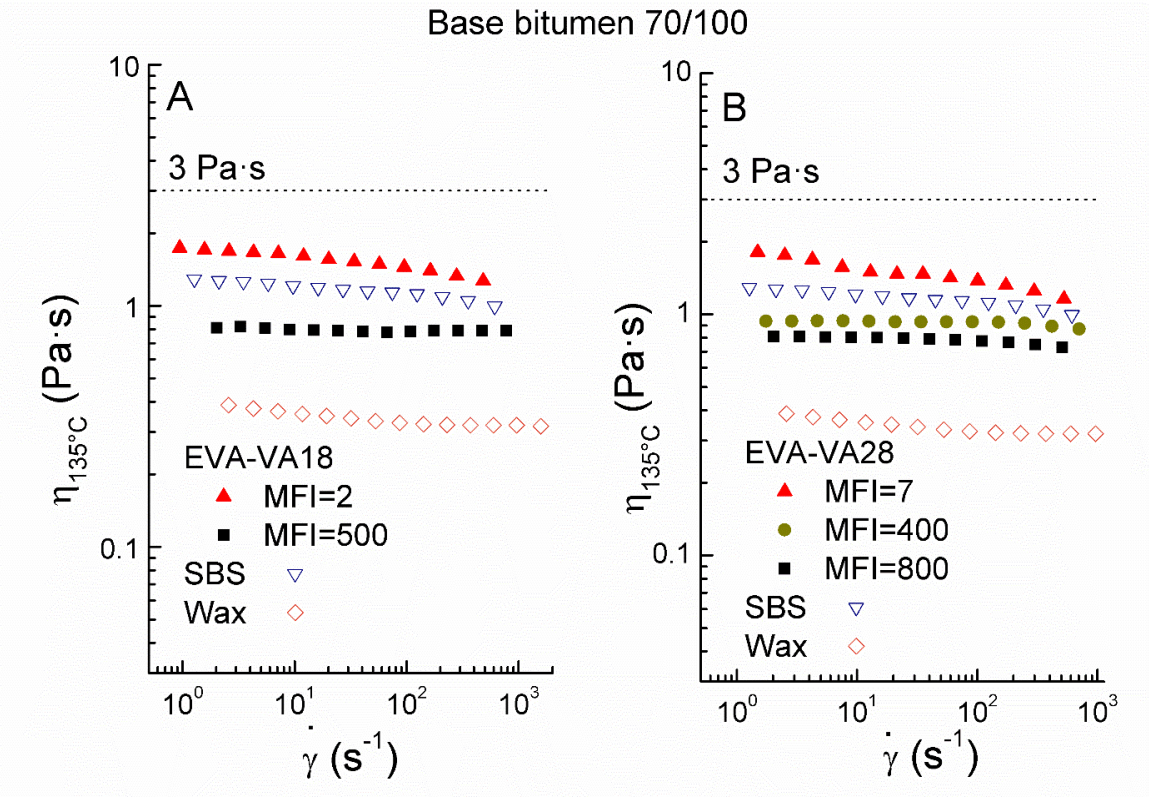

Figure 4. 1. 8 Viscous flow curves, at 135 °C, for the 5 wt. % EVA-binders prepared with either (a) EVA-VA18 or (b) EVA-VA28 and neat bitumen 70/100, as a function of the Melt Flow Index value.

For both VA contents, an increase in MFI yielded a decrease in the binder viscosity and, interestingly, EVA-binders with MFIs above 400 present lower viscosities than the SBS-modified bitumen. Likewise, it is worth noting that binder EVA-VA18-MFI500 containing 7.5 wt. % polymer (Figure 4. 1. 5) shows lower viscosity at 135 °C than system EVA-VA18-MFI2 with 5 wt.% polymer (Figure 4.1.8A), confirming the importance of the EVA MFI parameter. Consequently, if these EVA PMBs present reduced viscosity at 135 °C, if compared to standard PMBs, we may also expect reduced working temperatures, with respect to standard PMBs. However, they are more viscous than the binder modified with the wax, a well-known viscosity reducer.

Moreover, no matter the selected VA content, Figure 4.1.8 has revealed the flow behaviour of EVA-binders at 135 °C to be dependent on MFI values. Thus, Figure 4. 1. 9

shows the viscosity at 135°C and two different shear rates (10 and 100 s^{-1}) of all the EVA-binders formulated with the 70/100 bitumen.

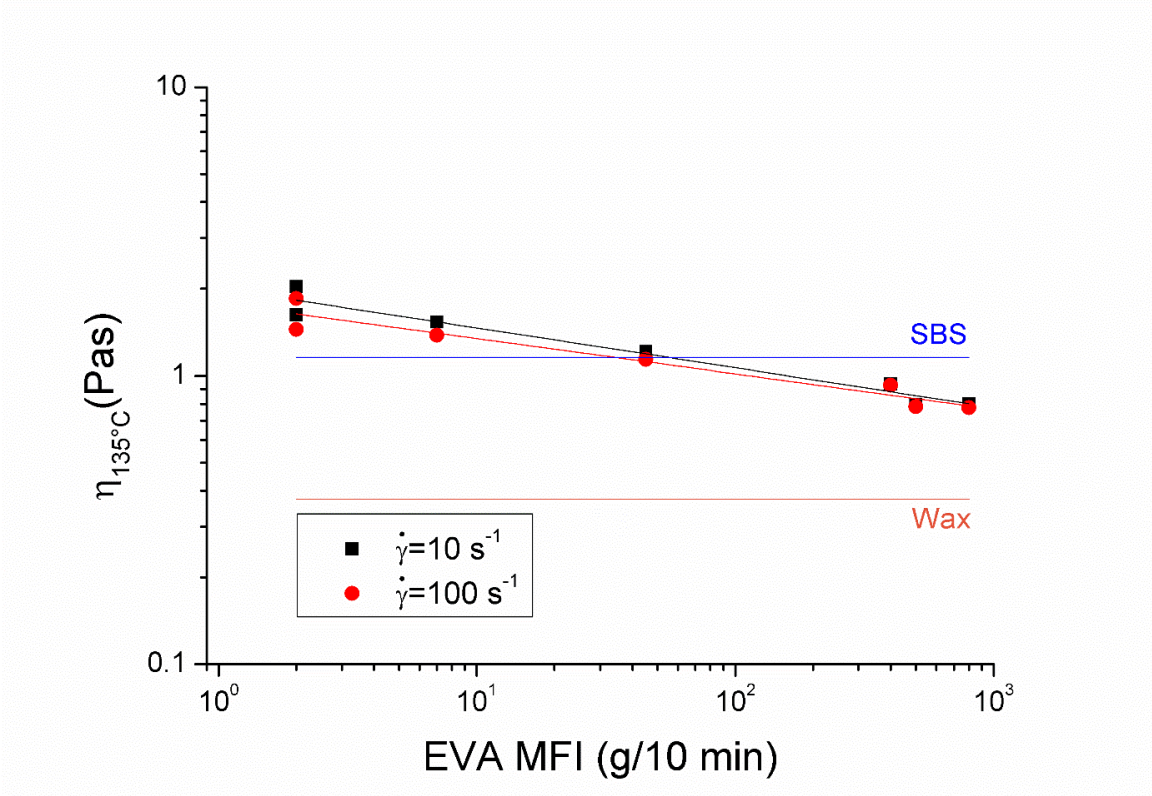

Figure 4. 1. 9 Viscosity evolution (at 10 and 100 s-1) for 5 wt. % EVA-binders, as a function of EVA MFI value used for the modification of a 70/100 bitumen. Comparison with SBS and wax modified binders formulated with the same bitumen.

As may be seen, bitumen viscosity undergoes a power law decrease, as MFI is raised, with the slope of the fitting curve being just slightly dependent on the shear rate, which evidences their nearly Newtonian behaviour at 135 °C. In any case, all the viscosity values at 135 °C satisfy the limiting value required (3 Pa·s) and are lower than SBS-binder's for MFIs above 45. Furthermore, the relevance of the MFI on the binder performance, at in-service conditions, is confirmed by Figure 4. 1. 10, which shows a power-law correlation between penetration of EVA-binders and their MFI, so that binder becomes softer with increasing the MFI values, no matter which VA content and neat bitumen are selected. Similarly, an acceptable dependence of R&B softening point

with MFI has been found, obtaining a lower value of this parameter as MFI becomes higher. However, this parameter also seems to be affected by the VA content.

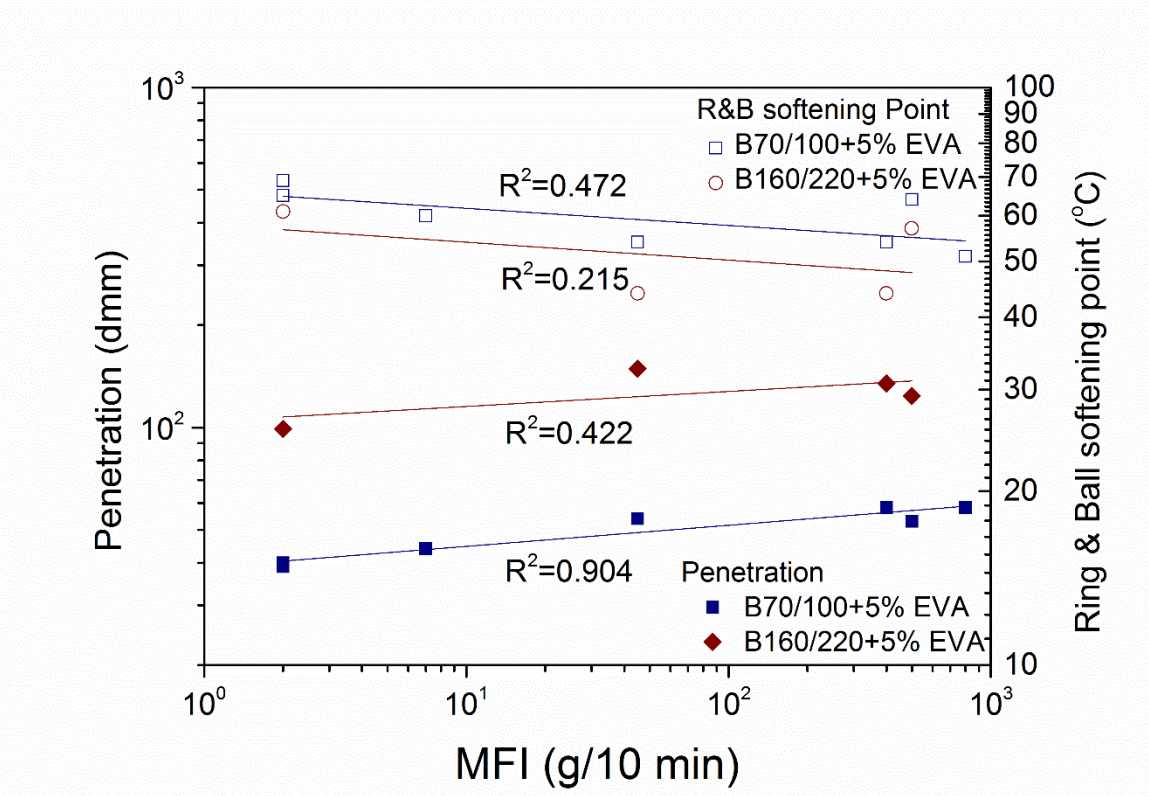

Figure 4. 1. 10 Dependence on MFI of EVA-binders (5 wt. % polymer) penetrations and ring & ball softening points.

4.1.4 Concluding remarks

The objective of this research was to develop EVA modified bitumens with in-service performance comparable to traditional PMBs but lower viscosity than these at the application temperatures, so enabling their use in reduced-temperature technologies. To that end, two EVA characteristics (vinyl acetate content and Melt Flow Index) need to be optimized.

On the one hand, bitumen modification with the EVA copolymers having the lowest VA contents (7 and 18 wt.%) yielded higher viscosity at 60°C, and improved elasticity and

thermal susceptibility at the medium-to-high in-service temperatures, if compared to their corresponding unmodified bitumens. Likewise, optical microscopy observations demonstrated the existence of large and uniformly distributed polymer-rich domains. Interestingly, these formulations showed reduced viscosity once the EVA melting point was exceeded and the reinforcing effect of the crystals disappeared. On the other hand, it was also found that the MFI strongly affects some of the binders' properties. Hence, a power-law correlation between the viscosity at 135°C and the MFI values was found, regardless the VA content.

We conclude that EVA modified bitumens with both improved in-service properties and reduced application temperature can be obtained by balancing VA content and MFI for a selected polymer concentration. In our case, for example, the results proved an optimum balance with a VA content of 18 wt.% and a MFI of 500 g/10 min. This formulation gave rise to a binder with similar performance at medium-to-high in-services temperatures to a reference modified bitumen with 3 wt.% SBS, but with lower viscosity at 135 °C. If compared to 1.5 wt.% wax-modified bitumen, the reduction in viscosity at 135 °C was not so significant, but it exhibited higher elasticity.

4.2 Selection of Ethylene-Vinyl-Acetate properties for modified bitumen with enhanced end-performance

Under review in :

Rheologica Acta

Publishing Company : Springer.

Editor in Chief : Jan Vermant

Volume: -, PP : -

Year : -

ISSN : -

DOI : -

.

ABSTRACT

Bitumen modification with ethylene vinyl acetate (EVA), in a wide range of temperatures (between -30 and 100°C), has been studied as a function of polymer concentration and EVA characteristics (vinyl acetate content, VA, and melt flow index, MFI). Viscous flow, dynamic shear (DSR) temperature sweep and technological tests were conducted to assess binder performance at medium-to-high in-service temperatures. Evaluation of binder low temperature viscoelastic behavior has been performed using a rectangular fixture (SRF) in torsional mode, either in the linear viscoelastic region or under non-linear conditions (by strain breakage tests between -30 and 0 °C). Further microstructural analysis based on modulated differential scanning calorimetry (MDSC) and optical microscopy was conducted to support rheological and technological results. Hence, total crystalline fraction (related to the VA content and polymer concentration) turned out to be a key parameter to achieve a suitable binder modification at medium-high temperatures. In addition, MFI appears to be an important EVA parameter at low temperatures, as it was found that lower MFI values enhanced resistance to low temperature cracking.

4.2.1 Introduction

Asphalt roads with improved performance are more demanded every day due to growth in traffic frequency and load (Zhu et al. 2014; Saboo 2015). Asphalt pavement itself is mainly composed of mineral aggregates and bitumen, stacked in several layers, where bitumen is only about 5 wt.% of the mix. However, bitumen portrays significant part to road performance since it is the only deformable component forming a continuous matrix in the mix. In warm climate regions, asphalt pavement is expected to undergo permanent deformation under frequent load at high in-service temperature. Conversely, lack of flexibility does not permit to absorb energy caused by traffic loading without breaking. So, thermal fracture is inevitable in regions where exceptionally low temperature makes materials too stiff during winter (Munera and Ossa 2014). Under such thermal conditions, bitumen properties become crucial for the prediction of asphalt pavement performance, and certainly require to be improved to cope with the aforementioned issues related to temperature (Cuadri et al. 2013a).

On these grounds, bitumen properties are either physically or chemically modified to match certain criteria of application, usually by the mechanical dispersion of polymers within the bituminous matrix (Lu and Isacsson 2000; Cuadri et al. 2014; Polacco et al. 2015). Physical modification is carried out by thermoplastic elastomers such as SBS, SBR, rubber, etc. (Navarro et al. 2010; Liang et al. 2015) or thermoplastic plastomers such as PE, PP, EVA, etc. (Fawcett and McNally 2000; Garcia-Morales et al. 2004). Alternatively, chemical modification has been performed by epoxy, polyurethane resin, etc. (Carrera et al. 2010; Partal and Martínez-Boza 2011).

The preferred polymers have the ability to form physical networks, which usually originate from the simultaneous presence of both rigid (below glass transition temperature or crystalline) and flexible segments (Polacco et al. 2015). Interestingly, EVA has both characteristics in its backbone (crystalline and amorphous fraction), the so-called semi-crystalline polymer. A recent study on EVA as modifying agent for road pavement has shown an interest of using it as co-blending modifier with recycled tire rubber to obtain combined benefit of each individual polymer by optimizing the processing parameter with the hierarchy of importance being time, temperature and shear at the last (Fang et al. 2016). Another study also focuses on searching optimum processing parameters to prevent storage separation of EVA from bituminous phase (Saboo 2015). Other studies have focused on the use of EVA as bitumen modifier (Dekhli et al. 2015). However, little attention has been paid to the importance of EVA selection based on its vinyl acetate content (VA) and/or melt flow index (MFI). In this sense, a previous study on EVA properties has pointed out the importance of MFI on the design of binders with improved workability for reduced-temperature asphalt technologies. Thus, the resultant binder was characterized by its lower viscosity during high temperature operations such as asphalt mixing, laydown and compaction, while keeping suitable properties at medium to high in-service temperatures (Yuliestyan et al. 2016a).

The present work further explores the effect of EVA selection (according to its VA and MFI characteristics) and concentration on the binder thermo-rheological behavior in a wide range of temperatures, from -30 to 100 °C, which covers low, medium and high in-service temperatures. To that end, binder properties at medium to high temperature have been assessed by traditional technological tests and viscous and

viscoelastic shear measurements performed with a plate-plate geometry between 30 and 100 °C. Instead, binder in the low temperature region, requires more exploration. Traditionally, thermo-mechanical analysis or viscoelastic properties of bitumen have been evaluated by bending beam rheometer (BBR) and dynamic shear rheometer (DSR) using plate-plate rheometry (Cuadri et al. 2013a). However, plate-plate geometry at low temperature may face considerable error on the moduli values measured due to instrument compliance when sample's stiffness is extremely high (Christensen and Anderson 1992; Lu et al. 2016). Alternatively, oscillatory rheological tests in torsional mode on solid rectangular fixture (SRF) have been proposed to eliminate this compliance error in this low temperature study. Moreover, this geometry allows breakage deformation tests to be conducted on bitumen at a temperature close to the material glass transition and under a load exceeding non-linear viscoelastic conditions.

4.2.2 Experimental

4.2.2.1 Materials and formulations

Modified binders were formulated by mixing neat bitumen, with a penetration grade interval of 70/100 (Table 4.2.1), with different ethylene vinyl acetate copolymers (EVA) used as binder modifiers, which were selected by their vinyl acetate content (VA) and melt flow index (MFI). VA contents relate to EVA melting point and MFI is a measure of polymer mass flowing at 190 °C under loading of 2.16 kg in a standard measuring device for 10 min, according to ASTM D1238. Both bitumen and EVA, with commercial names of Alcudia®, were kindly donated by Repsol SA, Spain.

Table 4. 2. 1 Penetration, ring-and-ball softening point and penetration index for EVA modified bitumen studied

	Neat bitumen	B70/100+VA7-MFI2 (wt.%)			B70/100+VA18-MFI500 (wt.%)		
	B70/100	2.5	5.0	7.5	2.5	5.0	7.5
Penetration [dmm] [a]	73	59	39	34	64	53	39
Ring-and-ball softening point [°C] [b]	46	52	65	79	52	64	69
Penetration index		-0.30	1.36	3.22	-0.11	1.94	2.04

[a]According to EN 1426:2007.

[b]According to EN 1427:2007.

Polymer concentration ranged between 2.5 and 7.5 wt.% for EVAs with 7 wt.% VA and MFI of 2 (referred to as VA7-MFI2) and 18 wt.% VA and MFI of 500 (VA18-MFI500). Additional binders having 5 wt.% EVA, as suggested for road application (Fuentes-Audén et al. 2008), were prepared with VA18-MFI2, VA28-MFI7 and VA28-MFI400. Finally, a neat bitumen (B70/100), a binder with 3 wt.% of Styrene-Butadiene-Styrene (SBS) Calprene® C501 (Dynasol) and a binder with 1.5 wt.% wax Sasobit® (Salsol Wax) were used as reference materials.

4.2.2.2 Binder sample preparation

Binder processing, which consisted in melting and blending EVA with neat bitumen at 150 °C, was performed using a high shear rotor-stator type laboratory mixer L5M at 5000 rpm for 1 h, in order to obtain homogenous EVA/bitumen blend. Immediately after blending, molten binders were poured onto flat surface aluminium containers to obtain a thin layer avoiding separation, and cooled at ambient environment for 24-h

before storing at – 20°C to preserve its microstructure from any molecular mobility. Particularly, for low temperature study, blends were molded into rectangular specimens with measurement of 40 mm x 10 mm x 2 mm.

4.2.2.3 Tests and measurements

Penetration (pen_{25}) and ring & ball softening point (SP) tests, according to EN 1426:2007 and EN 1427:2007 standards, respectively, were conducted on bituminous samples for technological characterization, and their results are gathered in Table 4.2.1. Penetration index (PI), predicting the changes in binder consistency with respect to temperature, was used to pre-identify binder thermal susceptibility and calculated as follows:

$$PI = \frac{1952 - 500\log(pen_{25}) - 20SP}{50\log(pen_{25}) - SP - 120} \quad (4.2.1)$$

In medium-high temperature range, binder rheological behavior was characterized by means of viscous and linear viscoelastic tests. Steady viscous flow curves at 60 °C were performed in a controlled-stress rheometer Physica MCR-301 (Anton Paar, Austria) using a parallel plate geometry (25 mm diameter and 1 mm gap). Dynamic shear temperature sweep tests on a continuous heating ramp of 1 °C/min from 30 to 100 °C at a constant shear stress of 100 Pa (within the linear viscoelasticity range, LVE) and frequency of 10 rad/s were performed in a controlled-stress rheometer RheoStress RS600 (Haake, Germany). ~~A~~ Parallel plate geometry (20 mm diameter and 1 mm gap) was used. Previously, stress sweeps were performed, at the same frequency and at selected constant temperatures within the 30 to 100 °C interval, for LVE determination.

Rheological tests at low temperature were carried out under oscillatory torsional mode, using solid rectangular fixture (SRF) samples, in a controlled stress rheometer Physica MCR-301 Anton Paar GmbH (Austria) equipped with a convection heating chamber (CTD 600) and liquid N_2 evaporation unit (EVU 10) for cooling. Firstly, stress sweep tests, within a shear stress range of 10 - 10^7 Pa, were performed to determine LVE region. These tests were also used to obtain the maximum strain upon which material underwent irreversible damage and collapsed ($\gamma_{breakage}$), perceived as a sudden drop of modulus when material broke up. Secondly, the frequency sweep tests, from 0.1 to 10^2 rad/s at a selected shear stress within LVE region, were performed at -30, -20, -10, 0 and 10 °C for each sample prepared with at least two replicates.

Modulated differential scanning calorimetry (MDSC), performed in a TA Q-100 (TA Instrument, USA), was used to study binder microstructure thermal transitions. The following testing procedure were applied to 5-10 mg ~~of~~ samples: (a) first heating and thermal equilibration above the polymer melting point for eliminating any discrepancy of thermal history, (b) cooling ramp to -60 °C and (c) a second heating ramp to the same final temperature as in step (a). The heating/cooling rate was set at 5 °C/min with an amplitude of modulation of ± 0.5 °C and an oscillation period of 60 s, in the presence of 50 mL/min of N_2 as purge gas. Degree of crystallinity (χ_C) of each EVA type was calculated as follows:

$$\chi_C = \frac{\Delta H_m}{\Delta H_{100}.\, C_{EVA}} \tag{4.2.2}$$

where ΔH_m is heat of melting on 2nd cycle DSC heating scans, ΔH_{100} is the melting enthalpy of 100% crystalline EVA polymer, 293 J/g (Meisenheimer and Zens 2008)

and C_{EVA} is wt.% of EVA in the binder. In addition, total crystalline fraction of EVA (w_C) in the binder was defined as the product $\chi_C \cdot C_{EVA}$.

To visualize samples microstructure, optical microscopy, obtained via light transmission through a thin layer of binder on a standard microscope slides (76 x 26 mm) layer, was carried out at room temperature using a standard Olympus BX51 microscope, by Olympus Optical (Japan).

4.2.3 Results and discussion

4.2.3.1 Medium-to-high temperature behavior

Aiming to evaluate the effect of EVA characteristics and its concentration on the binder performance at medium-to-high in-service temperatures, technological test, viscous flow curves at 60°C, dynamic shear temperature sweep tests, DSC analysis and optical microscopy were conducted on neat bitumen (as a reference) and on its EVA modified binders, prepared from VA7-MFI2 and VA18-MFI500 at three concentrations (2.5, 5.0 and 7.5 wt.%).

Figure 4. 2. 1 shows viscous flow curves for binders at 60 °C (usually considered as the maximum expectable temperature to be reached by pavements in warm climates).

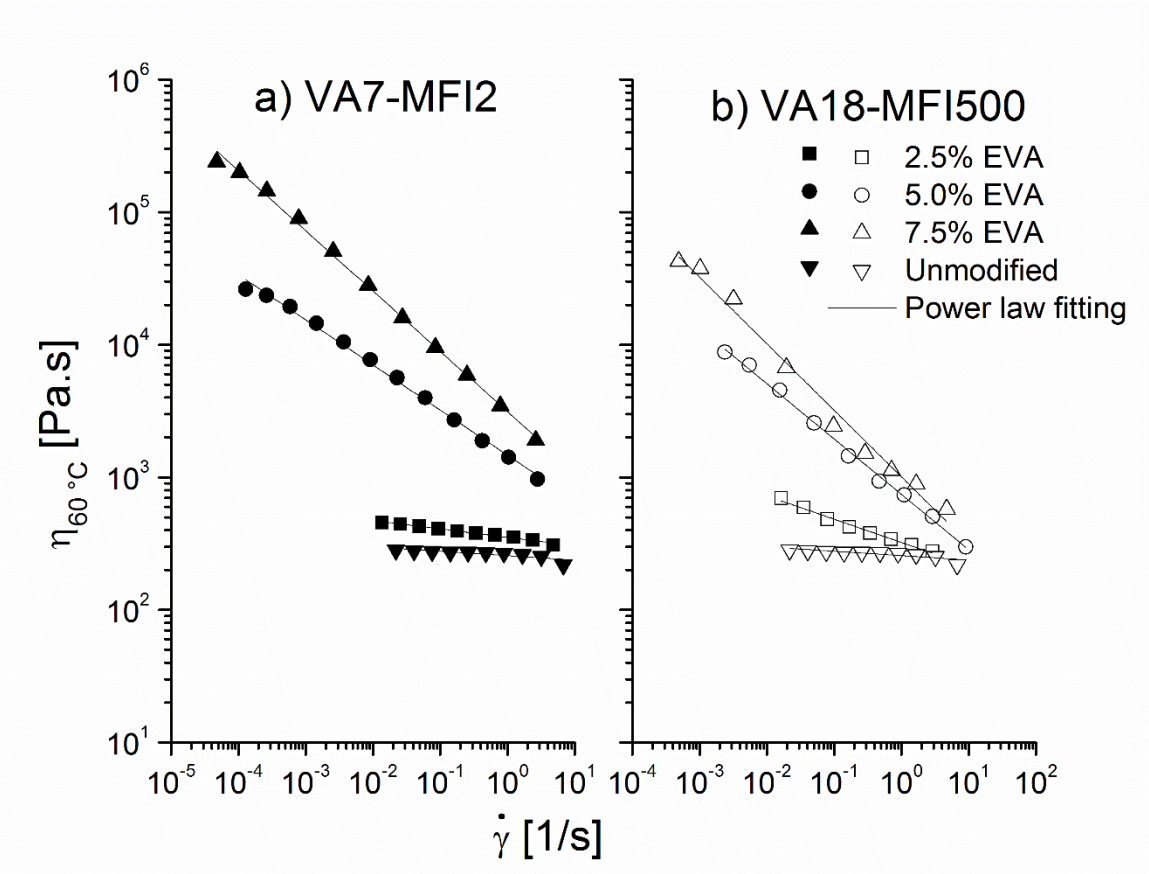

Figure 4. 2. 1 Steady shear flow behavior of 70/100 bitumen modified by EVA at 60 °C as a function of EVA copolymer weight percentage (2.5, 5 and 7.5 wt.%).

As can be observed, EVA addition at any weight percentage tested (of 2.5, 5.0, or 7.5 wt.%) increases the viscosity of the resulting modified binder and leads to the development of shear-thinning behaviors, which can be fitted by Ostwald-de Waele model fairly well:

$$\eta = k(\dot{\gamma})^{n-1} \tag{4.2.3}$$

where 'k' and 'n' are the consistency and flow indexes, respectively.

Table 4. 2. 2 Fitting parameters, 'k' and 'n' values, of the Ostwald-de Waele model and modification index, at 60 °C, for each EVA-binders, at 2.5, 5 and 7.5 wt.% .

EVA copolymer		At 60 °C		
Type	Conc. (wt.%)	k (Pa.s^n)	n	MI[a]
VA7-MFI2	2.5	358.26	0.95	4.6
	5.0	1443.15	0.65	57.7
	7.5	3025.01	0.53	245.7
VA18-MFI500	2.5	322.77	0.83	4.6
	5.0	745.38	0.58	24.4
	7.5	1003.72	0.49	65.9

[a] $MI = \eta^*_{Modified\ binder}/\eta^*_{Neat}$

As seen in Table 4. 2. 2, a lower 'n' value (within the shear rate considered) was observed as EVA concentration increased, confirming a more pronounced shear thinning response. On the other hand, an increase in consistency index, 'k', was seen as the concentration increased for both VA7-MFI2 and VA18-MFI500 modified binders, suggesting an improvement in binder performance at 60 °C (Garcia-Morales et al. 2004; González et al. 2004). On the whole, the use of EVA with less amount of VA (e.g. VA7-MFI2) led to higher modification degrees (i.e. higher viscosity or 'k' values) in the resulting binder.

Figure 4. 2. 2 presents the evolution of complex viscosity (η*) with temperature, of binders modified by increasing VA7-MFI2 and VA18-MFI500 concentrations, between 30 and 100 °C.

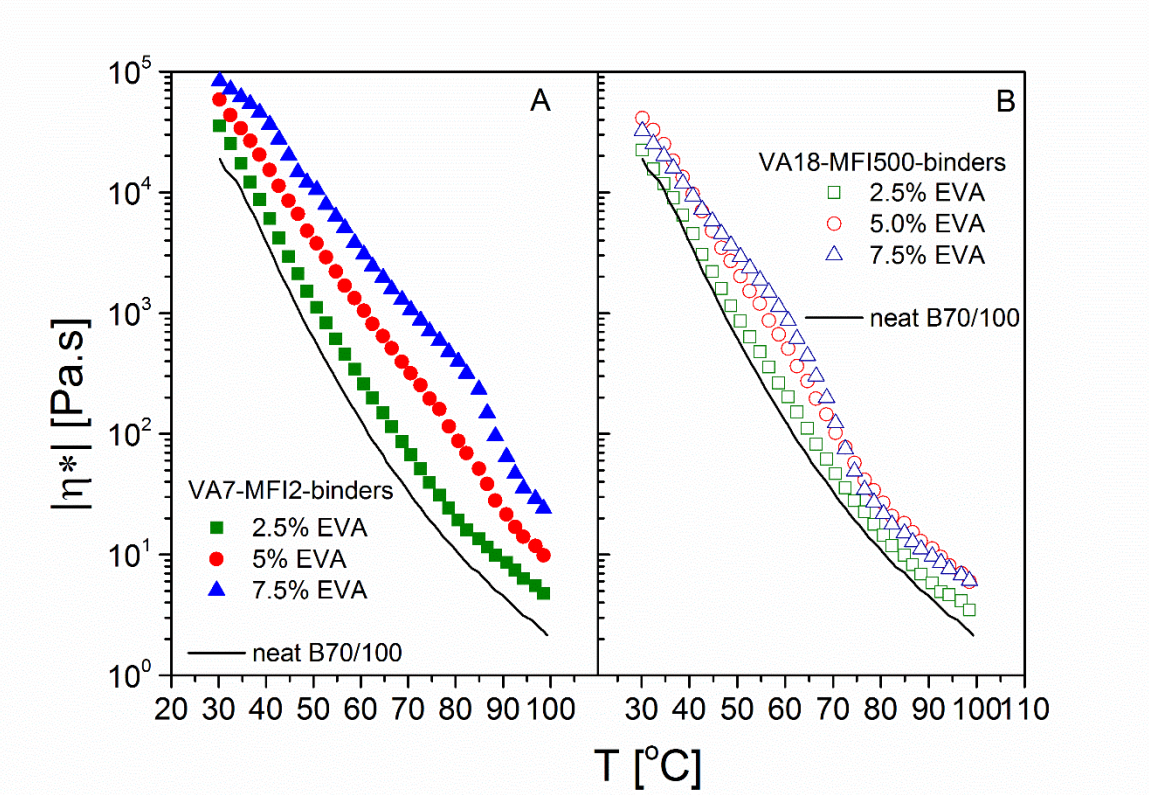

Figure 4. 2. 2 Evolution of complex viscosity with temperature, as a function of EVA concentration, for (a) VA7-MFI2 and (b) EVA-VA18.

Regarding binder modification achieved, binder with 7.5 wt.% VA7-MFI2 shows the highest increase in η* between 30-75 °C. For its quantification, a modification index ($MI_{60°C}$) has been defined as the ratio between complex viscosities of the modified and neat bitumens at 60 °C ($MI_{60°C}=\eta^*_{Modified\ binder}/\eta^*_{Neat}$), in Table 4. 2. 2. Thus, binder modified by 7.5 wt.% VA7-MFI2 presented the highest MI value of 57.7, which is followed by binder containing 7.5 wt.% VA18-MFI500 with $MI_{60°C}$ =24.4. This result confirms that asphalt permanent deformation could be better avoided by adding a higher amount of EVA with a lower VA content (Yuliestyan et al. 2016a).

Moreover, even though all binders show complex viscosity values decreasing with temperature (Figure 4. 2. 2), material thermal susceptibility becomes lower at in-service temperatures as EVA concentration rises (i.e. η* curve shows less slope from

30 to 60 °C or 80 °C, depending on the polymer used), as also predicted by higher penetration index (PI). However, above such threshold temperatures (80 and 60 °C for VA7-MFI2 and VA18-MFI500, respectively), η* values drop more sharply for the most concentrated systems (e.g. 5 or 7.5 wt.%) (Figure 4.2.2). In contrast, when only 2.5 wt.% EVA is involved, no change in η* slopes are noticed, regardless the selected EVA. The result points out that modified binder thermo-rheological properties are governed by both the selected EVA and its concentration.

The above threshold temperatures for the onset of the η* abrupt decay have been related to the EVA melting process, as may be deduced from MDSC analysis (Figure 4.2.3).

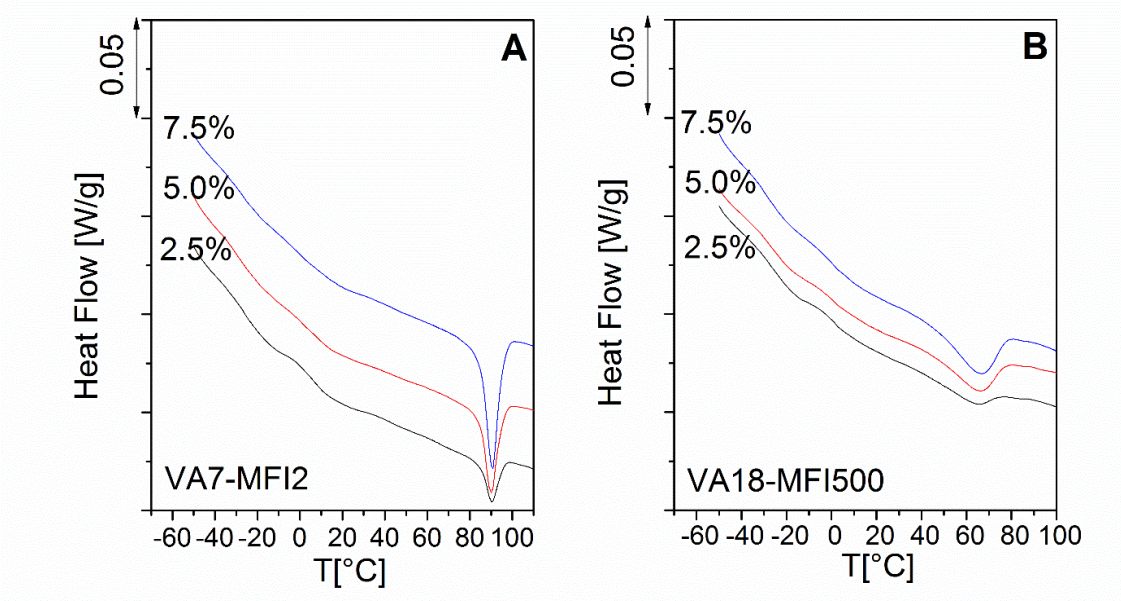

Figure 4. 2. 3 Total heat flow curve for: (a) EVA binder with VA7-MFI2; and (b) VA18-MFI500. Results obtained from MDSC 2nd heating cycle.

Table 4. 2. 3 Crystalline fraction properties; enthalpy of melting (ΔHm) , melting temperature (Tm), degree of crystallinity (χc), and total crystalline fraction (wc), obtained from 2nd cycle MDSC data

EVA copolymer				Binder - DSC 2nd Cycle calorimetric thermogram				
Name	VA (wt.%)	MFI (g/10 min)	T_m (°C)	Conc. (wt.%)	ΔH_m (J/g)	T_m (°C)	χ_c (%)	w_c (%)
VA7-MFI2	7	2	105	2.5	1.8	89	24.2	0.6
	7	2	105	5.0	4.5	89	30.7	1.5
	7	2	105	7.5	6.8	89	30.9	2.3
VA18-MFI500	18	500	84	2.5	0.6	65	7.5	0.2
	18	500	84	5.0	3.3	65	22.7	1.1
	18	500	84	7.5	5.0	65	22.9	1.7
VA18-MFI2	18	2	84	5.0	3.4	65	23.2	1.1
VA28-MFI400	28	400	69	5.0	--	--	--	--
VA28-MFI7	28	7	69	5.0	--	--	--	--

Polymer concentration hardly affects melting temperature (T_m) for each type of EVA, which seems to be only affected by the selected EVA (Figure 4.2.3 and Table 4.2.3). Thus, melting of VA7-MFI2 crystalline fraction leads to a peak in the modified bitumen, between 80-100 °C, at a higher temperature range than the one found for VA18-MFI500 (between 50-80 °C). Compared to their parent pure EVAs, T_m measured for such peaks in EVA modified binders have shifted to lower values (Table 4.2.3), as a consequence of migration of bituminous lighter fraction to polymer rich phase in the binder. Therefore, the change in slope of η* curves, found at ca. 80 and 60 °C, is

associated to the melting of swollen EVA crystallites at 89 °C and 65 °C, for VA7-MFI2 and VA18-MFI500, respectively (Figures 4.2.2 and 4.2.3, and Table 4.2.3).

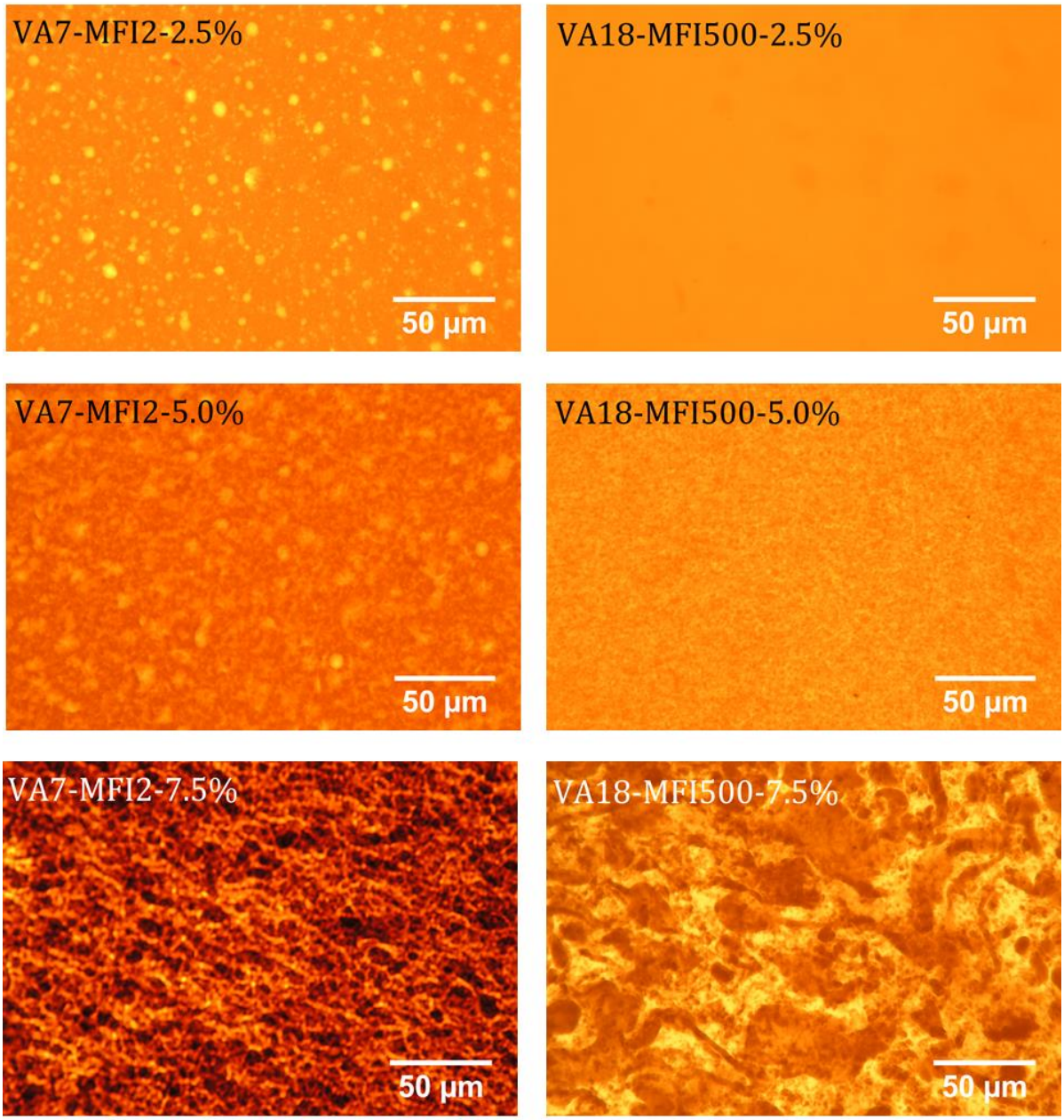

Figure 4. 2. 4 EVA binder morphology through transmission optical microscopy at 25 °C.

However, such a η* slope alteration was observed from 5 wt.% EVA onwards (Figure 4.2.2). Binder morphology, evaluated by optical micrographs, may shed some light to this issue (Figure 4.2.4). Two phases could be clearly distinguished where bituminous

phase appears as a darker region as opposed to a lightly toned region assigned for polymer phase. At a concentration of 2.5 wt.% VA7-MFI2, dispersed polymer droplets are observed all over the continuous bituminous phase (Airey and Rahimzadeh 2004; Sengoz et al. 2009). For the same concentration of VA18-MFI500 polymer-bitumen compatibility is such that polymer phase cannot be visually appreciated. Interaction of a larger content of VA pendant groups on VA18-MFI500 with bitumen yields a better dispersion (enhanced miscibility) which prevents visibility by optical microscopy observation (Sengoz et al. 2009). At 5 wt.%, a transition morphology, characterized by polymer network interconnecting polymeric beads, has been observed. VA7-MFI2 binder appears to have coarser well-defined polymeric beads, with a higher χ_c of 30 %, as compared to VA18-MFI500 binder having 22 % (Table 4.2.3). Finally, a continuous polymeric phase has formed at a concentration of 7.5 wt.% on both EVA types, although the specific effect of polymer-bitumen affinity on the final morphologies still remains. Therefore, binder morphologies shown in Figure 4.2.4 demonstrate VA content conditions the quality of polymer dispersion, whilst the EVA concentration determines the phase which governs the binder linear viscoelasticity. Consequently, at the highest concentrations of 5 and 7.5 wt.% EVA, the collapse of the molten polymer-rich microstructure would lead to the observed drop in η^* above the threshold temperatures of 60-80 °C.

In summary, binder properties seem to be affected by both EVA concentration and crystallinity, χ_c. In this regard, parameters such as consistency index (k), modification index (MI) and penetration index (PI) (Tables 4.2.1 and 4.2.2) are commonly used for the prediction of binder performance (Partal et al. 1999; Airey 2002a). Interestingly, the results obtained may be explained in terms of total crystallite fraction ($w_c = \chi_c \cdot C_{EVA}$)

fairly well (Figure 4.2.5). As may be seen, linear and exponential increases for those parameters with w_c have been found, suggesting a close dependence of binder performance at medium-to-high in-service temperatures on the amount of crystallites present (i.e. on combined contribution of EVA concentration and type).

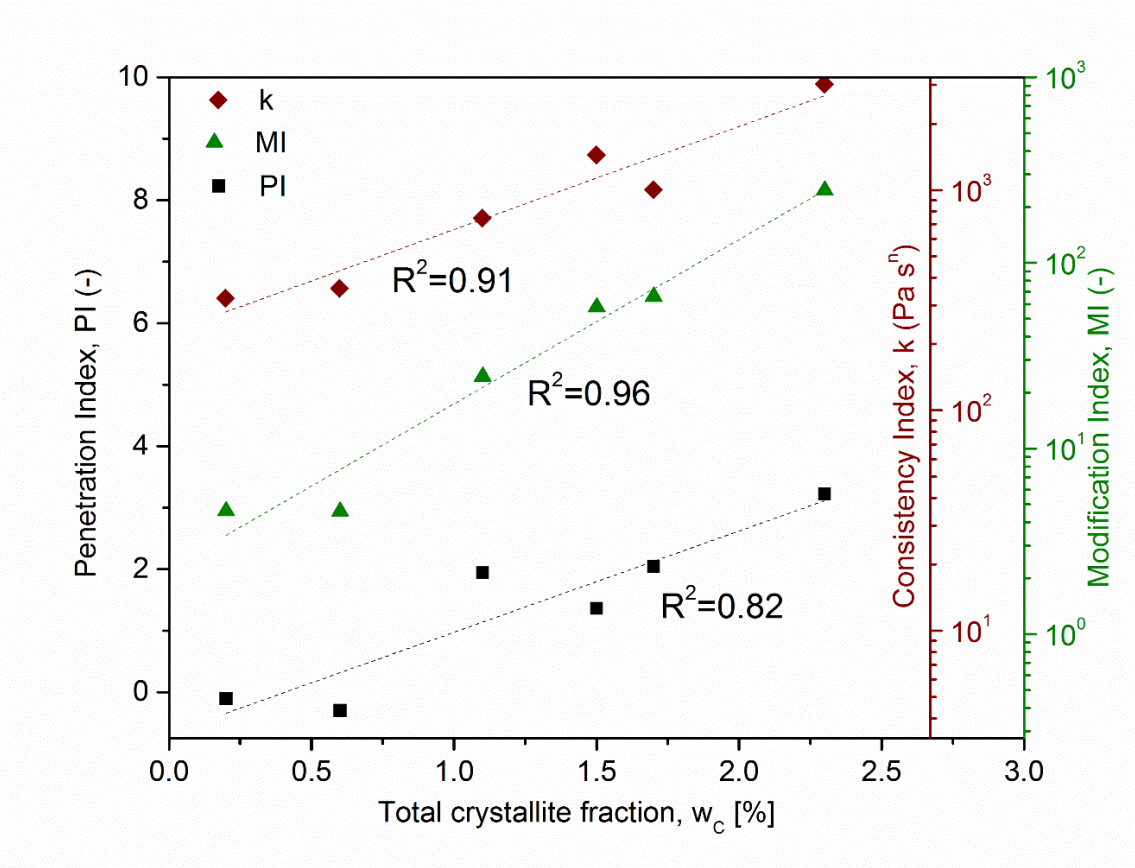

Figure 4. 2. 5 Penetration index (PI), consistency index, Ostwald de Waele parameter (k) and modification index ($MI_{60°C} = \eta^*_{MOD} / \eta^*_{UNMOD}$) as a function of total crystalline fraction (w_C).

4.2.3.2 Low temperature rheological behavior

Performance of neat bitumen, reference binders (modified by 3 wt.% SBS and 1.5 wt.% wax) and EVA-modified binders at low in-service temperatures (between -30 and 10 °C) has been assessed by means of dynamic torsional mode frequency sweeps. Figure 6 shows the effect of polymer concentration (Figure 4.2.6A) and VA content (Figure 4.2.6B) on the binder mechanical spectra at three selected temperatures.

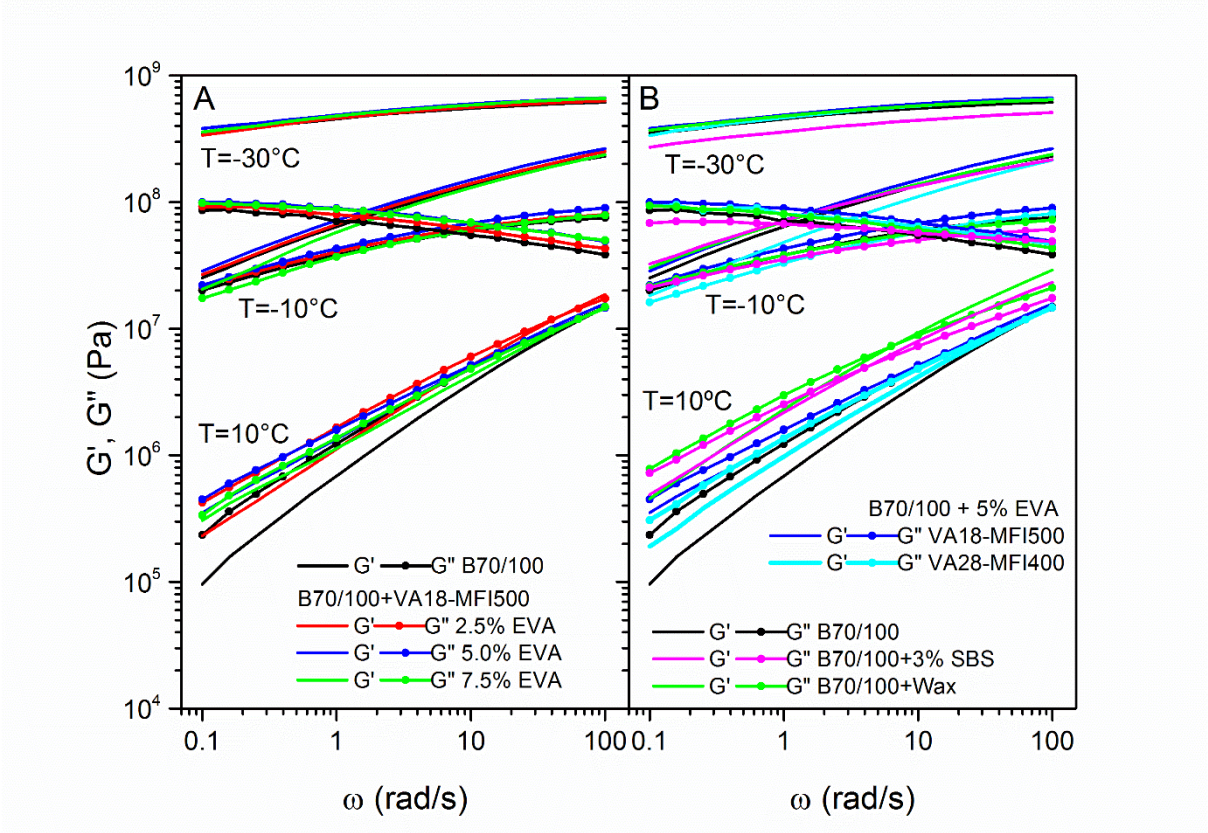

Figure 4. 2. 6 Frequency sweeps at -30, -10 and 10 °C of: (a) neat bitumen and EVA binders with varying concentration at 2.5, 5.0 and 7.5% w/w; and (b) EVA binders with VA18-MFI500 and VA28-MFI400.

For all binders, storage modulus (G') increases towards the material glassy region (close to 10^9 Pa) as temperature decreases or frequency increases. Likewise, loss modulus (G") decreases with frequency in that zone, located above a crossover point between both viscoelastic functions. As may be seen, binders modified by 2.5 or 5 wt. % VA18MFI500 (Figure 4.2.6A) and by 1.5 wt. % wax (Figure 4.2.6B) behave as the softer neat bitumen B70/100 at -10 and -30°C. A slightly improved behavior is found for the 7.5 wt. % VA18-MFI500-modified system which shows lower G' values than the neat bitumen at -10°C at low frequencies, suggesting a less brittle character for this high concentration (Figure 4.2.6A). Interestingly, a similar result can be obtained if bitumen 70/100 is modified by 5 wt. % VA28-MFI400 (Figure 4.2.6B). However, the enhancement is more apparent if 3 wt.% SBS is used as bitumen modifier, whose G'

values remains below the other binders at -30°C, still far from the glassy region (Figure 4.2.6B). Copolymer SBS is well known for its ability to enhance bitumen performance at low temperature, preventing asphalt from low temperature cracking (Munera and Ossa 2014; Polacco et al. 2015).

Frequency sweep curves plotted as phase angle (δ) vs. complex modulus |G*|, the so-called Black diagram, have been used to validate applicability to bituminous binders of time-temperature superposition principle (TTSP) (Airey 2002b; Sybilski et al. 2004). A fair continuity has been found connecting the frequency sweep curves at each temperature tested for neat bitumen and binders modified by wax or SBS (results not shown), suggesting they behave as thermo-rheologically simple materials. Some discontinuities were perceived around large δ or between isotherm curves of 10 and 0 °C for the most concentrated EVA-modified bitumens. In this regard, empirical master curves of complex modulus (|G*|) and loss angle (δ) vs. reduced frequency ($a_T \cdot \omega$) have been constructed by applying TTSP to all isotherms at a reference temperature (T_{Ref}) of -10 °C (Figure 4.2.7).

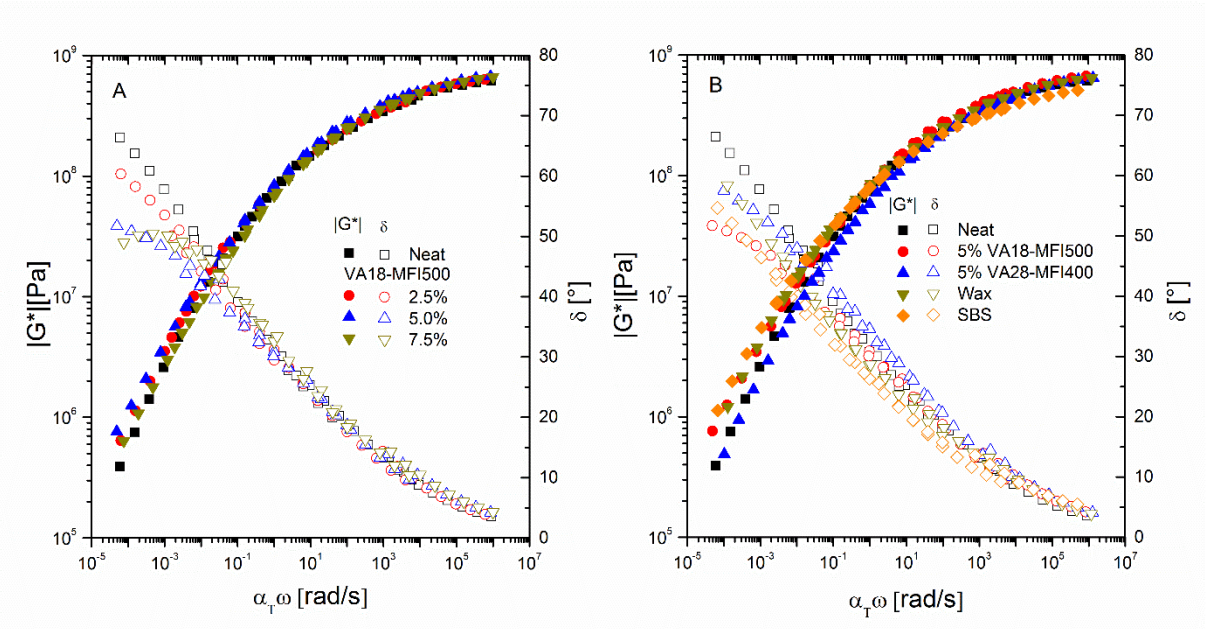

Figure 4. 2. 7 Empirical master curve of the oscillatory torsional |G*| and δ vs aTω , obtained at the reference temperature (T_{ref}) of -10 °C.

As a result, continuous master curves were obtained for neat bitumen and SBS and wax modified binders (Figure 4.2.7B), in agreement with their smooth Black diagrams. For EVA modified binders, semicrystalline structure is responsible for the broken TTSP, which is not visible when a low EVA dosage is added (Airey 2002b). Shift factor dependence on temperature can be described by Arrhenius-like equation (Ferry 1980; Airey et al. 2016):

$$a_T = \exp\left\{\frac{E_a}{R}\left(\frac{1}{T} - \frac{1}{T_{ref}}\right)\right\} \quad (4.2.4)$$

where 'E_a' and 'R' represent the activation energy and ideal gas constant, respectively. Table 4.2.4 shows the E_a values for all samples studied, which have been used to convert previous isothermal (T_{Ref} of -10 °C) master curves in Figure 4.2.7 (domain of frequency) into isochronal (ω_{Ref} of 10 rad/s) master curves (domain of temperature). With this aim, Equation 4.2.4 is re-arranged as follows (Cuadri et al. 2013a):

$$T = \frac{E_a \cdot T_{ref}}{R \cdot T_{ref} \cdot Ln(a_T) + E_a} \tag{4.2.5}$$

where shift factor (a_T) is defined as ratio of reduced frequency after shifting (ω_R) over reference frequency (ω_{Ref}), and ω_{Ref} is the frequency at which the resulting isochronal curve is obtained. Figure 4.2.8 presents the conversion plots of G' and G'' as a function of temperature at ω_{Ref}=10 rad/s, from neat and modified bitumen data.

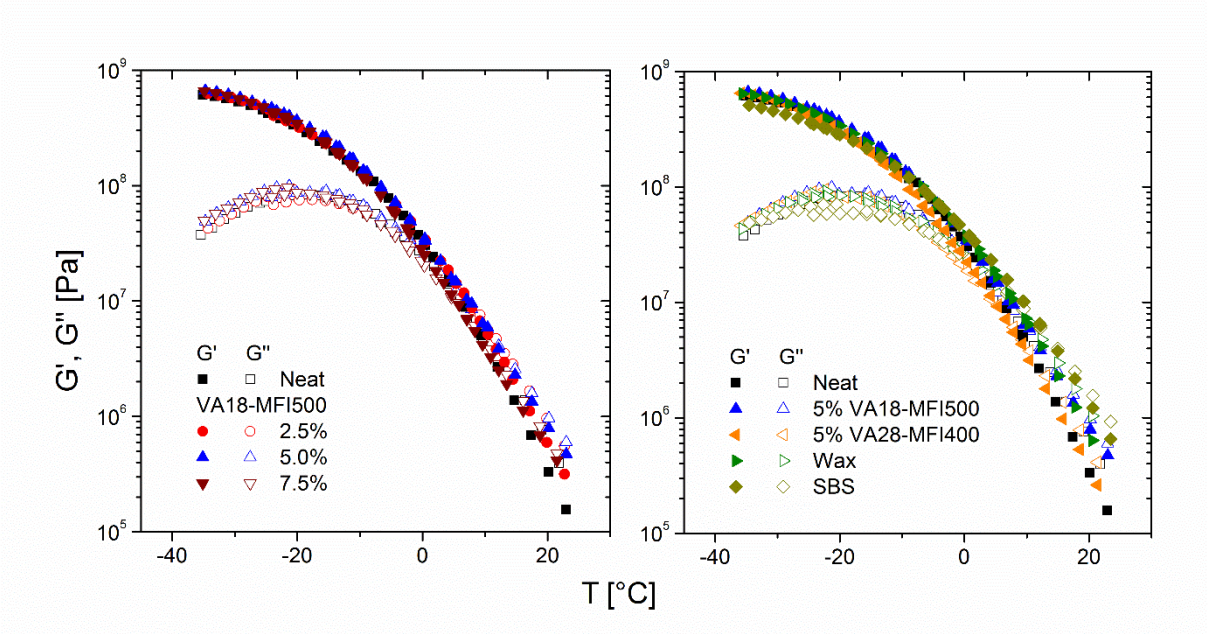

Figure 4. 2. 8 Temperature sweep curves calculated from Equation 4.2.5 at a reference frequency of 10 rad/s.

As can be observed, upon decreasing in temperature, material undergoes a transition to the glassy region where elastic modulus (G') begins to dominantly take over loss modulus (G''), below a crossover point. As further decrease, G'' modulus reaches the maximum value that is reported to be a "mechanical" glass transition temperature ($T_{g,DMTA}$) at 10 rad/s, below which material thermal cracking occur under much smaller deformations (Lu et al. 1999; Partal et al. 1999; Fawcett and McNally 2000). A

slight reduction of $T_{g,DMTA}$, as a result of polymer addition, has been observed as compared to neat $T_{g,DMTA}$ value, see Table 4.2.4.

Table 4. 2. 4 Mechanical glass transition temperature ($Tg_{,DMTA}$), activation energy (Ea) and elastic properties at -30 °C, derived from constructed master curve using Arrhenius type equation.

Sample	Polymer/wax (wt.%)	$T_{g,DMTA}$ [°C]	E_a [kJ/mol]	G'·10^{-8}, at -30°C (Pa)
B70/100	0	-18.5	236	5.5
VA18-MFI500-2.5	2.5	-19	237	5.8
VA18-MFI500-5.0	5	-19	239	5.9
VA18-MFI2	5	-21	225	4.7
VA18-MFI500-7.5	7.5	-19	241	5.8
VA28-MFI400	5	-19	236	5.5
VA28-MFI7	5	-20	239	5.5
Wax	1.5	-19	237	5.5
SBS	3	-20	230	4.5

Reduction of 1.5 °C is seen for SBS along with the smallest value for G' at -30°C ($G'_{-30\,°C}$=4.5·10^8 Pa), suggesting a delayed low temperature thermal cracking (i.e. a delay in attaining full brittleness) as the absorbed energy could be more easily dissipated at this temperature (González et al. 2004). However, at -30 °C, EVA having MFI of 400 or 500 (no matter the polymer concentration or VA content assessed) behave in a

different way presenting G' values that are slightly higher than neat bitumen value, despite their above commented reductions in $T_{g,DMTA}$.

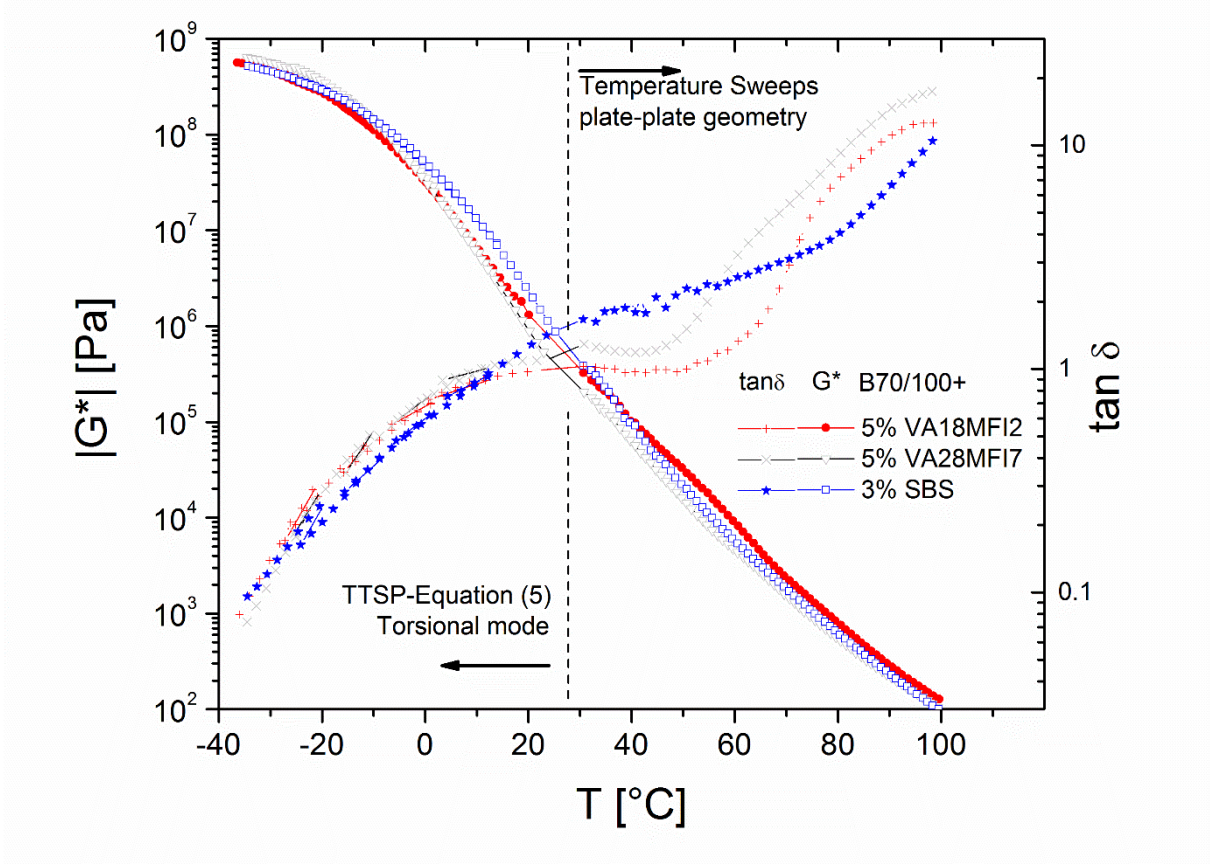

Figure 4. 2. 9 Comparison of complex modulus and loss tangent curves obtained from calculated temperature sweeps in torsion mode between -30 and 10 °C (Equation 4.2.5) and experimental oscillatory shear temperature sweeps between 30 and 100 °C.

Interestingly, SBS low temperature modification could be reproduced by using EVAs with lower MFI value for both VA18 and VA28 (Figure 4.2.9). Particularly by VA18-MFI2, which exhibits close values to SBS with $T_{g,DMTA}$= -21°C and $G'_{-30°C}$=4.8 10^8 Pa (Table 4.2.4). Figures 4.2.9 also points out the good agreement between experimental dynamic shear temperature sweeps conducted from 30 to 100°C at 10 rad/s, using plate-plate geometry and heating rate of 1 °C/min, and calculated temperature sweep curves obtained, from torsional tests between -30 and 10 °C, by application of

Equation 4.2.5. As can be seen, VA18-MFI2 modified bitumen shows a similar |G*| curve (from -30 to 100°C) to SBS reference system (Figure 4.2.9) and improved elastic properties between 10 and 70°C. Thus, tan δ exhibits an apparent plateau and lower values than SBS in this temperature range. Moreover, Figure 4.2.9 shows that if material performance is assessed in a wider range of in-service temperatures (e.g. from -20 to 70°C), the whole effect of EVA addition is a decrease in binder thermal susceptibility. Despite the fitting results to Equation 4.4.4, performed in a shorter temperature range between 10 to -30 °C, might be interpreted as polymer addition gives rise to more thermal susceptible materials, as may be deduced from the higher E_a values shown in Table 4.2.4 compared to neat bitumen (Garcia-Morales et al. 2004).

Thermodynamic glass transition temperatures can be also calculated by MDSC analysis from the evolution of first temperature derivative of heat capacity (Figure 4.2.10). Two peaks were seen at -30 and 2 °C for neat bitumen, which according to literature (Masson et al. 2002; Cuadri et al. 2013b) originate from the ordering of low molecular weight saturates fractions in bitumen. After addition of EVA, the peak at 2 °C disappears, suggesting that the fraction causing this peak has been absorbed by EVA polymer. Hence, it is likely that hardening is postponed towards lower temperatures, in agreement with previous results ($T_{g,DMTA}$). However, the peak at -30 °C seems to remain unaffected by EVA, which implies an individual and simultaneous structural conformation with its polymer, as observed at the same temperature in pure EVA curves for any VA content and MFI tested.

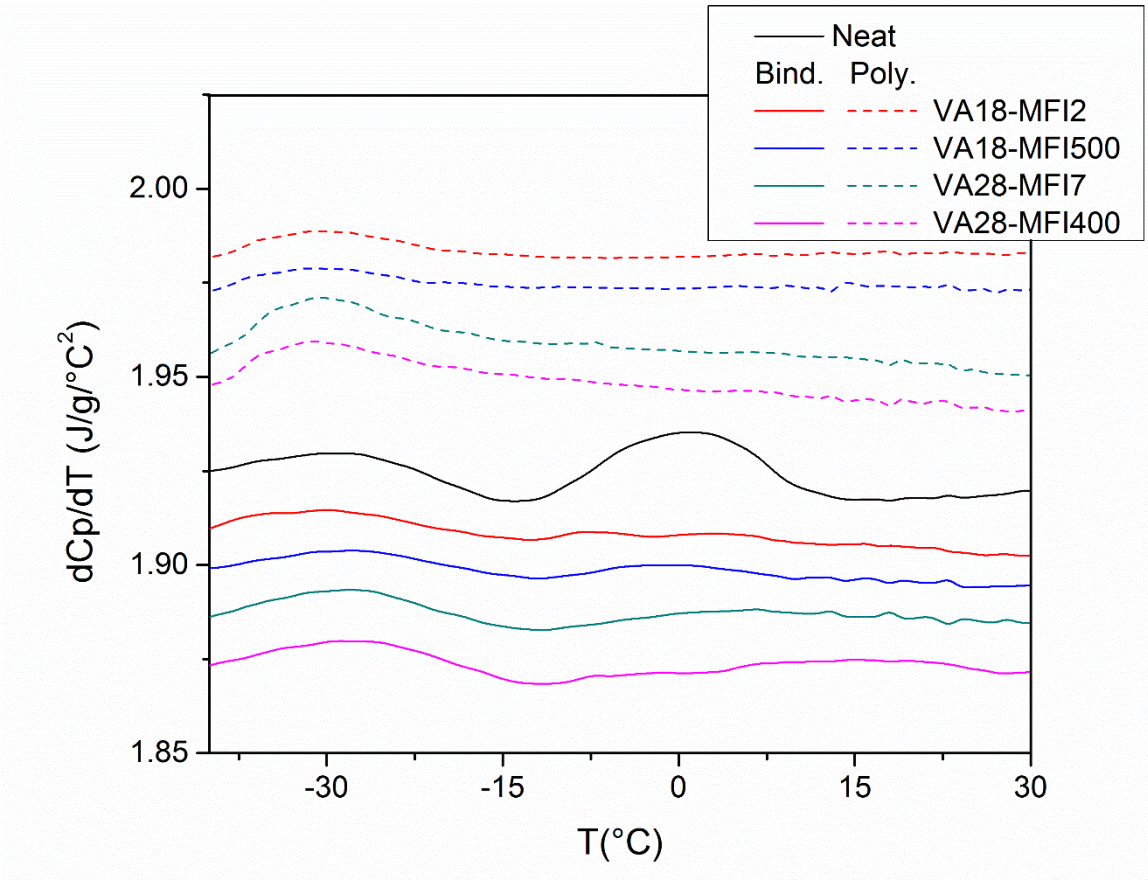

Figure 4. 2. 10 First temperature derivative of heat capacity (dCp/dT) for pure EVAs, neat bitumen and EVA modified binders. Results obtained from 2nd cycle of MDSC heating curve.

Finally, previous viscoelastic characterization has been conducted within the material linear viscoelastic region, at a strain (or stress) below γ_{nL} (i.e. under non-destructive conditions). In this regard, all materials tested presented a shortening of this region (lower values of γ_{nL}) as temperature decreased, evidencing a lower molecular motion (exemplified for |G*| vs γ curve of VA18-MFI500 binder as an inset in Figure 11A). If the non-linear viscoelastic limit is further exceeded at temperatures close to the material glass transition, cracking occurs. In order to assess this effect between -30 and 0 °C, strain breakage tests were performed by gradually increasing a dynamic torsional load exceeding the linear viscoelastic (LVE) region until the material could

not absorb more energy and cracked (inset Figure 4.2.11A). Results are plotted as strain at breakage ($\gamma_{breakage}$) vs temperature in Figure 4.2.11.

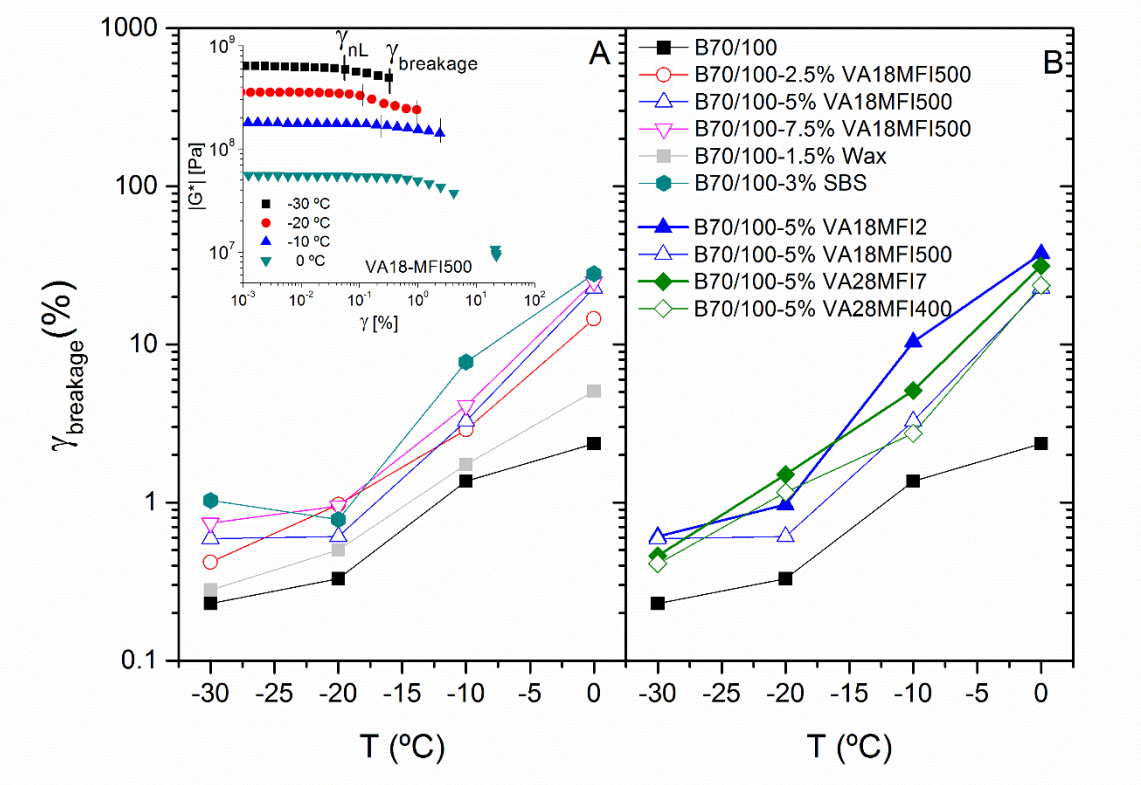

Figure 4. 2. 11 Dependence on temperature of binder strain at breakage ($\gamma_{breakage}$) as a function of VA18-MFI500 concentration (A), and EVA characteristics (B). Inset: Strain sweeps tests for determining non-linear viscoelastic region (γ_{nL}) and $\gamma_{breakage}$

As can be seen, $\gamma_{breakage}$ values decrease as temperature does for all systems (Figure 4.2.11). However, compared to neat bitumen, all PMBs resisted a higher strain before breakage. Polymer concentration in VA18MFI500 modified binders does not significantly affect values of $\gamma_{breakage}$, being their curves located between the SBS modified bitumen and the wax modified binder (Figure 4.2.11A). Similar results are found for the effect of VA content (Figure 4.2.11B). Conversely, a decrease in MFI parameter enhances binder performance (i.e. material becomes less brittle), as may be deduced from the higher $\gamma_{breakage}$ values obtained for VA18MFI2 compared to

VA18MFI500 or for VA28MFI7 compared to VA28MFI400 (Figure 4.2.11B). On the whole, SBS and VA18MFI2 modified bitumens seem to exhibit the best low temperature performance.

4.2.4 Concluding remarks

EVA modified binder properties over a wide range of temperature have been evaluated by means of rheological, calorimetric, microstructural and technological tests. At medium to high in-service temperatures, EVA addition (from 2.5 to 7.5wt.%) leads to improved rheological properties compared to the corresponding neat bitumen, either on binder flow behavior at 60 °C or viscoelastic properties up to 60-80°C. Rheological behaviors at such high temperatures depend on the selected polymer (VA7MFI2 or VA18MFI500), and are governed by the melting process of the polymer network formed (which becomes a continuous phase at 7.5 wt.% EVA), as deduced from MDSC results and optical micrographs. In this regard, linear and exponential relationships have been found between the total crystalline fraction (w_C) and binder parameters such as penetration, modification at 60 °C and consistency indexes. Hence, total crystalline fraction is considered a key parameter while using EVA to suitably modify binder performance from medium to high in-service temperatures.

Dynamic thermomechanical analysis at low temperature conducted in torsion mode has revealed the development of a thermo-rheologically complex behavior as EVA concentration is increased. Nonetheless, the frequency sweeps of viscoelastic functions between -30 and 10 °C were empirically superposed onto a master curve, which can be subsequently used to obtain temperature sweep curves at a selected

frequency (10 rad/s), by means of the Arrhenius-like temperature dependence of the shift factors. Such curves show a good agreement with those from oscillatory shear (plate-plate geometry) temperature sweep tests obtained at higher temperatures. Derived from calculated temperature sweep curves, binder "mechanical" glass transition temperatures ($T_{g,DMTA}$) showed a slight decrease by EVA addition, which might be seen by the absence of peak in MDSC analysis. Similarly, strain breakage tests have shown improved performance at low temperature for all modified binders. In this regard, MFI appears as the EVA key parameter to enhance binder performance at low temperature. Thus, lower MFI values led to less brittle materials, as may be deduced from the higher breakage strain values obtained for VA18MFI2 compared to VA18MFI500 or VA28MFI7 to VA28MFI400 (Figure. 4.2.11B). On the whole, SBS and VA18MFI2 modified bitumens seem to exhibit the best low temperature performance.

4.3 Binder design for asphalt mixture with reduced temperature: EVA modified bitumen and its emulsions

Published in :

Transportation Research Procedia
Publishing Company : Elsevier B.V.
Editor in Chief : Riccardo Rossi
Volume: 14, PP : 3512-3518
Year : 2016
ISSN : 2352-1465
DOI : 10.1016/j.trpro.2016.05.319

ABSTRACT

High energy consumption and environmental risks are both associated to the use of hot asphalt mixes. In response to the need of more sustainable pavements, the modification of bitumen with low melting point EVA copolymers is investigated. Firstly, different modified binders containing EVA with varying VA contents (and so different crystalline fractions and melting temperatures) and Melt Flow Index (MFI) values were investigated. In the second stage, emulsification was implemented, in which the above EVA modified bitumen was suspended in the form of micro-size droplets in aqueous phase, in the presence of a surfactant. The results suggest that an optimum balance between VA content and MFI value will improve the binder rheological performance at medium-high in-service temperatures as well as its workability, and will facilitate its emulsification. Additionally, the binder viscosity is tremendously reduced after its emulsification, which allows mixing to be performed at much lower temperature, so reducing both energy consumption and environmental risks.

4.3.1 Introduction

Bitumen, also found in natural deposits, is commonly a by-product of fractional distillation of crude oil (McNally 2011). Pavement is the top bitumen consumer, although other uses can be found in the roofing industry for this material. Bitumen is used as a binder to hold aggregates together in road pavement construction. Trend in the modification of bitumen arises as a consequence of the increasing demand of binders with improved resistance to permanent deformation, i.e. stiffer in the medium-high in-service temperature region, and more flexible at low in-service temperatures, i.e. preventing thermal cracking. In this sense, bitumen quality is often enhanced by polymer modification, to produce either physical or chemical interaction with the bituminous phase (Carrera et al. 2015). The selection of the type of polymer is important, as various polymers provide unique characteristics in the final performance, and also during production (Zhu et al. 2014).

Handling of modified bitumen requires an elevated temperature to achieve optimum aggregate coating, and the energy spent negatively affects the environment. To overcome this issue, reduced temperature technologies are highly encouraged. On the one hand, polymer modified bitumens with lower viscosity that can be handled at lower temperatures without affecting their in-service performance represent a current concern. On the other hand, bitumen emulsions provide two joint benefits: 1) eliminating polymer-bitumen separation issue during storage; and 2) viscosity reduction. In fact, polymer modified bitumen emulsions have been successfully used for several decades by road industry due to their high performance in the application of chip seals and microsurfacing for heavy trafficked pavements (Lesueur 2011).

With the vision of greener development, reduced temperature technology such as emulsion is greatly considerable. However, to the recent literature, lack of information has been published in the field of bituminous emulsion, particularly for in-line emulsification of modified bitumen, in which EVA modified bitumen emulsion has been considered. This work offers a systematic study in exploring the effect of VA content, coupled with its melting point, and MFI value of EVA copolymer in the design of binders for reduced temperature technologies. Two differentiated parts are involved: 1) performance and processability of binders modified by EVA copolymer; and 2) their emulsions, concerning the ratio of bitumen to water phase.

4.3.2 Experimental

4.3.2.1 Material and sample preparation

The bitumen selected for this study, supplied by Repsol (Spain) has a penetration grade of 70/100. EVA co-polymer, also supplied by Repsol (Spain), was used as bitumen modifier by 5 wt.% addition into 150 °C molten bitumen. Dispersion process was done in two steps with the assistance of a Silverson L5M high shear homogenizer: 1) melting step at 3500 rpm for 15 minutes and 2) mixing step at 5000 rpm for 1 hour. Two varying VA contents, 18 and 28 wt.%, were studied. Additionally, the effect of the MFI value was also envisaged, by choosing two different MFI values of 2 and 500 for the 18 wt.% VA copolymer, and 7 and 400 for the 28 wt.% one. From this standpoint, the modified binder was then coded as 'Binder'-'VA content'-'MFI', for instance EVAMB-VA18-MFI2.

Based on the optimum performance, the selected binder was then emulsified into aqueous phase in the presence of 0.5 wt.% surfactant. The emulsification process was

done in a colloid mill Denimotech DT03, and the emulsion collected in a pressurized vessel. Binder percentages chosen were 65 and 70 wt.% corresponding to typical applications of emulsion, such as microsurfacing and chip seals, respectively (Lesueur 2011).

4.3.2.2 Characterization

The binders were subjected to steady shear viscous flow tests at 60 and 135 °C. These measurements were performed in a controlled-stress rheometer Physica MCR 301 by Anton Paar, equipped with an electrically heated chamber. Serrated parallel plate geometry with 25 mm diameter was used. In addition, the viscoelastic properties of the binders, between 30-100°C, were characterized by oscillatory shear temperature sweep tests in a controlled-stress Haake RS600, equipped with a TC501 temperature controller, at the heating rate of 1 °C/min. Serrated parallel plate geometry with 20 mm diameter was used. In order to determine the LVE region, stress sweeps were previously performed.

With regard to the emulsions, droplet size distribution was measured using laser diffraction technique in a Malvern mastersizer 2000. To characterize the droplet surface charge, zeta potential value was tested in a Malvern zetasizer through electrophoresis method. The rheological analysis for emulsion has been done by means of steady shear viscous flow tests at 30 °C, also performed in Physica MCR 301, but now equipped with 27 mm diameter serrated coaxial cylinder geometry.

4.3.3 Result and discussion

4.3.3.1 Performance and processability of binder modified by EVA copolymer

The influence of EVA copolymer on the binder viscosity has been studied by means of steady shear flow tests at 60 °C and 135 °C (Figure 4.3.1). The selection of 60 °C was based on the average asphalt temperature expected in a warm climate region, and 135 °C is a reference value for laydown and compaction operations and emulsification.

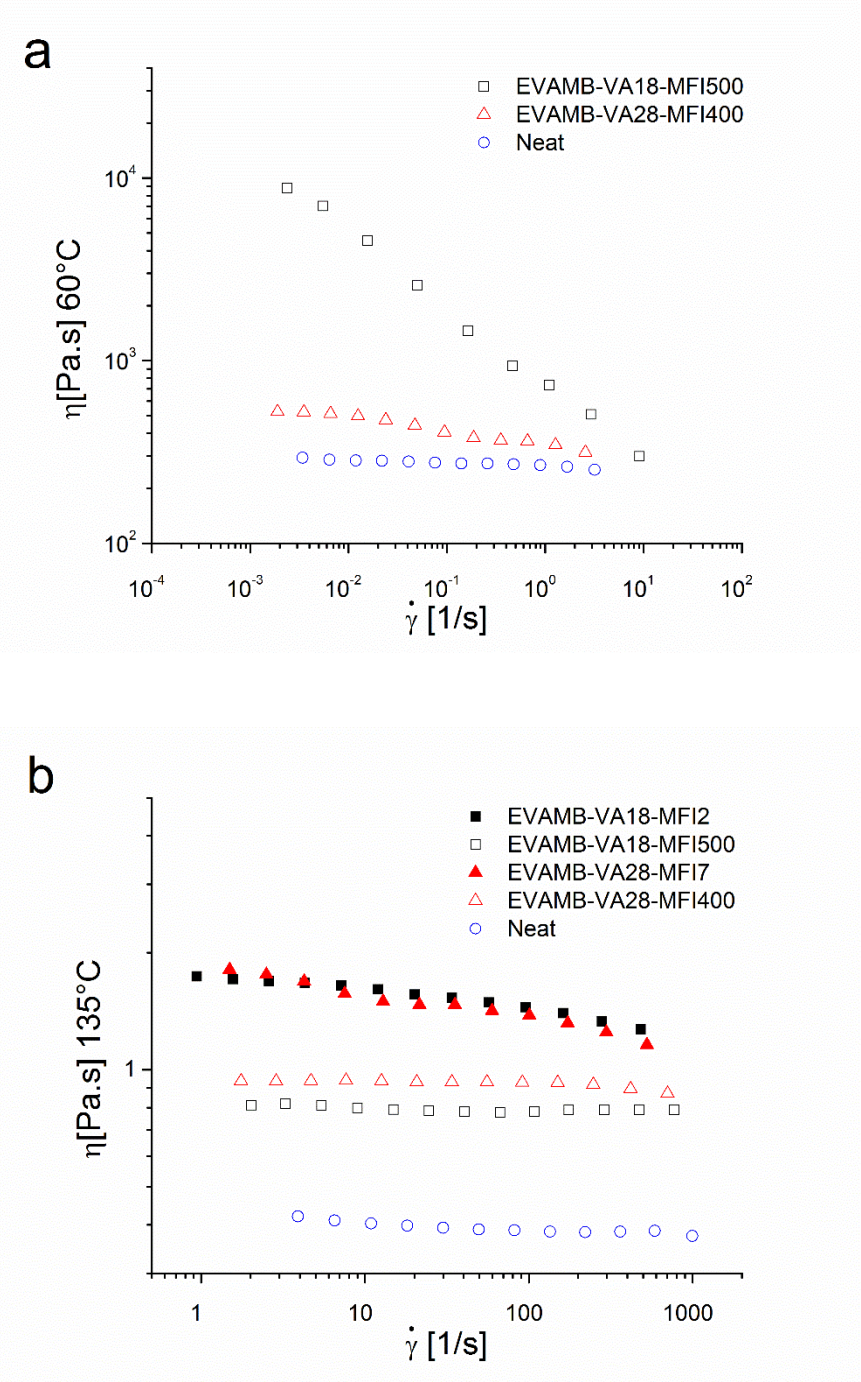

Figure 4. 3. 1 Flow behavior of EVAMB at (a) 60°C; and (b) 135°C

Binders modified with EVA copolymer exhibited improved resistance, as may be deduced from their viscosity increases observed at 60 °C, if compared to the neat 70/100 bitumen. The enhancement seemed to be significantly affected by VA content, so that the system VA18 was one order of magnitude more viscous than the PMB formulated with VA28 at low shear rates (Figure 4.3.1a). In contrast, flow behavior at 135 °C did not appear to follow similar dependence on VA. At that temperature, MFI turned out to be the most relevant parameter. For instance, EVAMB-VA18-MFI2 exhibits a viscosity close to the EVAMB-VA28-MFI7 one, which also applies for the other two cases (Figure 4.3.1b). Knowing that molecular weight and MFI of polymer are inversely proportional, the chain entanglement and internal friction affect polymer flow behavior (and, therefore, PMB viscosity) (Ravve 2012). As a result, binder viscosity decreases as EVA MFI value is higher, no matter the VA concentration studied (Figure 4.3.1b).

Binder thermomechanical properties have been measured through temperature sweep measurements in oscillatory shear in a wide temperature range, 30 - 100 °C. Figure 4.3.2 shows the evolution of the storage modulus, G', as a function of temperature. PMB viscoelastic moduli increased by the development of EVA copolymer in bitumen matrix. Such an increase in G' would lead to an improved elastic performance at medium to high in-service temperatures. Moreover, the influence of VA content in binder is reflected on the G' comparison between VA18 and VA28 that demonstrates greater elastic response in VA18 case, which is more apparent as temperature rises. Interestingly, at 65 °C, a sudden change in this slope appears for binder VA-18 cases, indicating a polymer molecular rearrangement inside bituminous matrix as a consequence of EVA crystallites melting, (Airey 2002a; García-Morales et

al. 2004). Conversely, a similar event is hardly seen for binder VA-28, due to a lower percentage of EVA crystalline fraction. The difference in percentage of crystal is related to the amount of non-crystallizable fraction in EVA, acetate pendant group, thereby, formation of crystal is more difficult in the case of binder with greater amount of VA content, (Somrang et al. 2004).

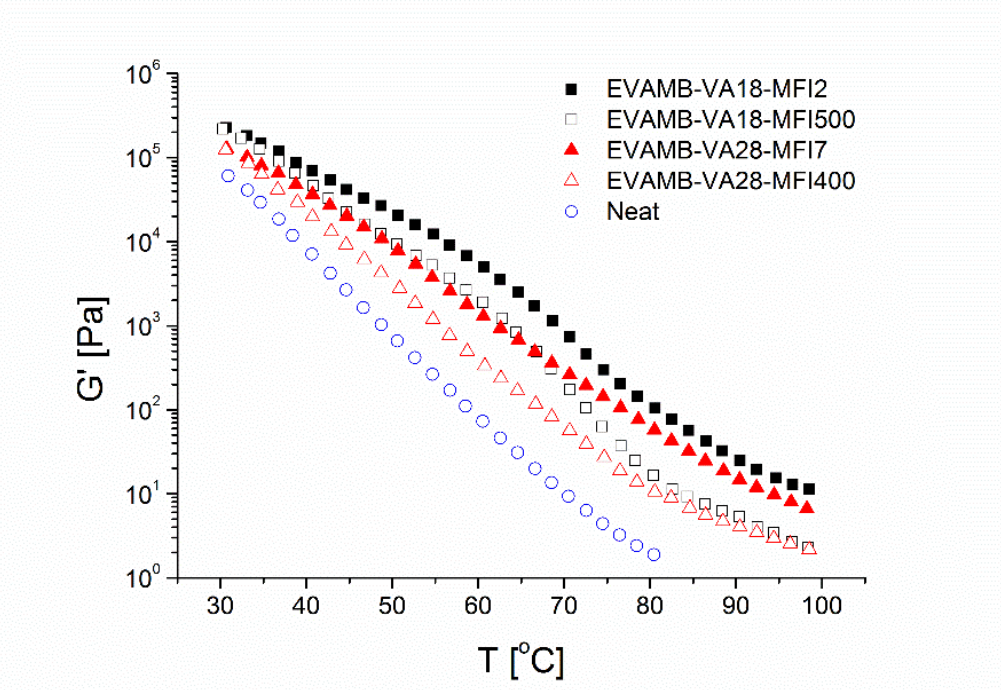

Figure 4. 3. 2 Storage modulus dependence on temperature, ranging 30-100°C

For the same reason, the above commented higher viscosity at 60 °C of VA18 binder is closely linked to a higher percentage of EVA crystallites that leads to improved binder resistance to permanent deformation. Nevertheless, above the melting of the EVA crystalline fraction, e.g. 135°C, MFI is a key parameter to understand binder flow behavior (Figure 4.3.1b). In this sense, EVAMB flowability was favored by selecting high MFI values, which would facilitate aggregate-binder mixing as well as other processes such as emulsification. On this ground, EVAMB-VA18-MFI500 was selected for being emulsified, due to its suitable balance between binder performance (i.e. high viscosity and elasticity at 60 °C) and processability (i.e. low viscosity at 135°C).

4.3.3.2 EVAMB emulsion

During emulsification, low viscosity of bituminous phase, as low as 200 mPas or less, is recommended to facilitate the breaking and dispersion process (Read and Whiteoak 2003) and with a water phase temperature at 50 °C, Salomon (2006). As seen in Figure 4.3.1b, viscosity of EVAMB-VA18-MFI500 at 135 °C laid around 782 mPas, beyond the recommendation. Therefore, a higher temperature, around 145 °C, was required with an attention paid for compensating water phase evaporation in colloid mill. Thus, pressure during emulsification was maintained above saturated water pressure at its corresponding temperature, above 5 bar.

Bituminous emulsion DSD curves are shown in Figure 4.3.3 as droplet size by volume fraction. Unimodal distributions were perceived for both modified bitumen emulsion cases, whilst neat emulsion appears as unimodal with a shoulder at low particle size. Conversion of DSD volume fraction to volume to surface mean diameter, the so called Sauter mean diameter, $D_{3,2}$, was carried out as follows:

$$D_{3,2} = \frac{\sum_i n_i d_i^3}{\sum_i n_i d_i^2} \tag{4.3.1}$$

where n_i is the number of droplets with diameter d_i. As may be seen in Table 4.3.1, EVAMB-E-65 exhibited larger $D_{3,2}$ values than its corresponding neat emulsion (Neat-E, having 65% bitumen), as a consequence of a more difficult droplet breaking during process (Lesueur 2011), derived from a more viscous bituminous phase. Likewise, processing of the most concentrated emulsion was also hindered by the higher bulk viscosity of the resulting emulsion, as deduced from $D_{3,2}$ value of EVAMB-E-70 being larger than EVAMB-E-65.

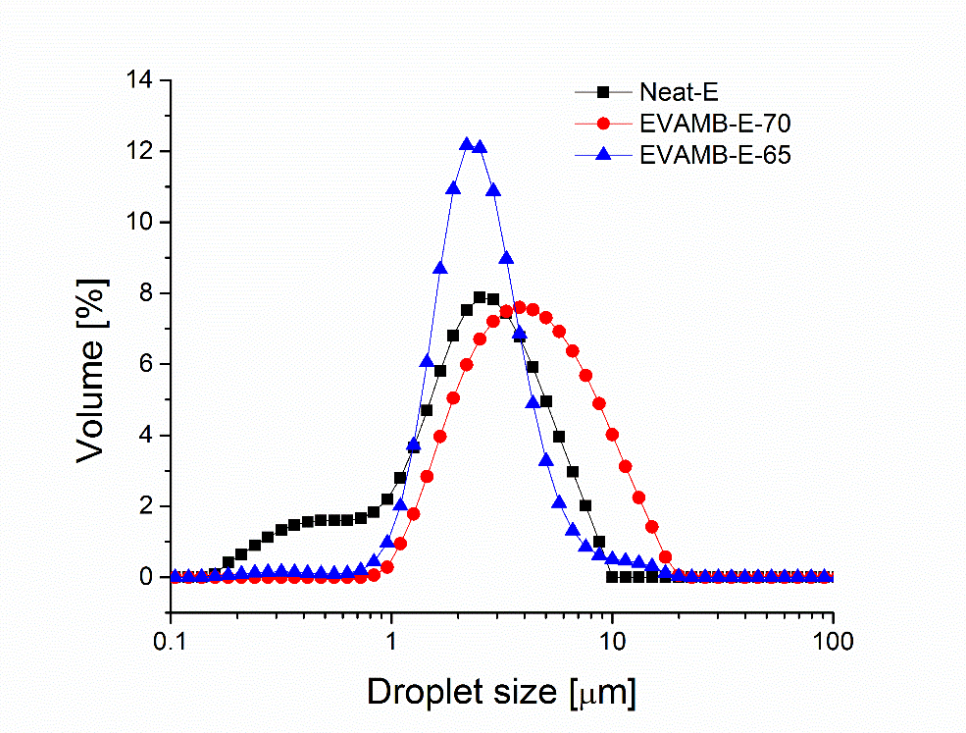

Figure 4. 3. 3 Droplet size distribution of the emulsions obtained

Table 4. 3. 1 Sauter mean diameter and zeta potential of emulsions at pH of 1 and ambient temperature

Emulsion	$D_{3,2}$ [μm]	ζ_{AVG} [mV]
Neat-E	1.443	74.68
EVAMB-E-65	2.287	68.15
EVAMB-E-70	3.641	82.45

N-tallow alkyl tri-methylene diamine has been used as surfactant (cationic type). The lipophilic (nonpolar) part interact with bituminous phase resulting the other end of diamine group (polar) available for water, Salager (2002). Surfactant has been prepared in acidic water phase to allow amine as a proton receptor being positively charged. In this sense, zeta potential measurement was performed to estimate the charged value, and the results are shown in Table 4.3.1. All emulsion studied present

positive charge value higher than 65, suggesting a high electrophoretic mobility that is equivalent to the estimated surface charge value, hence providing excellent stability.

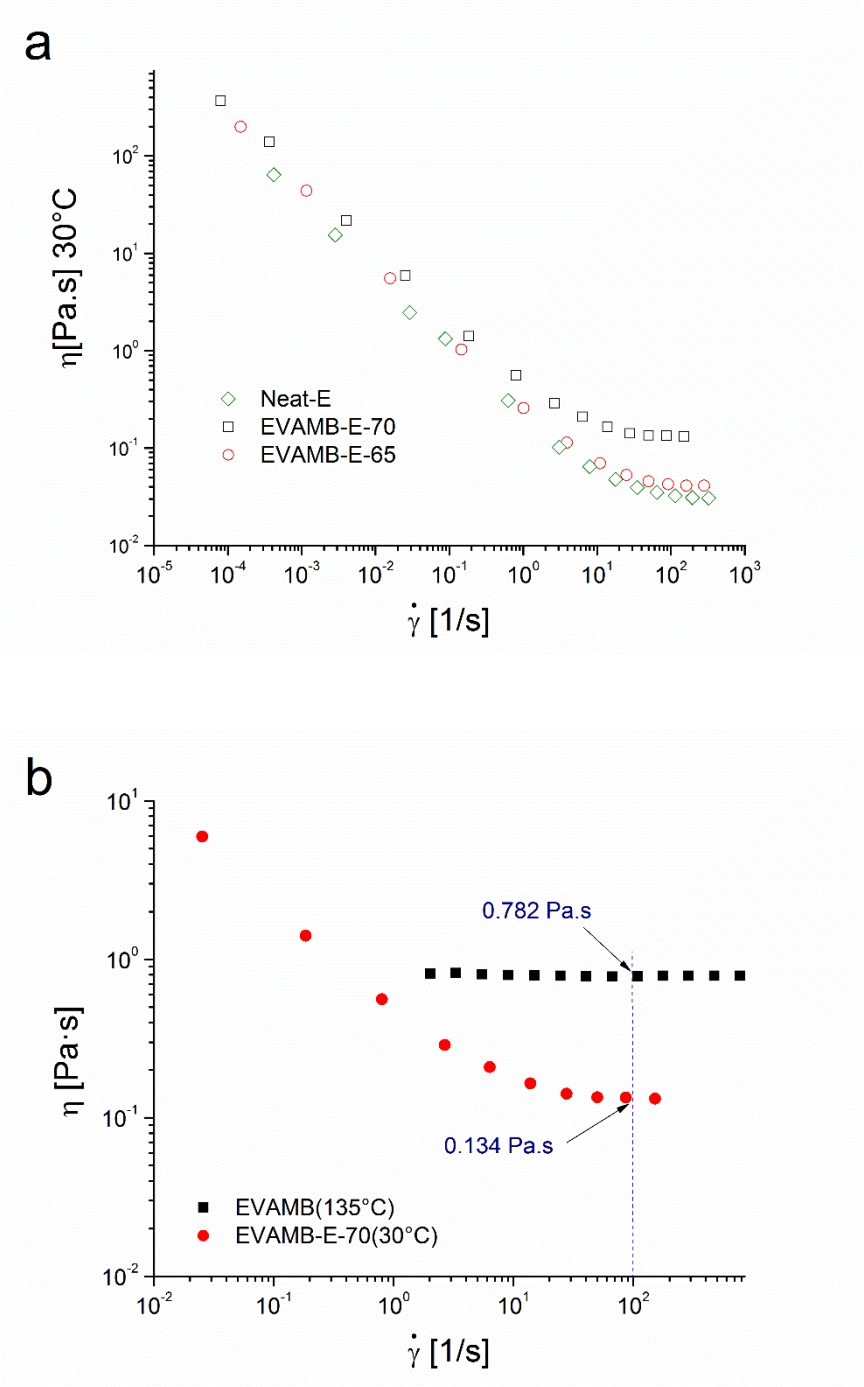

Figure 4. 3. 4 (a) Viscosity curve of emulsion at 30°C and (b) Viscosity comparison between EVAMB at 135 °C & EVAMB emulsion at 30 °C

Viscosity curves of emulsion for neat and both EVAMB cases at 30 °C are displayed in Figure 4.3.4a. The selection of 30 °C was based on emulsion application temperature, for cold mixes technology, typically from 25 to 60 °C (Rubio et al. 2012). For all emulsions tested, a shear thinning behavior was noticed from 10^{-4} s^{-1} to 10 s^{-1}, followed by a constant viscosity. Neat emulsion with 65 % suspended bituminous phase and EVAMB-E-65 gave a close value of high-shear-rate limiting viscosity, around 35 mPas, whilst EVAMB-E-70 has a value about 134 mPas. This result agrees with the larger volume fraction of disperse phase of system EVAMB-E-70, which leads to a higher packing density and, therefore, to a higher viscosity of the expected deflocculated emulsion at high shear rate (Otsubo and Prud'homme 1994b; Read and Whiteoak 2003; Carrera et al. 2015).

In the interest of comparing the two tested methods, binder viscosity curve at 135 °C (elevated temperature method) and its emulsion with 70% bituminous phase (reduced temperature method) were shown in Figure 4.3.4b. In that particular case, emulsion technology presented a viscosity difference by 6 times lower than the elevated temperature method for a more effective flowability.

4.3.4 Conclusion

The study of binder rheological behavior, through steady shear viscosity and oscillatory shear measurements, suggests that EVA copolymer containing lower VA content, 18%, affects more the viscoelastic parameter and thermal susceptibility of modified binder within its in-service temperature. Whilst, binder flow resistance was seen to decrease by increasing MFI after crystalline fraction vanished, suggesting better flowability for binder with higher MFI. The necessity of enhanced fluidity is to

promote a milder processing condition for the production of EVA modified bitumen emulsion. Thus, EVAMB-VA18-MFI500 was selected for emulsion process.

Bituminous to water phase ratio affects DSD and, mainly, high-shear-rate limiting viscosity of the emulsion. Coarser droplet size, as perceived in $D_{3,2}$, was reported for higher bitumen concentrations and/or for more viscous binders. In the interest of underlining the involvement of emulsion technology, emulsion viscosity at 30 °C was reported 6 times lower than binder viscosity at 135 °C, regardless the temperature difference that could suppress the energy consumption and environmental risk.

4.4 Design of lignin-based cationic emulsifier and emulsion formulation for road paving application

ABSTRACT

Lignin, apart from being the second most abundant natural polymer available, is a potential material to be value-added, rather than ending up burnt. This work aims to develop cationic lignin-based emulsifiers to be used in bitumen emulsions for road paving application. Cationic emulsifiers, highly demanded in road paving, cannot be manufactured directly from alkali lignin, thereby requiring modification. Amination through Mannich procedure is seen prospective since the attached amines can be positively charged in acidic medium. On these grounds, several parameters, including reaction route, reagents ratio and amines type were optimized by the assessment of the emulsification capability of silicone oil-in-water emulsions (used as bitumen emulsion prototypes). Resultant emulsion properties were evaluated through droplet size distribution (DSD), microstructural observations (by optical micrographs), Z-potential analysis and viscous flow/viscoelasticity tests. On the other hand, the effect of emulsion formulation was studied as a function of surfactant concentration, pH of aqueous phase and O/W ratio. Finally, a comparative analysis between bitumen emulsions prepared with cationic modified lignin and a commercial cationic emulsifier is presented. The results suggest that the proposed Mannich reaction, carried out under alkaline medium for a reagent ratio between 1/11/11 and 1/22/22 using tetra-ethylene penta-amine ($(NH_2C_2H_4NHC_2H_4)_2NH$) yields a surfactant which, if used at pH < 2 and 0.5 wt.% satisfies the performance expected for a typical bitumen emulsion at O/W ratios between 60/40 and 70/30.

4.4.1 Introduction

Bitumen emulsion is a class of bituminous binder that allows bitumen mixing with aggregate and further compaction operations to be performed even at ambient temperature. Issues associated to hot mixes asphalt (HMA), such as high energy consumption, dust and toxic fume released, are reduced based on the fact that emissions are 7 times lower (in kg eq. CO_2/ton product), and energy consumption is 7.5 times lower (in MJ/ton product) than HMA (Lesueur 2011). In such a bituminous product, bitumen is dispersed and stabilized in the form of droplets in an aqueous phase, giving rise to the so-called oil-in-water O/W emulsions. To that end, emulsion demands an emulsifier able to remain at the interface of two immiscible liquids.

As today's development is expected within the frame of sustainability, material environmental indicators such as energy, emissions, material (renewability) are concerned. In this regard, lignin is a natural polymer embedded in lignocellulose form that made the structural layer of woody plants. While the cellulose is used as the main input for paper-making industry, the rest of lignin, previously broken down, ends up burnt in cogeneration system, with only 5% used for other functionalities. In recent decades, vast researches in this topic have introduced various ways to value-add lignin in search of many novel advanced materials through modifications (e.g. by fragmentation, substitution and/or attachment of different functional groups) for broadening its potential application, including emulsification (Laurichesse and Avérous 2014; Norgren and Edlund 2014) .

For transport infrastructure materials, lignin and its derivatives present structural similarity with bitumen, hence, they result suitable for being used to partially replace bitumen role in asphalt mixture (Slaghek et al. 2015). In general, lignin is a polyanionic

polyelectrolyte, in which their functional groups of carboxylic acid and phenolic hydroxyl could be potentially dissociated into ions under high level of alkalinity (Gundersen 2001), thus presenting surface properties. In this regard, lignosulfonates have been already used as commercial anionic emulsifiers with a wide range of working pH values. Lignosulfonate is commonly produced from pulp plant adapting sulfite process that represents less than 15% worldwide production. Alternatively 85% pulp industry utilizes Kraft process, yielding alkali lignin or Kraft lignin (Carvajal et al. 2016). Furthermore, a large quantity of lignin from biomass-based biofuel production may also be expected in the next coming years. The absence of protonatable functional groups does not permit the three previously mentioned lignins to work as cationic emulsifier, thus requiring modification. Interestingly, phenolic derivatives largely available in the lignin aromatic structure are perceived as building blocks where protonatable functional groups, such as amines, are easily attached. Besides, in the blend with bitumen, amines may play roles as anti-oxidants (James and Stewart 1991) or antistripping agents (Zhu et al. 2014). In addition, lignin itself has demonstrated anti-aging properties indicated by their carbonyl index in bitumen blends (Thomas 2005).

A Mannich reaction is a widely-known method for amination, involving formaldehyde and amines as reagents (Mannich and Krösche 1912). The reaction could be performed under acidic or alkaline environment (Li 2006). A research work by Du et al. (2014) reports that the intermediate compound is a product of the amine-formaldehyde reaction attacking lignin on its aromatic ring C5, as shown in Figure 4.4.1. Another study (Liu et al. 2013) suggests that amino-alkylation occurs at lignin carbonyl groups. Once reacted, the modified lignin becomes positively charged in acidic environment. These charges, when used in cationic bitumen emulsions for

asphalt, stabilize bitumen-water interface and, more interestingly, promote binder interaction and adhesion to the negatively charged aggregate surface. The reason why cationic emulsifiers are preferred relies on the negative charge present on the surface of siliceous based derivatives (Si_xO_{2y}), which are commonly found in many aggregates (Ronald and Luis 2016). Thus, cationic bitumen emulsions dominate the market (Read and Whiteoak 2003).

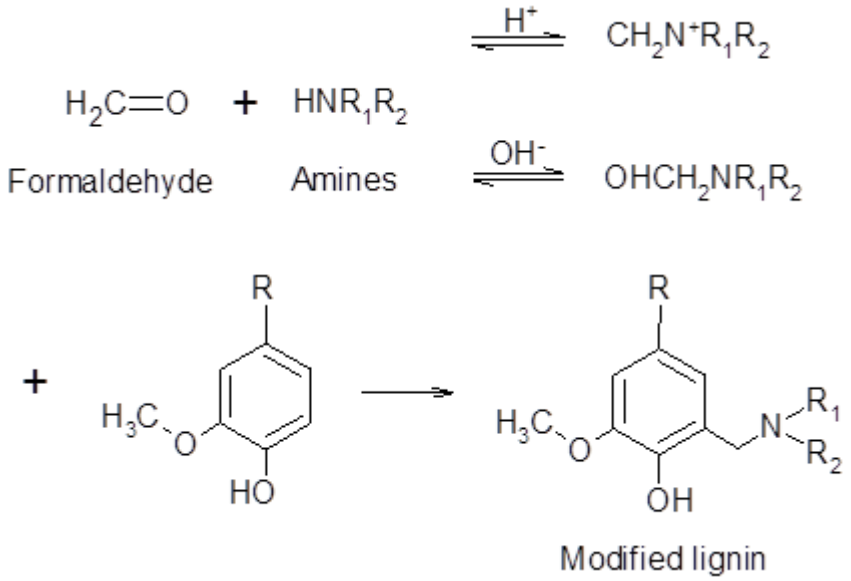

Figure 4. 4. 1. Mannich reaction mechanism (an example in alkaline environment): A) an intermediate compound formation from formaldehyde and amines (ie. TEPA) and B) complete reaction between Kraft lignin and previously formed intermediate compound, adapted from article (Du et al. 2014).

This work aims to develop alkali lignin-derived (Kraft lignin-derived, KL) cationic emulsifiers via the Mannich reaction. With that purpose, different variables such as reaction route (alkaline or acidic), types of amines and reagent ratios were studied. The performance of the resulting cationic surfactants was optimized by evaluating their emulsification capability on prototype silicone oil-in-water emulsions, in terms of droplet size distribution (DSD), microstructure (by optical micrographs), Z-potential, and rheological behavior. On the other hand, the effect of emulsion

formulation was studied as a function of emulsifier concentration, pH of aqueous phase and O/W ratio. Finally, a comparative analysis between bitumen emulsions prepared with cationic modified lignin and a commercial cationic emulsifier is presented.

4.4.2 Experimental

4.4.2.1 Materials

For the preparation of the cationic emulsifier, a non-commercial Kraft lignin (KL) was provided by *Instituto Nacional de Investigación y Tecnología Agraria y Alimentaria* (INIA), Spain. This lignin, with approximate molar mass of 3000 g/mol, was obtained from a Kraft process of *Eucalyptus globulus* hardwood. This material is soluble in alkaline aqueous solution at pH higher than 10 (with NaOH) and in the organic solvent used in this study under acidic conditions, 1,4 dioxane. For the Mannich reaction, two other reagents (formalydehyde 37 wt.%, FD, and different types of amines, AM) were purchased from Sigma Aldrich, Spain. Amines studied were: dimethylamine (DMA), diethylenetriamine (DETA), tetraethylene-pentamine (TEPA) and polyethyleneimine (PEI). Finally, a commercial cationic surfactant, n-tallow alkyl tri-methylene diamine, A100 (from Kao Chemicals, USA) was selected as a reference.

In the production of the prototype emulsions, silicone oil (FS100 from Esquim SA, Spain) with an approximate viscosity of 100 mPa·s at ambient temperature was chosen. The reason behind this selection was to imitate, without need of heating, bitumen viscosity prior to its emulsification at high temperature, which is recommended to be less than 200 mPa·s before entering colloid mill (Read and

Whiteoak 2003). Lastly, bitumen with a penetration grade of 500, kindly donated by Repsol SA Spain, was emulsified for the final stage of the study.

4.4.2.2 Preparations

As mentioned earlier, modified lignin (MKL) production can be conducted in either acidic or alkaline medium which, as shown in Figure 4.4.1, yields different routes, in terms of the intermediate compound formed. In case of acidic route, the KL has to be previously solubilized in 1,4 dioxane. Immonium ion and amino-alkylated products of FD and different types of AM formed before reaction with the solubilized ligninin acidic and alkaline media, respectively. The reactions were always performed in a rounded-bottom glass flask, with stirring at 1000 rpm, at 60 °C for 4 hours. Reagent ratios between KL, FD and AM ranged from1/5/5 to 1/44/44. After reaction completion, HCl 37 wt.% and distilled water were used to adjust aqueous phase pH and MKL concentration.

Emulsion prototypes (with O/W ratios of 60/40 and 70/30 by mass) were prepared by conveniently premixing FS100 and aqueous phase containing modified lignin at the required concentration. Emulsification was carried out in a rotor-stator homogenizer Ultraturrax T25 (IKA, Germany), with S25N dispersion element at 20000 rpm, for 4 minutes at room temperature. Finally, production of bitumen emulsion was conducted following a similar procedure. In this case, bitumen and aqueous phase required previous heating up to 90 °C.

2.3. Emulsion characterization

Laser diffraction, performed using Malvern Master Sizer 2000 (UK), was employed to measure droplet size distribution (DSD). Between 1 and 3 drops of concentrated

emulsion was dispersed into water in a dispersing chamber with stirring at 1500 rpm and pumping recirculation. Zeta potential tests, performed using Malvern Zetasizer (UK), allowed surface charges to be inferred. Sample was injected using syringe into inverted folded capillary zeta cell DTS 1070 for avoiding bubble formation. Three measurements were performed for each sample and the average value reported.

The rheological characterization was carried out by means of steady viscous flow tests and dynamic shear frequency sweeps, at 30 °C. Measurements were conducted in a controlled-stress Physica MCR-301 by AntonPaar (Austria). For steady shear tests, in order to avoid wall-slip phenomenon, serrated measuring cup and coaxial cylinder Z20-DIN (27 mm diameter, 1 mm gap) were used to accommodate 20 mL of emulsion. Tests at 30 °C were performed by progressively increasing the applied stress so that shear rate ranged from 0.01 and 50 s^{-1}. An equilibration time of 120 s guaranteed steady state conditions at every selected shear stress. For oscillatory shear tests, frequency sweeps within the linear viscoelasticity region were performed on the same device but using serrated plate-plate geometry with a diameter of 50 mm and 1 mm gap. Measurement conditions were applied in a frequency range between 1 and 100 rad/s, at a temperature of 30 °C. At least, two replications were always performed.

Optical micrographs were captured at ambient temperature using Olympus BX51 microscope on 50 µL of emulsion placed on a standard microscope slide (76 × 26 mm).

4.4.3 Results and discussion

4.4.3.1 Kraft lignin chemical modification

Emulsion properties such as droplet size and its distribution, viscosity and microstructure, are closely linked to emulsifier characteristics. The optimization of the

emulsifier was based on three variables involved in the Mannich reaction: reaction route, type of amines and reagents ratio, and the evaluation required emulsions formulated under identical conditions of emulsifier concentration, pH of aqueous phase and O/W ratio. Moreover, these parameters are further studied as they strongly affect the final properties of the emulsion, as suggested by Ronald and Luis (2016). The effect caused by processing was excluded from this study, by maintaining the procedure of preparation for all emulsion the same.

For studying the reaction route, Figure 4.4.2A compares droplet size distribution (DSD) curves of emulsions stabilized by cationic modified lignins, synthetized under acidic and alkaline conditions with DMA, and by the reference emulsifier A100. Lignin-based emulsifier was successfully produced using both reaction routes, as may be deduced from their DSD curves shown in Figure 4.4.2A. Compared to the reference emulsion (A100), which presented unimodal distribution with a peak centered at ~5 μm, the use of 1 wt.% of DMA-KL emulsifier modified through the acidic route could not approach the targeted reference peak value. In this case, the peak appeared centered at a too large size (about 300 μm). When employing 1 wt.% of alkaline-based DMA-emulsifier, the peak was observed at a smaller size range from 10 to 80 μm. Although particle size is still not comparable to the commercial emulsifier, the reaction was accommodated via alkaline route from this point forward.

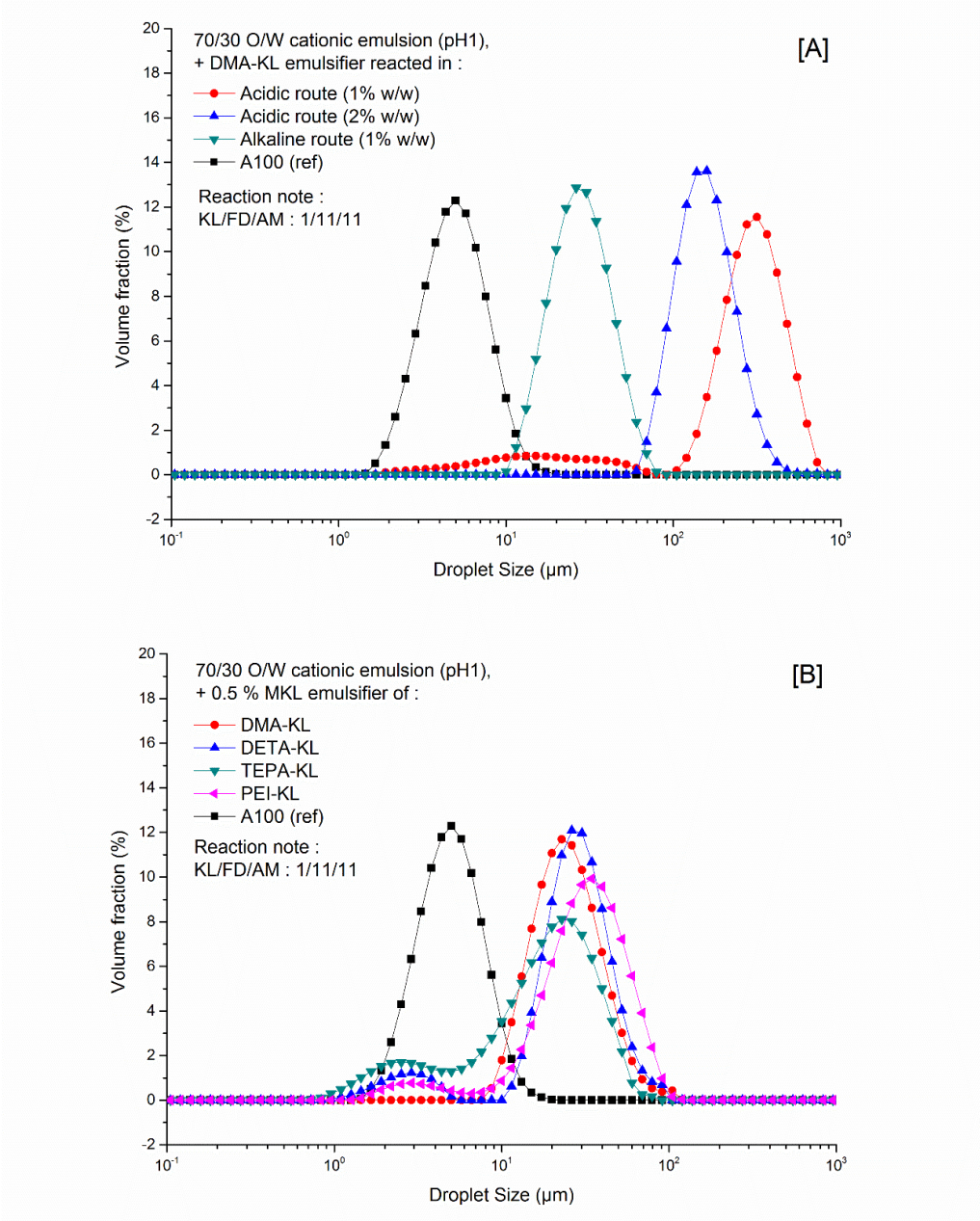

Figure 4. 4. 2. Droplet size distribution of emulsion stabilized by MKL emulsifier, previously prepared as a function of A) reaction route and B) type of amine reagents, and a commercial emulsifier (A100) as reference.

Optical micrographs shown in Figure 4.4.3 support the reaction route selected. Firstly, those micrographs confirm the average droplet size measured by laser diffraction illustrated in Figure 4.4.2A. The second interesting observation is the presence of some black particles in Figure 4.4.3A that may refer to solid unreacted KL raw material (inset of Figure 4.4.3A), which remains in the acidic route. On the contrary, no sign of

black particles was arisen for emulsions stabilized by alkaline-prepared emulsifier (Figure 4.4.3B). Thus, qualitatively, the success of alkaline route might be asserted from its higher quantity of cationic emulsifier soluble in aqueous phase at pH 1, given that peak shifting to lower drop sizes is presented in Figure 4.4.2A. It is worth noting that alkali lignin is naturally insoluble in acidic medium, such that 1,4 dioxane (organic solvent) is required for conducting single phase reaction in the acidic route. If the solvent is unable to completely dissolve the lignin, then multiphase reaction, governed by mass transfer (by diffusion) at the interface, may occur (Walas 1997). In consequence, under the selected reaction conditions specified in experimental section, of this study, the alkaline route is seen more effective.

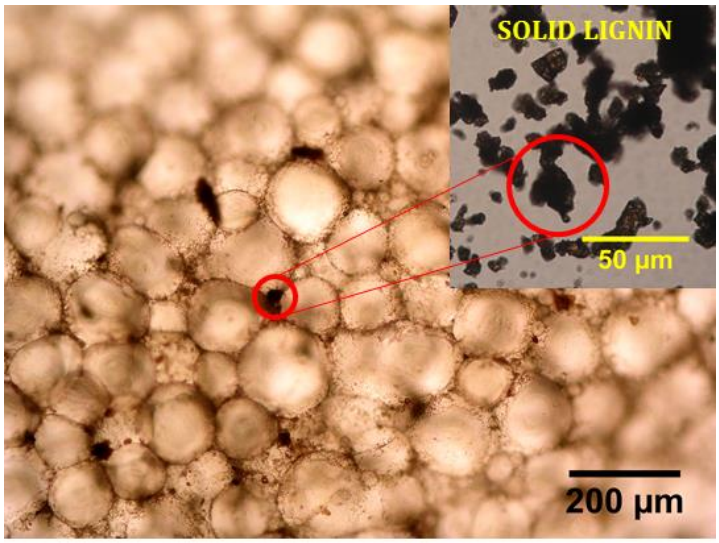

[A] Acidic route on DMA-KL

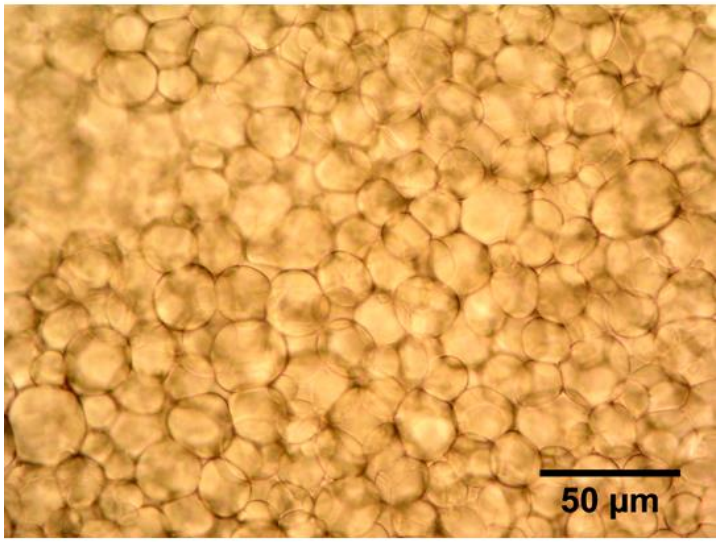

[B] Alkaline route on DMA-KL

Figure 4. 4. 3. Optical micrograph of emulsion prepared using emulsifier, previously reacted in (A) acidic and (B) alkaline route, and solid lignin (inset 3A).

In an attempt to find a relationship between surfactant performance and the number of protonatable units (N atoms), different amine molecules were studied: DMA (1N), DETA (3N), TEPA (5N) and PEI (~20N). Figure 4.4.2B presents DSD curves of emulsions stabilized with alkaline-prepared emulsifiers previously reacted with the above listed types of amines. Apart from DMA-KL and A100 emulsion, the remaining

emulsions have shown bimodal curves, with the second peak arising between 1 and 10 µm. No qualitative differences among all those lignin emulsifiers, in terms of DSD distributions, were found. Such DSDs were quantitatively compared using Sauter mean diameter ($D_{3,2}$), calculated as follows:

$$D_{3,2} = \frac{\sum_i n_i \cdot D_i^3}{\sum_i n_i \cdot D_i^2} \qquad (4.4.1)$$

where n_i is the number of droplets with diameter D_i. Results are shown in Figure 4.4.4 for the four types of amine studied, for two selected O/W ratios of 60/40 and 70/30.

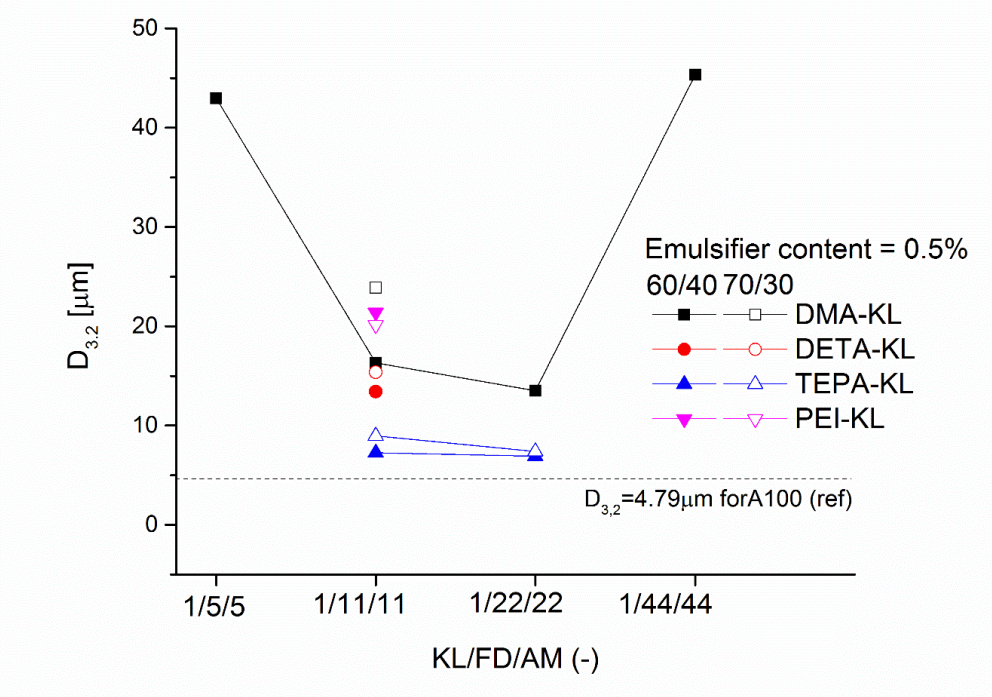

Figure 4. 4. 4. Surface mean diameter ($D_{3,2}$) of 60/40 and 70/30 cationic emulsion vs reagent ratio (KL/FD/AM) used to prepare MKL emulsifier, as a function of type of amines.

In the case of DMA-KL and TEPA-KL, results are also given, as a function of the reagents ratio (KL/FD/AM of 1/5/5, 1/11/11, 1/22/22 and 1/44/44 for DMA-KL and of 1/11/11 and 1/22/22 for TEPA-KL). The reagent ratios were initially opted referring

to the number of estimated active sites available for reaction. Based on a generally accepted mechanism for Mannich reaction on lignin, the amine-formaldehyde intermediate compound selectively attacks the aromatic C_5 and carbonyl group (Liu et al. 2013; Du et al. 2014), which may potentially occur on Guaiacyl (G) and p-hydroxyphenyl propane (p-H) units. However, the presence of both active sites is ruled by lignin origin related to the wood source and process applied before its isolation and purification (Laurichesse and Avérous 2014). On those uncertainties, this part of the study merely focused on which reagents ratio and amine type yielded the emulsifier which was able to provide the smallest droplet size. As shown in Figure 4.4.4, minimum $D_{3,2}$ values were observed at a ratio between 1/11/11 and 1/22/22 for DMA. This result may suggest that at the lowest reagents ratio the stabilization originated by electrostatic repulsion may be insufficient. In other words, the charge density on the lignin molecule may not be enough. On the contrary, at a fixed emulsifier concentration of 0.5 wt.%, a too high ratio means much less lignin (building blocks) available as emulsifier units. Based on that, 1/11/11 was selected for the remaining AMs study. As observed, the relationship found, whereby $D_{3,2}$ decreases as N atom per amine molecule increases, is valid for DMA-KL, DETA-KL, and TEPA-KL emulsion, whilst fails for PEI-KL emulsion. For the same reason as before, PEI, with very high molar mass if compared to the other amines (see Table 4.4.1), yields much less modified lignin units. When used at a constant concentration of 0.5 wt.% as in Figure 4.4.4, this means poor stabilization if compared to the other emulsifiers. Finally, TEPA-KL $D_{3,2}$ was shown the closest to reference value of about 5 μm, even better when formulated with ratio of 1/22/22, which yielded average size of about 7 μm. Hence, Figure 4.4.4 makes clear the importance of the electrostatic repulsion among bitumen drops just formed upon breaking-up occurring at the dispersing tool, in terms of the

expected DSD of the emulsion leaving the colloid mill. For this reason, TEPA-KL was the emulsifier selected for further optimization of the emulsion formulation.

In addition, a slightly smaller $D_{3,2}$ was observed for smaller O/W ratio, at 60/40 than 70/30, for the majority of amine group except for PEI-KL emulsion. At the smallest O/W ratio, the emulsification device efficiency (related to stirring energy transferred per unit volume) is higher, yielding the formation of a larger droplet surface area (Gingras et al. 2005).

4.4.3.2 Effect of emulsion formulation

The effect of TEPA-KL emulsifier concentration and pH of aqueous phase on DSD of 70/30 emulsions is shown in Figure 4.4.5. As seen in Figure 4.4.5A, at 0.5 wt.% of emulsifier, a bimodal distribution is shown, with peak maximums located at ~15 μm and ~2 μm (this latter slightly superposed to reference peak). When the concentration was reduced to 0.25 wt.%, the smaller peak disappeared and the main peak shifted to ~40 μm. Further decrease to 0.125 wt.% of emulsifier caused a shift to ~70 μm, as a consequence of a thinner adsorbed emulsifier layer which upon compression (driven by attraction interaction) cannot sustain droplet stability, giving rise to coalescence up to the point at which a stable layer thickness is attained (Tadros 2014). Thus, the reduction of TEPA-KL emulsifier concentration at the interface yielded the decrease of total droplet surface, i.e. larger droplets were formed.

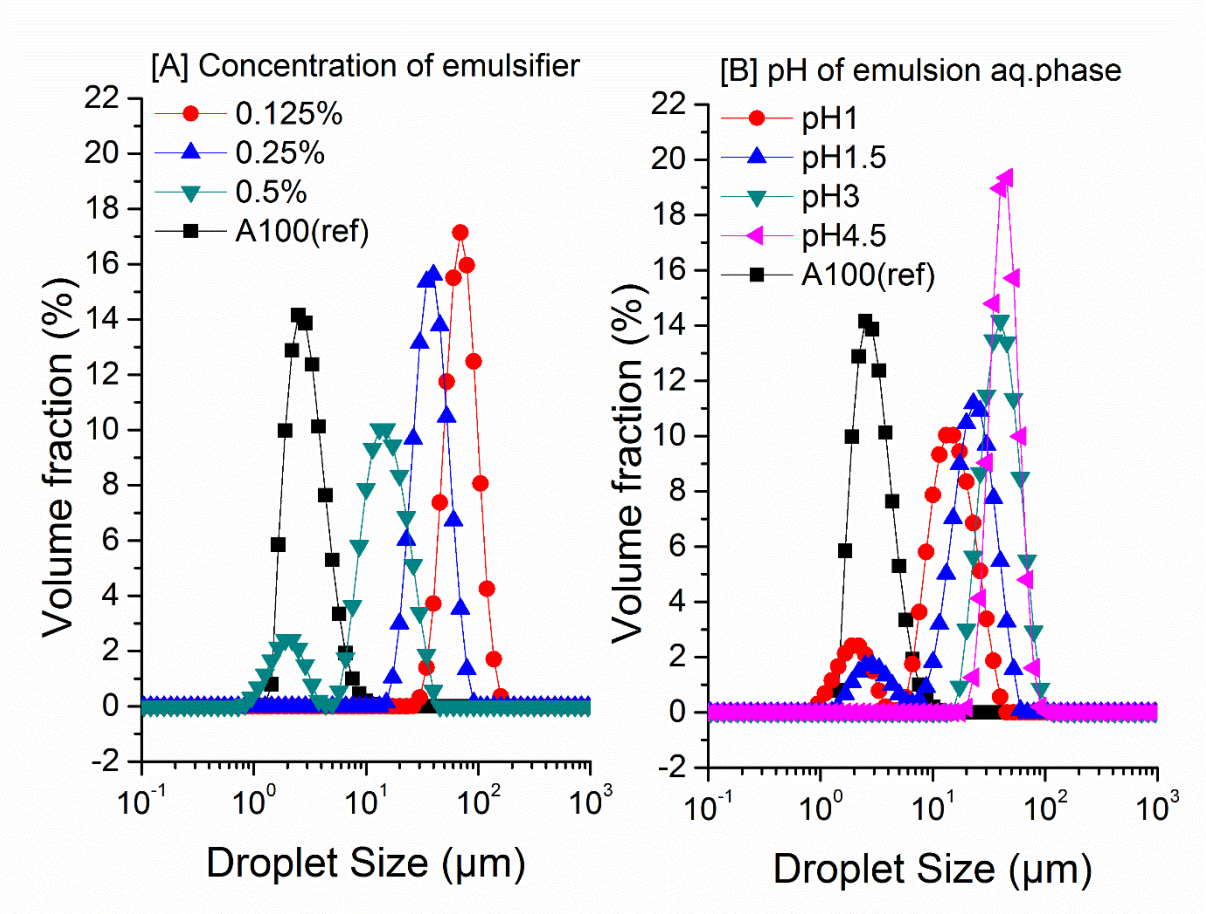

Figure 4. 4. 5. Droplet size distribution of emulsion containing TEPA emulsifier as a function of (A) Emulsifier concentration in interval range of 0.125 – 0.5% and (B) aqueous phase pH in interval range of 1 – 4.5, including emulsion with A100 as reference.

Similar trend was observed in Figure 4.4.5B, with bimodal curves for emulsions prepared at low pH of aqueous phase, of 1 and 1.5, which became unimodal (and shifted to larger size domains) by increasing pH. At low pH, the charge density of the emulsifier increases, due to the presence of a higher number of protonated groups ($>NH^+$). This improves the repulsive action against Van-der-Waals attraction forces (Tadros 2011), so that the chance for coalescence is minimized, and smaller droplets can be maintained.

4.4.3.3 Emulsion rheology and stability

Figure 4.4.6 presents viscous flow curves of emulsions, at 30 °C, as a function of the amine type used for obtaining modified lignin emulsifier and the O/W ratio.

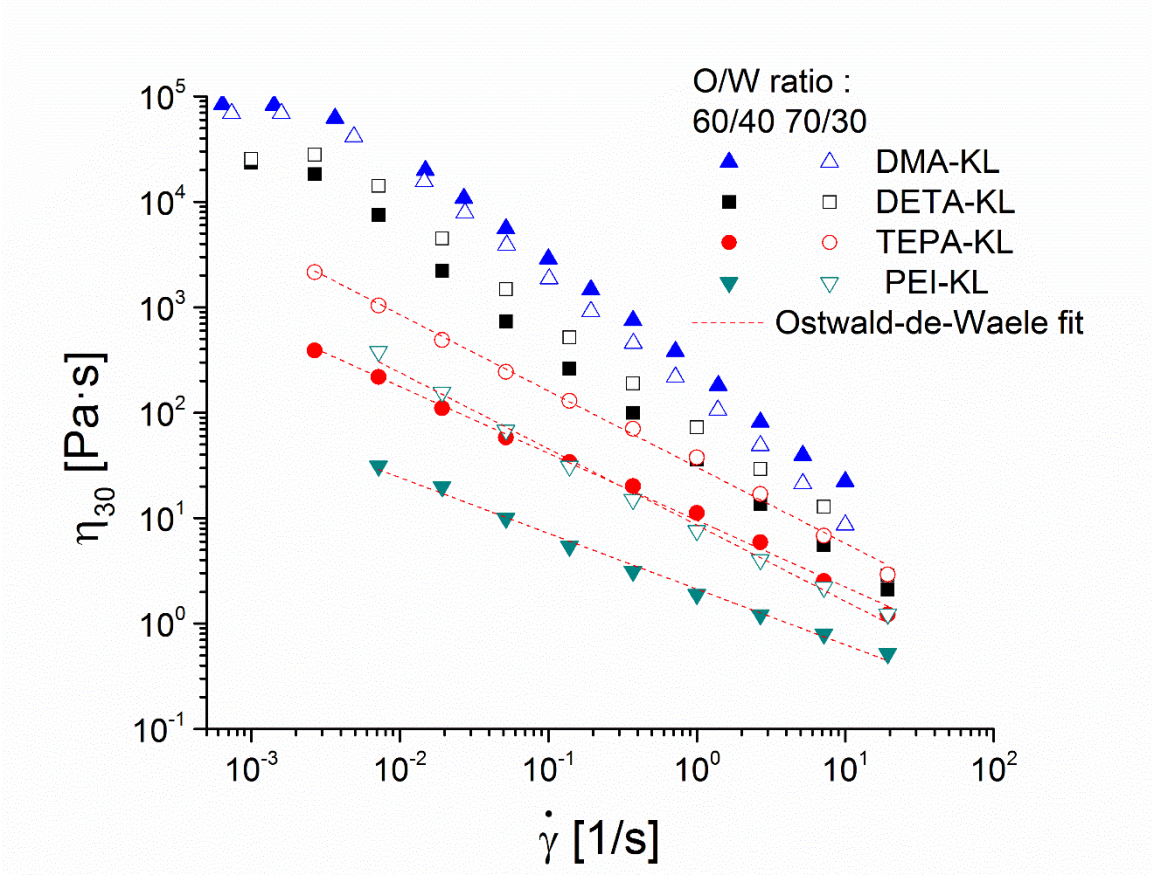

Figure 4. 4. 6. Viscous flow behavior of emulsion as a function of amines group used to modify lignin at O/W ratio of 60/40 and 70/30.

The selection of the test temperature relied on the expected bitumen emulsion application (Vaitkus et al. 2016), that is, cold mixed asphalt technology in this case. As can be observed, all emulsions, no matter their bitumen concentration (60/40 and 70/30 O/W ratio), showed a shear thinning behavior between 0.01 and 30 s^{-1}. The viscous behavior of emulsions stabilized by TEPA-KL and PEI-KL was described fairly well by the Ostwald-de-Waele model:

$$\eta(\dot{\gamma}) = k \cdot \dot{\gamma}^{n-1} \quad (4.4.2)$$

where k and n are consistency and flow indexes, respectively. As shown in Table 4.4.1, the highest k value was found for emulsion formulated with TEPA-KL, and the opposite trend was shown for n index, what implies that TEPA-KL emulsion is more structured than PEI-KL emulsion (Barnes 1994). As previously commented, the balance between building block units and protonatable sites, that is, charge density at the droplet surface, seems to be more favorable for TEPA-KL emulsion in such a way that enables stronger droplets interactions (Yuliestyan et al. 2017).

Table 4. 4. 1. Oswald-de-Waele fitting parameters, of power law (n) and consistency (k) indexes, of emulsion with 60/40 and 70/30 of O/W ratio as a function of amines at various MW (and quantity of protonatable N unit) used to prepare modified lignin emulsifier, and its corresponding zeta potential values (ζ).

Emulsion		60/40		70/30		ζ, mV
modified with amines	$MW_{(amines)}$, g/mol	k, Pa·s^n	n, -	k, Pa·s^n	n, -	
DMA	45.08	--	--	--	--	5.6
DETA	103.17	--	---	--	--	8.5
TEPA	189.30	9.58	0.36	30.56	0.27	18.7
PEI-	~800	2.08	0.47	8.46	0.30	20.9

No rheological model was used to describe the viscous flow behaviors of DMA-KL and DETA-KL emulsions. They exhibited a complex flow behavior with a Newtonian region at the lowest shear rates studied, followed by a sharp decrease in viscosity as shear rate increased (Figure 4.4.6). Such a steep slope of the shear rate dependence of viscosity for DMA-KL and DETA-KL emulsions gave inconsistent negative values for n,

which for a shear-thinning fluid has to be between 0 and 1. This flow behavior arises from flow instabilities due to microstructure collapse, which might involve deflocculation, droplet coalescence and, eventually, emulsion destabilization.

The result in Figure 4.4.6 might be explained by means of zeta potential 'ζ' results shown in Table 4.4.1. Firstly, it is necessary to highlight that the positive ζ values observed mean that the emulsifiers (also their derived emulsions) present positive surface charge, as a consequence of protonated amine groups. TEPA-KL and PEI-KL emulsifiers presented the highest ζ values. A higher surface charge density favors electrostatic repulsion and hinders flocculation, Thus, the emulsions formulated with those emulsifiers showed reduced viscosity and less pronounced shear-thinning behavior within the shear rate interval tested. As opposed, the ζ value of DMA-KL emulsion, 5.6 mV was the smallest. The contribution of the emulsifier charge to the emulsion stability is low. Moreover, due to the low molecular weight of DMA reagent, the DMA-KL emulsifier has the highest fraction of lignin, promoting more intense hydrophobic interactions between drops that favors their flocculation. This phenomenon contributes to an important viscosity increase by formation of a gel structure (explained below). As a result, emulsion instability is favored by means of flocculation or even partial coalescence (Tadros 2014). However, this flocs formation does not necessarily involve complete coalescence, as reversibility was found upon re-dispersion. Based on that, the structured-flocs formed can be severely disrupted upon applying an increasing shear stress ramp, as in Figure 4.4.6. Padmanabhan and Bhattacharya (1991) explanation also negative 'n' values found during extrusion of corn materials. They attributed its origin to molecular degradation, viscous dissipation and wall slip under shear. In our case, wall slip and viscous dissipation are excluded due to the use of serrated sensor system. Thus, considering molecular degradation

analogy, low internal friction upon de-flocculation phenomenon would turn out in a very severe shear thinning, which could give rise to inconsistent negative values for 'n' index. This behavior results more pronounced for the most concentrated 70/30 emulsions.

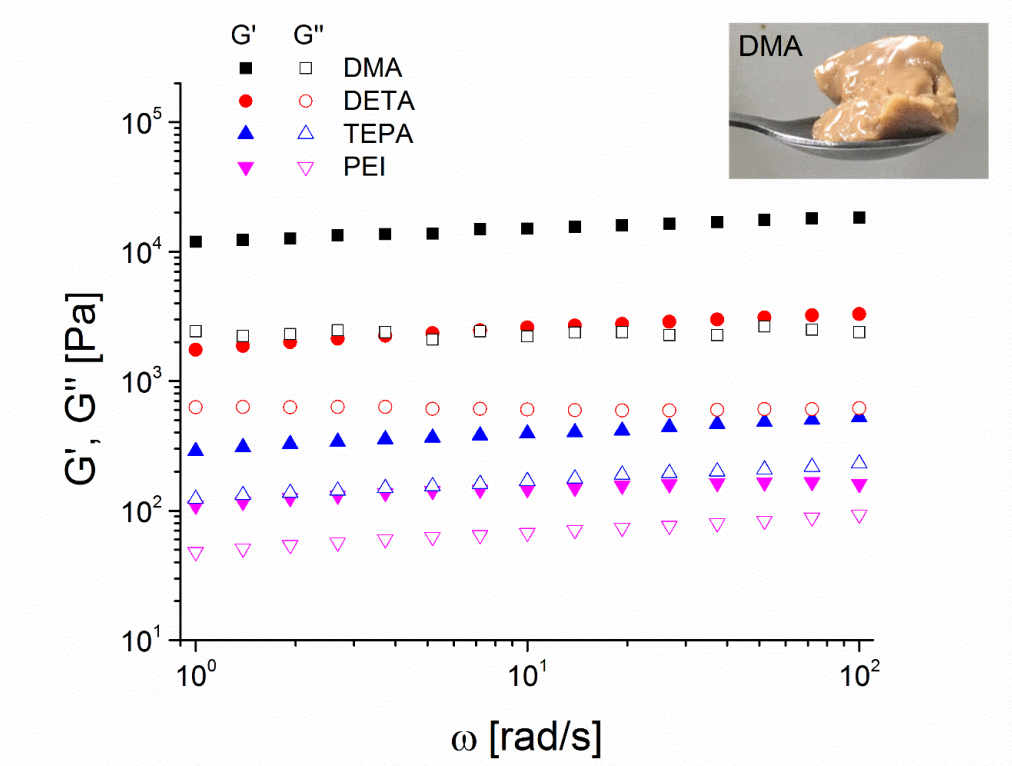

Figure 4. 4. 7. The evolution viscoelastic properties, of storage (G') and loss (G'') modulus, in frequency domain of 60/40 emulsion with 0.5% of lignin-emulsion, previously prepared with different amines.

Figure 4.4.7 presents the evolution of viscoelastic properties with frequency of 60/40 emulsions. In all cases, storage modulus was always higher than loss modulus, which implies a prevailing elastic behavior, with G' and G'' largely frequency insensitive. This is the typical behavior of gel systems. Within the range tested, the highest values of storage (G') and loss (G'') moduli are found for DMA-KL emulsion. Amines with higher quantity of protonatable units (with higher ζ values according to Table 4.4.1) yielded decreased moduli values. Moreover, from DMA to PEI emulsions, the distance between

G' and G'' became smaller and, so, the loss tangent (tan (δ) = G'' / G') values increased from 0.15 to 0.45, respectively. The lowest value of 0.15 reveals a more developed structural network (Barnes 1994; Tadros 2011). Thus, a value loss tangent of 0.15 and the visual appearance in Figure 4.4.7 suggest that DMA emulsion can be classified as a weak gel with tan δ below 1 but approaching a strong gel (tanδ < 0.1) and on the contrary to the case of PEI emulsion (Clark et al. 1987). In fact, Figure 4.4.6 shows extremely low power-law exponent. These results seem to confirm that gelation, due to extensive flocculation, is more likely when using lignin emulsifiers prepared with amines with low number N atoms and high quantity of lignin units. In the case of DMA, the electrostatic repulsion due to positive charged sites does not compensate the strong attractive forces as a consequence of hydrophobic interactions between lignin molecules. Hence, despite flocculation in DMA emulsion is merely a reversible physical state, its low values of ζ and tan δ are not desirable characteristics for bitumen emulsions which demand flowability for a better penetration and coating of the aggregate matrix during mixing. A better use of DMA-KL compound could be as a flocculating agent in acidic medium, studied by other authors (Fang et al. 2010). Therefore, considering DSD profile (Figure 4.4.2B) and viscous flow behavior (Figure 4.4.6), tetraethylene pentaamine (TEPA) is the best option for lignin amination, among other tested, to achieve the desired properties that allow its application in bitumen emulsions.

Besides the relation to emulsion behavior, all ζ values are small for an emulsion to be merely considered electrostatically stable. However, DSD evolution of DMA and TEPA emulsion over certain period of time (of 1 day, 1 week and 15 months) demonstrated an exceptional emulsion stability.

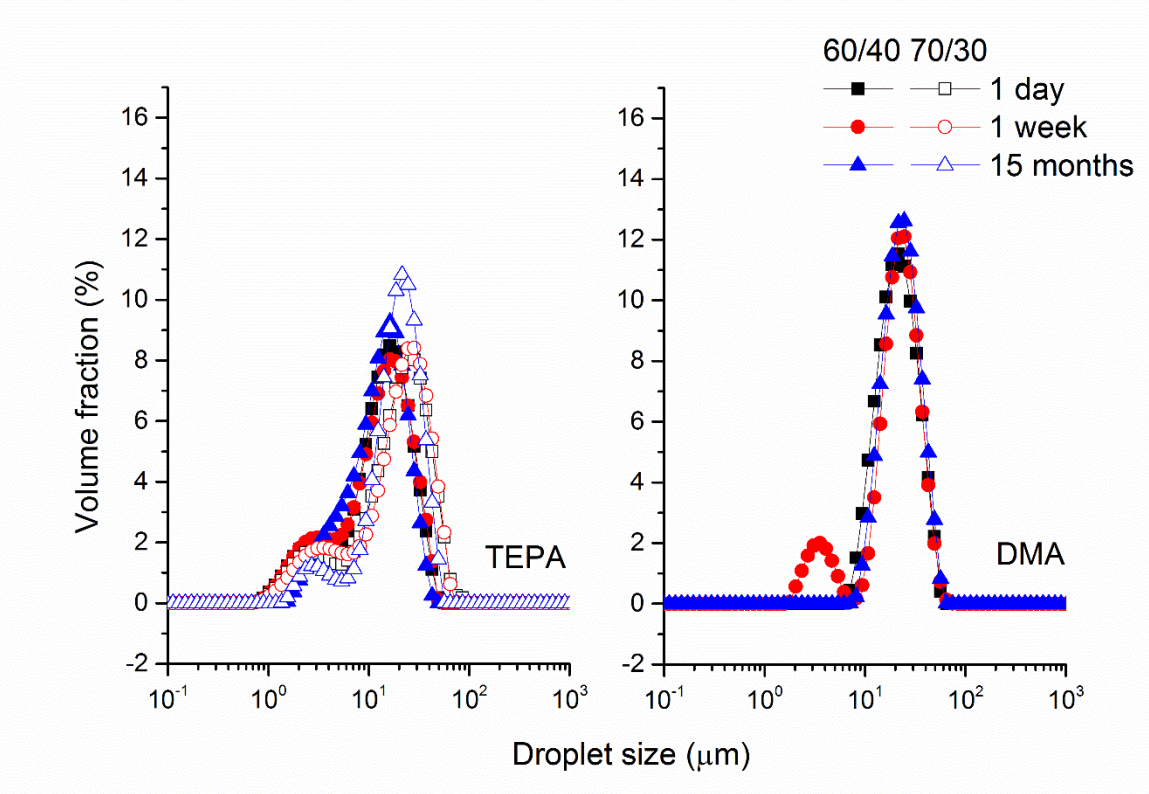

Figure 4. 4. 8. Droplet size distribution evolution, of 60/40 and 70/30 emulsion stabilized by TEPA-lignin and DMA-lignin, over period of 1 day, 1 week and 15 months.

Figure 4.4.8, which illustrates curves obtained after the emulsions re-dispersion, hardly shows shifting among DSD curves with time (and visual alteration was not observed, either). This suggests that stability mechanism is not only governed by electrostatic, but steric barrier as a secondary mechanism by mutual attraction (Fritz et al. 2002; Norgren et al. 2002), which was previously demonstrated by rheological characterization. Thus, aminated lignin, a macromolecule that (after amination) possess positive charge in acidic medium, is considered as polycation (polyelectrolyte), which in an appreciable thickness of adsorbed layer, laid at emulsion droplet interface, presented both electrostatic and steric characteristics, known as electrosteric.

4.4.3.4 Application to bitumen emulsions

Aiming to assess the ability of modified KL to stabilize bitumen emulsions for road paving, a 60/40 bitumen (B500) cationic emulsion was emulsified at pH 1 by a 0.5 wt.% of TEPA-emulsifier, which was reacted through the alkaline route at a 1/22/22 ratio.

Figure 4.4.9A presents DSD curve for the TEPA and the reference A100 bitumen emulsion. After 1 day storage, emulsion A100 shows a bimodal distribution whilst TEPA emulsion exhibits a unimodal curve of higher droplet sizes than the reference surfactant. If compared to silicone emulsions, surfactant A100 gave rise to a smaller size of $D_{3,2}$=2.56 μm for bitumen emulsion A100 (Table 4.4.2 and Figure 4.4.2). Conversely, bitumen emulsion emulsified by TEPA presents a higher Sauter mean diameter $D_{3,2}$ than its counterpart formulated with silicone (Table 4.4.2 and Figure 4.4.4). On the other hand, A100 bitumen emulsion DSD evolved over 1 week towards higher sizes, as the peak previously found at ~1 μm vanished. However, TEPA bitumen emulsion profiles superposed one onto another, exhibiting excellent stability, which agrees with previous results from silicone oil emulsion prototypes (Figure 4.4.8). Interestingly, A100 proved successful at electrostatically stabilizing small droplets upon rupturing of larger drops, whilst TEPA-KL mainly demonstrated a great ability to stabilize the final emulsion by steric mechanism.

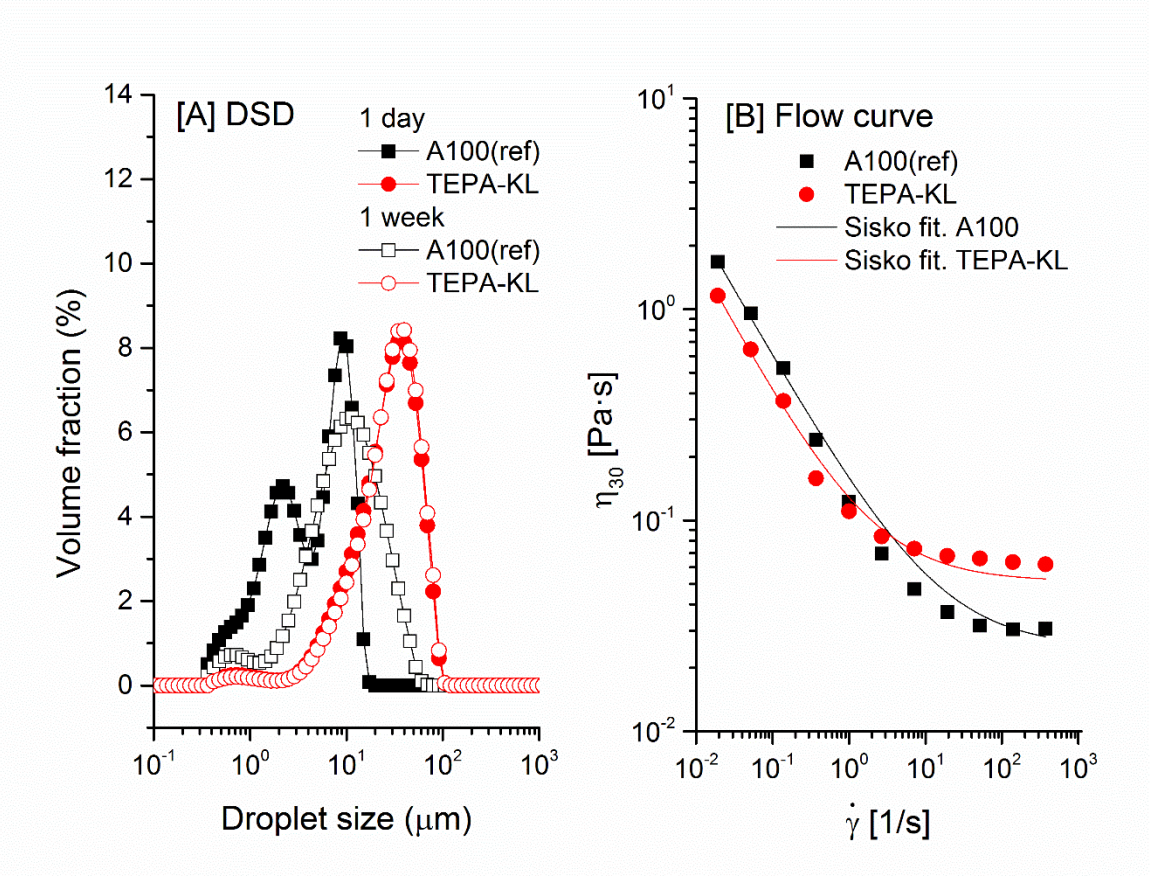

Figure 4. 4. 9. Characterization results, of (A) droplet size distribution curves over 1 day and 1 week and (B) viscous flow curves and its Sisko model fitting, for B500 bitumen emulsion with O/W ratio of 60/40, prepared using TEPA-KL and A100 as reference.

Figure 4.4.9B presents flow curves for TEPA and A100 bitumen emulsions. The dependency of viscosity on shear rate was apparent at low shear rates, between 0.01 and 1 s^{-1}, followed by a transition to a final region with a Newtonian response. This limiting value corresponds to a completely deflocculated system, as a consequence of the severe shear applied. These behaviors, different to those shown in Figure 4.4.6, are better described by Sisko model, which introduces a high shear limiting viscosity, 'η_∞', accounting for such a Newtonian region:

$$\eta(\dot{\gamma}) = \eta_\infty + k \cdot \dot{\gamma}^{n-1} \quad (3)$$

Table 4.4.2 summarizes consistency (k) and flow (n) indexes and η_∞.

Table 4. 4. 2 Sisko fitting parameter, $D_{3,2}$ and maximum packing volume fraction (Φ_M), of 60/40 bitumen (B500) emulsion prepared using 0.5% of TEPA emulsifier and A100 as reference

Bitumen emulsion	k, Pa·s^n	n, -	η_∞, Pa.s	$D_{3,2}$,µm	Φ_M
A100-emulsion	0.135	0.36	0.025	2.56	0.685
TEPA-emulsion	0.077	0.32	0.051	13.59	0.641

Both emulsions present quite similar shear thinning behaviors, as demonstrated by close values of the flow index. However, TEPA emulsion limiting viscosity is higher than that for the emulsion stabilized by A100 (despite they were formulated with the same bitumen concentration). Initially, a higher $D_{3,2}$ value means a smaller total surface area formed, or lesser droplet quantity, which would lead to a lower emulsion limiting viscosity. However, if the η_∞ value is considered to be influenced by no other parameters than the viscosity of the dispersing medium, dispersed phase volume fraction and its corresponding maximum value (Φ_M) (Barnes 1994), the DSD curves in Figure 4.4.9A may shed light on this issue. Bimodality of A100 emulsion, along with its wider size distribution, allows internal spaces among droplets to be filled by smaller size droplets, resulting in a higher Φ_M value. According to the above assumption, Φ_M values for A100 and TEPA emulsions were calculated by using the Frankel-Acrivos equation , and are shown in Table 4.4.2. TEPA and A100 show Φ_M values of 0.641 and 0.685, respectively. This means that the TEPA-emulsion (60 wt.% dispersed phase) is closer than A100-emulsion to the maximum packing volume fraction admissible. So, stronger interactions among droplets are expected during flow, giving rise to a higher limiting viscosity η_∞ for TEPA-emulsion.

The application of lignin-based emulsifier may depend on the desired final properties specified in standards (e.g. EN 13808), such as viscosity, breaking behavior, etc. However, most importantly, those properties are predictable considering parameters previously demonstrated in this work.

4.4.4 Concluding remarks

This work has evaluated physical, rheological and microstructural properties of model (silicon) and bitumen emulsions stabilized by cationic lignin-based surfactants. To that end, lignin modification has been accomplished, by a Mannich reaction procedure, optimizing variables such as reaction route (alkaline or acidic), types of amines, and reagent ratios. On the other hand, emulsion formulation has been modified as a function of emulsifier concentration, pH of aqueous phase and O/W ratio.

The results suggest that alkaline route is more effective than acidic one, for the specific reaction conditions of 60 °C for 4 hours. For a typical bitumen emulsion, lignin modified by tetraethylene pentamine is preferred as cationic emulsifier, presenting sufficient stability and a suitable viscous behavior. Nonetheless, the other amines, used as sources of protonatable groups for lignin, have demonstrated excellent emulsification ability of silicone dispersions. For a fixed concentration value, the reagent ratio (KL/FD/AM) was found optimum for 1/11/11 and 1/22/22. Based on those adjusted emulsifier parameters, the cationic O/W bitumen emulsions are desirably formulated with 0.5% w/w lignin modified by TEPA, dispersed in a aqueous phase at pH 1, for a bitumen concentration between 60% and 70%, range commonly used in asphalt industry.

4.5 Assessment of modified lignin cationic emulsifier for bitumen emulsions used in road paving

Published in :

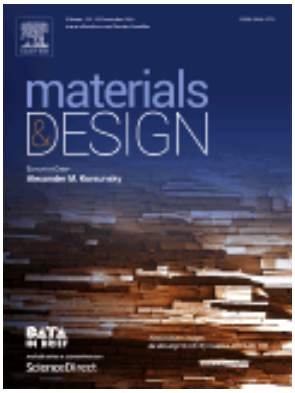

Materials & Design

Publishing Company : Elsevier B.V.

Editor in Chief : Alexander M. Korsunsky

Volume: 131, PP : 242-251

Year : 2017

ISSN : 0264-1275

DOI : 10.1016/j.matdes.2017.06.024

ABSTRACT

The utilization of Kraft lignin as cationic emulsifier in the preparation of bitumen emulsions has been assessed in this work. Thus, Kraft lignin was previously modified in alkaline medium in presence of tetraethylene pentamine (TEPA) and formaldehyde, according to the Mannich reaction. Solubility in water phase as a function of pH demonstrated the amphoteric nature of the reaction product, which enables its potential application in cationic bitumen emulsions. Bitumen emulsions stabilized by modified lignin (MKL) were further studied. Different B/W ratios, which mainly affected the high-shear-rate-limiting viscosities, yielded more similar mean droplet diameters than different pHs, whose effect on viscosity was mainly at low shear rates. Moreover, viscous flow and linear viscoelasticity tests revealed enhanced rheological performance of the MKL bitumen residue if compared to the parent base bitumen. Finally, half warm mix asphalt (HWMA) specimens containing reclaimed asphalt pavement (RAP) were studied, and the results compared with those corresponding to virgin aggregate. In both cases, the preparation of HWMA with a selected 60/40 MKL bitumen emulsion at 80°C by gyratory compaction was successful. Compared to the virgin aggregate, the specimen derived from 100% RAP showed much higher mechanical resistance due to a partial blending of fresh binder with RAP aged binder.

4.5.1 Introduction

Over the last decades, sustainable development policy is being strongly encouraged in many sectors, including transport infrastructure. In pavements construction, the massive consumption of fossil fuels and highly toxic pollutants emission associated to the use of the standard practice of hot mix asphalt (HMA) technology are two critical environmental concerns (Gómez-Meijide and Pérez 2014; Carrera et al. 2015). As an alternative, reduced-temperature paving technologies using bituminous emulsions may represent up to 7 times lower emission in kg eq. CO_2/ton product and up to 7.5 times lower energy consumption in MJ/ton product, as compared to HMA (Lesueur 2011). These great reductions come from the decrease in binder viscosity which allows for milder workability during manufacture. Hence, even at ambient conditions, mixing and compaction in the reduced temperature method is expected to perform better than in the standard method, as bitumen viscosity at 135 °C is 6 times higher than its corresponding 70/30 (B/W) bitumen emulsion under ambient conditions (Yuliestyan et al. 2016b).

Bitumen emulsions are composed of two immiscible phases, that is, 1-50 μm bituminous droplets dispersed into water medium in the presence of an emulsifier. The emulsifier is an amphiphilic substance with a hydrophilic head and a lipophilic coil. It resides at the interface between the bitumen droplet and the water phase, acting as a stabilizer which reduces the interfacial tension between both phases and facilitates the emulsification process. In terms of the surface charge of the hydrophilic end, cationic emulsifiers are used, by far, in a larger scale than anionic or non-ionic emulsifiers in the bitumen emulsion industry (Read and Whiteoak 2003). This is due to its ability to adhere to electronegative siliceous solid aggregates, the most common

mineral type on Earth (Mallawarachchi et al. 2016; Ronald and Luis 2016). In this regard, functional groups containing nitrogen, i.e. amine, amidoamine and imidazoline, are widely used in the hydrophilic end of cationic emulsifiers (Read and Whiteoak 2003) due to its known ability as adhesion promoters (Gawel et al. 2016).

Interestingly, lignin, a by-product of pulping industry, has presented a potential use as a building unit for cationic emulsifiers (Laurichesse and Avérous 2014; Windeisen and Wegener 2016). Depending on the sources, from hardwood or softwood, and importantly the previous treatment used, i.e. sulfate (Kraft) process, sulfite process, etc., a wide variety of lignin is available. Together with cellulose, lignin represents the most abundantly available biopolymer on Earth. However, only a small amount of it is being utilized to manufacture commercial products, and the rest is mainly burnt for energy (Matsushita 2015; Windeisen and Wegener 2016). To obtain a cationic emulsifier product based on the Mannich reaction, a compound containing an amine functional group is attached to lignin, with formaldehyde as a second reagent (Matsushita and Yasuda 2003; Du et al. 2014; Laurichesse and Avérous 2014). In alkaline medium, the reaction occurs between a lignin carbon with high electron density and an intermediate substance (aminomethanol) which was initially formed from the reaction of formalydehyde and the amine (Laurichesse and Avérous 2014), shown in Figure 4.5.1.

This type of modification permits the use of various types of lignin, among them, lignin extracted by a Kraft process, which is a highly adopted technology in pulping industry (Du et al. 2014). Hence, selection of Kraft lignin as raw material is of high interest, that also presents a potential use as properties modifier (Kaewtatip and Thongmee 2013). Similarly, options are also available for the amine group selection, though it is limited

to primary (-NH_2) or secondary (-NH) amine. In this study, tetraethylene pentamine (TEPA), where in Figure 4.5.1 R1=$C_{2n}H_{1+5n}N_n$ and R2=$C_{2(4-n)}H_{1+5(4-n)}N_{4-n}$, for $0 \leq n \leq 2$, with three secondary and two primary amine, was chosen as reagent. High expectation was put on its emulsifying ability and further adhesive properties of its binder, given the high number of amine groups involved in the molecule.

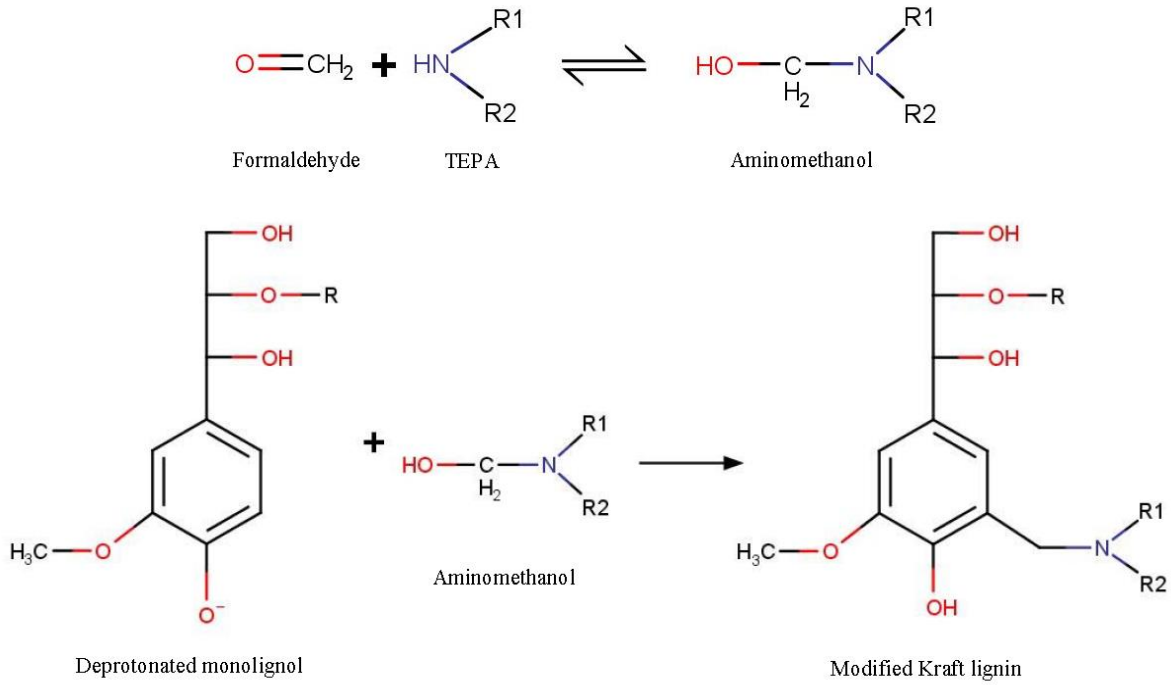

Figure 4. 5. 1 Molecular structure prediction during Mannich reaction for the preparation of MKL, represented as monolignol, formaldehyde and amine functional group reaction, adapted from (Du et al. 2014)

For that purpose, this work assesses the potential use of TEPA modified lignin (MKL) as cationic emulsifier of bitumen emulsions. In that sense, the methodology was established as follows: a) influence of pH on the solubility in aqueous medium of the cationic emulsifier; b) investigation on the influence of pH, B/W ratio and processing on the MKL bitumen emulsions droplet size distribution and their flow behaviour at 30 °C; c) evaluation of the MKL bitumen emulsions breaking rate and further study on

the relation between the rheological properties and microstructure of their residues; and d) feasibility of developing half warm mix asphalt (HWMA) containing reclaimed asphalt pavement (RAP) with the use of MKL cationic bitumen emulsions.

4.5.2 Experimental

4.5.2.1 Materials

Alkali or Kraft lignin (KL) CAS no.: 8068-05-1, brown powder (insoluble in acidic aqueous solution) with MW of 10000 g/mol, was used as a precursor to obtain MKL. This lignin presented ash content of 3.14 wt.% and elemental composition (wt.%) as follows: C: 61.15, H: 6.72, N: 2.18, O: 26.92, S: 2.54. In this case, if all the sulfur is assumed to be found as sulfonate groups, the $-SO_3^-$ content would be of 6.35 wt.%. Amination, through the Mannich reaction, was followed by reacting KL with tetraethylene pentamine (TEPA) and formaldehyde (supplied as 37 vol.% aqueous solution). All reagents were purchased from Sigma Aldrich, Spain. The bitumen used to manufacture the emulsions was kindly supplied by Repsol S.A. (Spain). Values of penetration of 190 dmm and Ring-and-Ball softening temperature of 39 °C were measured according to European Standards EN 1426:2007 and EN 1427:2007, respectively. Finally, in order to assess the potential use of the emulsions in HWMA, two types of aggregates were selected: a) RAP, provided by Repsol S.A. Spain, was extracted from a road in Madrid; and b) a siliceous aggregate, used as reference, from Arido Velilla S.A. Spain.

4.5.2.2 Emulsions and samples preparation

In the preparation of the emulsifier, previously optimized quantities of 1 g KL and 1.4 g TEPA were initially solubilized in 50 mL of alkaline (pH of 13) aqueous solution, at

60 °C, under stirring at 1000 rpm. Then, a quantity of formaldehyde equivalent to TEPA in moles was added to conduct the Mannich reaction for at least 4 h. To prepare the emulsion aqueous phase, the concentrated MKL was diluted up to the final desired concentration with deionized water and the pH was then adjusted using HCl in 37 vol.% aqueous solution.

The preparation of the bitumen emulsions was performed according to the following three different methods: A) batch mixing of bitumen at 140°C with water at 60°C in a homogenizer IKA UT T50 with a toothed rotor-stator G45M dispersing element at 10000 rpm for 4 min; B) one pass in-line mixing for 3 s, of both phases, in a colloid mill type C45-2939 (bitumen and water phases at same temperatures as before) at 6000 rpm; and C) similar as in (A) performed in a shorter processing time of 2 min. Aiming to investigate the influence of pH, B/W ratio and processing procedure on the emulsion properties, the nine emulsion cases presented in Table 4.5.1 were developed. Thus, pH was varied between 1 and 7, and the B/W ratio from 50/50 to 70/30. A constant concentration of the surfactant MKL of 0.75 wt.% (with respect to overall emulsion) was always used.

Table 4. 5. 1 Work plan developed for the emulsion study observing the influence of pH, bitumen-to-water (B/W) ratio and processing, with 0.75 wt.% of MKL (over the emulsion)

Case identifier	**Emulsion identifier**	**Emulsion definition**		
		pH	**B/W ratio**	**Processing**
pH	pH1-60-A	1	60/40	T50 at 10000 rpm for 4 min (A)
	pH3-60-A	3		
	pH5-60-A	5		
	pH7-60-A	7		
B/W	pH1-50-B	1	50/50	CM at 6000 rpm for 3 s (B)
	pH1-60-B		60/40	
	pH1-65-B		65/35	
	pH1-70-B		70/30	
Processing	pH1-60-C	1	60/40	T50 at 10000 rpm for 2 min (C)

Residual binders were obtained by the evaporation method outlined in UNE-EN 13074-1:2011. This method minimizes the damage provoked to the binder with a view to its further characterization. Alternatively, residual binder, in the form of mastics, might also be obtained by adding cement and filler to allow hydration and demulsification process (Dondi et al. 2014), though beyond the scope of this study. The influence of the MKL in the bitumen residues was studied at varying MKL concentrations from 0.41 to 2.08 wt.%, which represent from 0.25 to 1.25 wt.% of MKL in their parent 60/40 B/W emulsions (prepared by method A, at pH of 1).

The preparation of HWMA specimens was conducted, in a gyratory compactor, by initially mixing aggregates at 110 °C with a 0.5 % of water at 60 °C followed by MKL bitumen (60/40) emulsion at the same temperature, before compaction at 80 °C.

100% RAP specimens were prepared by pouring 2.5 wt.% of MKL emulsion (which represents 1.5 wt.% dry bitumen added) into 0/16 crushed RAP, composed of 40 wt.% fine and 60 wt.% coarse fraction. The 60/40 emulsion used was prepared by method B. In order to compare the effect of virgin and reclaimed asphalt, reference virgin aggregate asphalt mixes were prepared using a granulometry of AC 16 design (Figure 4.5.2) with a binder content of 5 wt.% (8.33 wt.% of MKL 60/40 emulsion). All mixtures were subjected to curing process inside oven at 50 °C for three days.

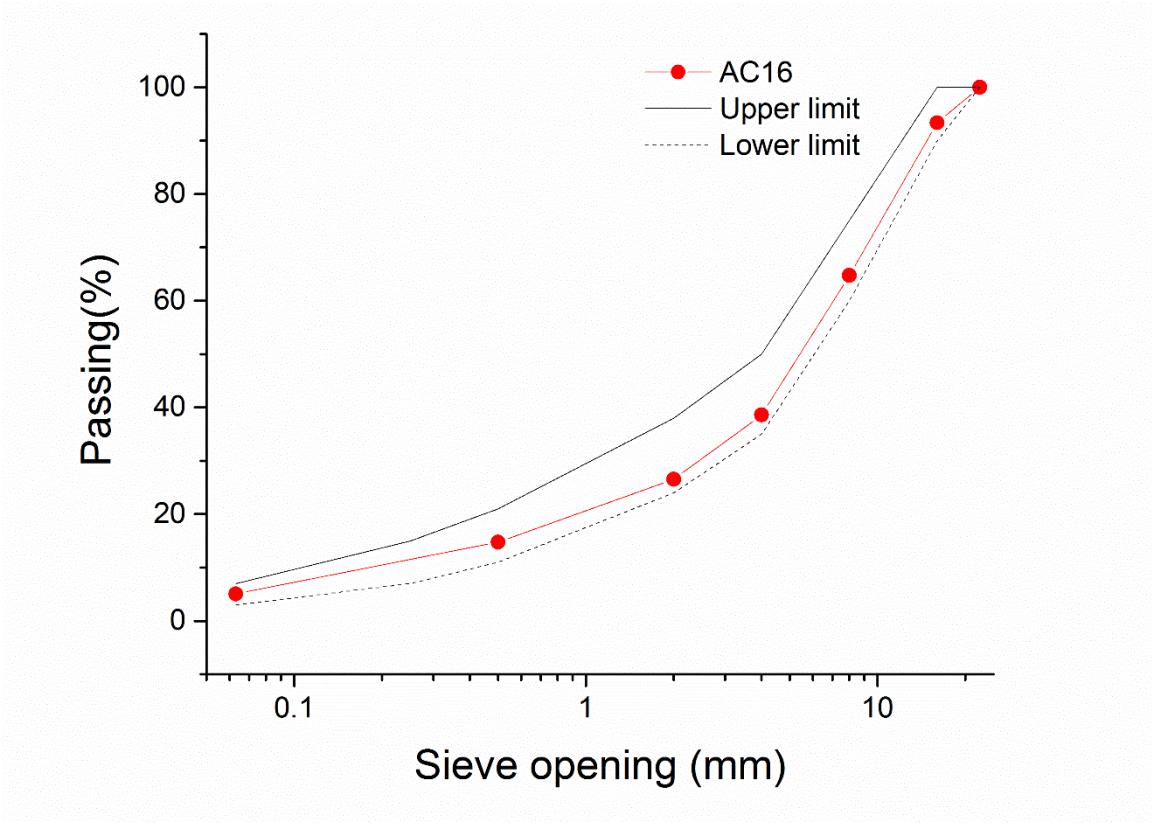

Figure 4. 5. 2 AC 16 grading curve with its corresponding maximum and minimum limit

4.5.2.3 Tests and measurements

Filtration tests, by passing MKL solution through filter paper with pore size between 7-9 and 45 µm, were conducted as a function of pH. The solubility was estimated using Equation 4.5.1:

$$\%\ Solubility\ = \left(1 - \frac{m_c}{m_i}\right) x100\% \qquad (4.5.1)$$

where mi and mc are the initial mass of MKL dispersed in aqueous medium and the mass of MKL in cake (retained by the filter), respectively. The absence of solid particles on the filter was interpreted as a proof of high solubility. Additionally, visual inspection of each MKL solution prior to filtration was used to relate color with solubility.

Fourier Transform Infra-Red (FT-IR) spectroscopy was performed to compare specific functional groups in Kraft lignin before and after modification. FT-IR spectra were obtained using FT/IR 4200 type A, manufactured by JASCO company, in transmission mode. Thin disks were prepared by mixing Kraft lignin or MKL powder with KBr (in a wt. ratio of 1:5), followed by hydraulic pressing at 5 bar for 5 minutes. Spectra were collected with a resolution of 4 cm-1 from 350 to 4000 cm^{-1}.

Two different tests were carried out to characterize bitumen emulsion properties: a) droplet size distribution tests were conducted in Mastersizer 2000 Malvern (UK), at ambient temperature; b) Viscous flow tests at 30 °C were performed using rough surface coaxial cylinders, to prevent wall-slip phenomena, in a controlled stress rheometer Physica MCR 301 by Anton Paar (Austria). Apart from this, the emulsion breaking index was also measured as the amount of Sikaisol filler needed for breakage upon contact with 100 gr of bitumen emulsion (according to EN 13075-1).

The rheological properties of the binder residue were revealed by means of: a) viscous flow tests at 60 °C, performed using serrated parallel plates (25 mm diameter) at 1 mm gap in Physica MCR 301 Anton Paar (Austria); and b) dynamic shear temperature sweeps at a frequency of 10 rad/s from 30 to 80 °C with a heating rate at 1°C/min,

with serrated parallel plates (20 mm diameter) at 1 mm gap on a controlled stress RS600 from HAAKE (Germany) within its linear viscoelastic (LVE) region.

The morphology of the binder residue, at ambient temperature, was evaluated through optical micrographs obtained using DFC495 Leica camera attached to DM2500 microscope. Samples, on standard microscope slides (76 × 26 mm2), were initially heated up to 70 °C to form very thin layers which allowed light to be transmitted through.

Furthermore, Vialit adhesion plate shock tests, referred to EN 12272-3, were prepared by placing 100 aggregates on a 20 × 20 cm2 standard plate previously filled with 70/30 bitumen emulsion (method B) which was allowed to set. Three test replicates were performed by dropping a standard ball onto an inverse facing plate. Visual observation was conducted on the aggregates.

With regard to the HWMA, the workability was evaluated through the gyratory compaction test, using Superpave gyratory compactor (by Matest, Italy), by applying a weak load of 0.6 MPa at 0.82° internal angle for a number of gyrations (Gn) of 200 at a speed of 30 rpm. The compactability was then fitted to Equation 4.5.2 (EN 12697-10):

$$h = h_1 - C \cdot ln(G_n) \tag{4.5.2}$$

where h is height, h1 is height at first gyration and C is a workability indicator.

Finally, the mechanical properties of HWMA were assessed via the following indirect tensile tests (IDT): a) indirect tensile stiffness modulus (ITSM) test at 20 °C, by applying repetitive dynamic non-destructive load pulse for causing 0.005% transient horizontal measured on cylindrical specimen using a linear variable differential

transformer (LVDT) mounted to the device, as per EN 12697-26; and b) indirect tensile strength (ITS) test at 15 °C, by applying destructive vertical force to cause a vertical deformation rate of 50 mm/min, and using Equation 4.5.3 (EN-12697-23) to calculate ITS mechanical failure:

$$ITS(MPa) = \frac{2 \cdot P}{t \cdot \pi \cdot D} \quad (4.5.3)$$

where P is maximum force (N); t and D, are the average thickness and diameter of specimen (mm), respectively. All the mechanical tests were done with four replicates.

4.5.3 Results and discussion

4.5.3.1 Characterization of MKL as potential cationic emulsifier

The potential use of the MKL as emulsifier in cationic bitumen emulsions resides in its ability to solubilize in acidic solution through protonation of the attached amine groups. Validation of the existence of amine groups attached to the lignin molecule after completion of the Mannich reaction was performed by Fourier Transform Infra-Red (FTIR) spectroscopy. Figure 4.5.3 presents FTIR spectra for Kraft lignin before and after modification. Before modification, typical lignin phenolic features are observed, with the O-H stretching and aromatic (skeletal) vibration being denoted by a wide broad peak centered at 3421 and peaks at 1605 and 1515 cm^{-1}, respectively. The origin of Kraft lignin used could be identified from its particular peaks between 1800-900 cm^{-1}. Thus, peaks at 1117 and 1328 cm-1, assigned for C-H and C-O deformation in Syringyl (S) aromatic unit, appear larger than those of guaiacyl (G) unit at 1159 and 1262 cm-1 (seen as overlapped shoulders) for the same assignment. A higher percentage of S (from synapyl alcohol-derived monolignol) than G (from

coniferyl alcohol monolignol) in their structural units indicates a hardwood origin, as opposed to softwood lignin which is mostly comprised of G units (Kubo and Kadla 2005; Laurichesse and Avérous 2014). After modification, the structural units appear different as observed by the following evidences on the MKL transmittance spectrum: a) bending in-plane of C-H in G and S units, between 1260 and 1060 cm^{-1}, have shown a lesser definition; and b) the presence of a newly developed peak centered at 770 cm^{-1} associated to N-H wagging out of plane. This would suggest that modification, with the inclusion of an amine functional group, has occurred in their aromatic unit.

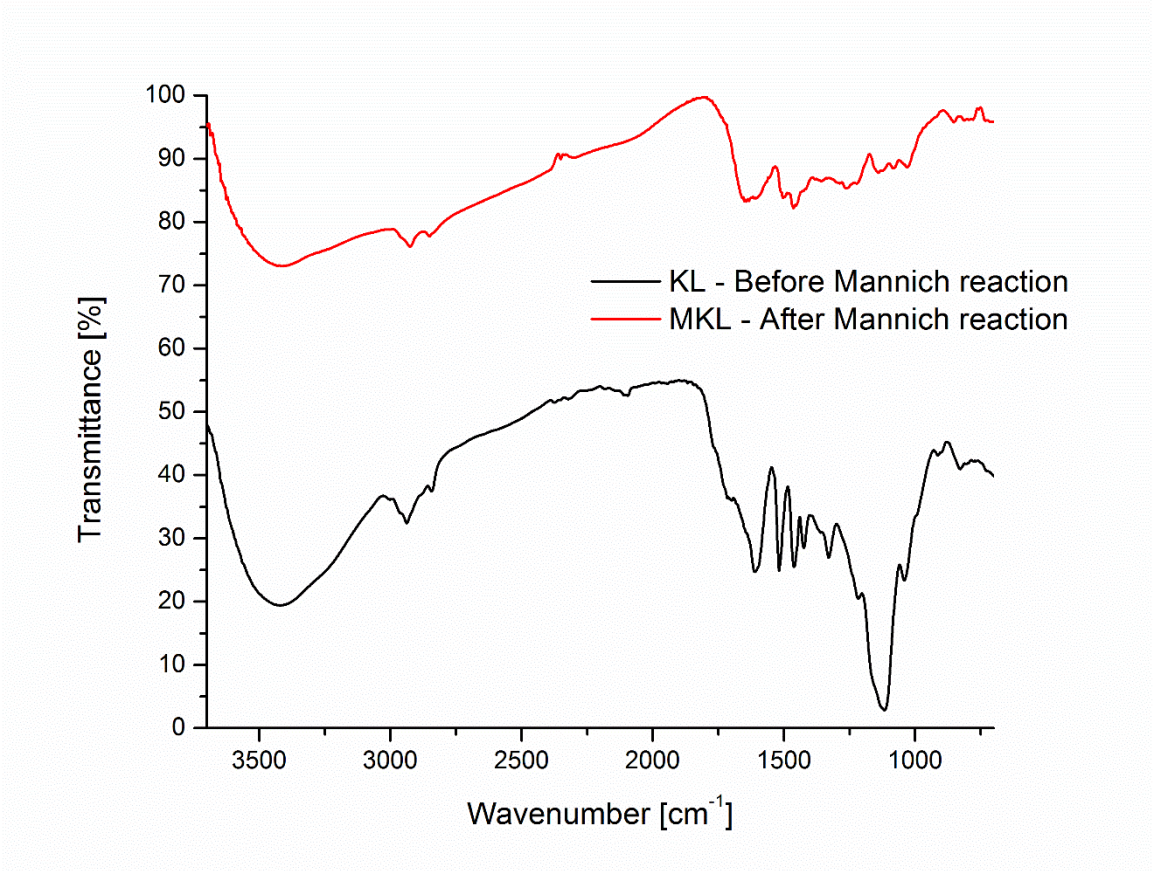

Figure 4. 5. 3Fourier transform infrared (FT-IR) spectrum of Kraft lignin/MKL, before and after Mannich reaction, between wavenumber range of 700 - 3700

In order to evaluate the effect of pH on the solubility of the MKL to be used as cationic emulsifier in aqueous medium, visual inspection was performed on dispersions of

MKL into water, at different pH between 1 and 11. The results are shown in Figure 4.5.4a. A transparent black/dark solution is seen at pH ≤ 5 and pH ≥ 10. In contrast, a turbid milky light brown dispersion is observed at 6 ≤ pH ≤ 9, as a result of the light beam scattering by insoluble MKL particles.

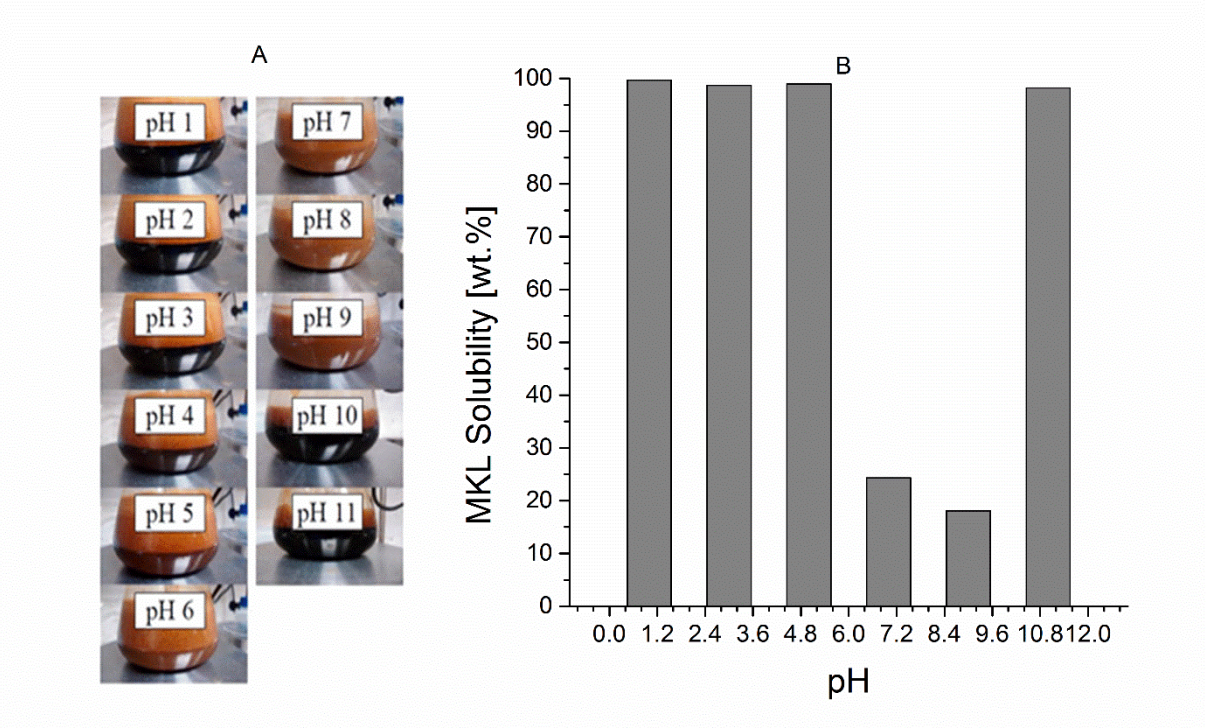

Figure 4. 5. 4 MKL solubility analysis via, a) visual inspection and b) filtration by means of MKL percentage in filtrate passing through 45 μm Φ pore size, as a function of pH

The above dispersions were further subjected to filtration tests, which allowed for the establishment of a relation with previous results. The percentage of MKL non-retained by the filter, as a function of pH, is presented in Figure 4.5.4b. When the solution appears as black/dark transparent, almost all MKL was retrieved in the filtrate. In contrast, about 80% of the total weight of MKL was collected either using filter with pore size of 7-9 or 45 μm at pH between 7 and 9, when the turbidity was high in the unfiltered solution. Based on that result, acid-base Brönsted-Lowry principle attempts

to explain that at pH ≤ 5, a large amount of MKL (lignin – NR_1R_2) is protonated in acidic medium to form the conjugate acid (lignin – N $R_1R_2H^+$), as a result of H^+ reception. The resulting positive charge alters the MKL solubility, as it is now able to form H-bond with water (Norgren and Edlund 2014). At intermediate pH, the equal presence between two opposite charge in MKL unit yield the net charge of solution nearly zero. In addition, the attraction among hydrophobic component of MKL form coacervates of coarse particle and finally co-precipitate. At pH ≥ 10, the hydroxyl groups naturally present in the Kraft lignin molecules are easily deprotonated in the presence of alkali, yielding the negatively charged conjugate base (lignin – O^-). As a consequence, the MKL becomes soluble again. The amphoteric nature of the MKL molecule makes solubility possible, depending on the pH, not only in alkaline (as raw Kraft lignin) but also in acidic medium. Therefore, it enables its potential application in cationic and anionic bitumen emulsions, simply, by adjusting pH of their aqueous phase.

4.5.3.2 Effect of pH, B/W ratio and processing on bitumen emulsions prepared with the MKL emulsifier

The evaluation of the droplet size distribution and viscous flow behavior of the bitumen emulsions helps understand their coating potential. Moreover, pH, bitumen/water (B/W) ratio and processing device are among the parameters which most influence the above properties. Hence, their effect on the nine MKL bitumen emulsions summarized in Table 4.5.1 was studied.

Figure 4.5.5 presents the results of particle size analysis, by laser diffraction, on the different bitumen emulsions, as a function of the three above parameters: a) pH, b) B/W ratio or c) processing.

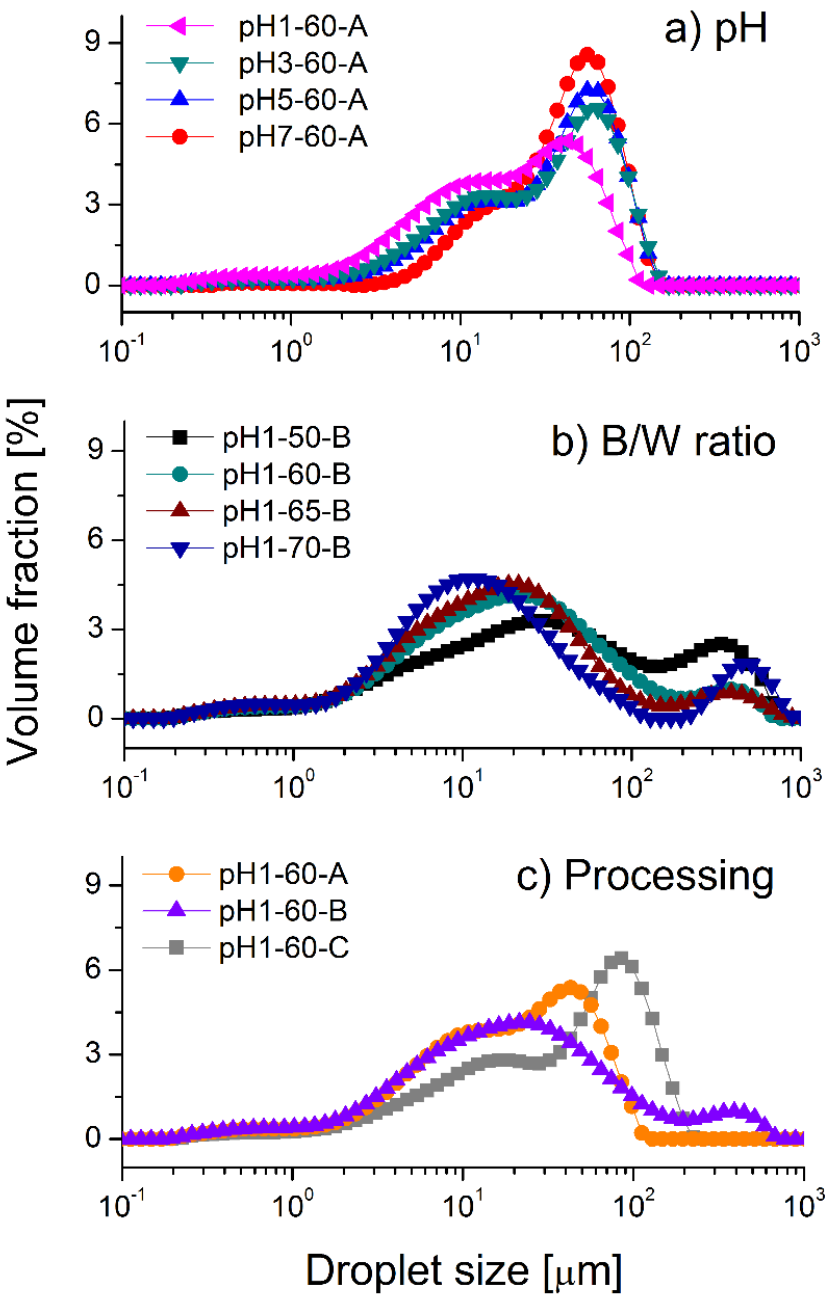

Figure 4. 5. 5 Droplet size distribution of emulsified bitumen with MKL concentration of 0.75 wt.%, measured at ambient condition via laser diffraction method, for the study of a) pH, b) B/W ratio and c) processing influence

In Figure 4.5.5a, each curve appears as a result of two overlapped peaks, with the largest one centered at 50 μm and the other one yielding a shoulder at a smaller droplet size (which increases as pH decreases). In general, within the pH interval

analyzed, the droplet size distribution (DSD) remains quite unaffected by pH, in terms of shape. On the other hand, a well-defined bimodal curve, with peaks at around 20 and 300 μm, was always exhibited at the different B/W ratios tested for emulsion obtained in the in-line homogenizer (processing B). As shown in Figure 4.5.5b, B/W did not cause much influence between 60 and 70 wt.% of bitumen, although some differences in the DSD are appreciated for the 50/50 emulsion. Interestingly, the DSD shape did not vary significantly with pH (in Figure 4.5.5a) or B/W ratio (in Figure 4.5.5b), provided that those emulsions were obtained by the same processing procedure. Instead, a comparison of different procedures, as in Figure 4.5.5c, led to differing DSD shapes, which suggests the strong influence of processing on this matter.

Moreover, in order to make easier a comparative analysis for every effect studied, Sauter mean diameter, $D_{[3,2]}$, was calculated using Equation 4.5.4:

$$D_{[3,2]} = \frac{\sum_i n_i \cdot D_i^3}{\sum_i n_i \cdot D_i^2} \tag{4.5.4}$$

where ni is the number of droplets with diameter Di. Table 4.5.2 depicts the mean diameters, as a function of all tested parameters (cases a, b and c). A may be seen, the droplet mean diameter increases with pH, from $D_{[3,2]}$ of 6 μm at pH 1 up to 45 μm for pH 7. Such explanation is derived from the MKL ability to capture a proton in acidic solution. Stronger acidic conditions prevent precipitation of previously dissolved MKL, which increases the effective concentration of the emulsifier in water. Moreover, pH also affects its emulsifying properties given the formation of a surfactant molecule with a larger surface charge density as a consequence of a more successful protonation (Ouellette et al. 2015). Thus, upon contact between bitumen and water phases and in the presence of mechanical energy for droplet breakage during emulsification, a large migration of strongly charged MKL molecules to the water-bitumen interface allows

for the formation of finer and more stable bituminous droplets. However, as pH increases up to 7, weaker surface charge densities increase the chance for coalescence of the new formed bitumen droplets (Rodríguez-Valverde et al. 2003). With regard to the bitumen concentration, B/W ratio seems to affect mean diameter of bitumen droplets in a lesser extent than pH. So, all the $D_{[3,2]}$ values ranged from 5 to 7 μm, being lowest droplet size for emulsion 70/30. This result is related to the higher emulsion bulk viscosity of system 70/30, which hinders droplet motion, along with an emulsion continuous phase more concentrated in MKL. Both facts would prevent droplet coalescence after emulsification and, therefore, explain the lower droplet size as bitumen concentration increases. Furthermore, the results seem to demonstrate that, for a MKL concentration of 0.75 wt.%, pH=1 yields highly protonated MKL particles which performs equally well at any of the B/W ratios studied. Also, even though stirring efficiency decreases for a higher number of drops, the viscosity increase caused by a high internal phase concentration which approaches phase inversion (turbulent flow might approach laminar) significantly improves the stirring energy transfer from the device to the droplet to be broken (Salager et al. 1996). Finally, the influence of processing on mean droplet size is shown Table 4.5.2. A comparison of pH1-60-A and pH1-60-C, both with the same formulation, prepared under the same batch conditions with the toothed rotor-stator apparatus IKA UT T50 (constant power density, ε), evidences the inversely proportional contribution of the agitation time, tag, on the $D_{[3,2]}$. Thus, $D_{[3,2]}$ scales with Ev-b, where Ev (energy density) is calculated as the product $\varepsilon \cdot t_{ag}$, and the exponent value depends on the flow regimen (Gingras et al. 2005, 2007b). Consequently, $D_{[3,2]}$ data was perceived smaller for longer emulsification time in pH1-60-A than in pH1-60-C. In case of in-line colloid mill emulsification, a similar scaling regime has been established, by calculating a

residence time in the dispersing zone as the ratio V_{EM}/Q, where V_{EM} is the volumetric capacity of the emulsification machine and Q is the flow rate (Gingras et al. 2005, 2007a). Yet, it is difficult to establish a comparison between these two types of emulsification because $D_{[3,2]}$ is largely influenced by geometrical considerations. DSD and Sauter mean diameters corresponding to pH1-60-A and pH1-60-B do not differ much, even though the rotor-stator speed and agitation time (10000 rpm and 4 min) were much higher than the colloid mill speed and residence time (6000 rpm and 3 s). However, a smaller gap between the shearing parts in the colloid mill as compared to the tooth spacing in the rotor-stator configuration may improve significantly its efficiency, due to higher values of shear rate.

Table 4. 5. 2 Sauter mean diameter ($D_{[3,2]}$) and Sisko model fitting parameters

Emulsion (case)	**k [Pa·s^n]**	**n**	**η_∞ [Pa·s]**	**$D_{3,2}$ [µm]**
pH				
pH1-60-A	0.192	0.08	0.035	6.01
pH3-60-A	0.067	0.15	0.029	9.20
pH5-60-A	0.046	0.24	0.026	10.61
pH7-60-A	0.016	0.31	0.026	20.32
B/W ratio				
pH1-70-B	0.115	0.13	0.090	4.87
pH1-65-B	0.103	0.17	0.039	5.24
pH1-60-B	0.077	0.22	0.020	5.85
pH1-50-B	0.003	0.38	0.004	6.98
Processing				
pH1-60-A	0.192	0.08	0.035	6.01
pH1-60-B	0.077	0.22	0.020	5.85
pH1-60-C	0.070	0.22	0.020	9.12

The viscous flow behavior of the above emulsions was also studied. Figure 4.5.6 presents the evolution of the steady state viscosity with shear rate, at 30 °C, as function of: a) pH, b) B/W ratio, and c) processing.

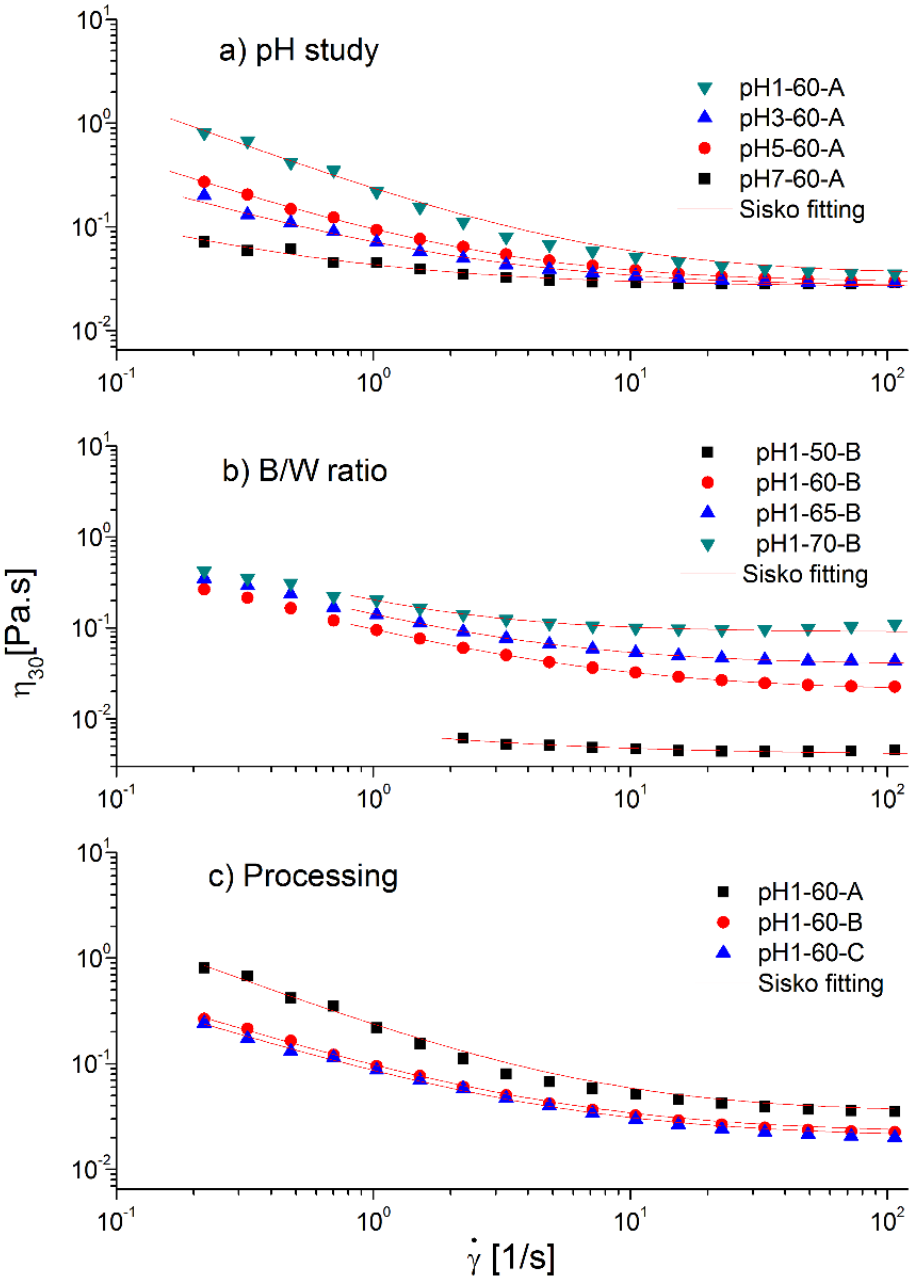

Figure 4. 5. 6 Viscous flow behaviour of bitumen emulsion at 30 °C, fitted with Sisko model, as a function of a) pH, b) B/W ratio and c) processing

Within the shear rate considered, all the emulsions presented shear thinning response at the low shear rate region, followed by a transition regime which evolves toward a constant viscosity, known as the high-shear-rate-limiting viscosity. Such flow behavior has been typically observed on concentrated colloids, emulsions or suspensions at droplet volume fraction $\phi \geq 0.3$ (Otsubo and Prud'homme 1992; Barnes 1994; Mueller, S., Llewellin, E.W., Mader 2009), and also applies for bitumen emulsions and polymer modified bitumen emulsions (Cuadri et al. 2016; Yuliestyan et al. 2016b). This viscosity evolution is well represented by the Sisko model, as follows:

$$\eta(\dot{\gamma}) = \eta_{\infty} + k \cdot \dot{\gamma}^{n-1} \qquad (4.5.5)$$

where η_{∞} is the high-shear-rate-limiting viscosity, k is consistency index, and n is the flow index. These fitting parameters were summarized in Table 4.5.2, for the three case studies considered. In the first case, the pH of the emulsion mainly affected the k index, which increased with decreasing pH. Stronger inter-drop interactions provoke an increase in the flow resistance at low shear rates, which is related to the consistency index k (Otsubo and Prud'homme 1994a). Similarly, η_{∞} at high shear rate values was observed to slightly increase as pH was lower.

The shear-thinning grade also increased ("n" became lower) as pH decreased (Table 4.5.2). This result is clearly observed from the low shear rate zone in Figure 4.5.6a and is explained by the fact that, at low pH, the MKL molecules own a higher surface activity, yielding a large amount of smaller droplets (i.e. a larger interfacial surface area per unit volume, as may be deduced from the lower $D_{[3,2]}$ found). Under those conditions, emulsion presents a well-developed three-dimensional network favored by entanglements among surfactant adsorbed at the bitumen-water interface. Such a flocculated microstructure mainly affects low-shear-rate emulsion behavior (n values)

and is destroyed by shear until hindrance no longer exists and Newtonian behavior is reached, η_∞.

Similarly, B/W ratio affects both low and the high shear rate viscous behavior of emulsions, and the differences in n, k and η_∞ are attributed to the different bitumen volume fractions, ϕ, (and $D_{[3,2]}$ values). Table 4.5.2 shows an increase in the emulsion viscosity and the development of shear thinning behavior (lower n values) as bitumen concentration is raised. Thus, a higher $\eta\infty$ of 0.090 Pa·s was obtained for pH1-70-B, as compared to pH1-50-B with η_∞ of 0.004 Pa·s.

With regard to processing, results in Figure 4.5.6c evidence nearly coincident viscosity curves (both with η_∞ of 0.020 Pa·s) for the emulsions pH1-60-B and pH1-60-C, and slightly higher η_∞ of 0.035 Pa·s for pH1-60-A. The latter characterized by a narrower DSD. With the aim to compare all these emulsions, a study on the influence of the DSD on the maximum packing volume fraction was conducted referring to Frankel-Acrivos model (Equation 4.5.6) with an assumption of cubical arrangement of solid spheres

$$\eta_R = C' \cdot \left[\frac{\left(\frac{\phi}{\phi_m}\right)^{1/3}}{1 - \left(\frac{\phi}{\phi_m}\right)^{1/3}} \right] \tag{4.5.6}$$

In Equation 4.5.6, η_R is relative viscosity (a ratio between the emulsion limiting viscosity and the continuous phase viscosity, measured as 1 mPa·s at 30°C); ϕ_m is dispersed phase maximum packing volume fraction; and C' is a constant with a theoretical value of 9/8 (Tanner 2002). Result of this relationship is presented in Figure 4.5.7. As can be observed, pH1-60-B and pH1-65-B were superimposed to fitting curves with ϕ_m = 0.70, whereas only a slightly higher ϕ_m of 0.72 was found for pH1-70-B (Figure 4.5.7). Interestingly, despite the different processing conditions

used for the manufacture of emulsion pH1-60-C, Frankel-Acrivos equation also predicts a ϕ_m of 0.7 for this system. This result indicates that, as shown by Figure 4.5.5b, differences in DSD among emulsions pH1-60-B, pH1-65-B and pH1-60-C are not so large. On the contrary, emulsion pH1-60-A exhibiting the narrower DSD would have the lowest ϕ_m of 0.67 (Figure 4.5.7), which turns out in a more dense droplet packing and, therefore, in a higher viscosity if compared to pH1-60-B and pH1-60-C (Table 4.5.2). In practice, such bi/multimodal DSD has the capability to form denser droplet conformation, or $\phi_m \gg$ value, that leads to lowering relative droplet fractions (ϕ/ϕ_m), and so lower η. In that sense, direct relation between ϕ/ϕ_m and emulsion η, as per equation 4.5.6, is applied, regardless their DSD curve.

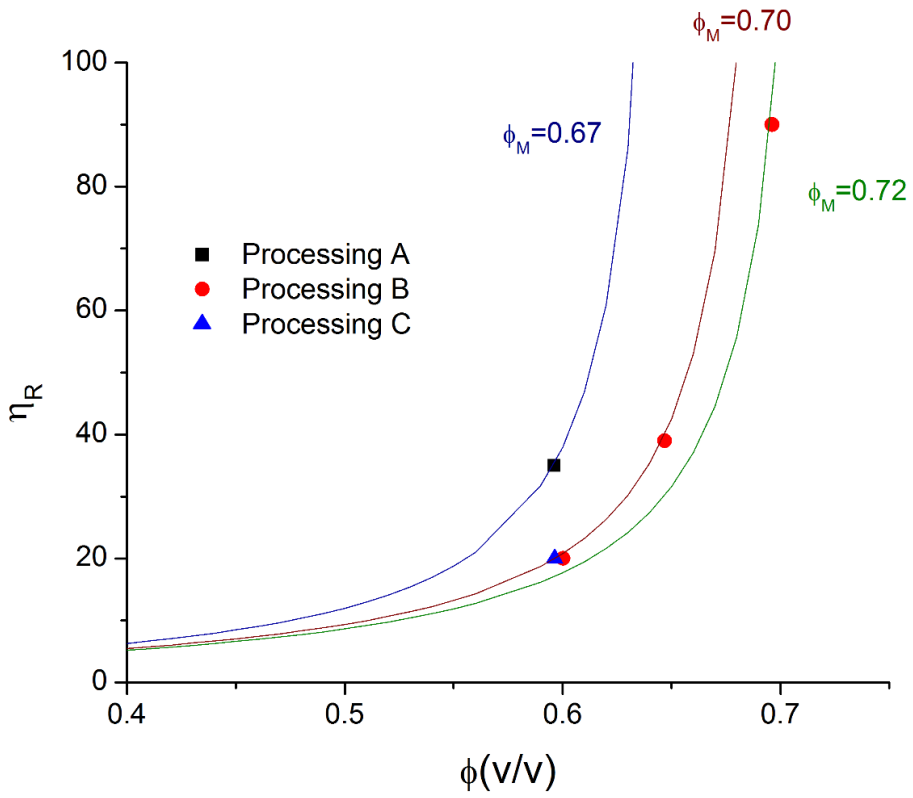

Figure 4. 5. 7 Emulsion relative viscosity (ηr) dependence on the dispersed phase volume fraction (ϕ) for all emulsion as function of processing procedure

4.5.3.3 Evaluation of the MKL emulsions breaking rate and characterization of their bituminous residues

Among other parameters, the current European specification EN 13808 identifies the type of cationic bitumen emulsion based on bitumen content (EN-16849) and breaking index class (EN-13075-1). Table 4.5.3 presents the results of these tests carried out on three bitumen emulsions prepared with the MKL emulsifier, at a typical range of 60-70 wt.% bitumen content.

Table 4. 5. 3 Results of bitumen content (EN 16849) and breaking index (EN 13075-1) tests for selected bitumen emulsions

Bitumen emulsion prepared	**Bitumen content (wt.%)**	**EN 16849 Classification**	**Breaking index value**	**EN 13075-1 Classification**	**Potential uses based on EN 13808 - Spanish national annex**
pH1-60-B	61.18	58-62 (class 6)	110	70-155 (class 3)	CUR
				110-195 (class 4)	IMP (if fluxant added)
pH1-65-B	65.79	63-67 (class 7)	102	70-155 (class 3)	TRG
pH1-70-B	70.64	67-71 (class 9)	90	<110 (class 2)	TRG

CUR – Curing coating for water proofing of bituminous mixture

IMP – Primary coating for water proofing of granular layer

TRG – Chipping surface dressing

For those selected emulsions, the bitumen content measured presented a slightly higher value than initially fixed, due most probably to evaporation of water during the emulsification. In addition, the bitumen content has also shown to affect the emulsion

breaking index, as found in Table 4.5.3. As a consequence of fewer interactions among a smaller bitumen fraction, a higher filler load is required in order to cause breakage for B/W ratio of 60/40 if compared to B/W ratio of 70/30. Such slower emulsion setting might be useful when a significant amount of fine aggregate is considered in several types of mixture applications such as slurry seal, primary coating of granular layer, dense-grade asphalt concrete, etc., in the event of avoiding premature breakage during mixing.

Further, with the objective to evaluate MKL influence on the final binder properties, 60/40 B/W emulsions (procedure A) with varying MKL concentrations of 0.25, 0.5, 1 and 1.25 wt.% were subjected to evaporation in order to obtain residues containing 0.41, 0.83, 1.67 and 2.08 wt.% MKL, respectively. Then, these residues were characterized by means of viscous flow tests, at 60°C, and dynamic temperature sweeps, in addition to analysis with optical microscopy.

Figure 4.5.8 presents the results of bitumen residues viscous flow tests, at 60°C, as a function of the MKL concentration (C_{MKL}) remained after water evaporation.

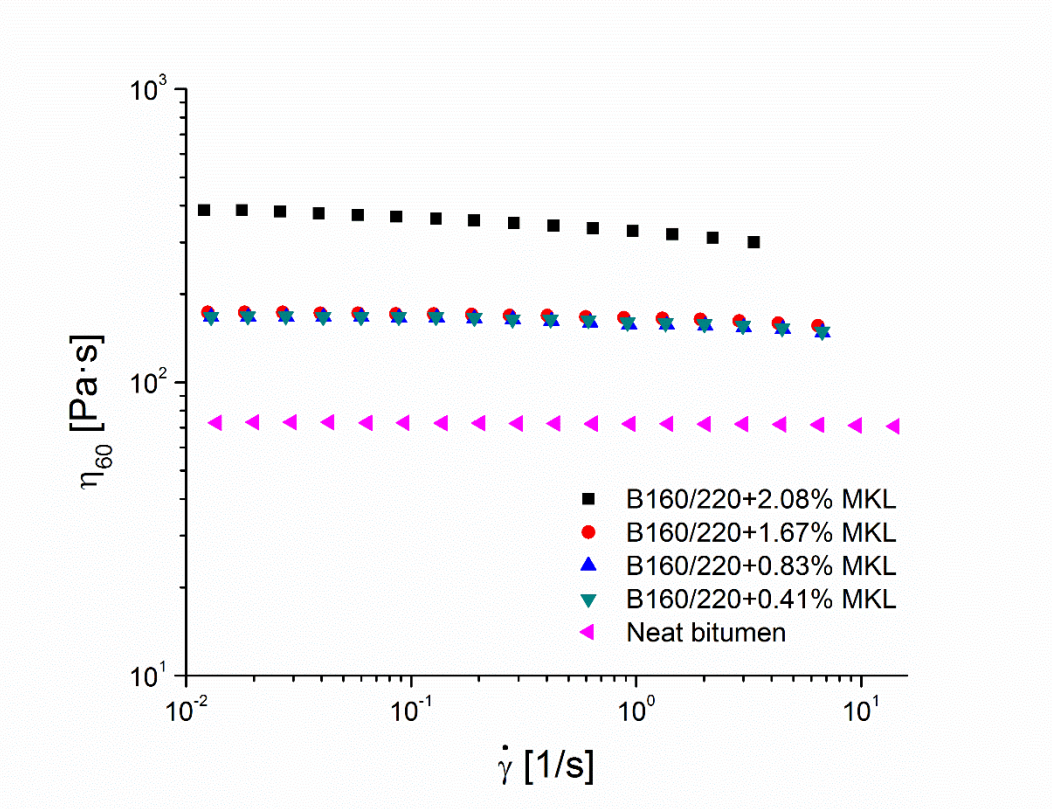

Figure 4. 5. 8 Viscous flow curves at 60 °C of bitumen residues containing the remaining MKL emulsifier at a concentration of 0.41, 0.83, 1.67, 2.08 wt.% and its neat bitumen

All the binders showed Newtonian (or nearly) behavior (no shear rate dependence). Residues with MKL concentrations of up to 1.67 wt.% proved comparable viscosity of about 160 Pa·s, significantly higher than those for the neat bitumen. However, a viscosity increase up to 350 Pa·s was observed after C_{MKL} was raised up to 2.08 wt.%, indicating enhanced modification which caused increased flow resistance.

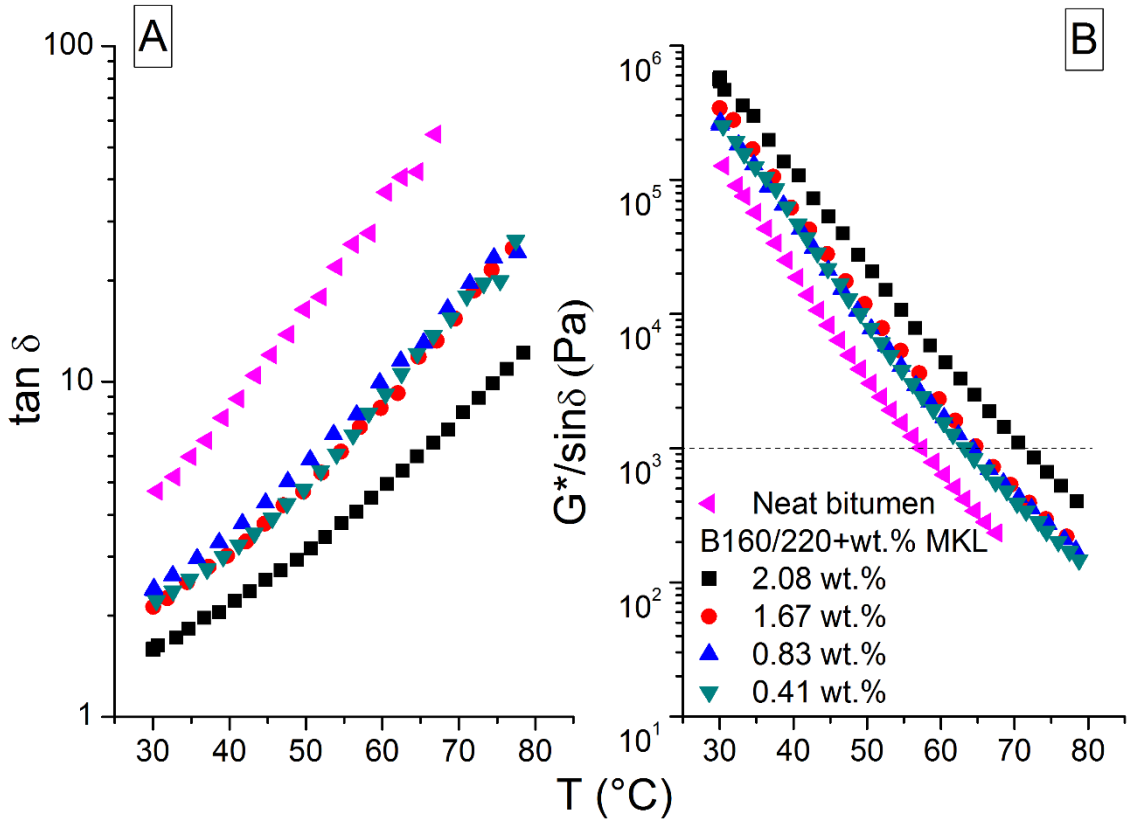

Figure 4. 5. 9 Viscoelastic behavior of bitumen residues containing the remaining MKL emulsifier at a concentration of 0.41, 0.83, 1.67, 2.08 wt.% and its neat bitumen: a) loss tangent between 30-80 °C; and B) rutting parameter.

In addition, their linear viscoelastic behaviors were evaluated and are presented in the form of the evolution of loss tangent with temperature (Figure 4.5.9a) and the "rutting parameter" derived from simple dynamic temperature sweep tests, |G*|/sin δ, (Figure 4.5.9b). In Figure 4.5.9a, the loss tangent (ratio of loss modulus to storage modulus, G''/G') of neat bitumen showed prevailing viscous behavior which became more notorious with increasing temperature from 30 to 80 °C. The presence of MKL at any concentrations, however, led to significantly lower tan δ and dampened thermal susceptibility in the temperature interval from 30 to 55°C. Moreover, "rutting parameter" may be considered an easier and more hands-on way to compare the

degree of improvement attained after modification. Thus, the values of temperatures at which |G*|/sin δ (under certain testing conditions outlined by AASHTO MP1 equals 1 kPa significantly increased from 57 °C for neat bitumen to 63-65 °C for 0.41-1.6 wt.% MKL and up to 71 °C for the 2.08 wt.% MKL modified bituminous residue (Figure 4.5.9b). So, the effect of the different MKL concentration on the elastic contribution results evident. It seems that a new developed structure is causing further increase in the elastic response when C_{MKL} is raised from 1.67 to 2.08 wt.%.

In order to contrast such a hypothesis, the morphology of the four bitumen residues was observed by optical microscopy. Their corresponding optical micrographs, at room temperature, are shown in Figure 4.5.10. As seen, the micrographs reveal fairly well distributed black/dark-brown particles on a lighter bitumen background. Those black/dark-brown particles are assigned for the MKL, and their number clearly increases as the concentration of emulsifier added does. However, even though some larger particles are observed in Figure 4.5.10c, there does not seem to be significant differences in terms of particle size and their round shape for MKL concentrations between 0.41 and 1.67 wt.%. On the contrary, larger and non-spherical particles are found when C_{MKL} is 2.08 wt.%. This particle anomaly might be explained in terms of flocculation of MKL particles. In fact, at 1.67 wt.% MKL, a small number of larger particles proves to be, probably, the onset of the flocs formation. For this reason, a notorious change in the viscous and viscoelastic response was observed when the MKL concentration was increased from 1.67 to 2.08 wt.%.

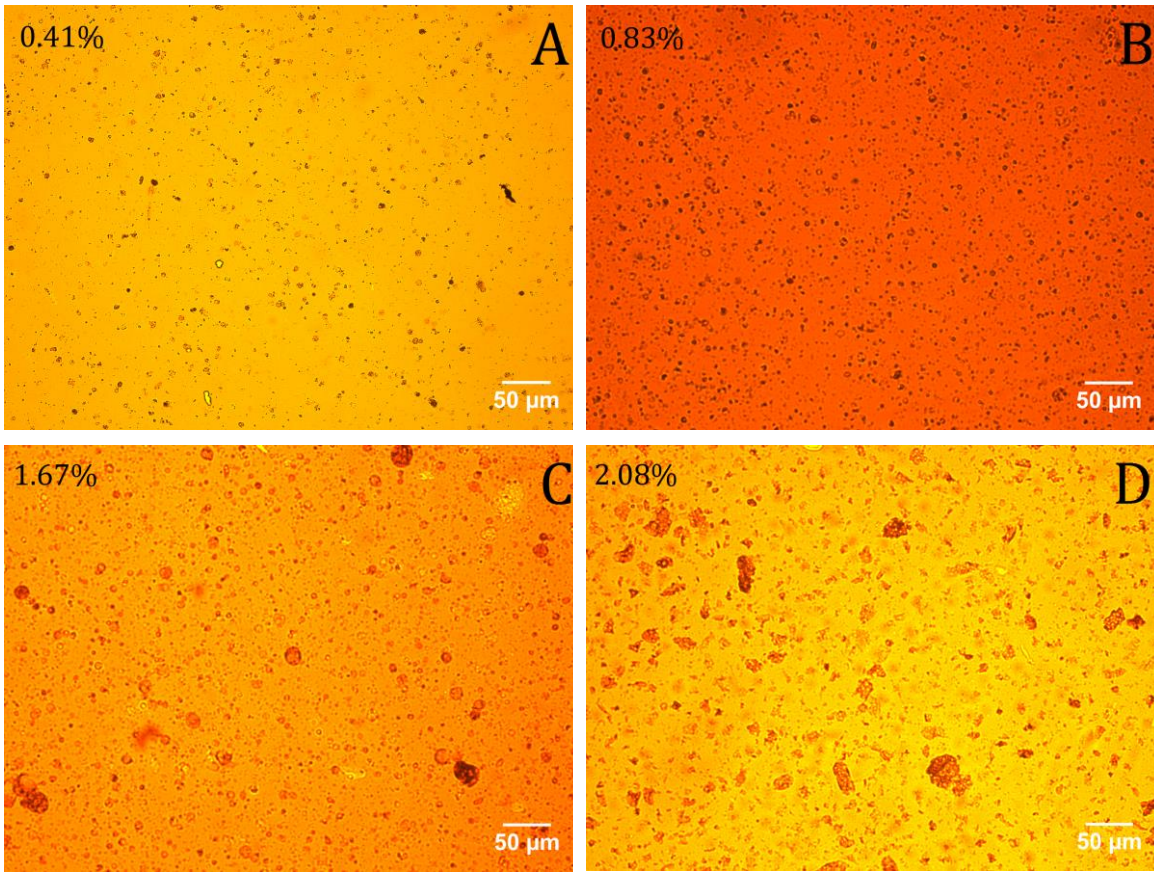

Figure 4. 5. 10 Optical micrograph of bitumen residue as a function of MKL percentage in bitumen; A) 0.41, B) 0.83, C) 1.67 and D) 2.08%

4.5.3.4 MKL bitumen emulsions applications

Based on the results in Table 4.5.3, two potential applications may be proposed: chipping surface dressing and asphalt mixes (EN13808 2013). Related to the chipping application, Vialit adhesion plate shock test was performed on two selected siliceous mineral aggregates (sizes 4/6 and 8/11), as presented in Figure 4.5.11. As can be observed, some aggregates persisted attached to bitumen on the plate and others, though detached, were stained with bitumen. Thereby, the absence of unstained aggregates on both sizes suggests 100% adhesivity at the tested temperature of 5°C. Furthermore, fragility temperature of 4/6 aggregates could be reported to be about 5°C, as 91% of them remained bonded to the plate (EN 12697-3).

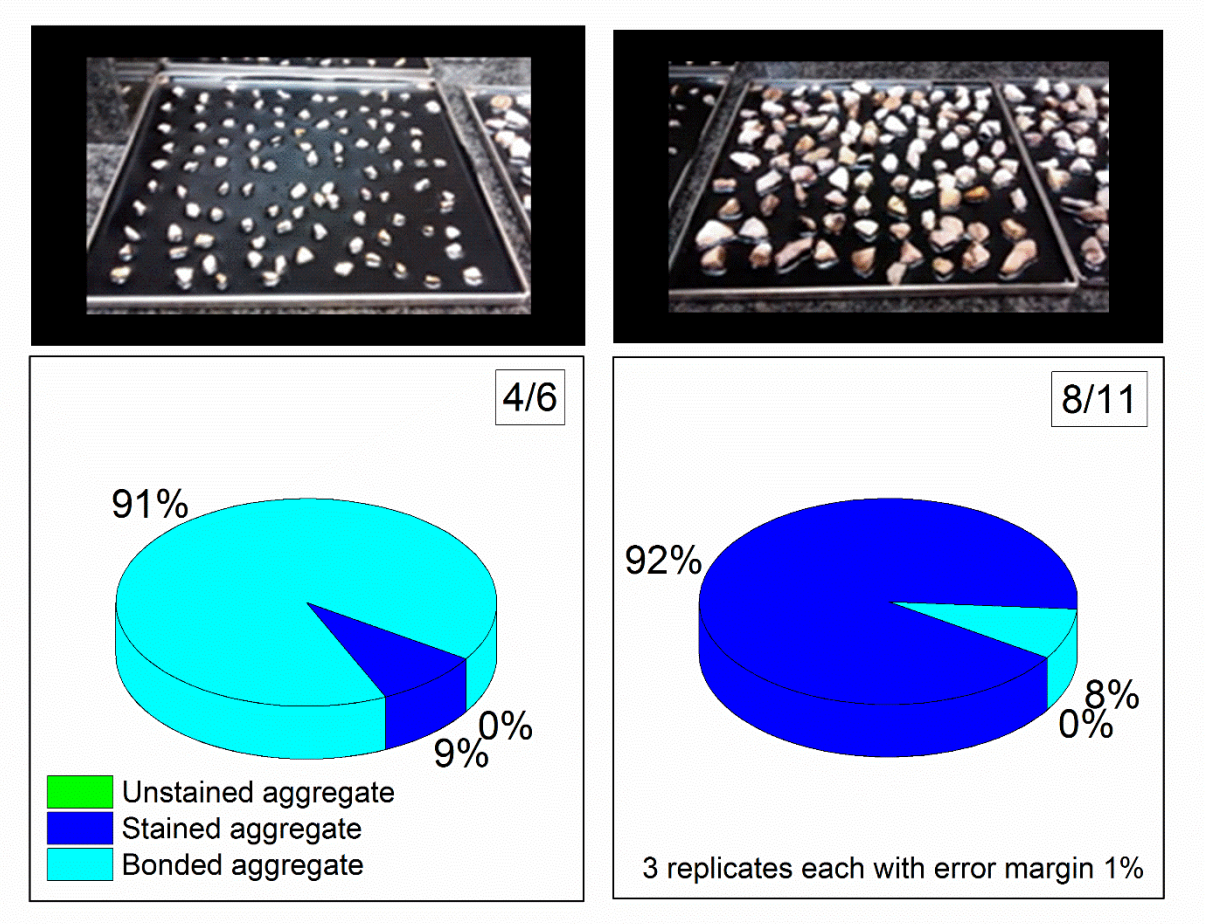

Figure 4. 5. 11 Vialit plate shock test results at 5°C

As for the potential application in asphalt mixes, several mechanical tests, including gyratory compaction, ITSM at 20 °C, and ITS at 15 °C, were performed on two HWMA, of AC 16 design, prepared with: a) 100% RAP and b) virgin aggregates (as reference). Figure 4.5.12 presents the evolution of the height of specimen with the number of gyrations, performed in a gyratory compactor, and includes the linear fitting compaction model curve. The workability indicator value (C), calculated according to the compaction model defined by Equation 4.5.2, has shown minor difference between both cases. This suggests a relatively comparable grading curve, as per LPC bituminous mixture design guide and/or EN 12697-10. However, a non-linear response on the 100% RAP curve, as not being able for significant further compaction, implies several issues in mixture design; ie. a too high percentage of fine fraction, an

excess of bitumen emulsion, or a partial blending (aged and fresh bitumen) to yield a sudden increase in binder viscosity. In that sense, a further design investigation of those parameters for bituminous mixtures involving 100% RAP in HWMA technology using particularly MKL emulsion would result of great interest, though uncovered in this article.

Indirect tensile test (IDT) results for indirect tensile stiffness modulus (ITSM) at 20 °C and indirect tensile strength (ITS) at 15 °C are presented in inset of Figure 4.5.12. Both ITSM and ITS results for 100% RAP present higher values than the reference specimen. The fraction of aged binder in the RAP (partially blended with the fresh binder coming from the bitumen emulsion) contributes to an increase in ITSM and ITS, if compared to the reference specimen which only contains fresh binder. This result has also been reported elsewhere (Zaumanis et al. 2014a; Dinis-Almeida et al. 2016) for technologies at higher temperature like WMA or even HMA. If compared to ITS values obtained by Gómez-Meijide et al. (2014) at 25°C for cold recycled mixtures, the ITS values in Figure 4.5.12 appear quite high. The reason is probably a lower testing temperature than that specified in the work above. Moreover, our higher preparation temperature enables a better diffusion of fresh binder into aged binder, which may contribute to raise the measured values in Figure 4.5.12, if compared to conditions used in (Gómez-Meijide and Pérez 2014). As for ITSM results, Graziani et al. (2016) carried out ITSM at 20°C on cold recycled mixes containing 2.5% cement. They found values higher than those in Figure 4.5.12. Interestingly, ITSM of 100% RAP mixture prepared using half warm technology and binder in the form of MKL emulsion has shown a ITSM value of 3.7 GPa, comparable to specimens commonly prepared with hot mixes procedure at 140 °C, for the same AC 16 design and test procedure followed (Pérez-Jiménez et al. 2014). However, as mentioned earlier, the use of MKL emulsion

for HWMA involving 100% RAP content requires further investigation, especially as far as the MKL emulsifier and aggregate grading curve contributions are concerned.

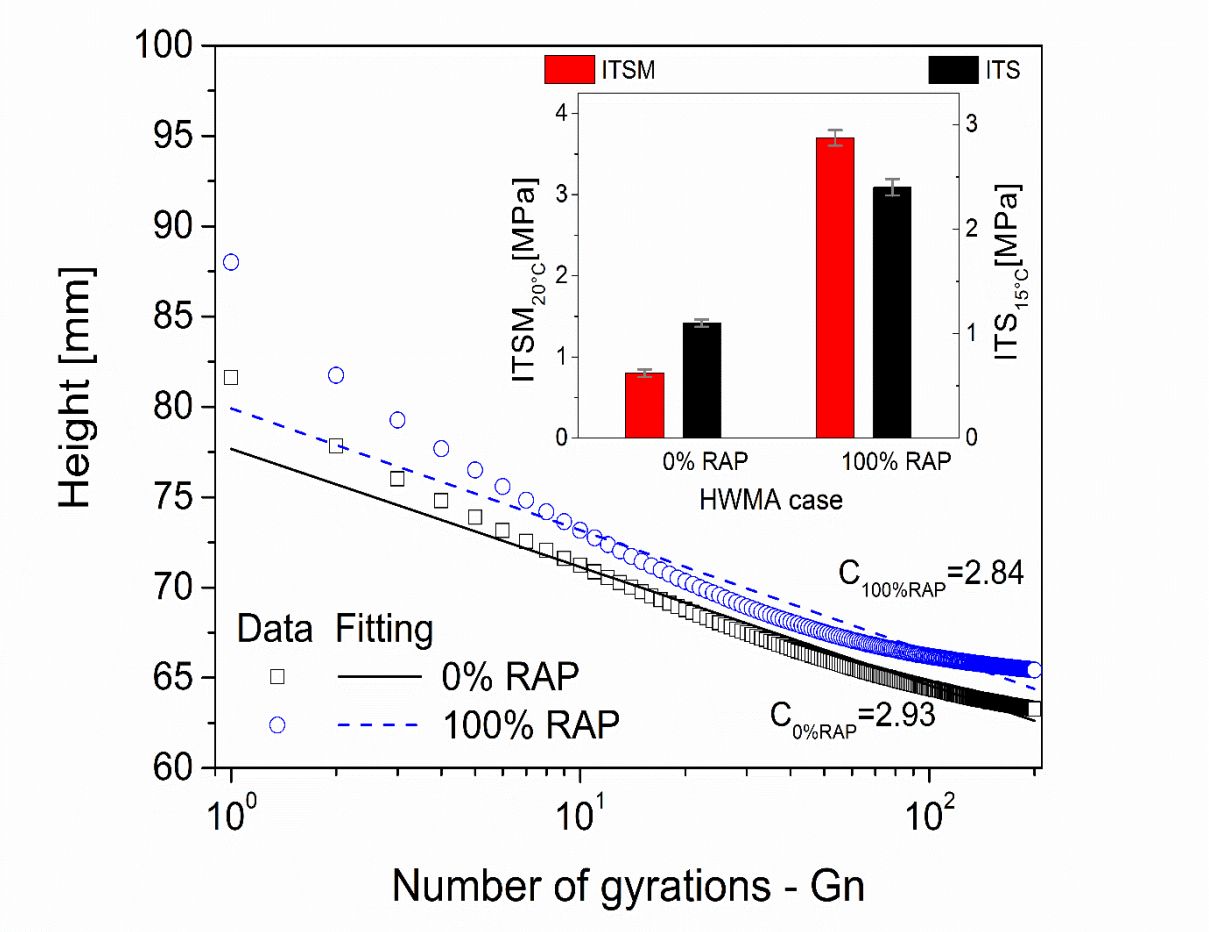

Figure 4. 5. 12 Compactability of specimen containing 100% RAP and virgin aggregate (0% RAP), adapting AC16 design, plotted as height of 100 mm diameter specimen vs number of gyrations. Inset-Indirect tensile test (IDT) results: indirect tensile stiffness modulus at 20 °C (ITSM) and indirect tensile strength 15 °C (ITS)

4.5.4 Concluding remarks

The Mannich reaction has proved its potential in the preparation of a cationic emulsifier for bitumen emulsions. The product obtained after reaction of Kraft lignin with tetraethylene pentamine and formaldehyde in alkaline medium (MKL) presented nearly 100% of solubility in acidic aqueous solution at pH ranging from 1 to 5, interval within which the raw Kraft lignin remained insoluble.

The use of MKL in the fabrication of cationic bitumen emulsions with a bitumen content of up to 70 wt.% was successful. The study on model MKL bitumen emulsions with constant surfactant concentration showed the significant effect of pH on Sauter mean droplet diameter and viscous flow behavior at low shear rates. At that region, emulsions proved to be more viscous and sensitive to shear rate as pH decreased. On the other hand, B/W ratio dominates the high shear flow behavior, seen as an increase in η_∞ with increasing B/W ratio. Under fixed pH and B/W ratio, different processing procedures led to evident differences in the emulsions DSD.

Additionally, MKL has shown to improve the viscous flow resistance of the emulsions residues, mainly above a threshold concentration of about 2 wt.%. Beyond this value notorious morphology changes (larger and non-spherical MKL flocs) were perceived by optical microscopy observations.

Lastly, HWMA specimens containing 100% RAP or virgin aggregates were successfully prepared at 80°C by gyratory compaction with a selected 60/40 MKL bitumen emulsion. The 100% RAP specimen showed much higher mechanical resistance as a consequence of the partial blending of fresh binder with RAP aged binder. However, further investigation on the role of MKL is required.

4.6 Sustainable asphalt mixes manufactured with reclaimed asphalt and reduced-temperature technologies, using modified-lignin-stabilized bitumen emulsions

ABSTRACT

This research aims to develop asphalt mixes with maximum recycling rate and minimum impact to environment. Their manufacture comprises the use of 100 % reclaimed asphalt pavements (RAP) as source of aggregates and a bitumen emulsion stabilized by amine-functionalized lignin, along with application of reduced-temperature asphalt technologies, between 80 to 130 °C. Previously, the effect of emulsification parameters such as emulsification device and time were evaluated by emulsion droplet size distribution and rheology measurements. Moreover, a study combining Pendant drop and Sessile drop (on a prototype polyethylene surface) tests proved enhanced values of the surface tension dispersive component upon addition of the modified lignin emulsifier to water phase. This result suggested that emulsion aqueous phase containing modified lignin would be able to wet the hydrophobic surface of RAP. Accordingly, reduced-temperature asphalt mixes (using bitumen emulsions stabilized by modified lignin) were successfully prepared to meet French design requirements. Asphalt mixes were subjected to four levels of characterization according to French design method for hot mixes, including gyratory compaction, rutting resistance, complex modulus and fatigue resistance tests. A semi-quantitative approach for estimating 'active' RAP binder content has been proposed, which would further minimize impact to environment, by balancing the manufacturing temperature and the fresh bitumen required.

4.6.1 Introduction

In the last decade, soaring pressure on the global environmental challenges demand immediate responses, as addressed in UN development agenda (Moon 2008). Particularly, issues involving sustainable-environmental–economic aspects are mostly discussed. In transport infrastructure construction sector, an example for such issues is the use of fresh bituminous and aggregate material, which has a high impact, up to 40% of CO_{2eq} (defined as mass of CO_2 emitted in kg over a ton of each layer needed during the lifecycle), if the extraction and production process are considered within the boundaries of analysis (Giani et al. 2015). Moreover, conventionally used hot mixes method during road construction may be perceived unsustainable due to energetically unfavorable process and highly potential pollutant emitted to the air (Lesueur 2011). In that sense, a reduction of virgin material (bitumen and aggregates) and the use of reduced-temperature processes would promote more sustainable road designs, attending both environmental and economic aspects.

Concerning the raw materials, the use of reclaimed asphalt pavement (RAP) is both economically and environmentally interesting due to the possible reduction of fresh binder, as well as the aggregates used. Such example reports a score, related to fossil depletion, lower down by 15% when RAP was employed considering ReCiPe method, an impact assessment according to two sets of impact categories: midpoint (single issue) and end-point (higher aggregation level) categories for easing the interpretation (Giani et al. 2015). That analysis is based on the comparison of three-structured layers (surface, binder and base) of which, one is manufactured with all virgin material and the other consist of up to 30% of RAP for the base layer. A reduction of 13-14 % in the cumulative energy demand has also been reported for

15% RAP recycled (Vidal et al. 2013). Besides those benefits, mechanical performance, of stiffness modulus and rutting resistance, could be improved (Apeagyei et al. 2013; Lopes et al. 2015; West et al. 2015). Obviously, such utmost benefit may be expected for a higher RAP recycling rate. Today, their uses (authorized in Europe – EN 13808-8) are yet limited to 10 % in surface layer and 20% in base layer (Delorme et al. 2007). The reason may be due to the difficulty in controlling the characteristics of aged binder and aggregates that potentially affect recomposed asphalt mixes final performance. For that reason, many studies focus on studying the influence of incorporating RAP at higher percentage, even up to 100% recycling, on their mechanical behavior, aiming at speeding up its authorization (Zaumanis et al. 2014a).

Partial blending phenomena, between RAP binder and fresh bitumen, yet requires understanding. This concept is widely accepted (Shirodkar et al. 2013; Lo Presti et al. 2016) that results in altering the performance of blended binder. For RAP recycled rate less than 25%, a study reports no particular change in binder grade is necessary (Kriz et al. 2014). Another study suggests an increase in the degree of partial blending from 70 to 96 % when mix compositions have been changed from involving 25% RAP and binder with PG70/28 specification to 35% RAP and PG50/28 (Shirodkar et al. 2011). From diffusion point of view, in which diffusion coefficient and viscosity are related by Arrhenius function with temperature, the lower the viscosity of bitumen at a particular temperature (or softer characteristics), the more favorable the diffusion to occur due to high diffusion coefficient (Oliver 1974). The comprehension of partial blending in HMA seems to drive in a converging direction, yet debatable on the investigation method for the moment. Unfortunately, when RAP is recomposed following a reduced-temperature mixing procedure, partial blending is another challenge. Many works done on recycled warm mix mostly explain about bitumen

content selection (Lopes et al. 2015; Dinis-Almeida et al. 2016), with the assumption of fully recovered RAP binder and without partial blending. In this work, a semi-quantitative approach, referred to thin-film diffusion phenomenon, has been proposed trying to understand partial blending under reduced-temperature mixing conditions. As a result, the fraction of 'active' RAP binder blended with the fresh bitumen could be estimated.

Another interesting material that can be potentially be used in road infrastructure is lignin. A previous study reports that lignin seems to be compatible with bitumen due to the similarity in their aromatic molecular structure (Slaghek et al. 2015). Lignin is a renewable material, derived from wood in the form of lignocellulose. While the cellulose is the main input of pulp plant, lignin mainly ends up burnt in heat regenerator (Laurichesse and Avérous 2014). Due to the aromatic structure, lignin potential as a precursor for advanced materials could be opened through chemical modification. By lignin amination, for instance, cationic emulsifier for bitumen emulsion application could be obtained. Previous study shows that modified lignin (MKL) may prevent coalescence, as observed by insignificant change in average droplet size and its distribution profile over 15 months, hence providing good stability. Despite stability during storage, bitumen emulsion also requires to wet the aggregate surface upon application, by a balance between the negative charge of the fresh aggregate and the positive charge of the cationic surfactant (Ronald and Luis 2016). However, if the bitumen emulsion (and the emulsifier) is designed to coat a 100% RAP, its physical properties may not be treated equivalently to coat virgin aggregates, due to the difference in surface characteristics. Thus, further research regarding emulsion/surfactant wettability on a hydrophobic surface is required to assess their interactions with RAP surface.

With the main objective to design asphalt mixes with maximum recycling and minimum impact to environment, this study is divided into three subtopics with the aims of: developing emulsifiers from lignin, able to partially wet RAP surface; optimizing processing parameters during the manufacture of bitumen emulsion; and producing reduced-temperature asphalt mixes containing 100% RAP without sacrificing their mechanical performance.

4.6.2 Experimental

4.6.2.1 Materials

Kraft lignin (KL), tetra-ethylene-pentamine (TEPA) and formaldehyde (supplied as 37 vol.% aqueous solution), purchased from Sigma-Aldrich (France), were used as reagents for producing cationic modified lignin (MKL). Kraft lignin used has a molecular weight of 10000 g/mol, an ash content of 3.14 wt.% and elemental composition (wt.%) consisting 61.15 of C, 6.72 of H, 26.92 of O, 2.18 of N and 2.54 of S. As for the reference, n-tallow alkyl tri-methylene diamine, under commercial name of Asfier100 from Kao Chemicals (USA) was selected. Bitumen used to manufacture the emulsions was kindly supplied by Repsol S.A. (Spain). Penetration test and Ring-and-Ball softening temperature, according to EN 1426:2007 and EN 1427:2007, were performed on bitumen to obtain the values of 190 dmm and of 39 °C, respectively. Finally, RAP was kindly supplied by IFSTTAR (France) that came from the fatigue carrousel of a real scale road fatigue simulator under accelerated heavy traffic.

4.6.2.2 Preparations

MKL emulsifier reaction procedure was presented elsewhere (Yuliestyan et al. 2017). Afterwards, concentrated MKL was diluted with acidic water at pH 1 to attain final

concentrations between 0.625 and 3.75%. Bitumen emulsions were prepared by emulsifying 60 wt.% of bitumen into that aqueous phase, at a selected concentration of 1.5 wt.% of MKL emulsifier. For sake of comparison, three emulsification devices were used in this study: A) three batch homogenizers UltraTurrax T25 and T50 from IKA (Germany) and a L5M from Silverson (US); and B) an inline three-stage high-shear homogenizer IKA Process-Pilot 2000/4-HT (Germany), referred to as 3STCM. The first three devices are small capacity processing units (200 – 500 gr). A premix of 145 °C bitumen and 60 °C of aqueous surfactant solution yielded a blend with an approximate temperature of 90 °C, to avoid water evaporation. Short after, emulsification at the maximum speed was done for 4 min. The difference with the in-line homogenizer type is in the capacity and the ability for continuous recirculation of the emulsion. When recirculation line was employed, the maximum capacity is 5 kg, and emulsification time was further evaluated on 3STCM by taking sample through recirculating line starting from 1 to 12 minutes. For the reference emulsion, 0.5 wt.% was dissolved in aqueous phase with pH 1 and the rest of procedures were similarly followed

For RAP binder analysis, sample was extracted using perchloroethylene solvent on automatic asphalt analyser (EN 12697-1) followed by binder recovery process in rotary evaporator (EN 12697-3). Details on the conditioning for mixing and compaction and the quantity of added water and fresh bitumen are presented in Table 4.6.1. The mixing was performed in two steps: first water addition for moisturizing RAP surface followed by bitumen emulsion addition for a total mixing time of 2.5 min. Compaction, apart from compaction study using gyratory compactor, was done using tire roller compactor. Once compacted, slabs were allowed for three days curing at 50 °C. For complex modulus and fatigues resistance tests, slabs were cut into trapezoidal specimen with sawing machine.

Table 4. 6. 1 Asphalt mixes preparation

	White aggregate		Black aggregate	
	WMA	**HWMA**	**HWMA-1**	**HWMA-2**
RAP aggregate				
Temperature °C	130	80	110	80
Binder				
RAP binder (%)	3.92	3.92	4.47	4.47
Additional bitumen (lignin emulsion C60) (%)	1.6	1.6	2.6	3.4
Bitumen emulsion	2.7	2.7	4.3	5.7
Added water (%)	0.75	0.75	0.75	1.5
Processing				
Compaction temp. °C	120	60	90	60

4.6.2.3 Tests and measurements

Surface tension measurements on acidic aqueous phase solution containing MKL emulsifier were done by the pendant drop method. The device consists of a camera with fixed focal length lens, pendant drop injector and LED lamp. The pendant drop was formed by a needle injector with outer diameter of 0.8 mm, and images were captured and analysed in real-time using Dinaten software, developed by the Department of Applied Physics at the University of Granada (Spain). Accurate surface tension measurements were obtained at the point that the drop was close to detach from the tip, when a more favorable deformation is caused by a bigger drop weight. With the same apparatus setup, the Sessile drop approach was used to test the contact

angle between a polyethylene surface (used as reference hydrophobic prototype) and a drop of aqueous solution at varying concentrations of the lignin surfactant studied. The procedure was adapted from general methodology explained elsewhere (Rodríguez-Valverde et al. 2002).

Bitumen emulsion properties was characterized by means of droplet size distribution (DSD) and viscous flow tests. DSD measurements were conducted in a Mastersizer 2000 laser diffraction analyzer from Malvern (UK), at ambient temperature. The refractive indices for bitumen and water were set at 1.61 and 1.33, respectively. Viscous flow tests at 30 °C were carried out in a controlled-stress rheometer Physica MCR-301 by AntonPaar (Austria), using a coaxial cylinder Z20-DIN (27 mm diameter) geometry, on steady rotational shear mode. Tests were performed by progressively increasing shear stress applied so that shear rate ranges are between 0.1 and 500 s^{-1}, with an equilibration time of 2 min, at every stress applied, to achieve steady state conditions. Geometry used was serrated type for avoiding wall-slip phenomena (Dealy and Larson 2006). For binders, flow tests between 0.01 – 50 s^{-1} were performed on extracted RAP bitumen and fresh bitumen, using plate-plate geometry in a Kinexus rheometer from Malvern (UK), at four temperatures of 60, 90, 120 and 150 °C.

Characterization of asphalt mixes was performed at four levels according to French design method (Delorme et al. 2007). In the first level, PCG3 mlpc® gyratory compactor was used to analyse their compaction behaviour. Loose mixes specimen was compacted in a rotating 150 mm diameter cylindrical mould, inclined at 0.82° (internal angle), with vertical pressure of 0.6 MPa according to EN-12697-10. The second level deals with rutting resistance that was done in wheel tracking device ORNIEREUR mlpc® (Vectrafrance, France), based on EN-12697-22. A 100 mm

thickness of parallelepiped specimen were subjected to sustain a 5 kN load of alternating wheel/tire at a frequency of 1 Hz (inside chamber at 60 °C) for up to 30000 cycles. Afterward, complex modulus was measured using MLPC-3MC® machine (Vectrafrance, France), according to EN-12697-26, by applying a sinusoidal small deformation on trapezoidal specimen at a ramp of frequency from 1 to 40 Hz, for each specified temperature between -10 and 40 °C. The last test (fourth level), according to EN-12697-24, aimed to estimate mix service life by measuring the change of complex modulus of trapezoidal specimen, subjected to a repetitive load between 80 and 150 μstrain, up to reduced-value by half at certain cycles.

4.6.3 Results and discussion

4.6.3.1 Characterization of aqueous phase containing modified lignin emulsifier

As a preliminary attempt to foresee the expected wettability improvement caused by the surfactant, the polar and dispersive components of the surface tension of aqueous solutions containing increasing concentrations of the modified lignin (MKL) were determined. Calculations involved Sessile drop contact angle (θ) measurements on a prototype non-polar polyethylene surface, along with Pendant drop tests in order to find out the overall surface tensions (γ) values (Figure 4.6.1). Despite a little fraction of compounds providing polar interactions, bitumen nature is mainly hydrophobic, and its surface free energy is mostly dominated by the dispersive component, related to van der Waals interactions (Ziyani et al. 2016). As RAP is basically aged-bitumen-coated aggregates, a surfactant solution with enhanced values of the surface tension dispersive component, at the expense of lower values of the polar component, results

a sensible approach to promote the interaction between MKL emulsifier (stabilizing bitumen emulsion) and bitumen hydrophobic surface. The selection of PE as standard reference for the Sessile drop method is based on the fact that it lacks polar component. So, the dispersive component is obtained straightforward with just one test. If the total surface tension of the liquid is previously determined by Pendant drop, the difference between the total and dispersive components gives the polar component.

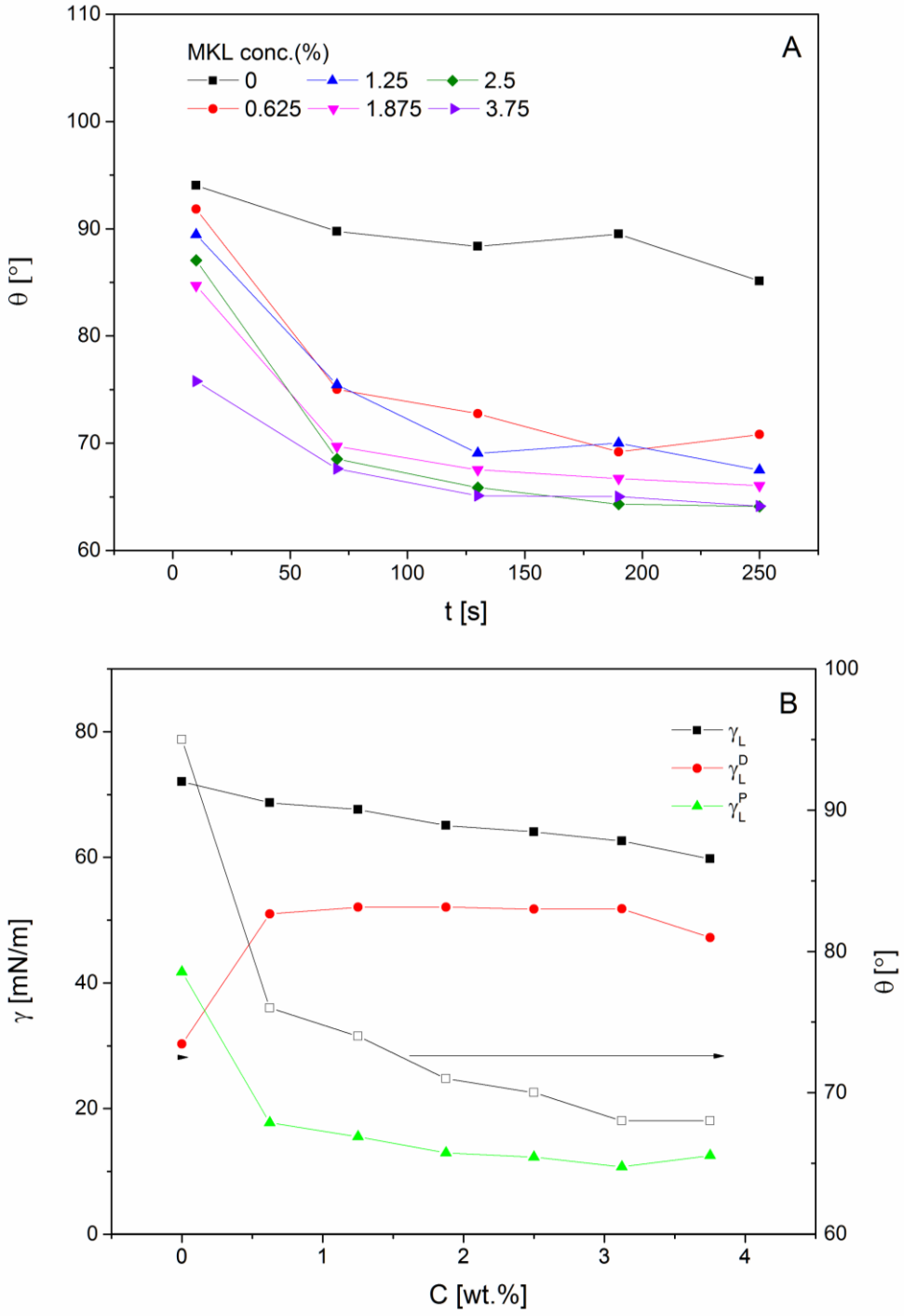

Figure 4. 6. 1 A) Evolution of contact angle (θ) on polyethylene substrate with respect to time and B) Contact angle (θ), liquid surface tension (γ_L), its disperse component (γ_L^D) and polar component (γ_L^P), of aqueous phase as a function of concentration.

As shown in Figure 4.6.1A, Sessile drop tests were conducted in static mode such that the time-dependent contact angles (θ) were monitored over an image capturing period of 250 s, for all cases studied. It is worth mentioning that evaporation influence was assumed negligible due to the closed-saturated system environment employed. For all MKL cases, a sharp decay in contact angle occurs at the beginning of the test, over the first 70s, followed by a milder decrease until steady values were achieved after 250 s.

The Sessile drop test is based on Young equation (Wu 1982), for a liquid drop on a solid surface, in equilibrium conditions, which can be conveniently arranged as follows:

$$\gamma_L \cdot (1 + cos\theta) \quad = \gamma_S + \gamma_L - \gamma_{S-L} \tag{4.6.1}$$

where γ_S, γ_L and $\gamma_{S\text{-}L}$ represent surface tensions (surface free energy) of solid and liquid, and interfacial tension solid-liquid, respectively, and $\gamma_L{\cdot}(1+\cos\theta)$ is the so-called "adhesion work". Using Owens-Wendt method (Mittal 2013), where the surface tension is calculated as the sum of dispersive (γ^D) and polar (γ^P) components:

$$\gamma = \gamma^D + \gamma^P \tag{4.6.2}$$

the adhesion work is expressed as follows:

$$\gamma_L \cdot (1 + cos\theta) = 2\sqrt{\gamma_L^D \cdot \gamma_S^D} + 2\sqrt{\gamma_L^P \cdot \gamma_S^P} \tag{4.6.3}$$

For the PE solid used as reference, with only dispersive component of γ_S^D = 35.3 mN/m (literature value), no polar interaction is expected (Starkweather 1965). Thus, by rearranging equation (4.6.1) and given that the overall value of surface tension of the

liquid (γ_L) is previously determined via pendant drop test, the dispersive contribution of the aqueous phase containing MKL can be obtained by equation (4.6.4):

$$\gamma_L^D = \frac{1}{\gamma_S^D}\left[\frac{(1+cos\theta)\cdot\gamma_L}{2}\right]^2 \quad (4.6.4)$$

and, then, the liquid polar component is calculated by equation (4.6.2).

As previously mentioned, the surface tension (γ) was first obtained from pendant drop technique, which is based on the fact that the curvature of the drop profile is the result of the balance between surface tension and gravitational forces (Stauffer 1965). As observed in Figure 4.6.1B, γ value of water (0 wt.% MKL), is 72 mN/m, and gradually decreased down to 59.74 mN/m when concentration of MKL in aqueous phase increases up to 3.75 wt.%, or equivalent to 1.5 wt.% MKL in a 60/40 emulsion. The contact angle (θ) on PE substrate (to the right Y axis) decreased fairly significant from 0 to 0.625 wt.% MKL, but less significant between 0.625 and 3.75 wt.% (probably the critical micelle concentration, CMC, has been already attained at 0.625 wt.%). This suggests improved wettability of hydrophobic substrate when MKL is added to the aqueous phase. Moreover, MKL addition altered both dispersive (γ^D) and polar (γ^P) surface tension components. Thus, with the addition of 0.625 wt.% MKL, γ^P is reduced and γ^D is increased.

It is worth noting that the higher the matched ratio of dispersive to polar component between liquid and solid, the more interaction may be expected (Mittal 2013). Therefore, the effect of the MKL may contribute to improve wetting on bitumen-coated RAP aggregates by the proposed emulsion.

4.6.3.2 Influence of processing parameter in the preparation of bitumen emulsion

Figure 4.6.2A presents droplet size distribution (DSD) of 60/40 bitumen emulsions stabilized by 1.5% modified lignin emulsifier, prepared using different emulsification devices. DSD of all emulsions are fairly similar, except for the one prepared in SilL5M. Apart from emulsification time, study demonstrates that $D_{3,2}$ values are governed by the dissipation energy, which is affected by processing parameters such as rotational speed 'N' where $D_{3,2} \sim N^{-1.2}$ (Gingras et al. 2007b). For emulsions emulsified for a similar time of 4 min, $D_{3,2} \sim N^{-1}$ seems valid, e.g. comparing homogenizers T25 at 20.000rpm ($D_{3,2(T25\ @20k\ rpm)}$ = 8.5 μm) and Sil5M at 5000 rpm ($D_{3,2(Sil5M\ @5k\ rpm)}$ =26 μm). Nevertheless, $D_{3,2}$ of homogenizer T50 is lower than that of T25, despite emulsion was manufactured with lower N. In this case, geometry of T50, with larger rotor/stator diameters than T25, also affects $D_{3,2}$ (Gingras et al. 2007b). Thus, the combined rotational speed and device configuration parameter results to improve energy dissipation, observed in the reduction of $D_{3,2}$.

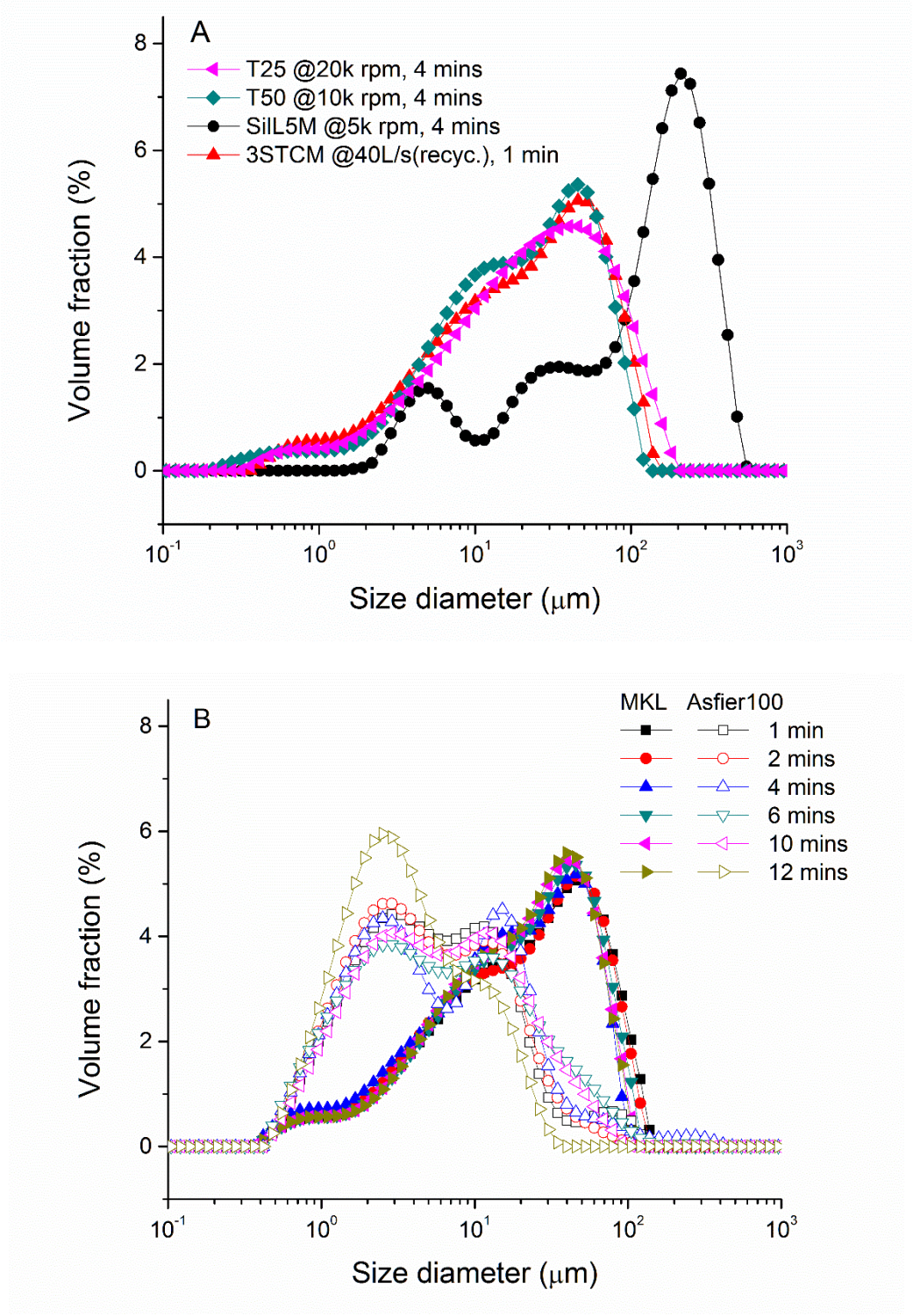

Figure 4. 6. 2 Droplet size distribution of bitumen (160/220) emulsion as a function of: A) different processing procedure followed (device and emulsification time); and B) effect emulsification time for a selected device three-stage in-line homogenizer - 3STCM

Table 4. 6. 2 Sauter ($D_{3,2}$) and De-Brouckere ($D_{4,3}$) mean diameters of emulsion produced using MKL and Asfier100 emulsifier as a function of emulsification time

Emulsification device	**Emulsification time**	**MKL**		**Asfier100**	
		$D_{3,2}$	**$D_{4,3}$**	**$D_{3,2}$**	**$D_{4,3}$**
IKA UT T25	4	8.45	39.04	-	-
IKA UT T50	4	6.01	26.69	-	-
Silverson L5M	4	25.56	141.26	-	-
3STCM	1	6.70	29.56	2.81	9.66
	2	6.46	28.33	2.68	8.07
	4	5.56	23.31	2.78	12.96
	6	6.63	26.73	2.81	12.19
	10	6.52	25.19	3.03	10.10
	12	6.55	24.92	2.27	5.08

For sake of comparison and scale-up, emulsification was also performed using an in-line homogenizer (3STCM), with a much more robust three-stage-emulsification geometry. As may be seen in Figure 4.6.2A and Table 4.6.2, DSD and $D_{3,2}$ values obtained were similar to those achieved by the T50 device, although in a much shorter emulsification time (1 min or less) and with a larger capacity (Figure 4.6.2A). Furthermore, Figure 4.6.2B presents DSD curves of 3STCM emulsions stabilized by MKL, for a longer emulsification time up to 12 mins. For comparison, emulsification with the reference Asfier100 emulsifier was also studied. Two major distinctive DSD profiles were observed at any time studied, assigned for MKL and Asfier100 cases. By using 3STCM, emulsification seems sufficient only in one minute of processing, regardless the type of emulsifier. Processing for a longer time does not cause any

significant DSD profile change. By analyzing average mean diameters (converted from DSD profile) in Table 4.6.2, the volume-weighted ($D_{4,3}$) mean diameter seems to be more affected than the surface-weighted $D_{3,2}$.

Flow behavior of emulsion as a function of O/W ratio between 30/70 to 60/40 is shown in Figure 4.6.3A. As commonly observed, bitumen emulsion presents shear thinning response at low shear rate, followed by Newtonian behavior at high shear rate, known as high-shear-rate limiting viscosity (η_∞). As may be seen, η_∞ values are affected by O/W ratio, presenting a higher value as more concentrated bitumen emulsions are, similar results have been already reported elsewhere (Gingras et al. 2005). All MKL-emulsions show a Newtonian region in a wide shear rate range, even when sheared between 0.1 and 1 s^{-1}. Compared to MKL-emulsions, Asfier100-emulsions present higher viscosity for each corresponding O/W ratio, showing their more highly-structured characteristics, clearly seen when the deformation is relatively small. Such phenomena might better be explained by internal phase fraction, related to the packing density (ϕ/ϕ_m), a ratio of emulsion volume fraction (ϕ) to its corresponding maximum packing (ϕ_m), and the relative viscosity (η_R). The value of η_R is calculated as the viscosity ratio of emulsion to its continuous phase, and can be fitted as a function of ϕ/ϕ_m by a model for concentrated suspensions, proposed by Frankel-Acrivos, as follows (Frankel and Acrivos 1967):

$$\eta_R = \frac{\eta_\infty}{\eta_{aqueous\ phase}} = 1.125 \cdot \left[\frac{\left(\frac{\phi}{\phi_m}\right)^{1/3}}{1 - \left(\frac{\phi}{\phi_m}\right)^{1/3}} \right] \qquad (4.6.5)$$

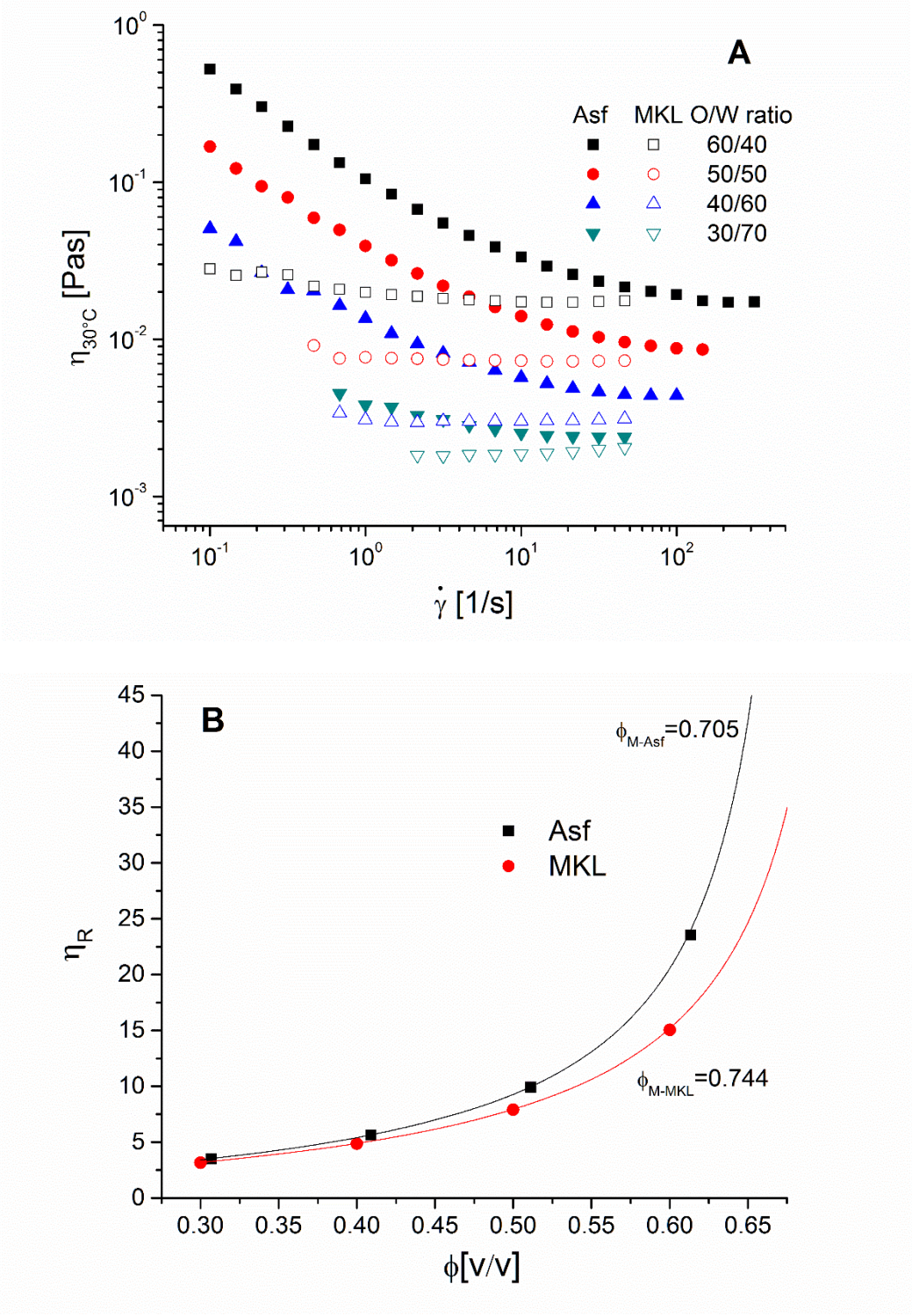

Figure 4. 6. 3A) Bitumen emulsion flow curves for O/W ratio within interval range of 60/40 to 30/70 and B) Frankel-Acrivos dependence of relative viscosity with dispersed phase volume fraction for emulsions stabilized by MKL and reference surfactant

In Figure 4.6.3B, the Frankel-Acrivos fitting curve describes fairly well experimental data. This result suggests η_∞ can be predicted from any O/W ratio higher than 30/70, given that the maximum internal phase value fraction (ϕ_m) is expected to be the same due to relatively similar DSD profiles of each set of emulsions (Figure 4.6.2B). In addition, the maximum packing of Asfier100 emulsion (ϕ_m = 0.705) is smaller. Therefore, for a given O/W ratio, their packing density (ϕ/ϕ_m) is always higher than MKL-emulsion. Such densely concentrated systems, governed by the increase in total interfacial area (and, therefore, by more interactions among droplets), result in more viscous emulsions (Otsubo and Prud'homme 1992; Barnes 1994).

4.6.3.3 Reduced-temperature asphalt mixes study

Manufacture of asphalt mixes composed of 100% RAP and fresh bitumen (from previous MKL modified bitumen emulsions), using reduced temperature technologies such as WMA and HWMA, will be assessed according to the standards of French design method for hot mixes.

To that end, bitumen emulsion containing modified lignin as emulsifier was mixed with 100% RAP as aggregates, with the aim of recovering RAP binder. Previously, RAP (with grading 0/10) was fractioned into four, of 0/2, 2/4, 4/8, and 8/10 fractions (Figure 4.6.4A). This splitting into fractions is advised for better homogeneity (De la Roche et al. 2010). Then, sieving on 'cleaned' white aggregates, after aged bitumen being stripped down, was performed to obtain the gradation of each fraction, as presented in Figure 4.6.4A. The quantity of each fraction was adjusted to superpose the recomposed profile with the targeted gradation for AC-BBSG 10 design, as in Figure 4.6.4B. A first approach, called "white aggregate", was followed for mix design that fixed the total bitumen (RAP binder and fresh B160/200) added to 5.5% (Table

4.6.1) and the grading curve was adjusted with fractions 2/4, 4/8, and 8/10, considering the size of cleaned RAP aggregates. Thus, "white aggregate" approach gave rise to the so-called WMA and HWMA mixes, prepared at 130 and 80 °C, respectively (Table 4.6.1).

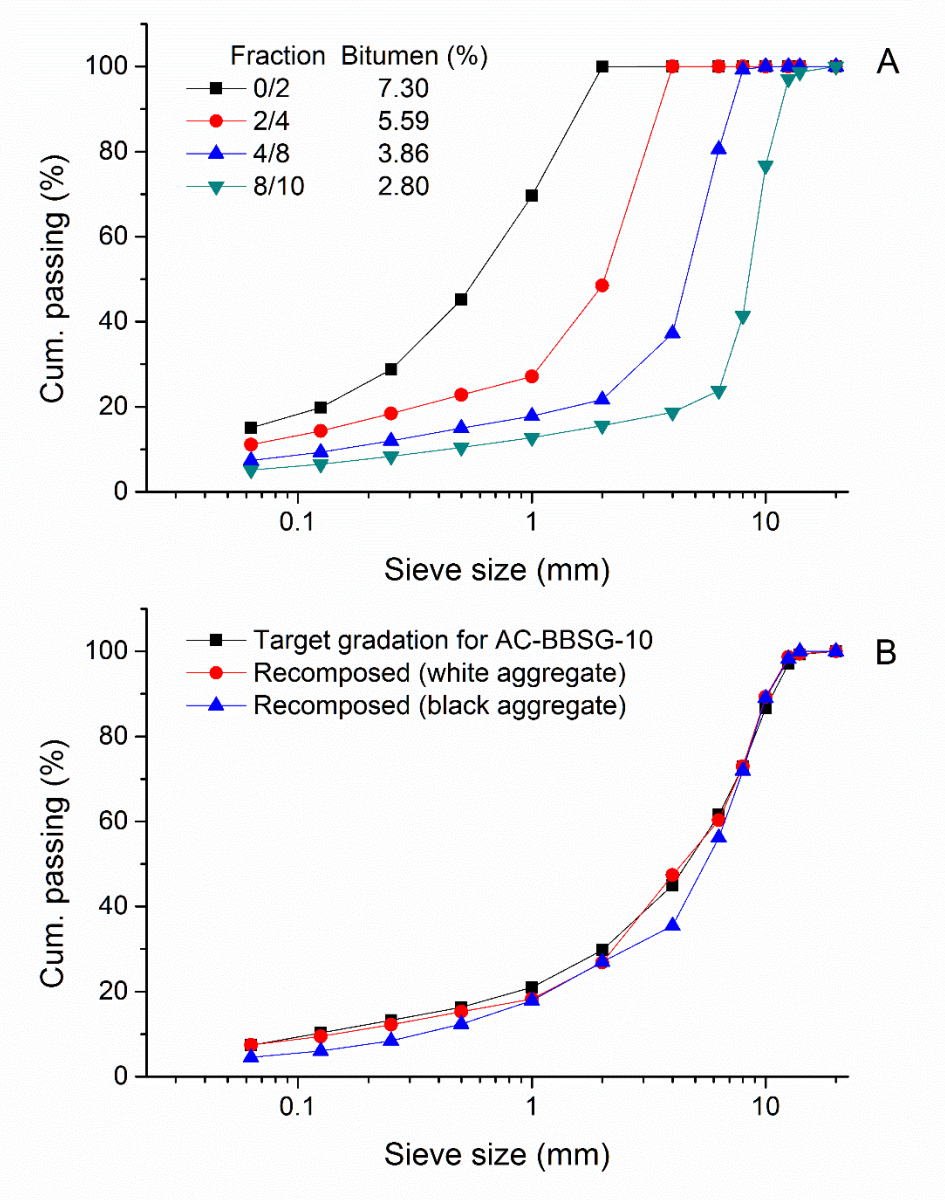

Figure 4. 6. 4 A) Sieve test results of separated RAP fractions (white aggregate), of 0/2, 8/4, 4/8, and 8/10, from which aged binder was previously stripped; and B) their recomposed aggregate gradation referred to AC-BBSG-10 design.

The first level of evaluation, according to French design method deals with compactibility performance in French gyratory compactor – PCG, as presented in Figure 4.6.5. There are several analysis methods to observe the curve of void percentage evolution vs number of gyration. The first study was screened based on the percentage of void (% v/v) at a given gyrations. European standard EN 12697-31 specifies an interval of void values between 5 and 10 % v/v at 60 gyrations for that intended design. As may be seen in Figure 4.6.5, for the white aggregate assumption (with a final 5.5% bitumen, composed of 3.92% RAP binder and 1.6 % of fresh bitumen), WMA reached a 9% void whereas HWMA ("white aggregate") fell beyond expected design value, with 24.4% void.

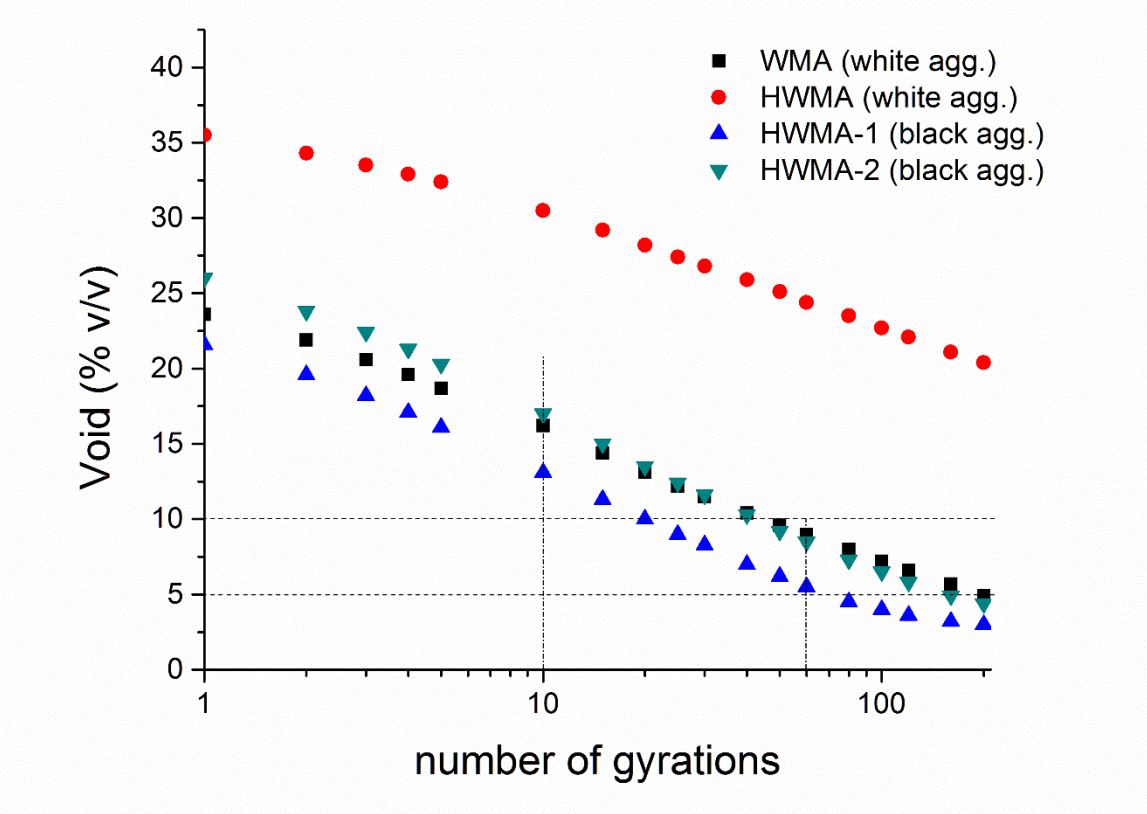

Figure 4. 6. 5 Gyratory compaction performance presenting mix void percentage and number of gyrations

As an alternative, a semi-quantitative approach consisted in adding more fresh bitumen, as mixing temperature decreased (Table 4.6.1). Furthermore, a new grading curve that considered "black aggregate" sizes (coated by RAP binder) and all RAP fractions (from 0/2 to 8/10) was proposed. This approach, based on previous studies (Shirodkar et al. 2011), assumes that a partial blending of RAP binder and fresh bitumen takes place in a higher extent for hot mixes asphalt (HMA). However, for reduced-temperature (e.g. WMA and HWMA) asphalt technologies, its blending level is expected to decrease, together with RAP binder quantity able to be rejuvenated, due to the high viscosity of RAP at such low mixing temperatures.

Regarding binders involved upon mixing, viscous behavior of RAP binder and fresh bitumen were characterized as a function of temperature (Figure 4.6.6A). A Newtonian behavior starting from low shear rates, known as zero-shear-rate limiting viscosity (η_0), was always found for both binders, being the aged (harder) bitumen more viscous than the fresh binder. Viscosities decreased with increasing temperature from 60 to 150 °C and were fitted to Arrhenius and WLF in equation 4.6.6 and 4.6.7, respectively (Dealy and Larson 2006):

$$a_T(T) = exp\left[\frac{Ea}{R}\left(\frac{1}{T} - \frac{1}{T_0}\right)\right] \quad (4.6.6)$$

$$a_T(T) = \frac{-C_1(T - T_0)}{[C_2 + (T - T_0)]} \quad (4.6.7)$$

Where a_T is the shift factor, Ea is the activation energy, R is the universal gas constant, T and T_0 are temperature and its arbitrarily selected reference and C_1 and C_2 are WLF constants.

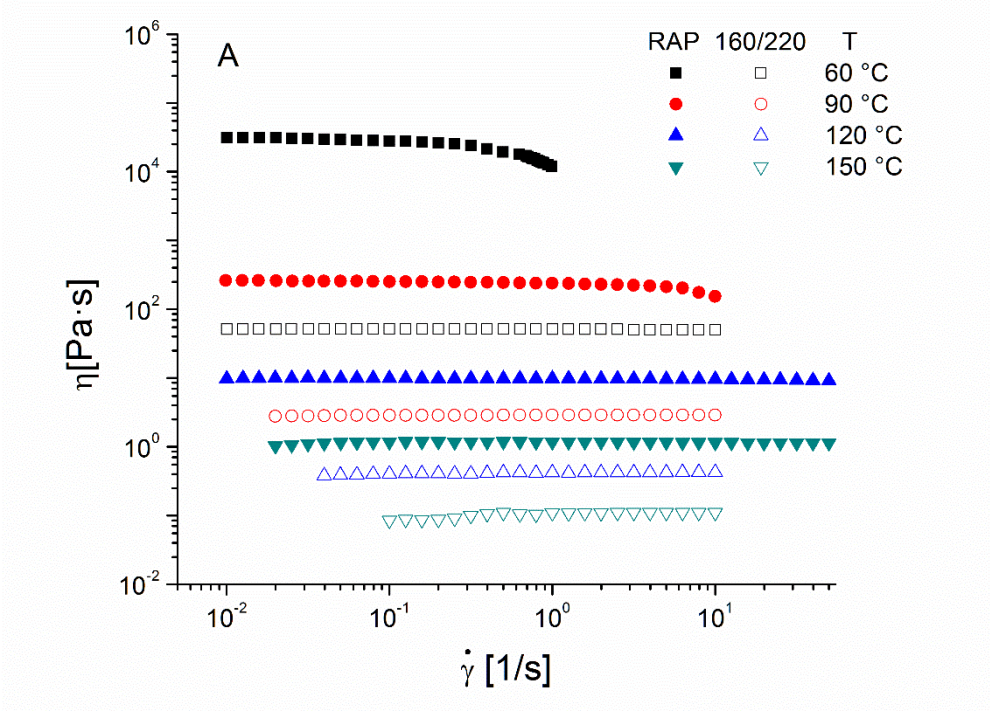

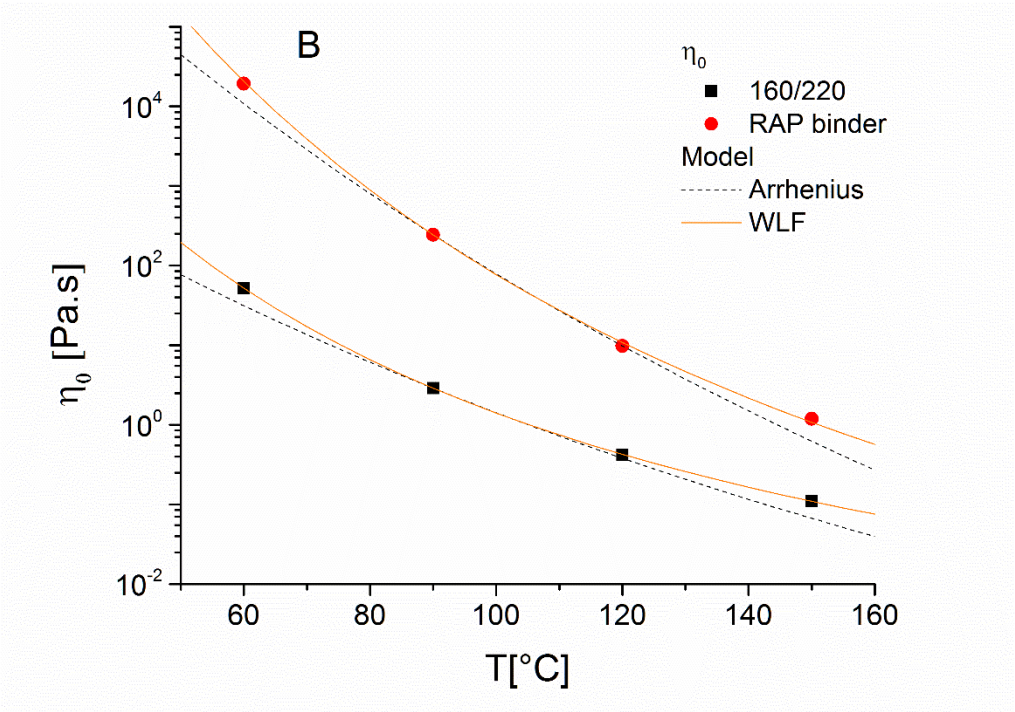

Figure 4. 6. 6 A) Flow curve of aged binder (extracted from RAP) and bitumen 160/220 (used as raw material for bitumen emulsion) at 60, 90, 120, and 150 °C and B) zero shear-rate limiting viscosity as a function of temperature and their corresponding fitting using Arrhenius and WLF equations.

As may be seen in Figure 4.6.6B, WLF model, with C_1 and C_2 of 4.9 and 147.1 for fresh bitumen and 9 and 171.8 for RAP binder, fits better than Arrhenius model the viscosity

dependence, in the whole temperature range studied, from 60 to 150 °C. However, for sake of simplicity and for estimation of fresh bitumen diffusion studied below, Arrhenius equation was used to describe binders viscosity in the mixing temperature range used for WMA and HWMA (80-120 °C). Thus, Ea will be used for estimating the quantity of fresh bitumen required, based on a thin film diffusion approach. Comparing both bitumens, the higher Ea value of 127 KJ/mol for RAP binder, as compared to fresh bitumen with 80 KJ/mol, suggests a material more susceptible to temperature, arising from a more complex microstructure. Moreover, its higher viscosity and non-Newtonian character are due to the change in chemical composition (e.g. increase in carbonyl and sulfoxide groups, molecular association, etc.), which has been associated to long-term aging that leads to a more complex intermolecular interactions within the microstructure (Masson et al. 2001; Lu and Isacsson 2002).

Trying to maintain "rejuvenated binder" content similar for both WMA ("white aggregate" approach) and HWMA ("black aggregate") technologies, it is necessary to estimate the amount 'active' RAP binder (i.e. RAP thickness) available for blending with the fresh bitumen added. This approach based on the diffusion of fresh bitumen penetrating RAP binder film thickness. The fraction of penetration 'x_T', for a certain length of aged binder coating RAP aggregates, may be estimated for every temperature of mixing (WMA, HWMA-1 and HWMA-2), with respect to a reference conditions (e.g. Hot Mix Asphalt-HMA processing conditions (Shirodkar et al. 2011)) as follows,

$$\frac{x_T}{x_{ref}} \approx \left(exp\left(\frac{-E_a}{R}\left(\frac{1}{T} - \frac{1}{T_{ref}} \right) \right) \right)^{0.5} \qquad (4.6.8)$$

where for a HMA T_{ref} is 150 °C and x_{ref} takes values between 0.9 and 1 (leading to red and black curves of Figure 4.6.7, respectively), assuming a high partial blending (within the range of 90 to 100% penetration depth of binder RAP (Shirodkar et al. 2011)). As for Ea value, based on a linear relationship between diffusion coefficient and apparent viscosity (Oliver 1974), diffusion coefficient can be estimated by the Arrhenius equation on diffusion (Oliver 1974; Kriz et al. 2014) and Ea in Equation 4.6.8 could take value previously calculated from Figure 4.6.6B for the soft bitumen. As a result, x_T values calculated for WMA, HWMA-1 and HWMA-2 can be used for the estimation of the RAP concentration involved in the diffusion process (Figure 4.6.7),

$$\text{“Active” RAP binder (\%)} = x_T \cdot [\text{Total RAP Binder (\%)}] \qquad (4.6.9)$$

Based on those results, the quantity of fresh bitumen, required to maintain the designed binder content should increase as manufacturing temperature decreases, e.g. by increasing the amount of added MKL-stabilized bitumen emulsion. Thus, Figure 4.6.7 estimates about 1.8 % “active” RAP in WMA and Table 4.6.1 shows 1.6% fresh bitumen was added, giving 3.4% total binder involved in compaction and performance of the mix. Accordingly, it can be estimated from Figure 4.6.7 and Table 4.6.1 that 3.4% and 3.6% bitumen (“Active” RAP+B160/220) should be involved in HWMA-1 and HWMA-2, respectively.

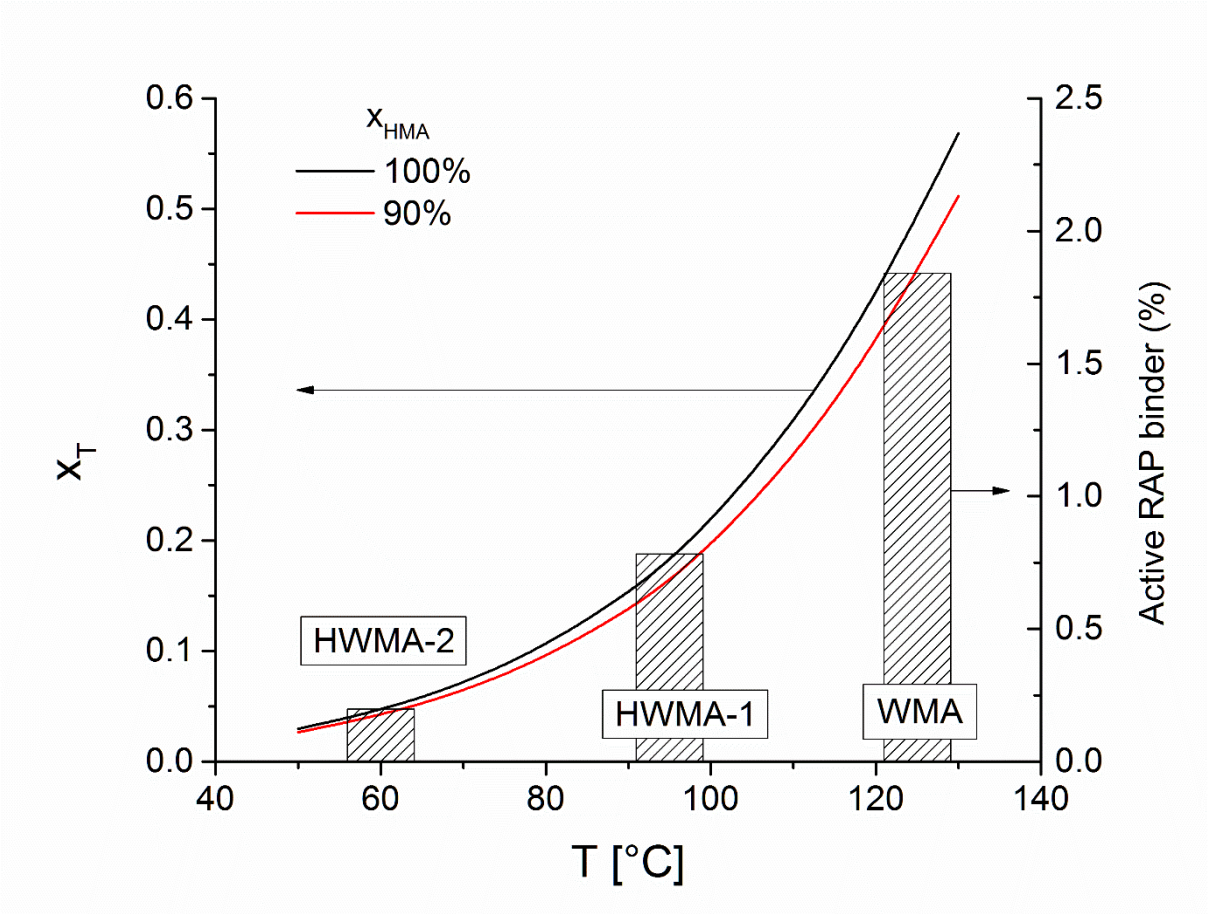

Figure 4. 6. 7 Semi-quantitative approach for estimating rejuvenated "active" RAP binder as a function of temperature, based on fraction of penetration into the RAP film (x_T) of the fresh bitumen.

In any case, when black aggregate assumption (or semi-quantitative approach) is used, with design values of 3.4-3.6% total bitumen involved, both HWMA-1 and HWMA-2 were sufficiently compacted (Figure 4.6.5). However, when using "white aggregate" assumption, mixes prepared at 80 °C (HWMA in Table 4.6.1) suffered from poor workability and were unable to be compacted to the expected void percentage (Figure 4.6.5). This would be related with the small amount of fresh (soft) bitumen added, in combination with the high RAP binder viscosity at 80 °C (Figure 4.6.6), which affected mix deformation and flow during compaction. According to Figure 4.6.7, about 0.20 % "active" RAP is expected to be available in HWMA ("white aggregate"),

which makes only 1.8% total binder involved in compaction of the mix, when 1.6% fresh bitumen was added (Table 4.6.1). Thus, "black aggregate" assumption was proposed for HWMA technology.

Furthermore, analysis of void content at 10 gyrations, that represents the state of materials subjected to low load, was performed to estimate the rutting performance (Figure 4.6.5). For this analysis, EN 12697-31 specifies a minimum value of 11% voids. HWMA-1 presented the lowest value at 13% that suggests a good workability with a drawback of the increasing chance of a poorer rutting performance. In this sense, the rutting resistance to permanent deformation was assessed according to EN 12697-22+A1 using wheel tracking device. Figure 4.6.8 shows the evolution of deformation depth to the number of cycles. HWMA-2 ("Black aggregate") specimen for rutting test could not be well-compacted with the common method using a tire roller compactor, which was probably due to inability for water removal, even though the good workability previously exhibited in the gyratory compactor (Figure 4.6.5). During preparation with gyratory compactor, clean water was observed expelled from the specimen to allow void content at 60 gyrations to be within the specification. The presence of clean water also means that bitumen (and emulsifier) adheres to aged binder surface, and the remaining water (with the lowest viscosity) leaves the specimen mix. Conversely, the absence of such phenomenon may suggest that water remains in the specimen and only moves from one side to the other depending on which part is subjected to the load. For this reason, only WMA and HWMA-1 rutting performance are evaluated in Figure 4.6.8. After 30000 cycles, the deformation depths are 5.2 and 8% for WMA and HWMA-1 respectively, which are within specification below the maximum admissible value of 10% for class 1. A higher penetration depth

value for HWMA-1 come to agreement with one predicted by the lowest value of void content after 10 gyrations.

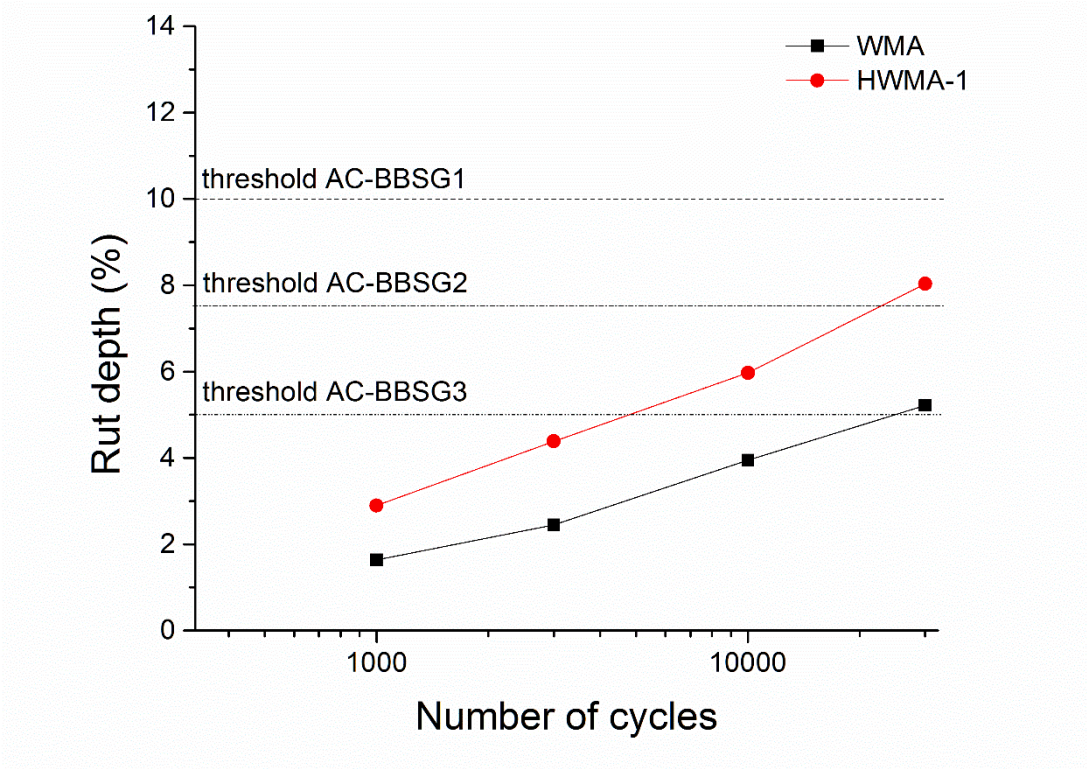

Figure 4. 6. 8 Rutting performance at 60 °C (by rut depth) as a function of number of tire-cycles, of 1000, 3000, 10000, and 30000 cycles.

The evolution of complex (E*) and loss (E") moduli as a function of reduced frequency is presented in Figure 4.6.9A. Similar to rutting test preparation, HWMA-2 specimen underwent compaction issues in the tire roller compactor, which resulted in high 13 % void. Although trapezoidal specimen for complex modulus test and fatigue tests were successfully cut from the slab. Conversely, WMA and HWMA-1 were within the designed void percentage that correlate to the prediction made by gyratory test.

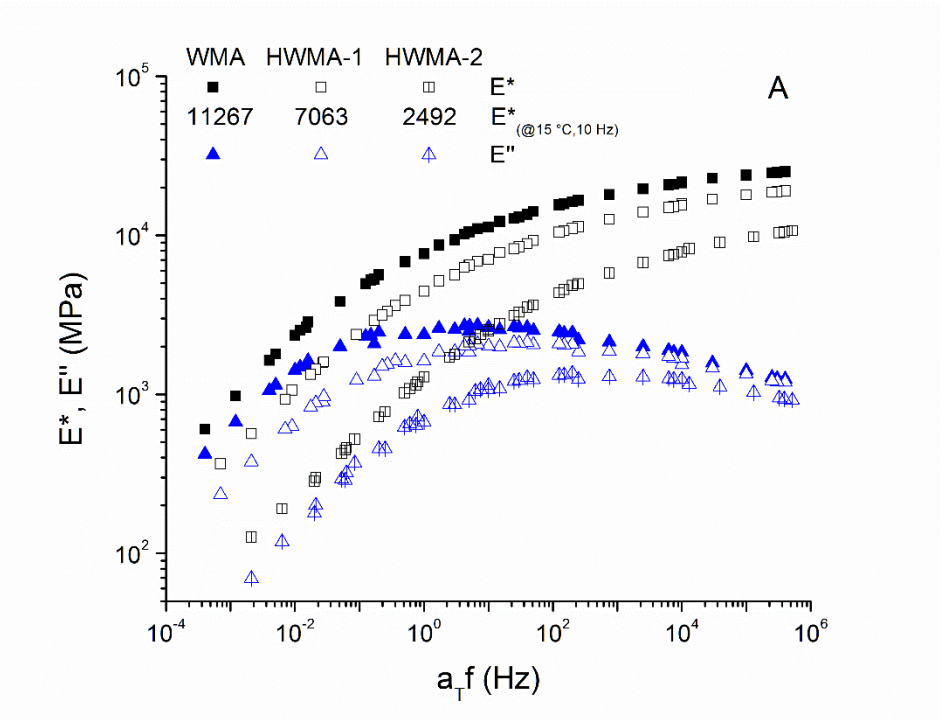

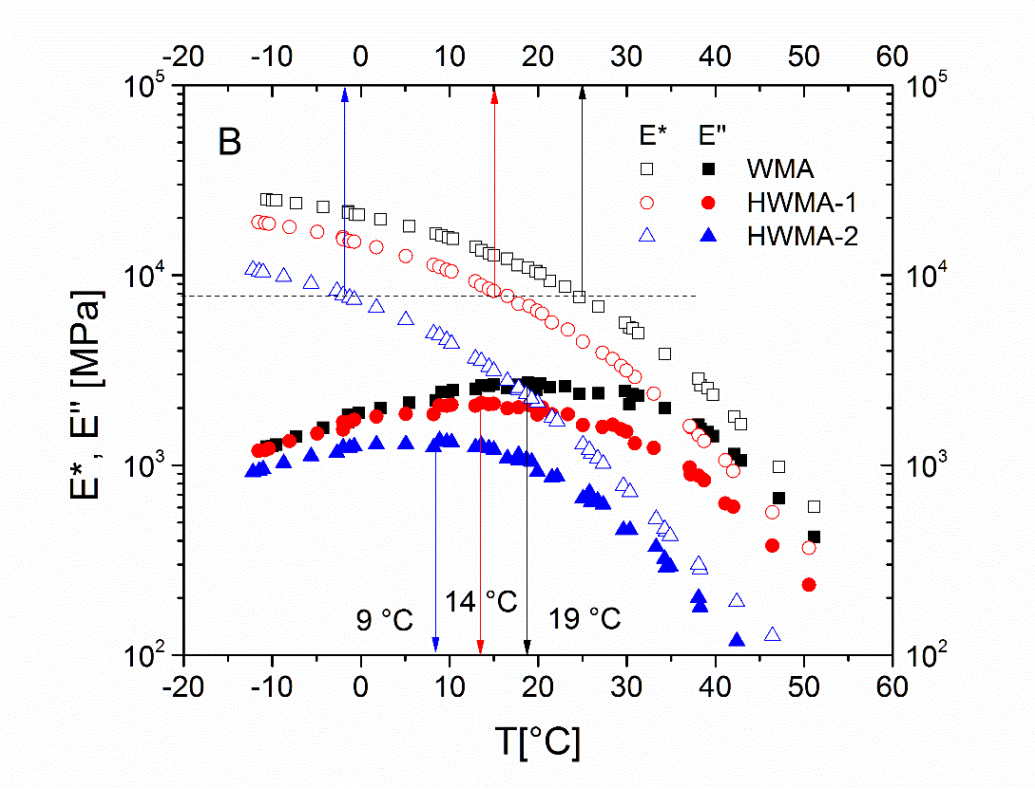

Figure 4. 6. 9Master curve by applying time-temperature superposition, of A) isothermal plot of moduli vs reduced frequency and B) isochronal plot of moduli vs temperature (obtained by using modified Arrhenius equation)

For AC-BBSG 10 mix, the complex modulus (E*) at 15 °C and 10 Hz should be either higher than or equivalent to 5500 MPa for class 1 or 7000 MPa for class 2 and 3. E* of WMA is 11267 MPa and E* of HWMA-1 is 7063 MPa that satisfy the requirement for class 1. However, test failed for HWMA-2 with E* of 2492 MPa (Figure 4.6.9). The differences in the magnitude among them are likely related to the theoretical blended binder properties, which can be measured for instance by means of technological penetration value (Pen). Thus, by applying logarithmic mixing rule,

$$\log(Pen\_AB) = a \cdot log(Pen_A) + b \cdot log(Pen\_B) \qquad (4.6.10)$$

where the estimated fraction 'a' of RAP binder (with Pen_A in Table 4.6.1) and fresh binder fraction 'b=1-a' (with Pen_B in Table 4.6.1) are calculated from Figure 4.6.7 and added fresh bitumen gathered in Table 4.6.1. By using Equation 4.6.10, the blended binder penetrations (Pen_AB) for WMA, HWMA-1 and HWMA-2 are expected to be 40, 99 and 162 dmm, respectively, assuming "active" RAP binder and total fresh bitumen are fully blended. Therefore, as emulsion-RAP mixing temperature decrease, the observed lower E* values of asphalt mixes at particular reduced frequency (Figure 4.6.9A) and poorer rutting performances (Figure 4.6.8) may be due to the increase in penetration values of the resulting blended binder. It is worth noting LCPC design advises the use bitumen with penetrations 35/50 and 50/70 for AC-BBSG-10 (Delorme et al. 2007).

Aiming to further predict mixes behavior for its low temperature performance, a conversion of moduli (E) vs reduced frequency ($a_T \cdot f$) into temperature domain (T) could be performed based on empirical application of time-temperature superposition principle and using a rearranged Arrhenius equation relating shift factor and temperature (Cuadri et al. 2013a):

$$T = \frac{Ea \cdot T_{ref}}{R \cdot T_{ref} \cdot \ln(a_T) + Ea} \quad (4.6.11)$$

The activation energy is initially obtained by taking the slope of a regression line of ln (a_T) vs T plot (not shown) at a reference temperature of T_{ref}=15 °C. Where the activation energy for WMA is 237 KJ/mol, whilst for HWMA-1 is 228 KJ/mol. Figure 4.6.9B presents the converted master curve into temperature domain that shows a shift in the maximum peak of loss modulus, a representative event of the glassy region onset (Partal et al. 1999), to a lower temperature for HWMA-1 and, much lower, for HWMA-2 (Figure 4.6.9B). Changing binder type, from soft to hard characteristics (i.e. lowering Pen_{25}), a statistically higher fracture temperature on porous and dense graded asphalt mixture is expected (Isacsson and Zeng 1998). Thus, this is perhaps relevant with WMA, having a low penetration blended binder (54% 'active' RAP binder and 46% fresh bitumen), which exhibits high mechanical glass transition temperature (from E'' max) at 19 °C. Accordingly, it is expected a poorer low temperature fracture behavior for this system, compared to others studied. In addition, given a WMA E* at 25 °C of 8 GPa and pulling a line crossing HWMA-1 and HWMA-2 E* vs T profiles, readings yield temperatures of 15 and -2 °C, respectively. Such reduction in temperature for a given E* value is attributed to the changes in binder hardness toward softer characteristic, that was similarly reported by others (Quintero Q. et al. 2016). This result may validate that the semi-quantitative approach works.

Finally, in level 4, fatigue resistance was evaluated by means of fatigue tests, determining parameter ε_6, a term that represents a maximum deformation for a flexible pavement to cause the stiffness reduction by half over a million cycles. This

value was obtained on a regression line of twelve data points in the logarithmic plot of number of cycles vs deformation (Figure 4.6.10).

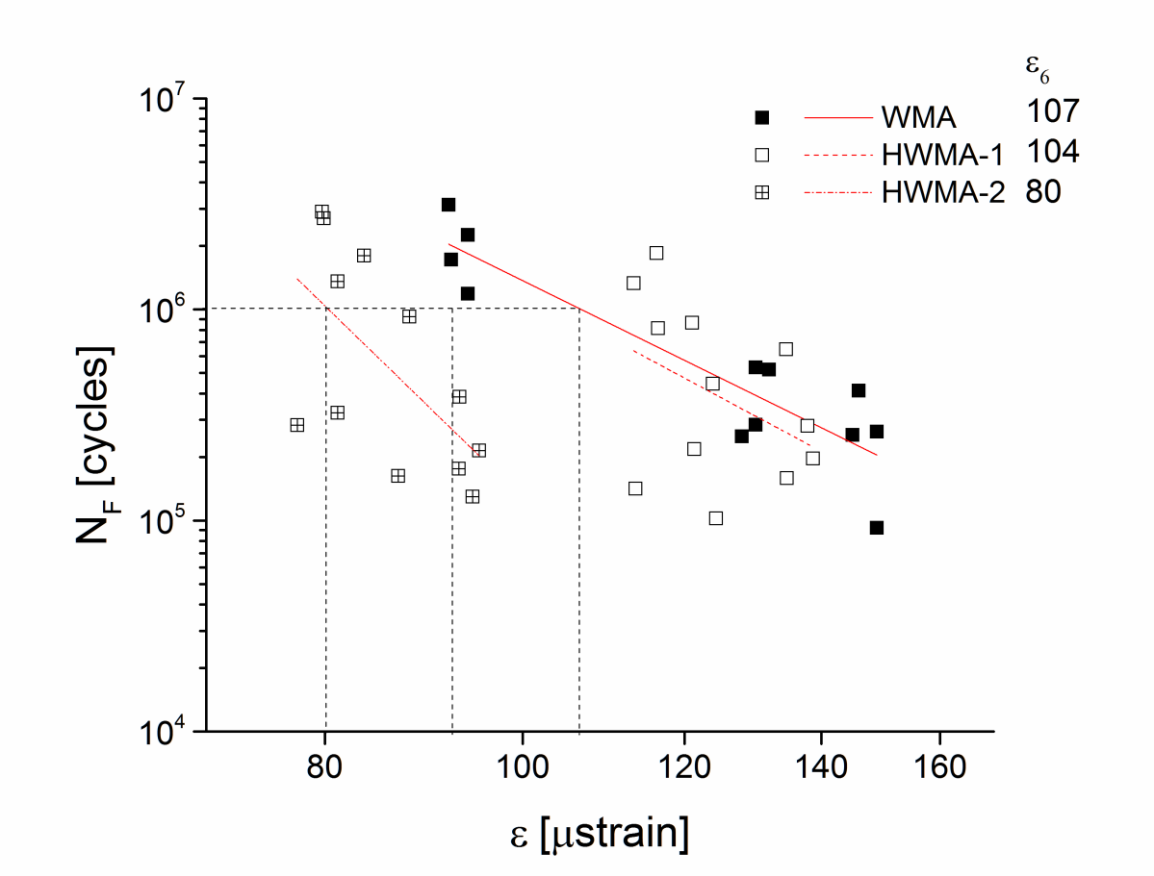

Figure 4. 6. 10 Fatigue life test by flexion, via two-points bending procedure, and fitting curve of load deformation (μstrain) vs number of cycles (N_F)

The design specification mentioned a minimum value of 100 for ε_6, and both WMA and HWMA-1 satisfactorily meet the specification, unlike HWMA-2. For a comparative analysis, a correction to ε_6 could be applied for a certain value of compaction degree, which in this case was 7%, using equation 4.6.12 (Delorme et al. 2007; Lopes et al. 2015).

$$\Delta\varepsilon_6 = 3.3 \cdot \Delta(\%v/v) \qquad (4.6.12)$$

Where Δ means the difference between the measured and targeted value for fatigue parameter (ε_6) and void percentage (%v/v). Hence, WMA with 6% and HWMA-1 with 8% have ε_6 corrected value of 103.7 and 107.3 μ_{strain}, respectively. If HWMA-2 was successfully compacted from 13% to 7%, its ε_6 is 99.8 which is fairly close the range to satisfy that criteria. LCPC design guide advice an increase of 25 μ_{strain} for an increase in binder content by 1 % (for asphalt mixes with binder content less than 7%), which was not observed if the assumption used in partial blending with semi-quantitative approach does not proceed. Based on that, it is difficult to analyze fatigue performance on one specific temperature, which in this study was at 10 °C for all mixes, when blended binder properties changes. This is based on other studies that report the change in critical temperature to cause minimum ε_6 is affected by binder hardness (Quintero Q. et al. 2016).

Finally, considering a minimum quantity of 5.5% bitumen is required for AC-BBSG-10 design [8], a saving of fresh bitumen by 70 and 50 % could be obtained for WMA and HWMA-1, thus expectedly reduce the impact to environment, in addition to the fact that performance quality fits the specification.

4.6.4 Concluding remarks

Asphalt mixes with maximum recycling and minimum impact to environment may be manufactured, between 80 and 130 °C, with a 100 % reclaimed asphalt pavements (RAP) as aggregates and a bitumen emulsion stabilized by modified lignin. The assessment of aqueous phase containing modified lignin suggests that MKL can play roles of emulsion stabilizer along with RAP coating agent. As for the latter, a partial RAP wetting is likely to occur, as may be deduced from its lower contact angle with polyethylene substrate (hydrophobic) compared to water. Regarding its surfactant

activity, the surface tension decreased with the increase in concentration from 0 to 0.625% and both polar and dispersive components of surface energy remained constant for higher concentrations.

By using a three-stage in-line homogenizer, the emulsification time shortens below 1 min, since no significant change in $D_{3,2}$ (about 6 μm) is observed for longer times. Compare to reference Asfier100 emulsions, MKL-stabilized bitumen emulsions show a lower viscosity, related to its higher maximum packing volume fraction, and a less non-Newtonian character, both factors would favour their use in reduce-temperature asphalt technologies.

Asphalt mixes prepared by WMA and HWMA procedures fulfilled up to the 4th level of French design method. In addition, a reduction of fresh bitumen content of 70 and 50 % was reported for WMA and HWMA-1 mixes, respectively, according to minimum binder requirement for a mix AC-BBSG 10. In this regard, a semi-quantitative approach becomes relevant in the design of mixes using reduced-temperature method, especially when high rate of recycled asphalt is used. Based on the relation between mixing temperature and fresh bitumen penetration into RAP binder film, a lower manufacturing temperature needs to be compensated by a higher amount of fresh bitumen. Thus, a balance between both parameters should be considered in search of the optimum reduction in lifecycle impact.

Chapter 5

General Conclusions

This work has been conducted under European research framework of Marie Curie "Sustainable Pavement and Railways Initial Training Network", which aims to investigate alternative sustainable technologies, for both road pavement and railways. Particularly, the results contained in this manuscript have focused on the development of more sustainable asphalts through: A) the use of reduced-temperature technologies based on polymer-modified bitumens applicable at lower temperatures and bitumen emulsions; B) use of a bio-based surfactants and bitumen modifiers such as the synthetized lignin-derived cationic emulsifiers; and C) use of reclaimed asphalt pavement materials. Referring to each specific topic, main conclusions achieved are listed as follows:

- EVA modified bitumen performance-related properties at medium-to-high in-service temperatures, like resistance to permanent deformation, were strongly affected by the vinyl acetate (VA) content in the copolymer in such a way that the lower the VA content (higher crystallinity), the better performance.
- In relation to the first conclusion, the total crystalline fraction in the modified binder, resulting from the product of EVA copolymer concentration and its crystalline fraction, governs the aforementioned performance.
- The use of EVA copolymers with high Melt-flow indexes (MFI) facilitates its mixing with bitumen and workability of the final asphalt mix, with the consequent reduction in process temperatures. On the other hand, the addition of EVA copolymers with low MFI seems to provide better rheological performance at low in-service temperature, as denoted by a shift of the mechanical glass transition to lower temperatures and the enhanced ability of the PMB to sustain higher strains before experiencing thermal fracture.

- If material performance in a wide temperature range and its facility of processing are put in priority, balancing low VA content and high MFI is a must.
- The Mannich reaction enabled to valorize lignin through the inclusion of amine groups which gave rise to cationic emulsifiers for road paving applications.
- Within the set of reaction conditions studied, an alkaline medium reaction route and tetraethylene-pentamine (TEPA) as amine reagent were chosen as optimum preparation conditions, such that the resulting cationic surfactant provided the expected emulsion stability and workability when used with typical formulation for road paving applications.
- The steady shear flow viscous behavior of modified-lignin-stabilized bitumen emulsions are governed by: emulsifier concentration, pH of aqueous phase, bitumen phase concentration, and energy input during emulsification.
- Water was able to wet a hydrophobic polyethylene surface upon addition of the modified-lignin emulsifier above, because the resulting aqueous phase presented increased and decreased values of surface free energy dispersive and polar components, respectively.
- The preparation of reduced-temperature asphalt mixes containing 100% reclaimed asphalt pavement (RAP) by using modified-lignin-stabilized bitumen emulsion was successful.
- For reduced-temperature asphalt technologies, calculations based on thin film diffusion proved to be a useful approach in order to predict the quantity of fresh bitumen needed for aged RAP to achieve a certain level of rejuvenation and a suitable mix workability and performance.

Bibliography

Airey GD (2002a) Rheological evaluation of ethylene vinyl acetate polymer modified bitumens. Constr Build Mater 16:473–487. doi: 10.1016/S0950-0618(02)00103-4

Airey GD (2002b) Use of Black Diagrams to Identify Inconsistencies in Rheological Data. Road Mater Pavement Des 3:403–424. doi: 10.1080/14680629.2002.9689933

Airey GD, Grenfell JRA, Apeagyei A, et al (2016) Time dependent viscoelastic rheological response of pure, modified and synthetic bituminous binders. Mech Time-Dependent Mater. doi: 10.1007/s11043-016-9295-y

Airey GD, Rahimzadeh B (2004) Combined bituminous binder and mixture linear rheological properties. Constr Build Mater 18:535–548. doi: 10.1016/j.conbuildmat.2004.04.008

Airey GD, Thom N (2015) Stiffness of cold asphalt mixtures with recycled aggregates from construction and demolition waste. Constr Build Mater 77:168–178. doi: 10.1016/j.conbuildmat.2014.12.045

Al-Mansob RA, Ismail A, Alduri AN, et al (2014) Physical and rheological properties of epoxidized natural rubber modified bitumens. Constr Build Mater 63:242–248. doi: 10.1016/j.conbuildmat.2014.04.026

Apeagyei AK, Clark TM, Rorrer TM (2013) Stiffness of High-RAP Asphalt Mixtures: Virginia's Experience.

Bahia HU, Hislop WP, Zhai H, Rangel A (1998) Classification of asphalt binders in to simple and complex binders. J Assoc Asph Paving Technol 67:1–41.

Barnes HA (1994) Rheology of emulsions - a review. Colloids Surfaces A Physicochem Eng Asp 91:89–95.

Barnes HA (2000) A Handbook of Elementary Rheology. The University of Wales Institute of Non-Newtonian Fluid Mechanics, Department of Mathematics

Barthel W, Marchand J-P, Devivere M von (2004) Warm asphalt mixes by adding a synthetic zeolite. Proc 3rd Eurasphalt Eurobitume Congr Held 12. doi: 10.1017/CBO9781107415324.004

Birgisdóttir H, Pihl KA, Bhander G, et al (2006) Environmental assessment of roads constructed with and without bottom ash from municipal solid waste incineration. Transp Res Part D Transp Environ 11:358–368. doi: 10.1016/j.trd.2006.07.001

Boucard L, Schmitt V, Farcas F, Gaudefroy V (2015) Bitumen emulsions formulation and destabilisation process relationship: influence of salts addition. Road Mater Pavement Des 16:330–348. doi: 10.1080/14680629.2015.1030910

Bueno M, Luong J, Terán F, et al (2014) Noise Reduction Properties of an Experimental Bituminous Slurry with Crumb Rubber Incorporated by the Dry Process. 602–613. doi: 10.3390/coatings4030602

Bulatović VO, Rek V, Marković KJ (2013) Rheological properties and stability of ethylene vinyl acetate polymer-modified bitumen. Polym Eng Sci 53:2276–2283. doi: 10.1002/pen.23462

Carrera V, Cuadri AA, García-Morales M, Partal P (2015) The development of

polyurethane modified bitumen emulsions for cold mix applications. Mater Struct Constr 48:3407–3414. doi: 10.1617/s11527-014-0408-2

Carrera V, Garcia-Morales M, Partal P, Gallegos C (2010) Novel bitumen/isocyanate-based reactive polymer formulations for the paving industry. Rheol Acta 49:563–572. doi: 10.1007/s00397-009-0399-z

Carvajal JC, Gómez Á, Cardona CA (2016) Comparison of lignin extraction processes: Economic and environmental assessment. Bioresour Technol 214:468–476. doi: 10.1016/j.biortech.2016.04.103

Christensen DW, Anderson DA (1992) Interpretation of dynamic mechanical test data for paving grade asphalt cements. J Assoc Asph paving Technol 61:67–116.

Clark AH, Kamide K, Ross-Murphy SB, Saito M (1987) Structural and mechanical properties of biopolymer gels. In: Biopolymers. pp 57–192

Collins P, Masson J-F, Polomark G (2006) Ordering and Steric-Hardening in SBS-Modified Bitumen. Energy & Fuels 20:1266–1268. doi: 10.1021/ef050403q

Cuadri AA, Carrera V, Izquierdo MA, et al (2014) Bitumen modifiers for reduced temperature asphalts : A comparative analysis between three polymeric and non-polymeric additives. Constr Build Mater 51:82–88.

Cuadri AA, García-Morales M, Navarro FJ, et al (2013a) End-performance evaluation of thiourea-modified bituminous binders through viscous flow and linear viscoelasticy testing. Rheol Acta 52:145–154. doi: 10.1007/s00397-012-0671-5

Cuadri AA, García-Morales M, Navarro FJ, Partal P (2013b) Isocyanate-functionalized castor oil as a novel bitumen modifier. Chem Eng Sci 97:320–327. doi: 10.1016/j.ces.2013.04.045

Cuadri AA, Roman C, García-Morales M, et al (2016) Formulation and processing of recycled-low-density-polyethylene-modified bitumen emulsions for reduced-temperature asphalt technologies. Chem Eng Sci 156:197–205. doi: 10.1016/j.ces.2016.09.018

D'Angelo J, Harm E, Bartoszek J, et al (2008) Warm-mix Asphalt: Europe Practice. Federal Highway Administration (2008) U.S. DoT, AASHTO, NCHRP, Report no. FHWA PL-08-007.

De la Roche C, Gabet T, Van de Ven M, et al (2010) Results of interlaboratory tests on a laboratory bituminous mixtures ageing protocol. In: Proceed-ings of the 11th international conference on asphalt pavements, France.

Dealy JM, Larson RG (2006) Structure and Rheology of Molten Polymers. Hanser

Dekhli S, Mokhtar KA, Hammoumm F, Bachir DS (2015) Rheological Behaviour of Ethylene-Vinyl-Acetate (EVA) Modified Road Bitumen. J Appl Sci 15:444–455.

Delorme J-L, Roche C de la, Wendling L (2007) LPC Bituminous Mixtures Design Guide.

Dinis-Almeida M, Castro-Gomes J, Sangiorgi C, et al (2016) Performance of Warm Mix Recycled Asphalt containing up to 100% RAP. Constr Build Mater 112:1–6. doi: 10.1016/j.conbuildmat.2016.02.108

Dondi G, Mazzotta F, Sangiorgi C, et al (2014) Influence of Cement and Limestone Filler on the Rheological Properties of Mastic in Cold Bituminous Recycled Mixtures. In: Sustainability, Eco-efficiency and Conservation in Transportation Infrastructure Asset Management. Taylor & Francis Group, pp 61–67

Doyle T a., McNally C, Gibney A, Tabaković A (2013) Developing maturity methods for the assessment of cold-mix bituminous materials. Constr Build Mater 38:524–

529. doi: 10.1016/j.conbuildmat.2012.09.008

Du X, Li J, Lindström ME (2014) Modification of industrial softwood kraft lignin using Mannich reaction with and without phenolation pretreatment. Ind Crops Prod 52:729–735. doi: 10.1016/j.indcrop.2013.11.035

Ecker A (2001) The Application of Iatroscan-Technique for Analysis of Bitumen. Pet Coal 43:51–53.

EN13808 (2013) Bitumen and bituminous binders. Framework for specifying cationic bituminous emulsions.

Fang C, Qiao X, Yu R, et al (2016) Influence of modification process parameters on the properties of crumb rubber/EVA modified asphalt. J Appl Polym Sci. doi: 10.1002/app.43598

Fang R, Cheng X, Xu X (2010) Synthesis of lignin-base cationic flocculant and its application in removing anionic azo-dyes from simulated wastewater. Bioresour Technol 101:7323–7329. doi: 10.1016/j.biortech.2010.04.094

Fawcett AH, Mcnally T (2001) Studies on Blends of Acetate and Acrylic Functional Polymers with Bitumen. 126–137.

Fawcett AH, McNally T (2001) Blends of bitumen with polymers having a styrene component. Polym Eng Sci 41:1251–1264. doi: 10.1002/pen.10826

Fawcett AH, McNally T (2000) Blends of bitumen with various polyolefins. Polymer (Guildf) 41:5315–5326. doi: 10.1016/S0032-3861(99)00733-8

Ferry JD (1980) Viscoelastic Properties of Polymers, 3rd. editi. Wiley, New York

Frankel NA, Acrivos A (1967) On viscosity of a concentrated suspension of solid

spheres. Chem Eng Sci 22:847–853.

Fritz G, Schdler V, Willenbacher N, Wagner NJ (2002) Electrosteric Stabilization of Colloidal Dispersions Electrosteric Stabilization of Colloidal Dispersions. Langmuir 18:6381–6390. doi: 10.1021/la015734j

Fuentes-Audén C, Sandoval JA, Jerez A, et al (2008) Evaluation of thermal and mechanical properties of recycled polyethylene modified bitumen. Polym Test 27:1005–1012. doi: 10.1016/j.polymertesting.2008.09.006

Garcia-Morales M, Partal P, Navarro FJ, et al (2004) The rheology of recycled EVA/LDPE modified bitumen. Rheol Acta 43:482–490. doi: 10.1007/s00397-004-0385-4

García-Morales M, Partal P, Navarro FJ, et al (2007) Processing, rheology, and storage stability of recycled EVA/LDPE modified bitumen. Polym Eng Sci 47:181–191. doi: 10.1002/pen.20697

García-Morales M, Partal P, Navarro FJ, et al (2004) Viscous properties and microstructure of recycled EVA modified bitumen. Fuel 83:31–38. doi: 10.1016/S0016-2361(03)00217-5

Gaudefroy V, Viranaiken V, Paranhos R, et al (2010) Laboratory Assessment of Fumes Generated by Bituminous Mixtures and Bitumen. Road Mater Pavement Des 11:83–100. doi: 10.3166/rmpd.11.83-100

Gawel I, Czechowski F, Kosno J (2016) An environmental friendly anti-ageing additive to bitumen. Constr Build Mater 110:42–47. doi: 10.1016/j.conbuildmat.2016.02.004

Giani MI, Dotelli G, Brandini N, Zampori L (2015) Comparative life cycle assessment of

asphalt pavements using reclaimed asphalt, warm mix technology and cold in-place recycling. Resour Conserv Recycl 104:224–238. doi: 10.1016/j.resconrec.2015.08.006

Gingras JP, Fradette L, Tanguy P, Bousquet J (2007a) Inline bitumen emulsification using static mixers. Ind Eng Chem Res 46:2618–2627. doi: 10.1021/ie0611913

Gingras JP, Fradette L, Tanguy P, Jorda E (2007b) Concentrated bitumen-in-water emulsification in coaxial mixers. Ind Eng Chem Res 46:1818–1825. doi: 10.1021/ie061169+

Gingras JP, Tanguy PA, Mariotti S, Chaverot P (2005) Effect of process parameters on bitumen emulsions. Chem Eng Process Process Intensif 44:979–986. doi: 10.1016/j.cep.2005.01.003

Gómez-Meijide B, Pérez I (2014) A proposed methodology for the global study of the mechanical properties of cold asphalt mixtures. Mater Des 57:520–527. doi: 10.1016/j.matdes.2013.12.079

González O, Muñoz ME, Santamaría a., et al (2004) Rheology and stability of bitumen/EVA blends. Eur Polym J 40:2365–2372. doi: 10.1016/j.eurpolymj.2004.06.001

González O, Peña JJ, Muñoz ME, et al (2002) Rheological techniques as a tool to analyze polymer-bitumen interactions: Bitumen modified with polyethylene and polyethylene-based blends. Energy and Fuels 16:1256–1263. doi: 10.1021/ef020049l

Goodrich JL, Goodrich JE, Kari WJ (1986) Asphalt composition tests: their application and relation to field performance. In: Transportation Research Record.

Graziani A, Godenzoni C, Cardone F, Bocci M (2016) Effect of curing on the physical and mechanical properties of cold-recycled bituminous mixtures. Mater Des 95:358–369. doi: 10.1016/j.matdes.2016.01.094

Gudimettla, L.M., Cooley, L.A., Brown, E.R. (2003) NCAT Report 03-03 : Workability of hot mix asphalt.

Gundersen S (2001) Langmuir surface and interface films of lignosulfonates and Kraft lignins in the presence of electrolyte and asphaltenes: correlation to emulsion stability. Colloids Surfaces A Physicochem Eng Asp 182:199–218. doi: 10.1016/S0927-7757(00)00739-1

Irvine GM (1985) The significance of the glass transition of lignin in thermomechanical pulping. Wood Sci Technol 19:139–149. doi: 10.1007/BF00353074

Isacsson U, Zeng H (1998) Cracking of asphalt at low temperature as related to bitumen rheology. J Mater Sci 33:2165–2170. doi: 10.1023/A:1004383506240

Isacsson ULF, Lu X (1999) Characterization of bitumens modified with SEBS , EVA and EBA polymers. 4:3737–3745.

Izquierdo MA, Navarro FJ, Gallegos C (2012) Bituminous polyurethane foams for building applications : Influence of bitumen hardness. Constr Build Mater 30:706–713. doi: 10.1016/j.conbuildmat.2011.12.088

Jäger A, Lackner R, Eisenmenger-Sittner C, Blab R (2004) Identification of four material phases in bitumen by atomic force microscopy. Road Mater Pavement Des 5:9–24. doi: 10.1080/14680629.2004.9689985

James AD, Stewart D (1991) The Use of Fatty Amine Derivatives To Slow Down the Age-Hardening Process in Bitumen. In: The Chemistry of Bitumen. pp 671–684

Kaewtatip K, Thongmee J (2013) Effect of kraft lignin and esterified lignin on the properties of thermoplastic starch.

Kriz P, Grant DL, Veloza BA, et al (2014) Blending and diffusion of reclaimed asphalt pavement and virgin asphalt binders. Road Mater Pavement Des 15:78–112. doi: 10.1080/14680629.2014.927411

Król JB, Kowalski KJ, Niczke Ł, Radziszewski P (2016) Effect of bitumen fluxing using a bio-origin additive. Constr Build Mater 114:194–203. doi: 10.1016/j.conbuildmat.2016.03.086

Kubo S, Kadla JF (2005) Hydrogen bonding in lignin: A fourier transform infrared model compound study. Biomacromolecules 6:2815–2821. doi: 10.1021/bm050288q

Laurichesse S, Avérous L (2014) Chemical modification of lignins: Towards biobased polymers. Prog Polym Sci 39:1266–1290. doi: 10.1016/j.progpolymsci.2013.11.004

Lesueur D (2011) Polymer modified bitumen emulsions (PMBEs). Elsevier

Lesueur D (2009) The colloidal structure of bitumen: consequences on the rheology and on the mechanisms of bitumen modification. Adv Colloid Interface Sci 145:42–82. doi: 10.1016/j.cis.2008.08.011

Lesueur D (1996) A Structure-related model to describe asphalt linear viscoelasticity. J Rheol (N Y N Y) 40:813. doi: 10.1122/1.550764

Lesueur D, Ezzarougui M, Hervé G, et al (2003) The Rheological Properties of Bitumen Emulsions Part II — Experimental Characterization The Rheological Properties of Bitumen Emulsions Part II – Experimental Characterization. 4:169–184. doi:

10.1080/14680629.2003.9689945

Lesueur D, Potti JJ (2004) Cold mix design: A rational approach based on the current understanding of the breaking of bituminous emulsions. Road Mater Pavement Des 5:65–87. doi: 10.1080/14680629.2004.9689988

Li J-J (2006) Name Reactions : A Collection of Detailed Reaction Mechanism.

Liang M, Liang P, Fan W, et al (2015) Thermo-rheological behavior and compatibility of modified asphalt with various styrene–butadiene structures in SBS copolymers. Mater Des 88:177–185. doi: 10.1016/j.matdes.2015.09.002

Liu Z, Zhao L, Cao S, et al (2013) Preparation and evaluation of a novel cationic amphiphilic lignin derivative with high surface activity. BioResources 8:6111–6120.

Lo Presti D, Jiménez Del Barco Carrión A, Airey G, Hajj E (2016) Towards 100% recycling of reclaimed asphalt in road surface courses: Binder design methodology and case studies. J Clean Prod 131:43–51. doi: 10.1016/j.jclepro.2016.05.093

Loeber L, Sutton O, Morel J, et al (1996) New direct observations of asphalts and asphalt binders by scanning electron microscopy and atomic force microscopy. J Microsc 182:32–39.

Lopes M, Gabet T, Bernucci L, Mouillet V (2015) Durability of hot and warm asphalt mixtures containing high rates of reclaimed asphalt at laboratory scale. Mater Struct 48:3937–3948. doi: 10.1617/s11527-014-0454-9

Lu X, Isacsson U (1997) Compatibility and storage stability of styrene-butadiene-styrene copolymer modified bitumens. Mater Struct 30:618–626.

Lu X, Isacsson U (2000) Modification of road bitumens with thermoplastic polymers. Polym Test 20:77–86. doi: 10.1016/S0142-9418(00)00004-0

Lu X, Isacsson U (2002) Effect of ageing on bitumen chemistry and rheology. Constr Build Mater 16:15–22. doi: 10.1016/S0950-0618(01)00033-2

Lu X, Isacsson U, Ekblad J (1999) Rheological properties of SEBS, EVA and EBA polymer modified bitumens. Mater Struct 32:131–139. doi: 10.1007/BF02479440

Lu X, Uhlback P, Soenen H (2016) Rheological Testing of Bitumen at Low Temperatures with 4-mm DSR. In: 8th RILEM International Symposium on Testing and Characterization of Sustainable and Innovative Bituminous Materials. pp 643–653

Mallawarachchi DR, Amarasinghe ADUS, Prashantha MAB (2016) Suitability of Chitosan as an emulsifier for cationic bitumen emulsions and its behaviour as an additive to bitumen emulsion. Constr Build Mater 102:1–6. doi: 10.1016/j.conbuildmat.2015.10.111

Mannich C, Krösche W (1912) Ueber ein Kondensationsprodukt aus Formaldehyd, Ammoniak und Antipyrin. Arch Pharm (Weinheim) 250:647–667. doi: 10.1002/ardp.19122500151

Markanday SS, Stastna J, Polacco G, et al (2010) Rheology of bitumen modified by EVA-Organoclay nanocomposites. J Appl Polym Sci 118:557–565. doi: 10.1002/app.32373

Martin-Alfonso JE, Franco JM (2014) Ethylene-vinyl acetate copolymer (EVA)/sunflower vegetable oil polymer gels: Influence of vinyl acetate content.

Polym Test 37:78–85.

Masson J-F, Polomark GM (2001) Bitumen microstructure by modulated differential scanning calorimetry. Thermochim Acta 374:105–114.

Masson J-F, Polomark GM, Collins P (2002) Time-Dependent Microstructure of Bitumen and Its Calorimetry. Energy & fuels 16:470–476.

Masson JF (2008) Brief review of the chemistry of polyphosphoric acid (PPA) and bitumen. Energy and Fuels 22:2637–2640. doi: 10.1021/ef800120x

Masson JF, Leblond V, Margeson J (2006) Bitumen morphologies by phase-detection atomic force microscopy. J Microsc 221:17–29. doi: 10.1111/j.1365-2818.2006.01540.x

Masson JF, Price T, Collins P (2001) Dynamics of bitumen fractions by thin-layer chromatography/flame ionization detection. Energy and Fuels 15:955–960. doi: 10.1021/ef0100247

Matsushita Y (2015) Conversion of technical lignins to functional materials with retained polymeric properties. J Wood Sci 61:230–250. doi: 10.1007/s10086-015-1470-2

Matsushita Y, Yasuda S (2003) Reactivity of a condensed–type lignin model compound in the Mannich reaction and preparation of cationic surfactant from sulfuric acid lignin. J Wood Sci 49:166–171. doi: 10.1007/s100860300026

Maupin GW, Diefenderfer SD, Gillespie JS (2008) Evaluation of using higher percentages of recycled asphalt pavement in asphalt mixes in Virginia.

McNally T (2011) Polymer Modified Bitumen. Elsevier

Meisenheimer H, Zens A (2008) Ethylene vinyl acetate elastomers (EVM). In: Klingender RC (ed) Handbook of specialty elastomers. CRC Press,

Mittal KL (2013) Adhesion and Adhesives: Fundamental and Applied Aspects : Advances in Contact Angle, Wettability and Adhesion, Volume One (1).

Moon BK (2008) Overcoming Global Obstacles to Achieve Develpment Goals. In: Achieving Sustainable Development and Promoting Development Cooperation. pp 9–14

Morrison FA (2001) Understanding Rheology. Oxford University Press

Mueller, S., Llewellin, E.W., Mader HM (2009) The rheology of suspensions of solid particles. Proceeding R Soc A 39:291–300. doi: 10.1007/BF01432034

Munera JC, Ossa EA (2014) Polymer modified bitumen: Optimization and selection. Mater Des 62:91–97. doi: 10.1016/j.matdes.2014.05.009

Navarro FJ, Partal P, Martínez-Boza F, Gallegos C (2005) Effect of composition and processing on the linear viscoelasticity of synthetic binders. Eur Polym J 41:1429–1438. doi: 10.1016/j.eurpolymj.2004.12.006

Navarro FJ, Partal P, Martínez-Boza FJ, Gallegos C (2010) Novel recycled polyethylene/ground tire rubber/bitumen blends for use in roofing applications: Thermo-mechanical properties. Polym Test 29:588–595. doi: 10.1016/j.polymertesting.2010.03.010

Needham D (1996) Developments in bitumen emulsion mixtures for road. University of Nottingham

Nellensteyn FJ (1923) Bereiding en Constitutie van Asphalt.

Norgren M, Edlund H (2014) Lignin: Recent advances and emerging applications. Curr Opin Colloid Interface Sci 19:409–416. doi: 10.1016/j.cocis.2014.08.004

Norgren M, Edlund H, Wågberg L (2002) Aggregation of lignin derivatives under alkaline conditions. Kinetics and aggregate structure. Langmuir 18:2859–2865. doi: 10.1021/la011627d

Oliver JWH (1974) Diffusion of Oils in Asphalts. Ind Eng Chem Prod Res Dev 13:65–70. doi: 10.1021/i360049a013

Ortiz O, Castells F, Sonnemann G (2009) Sustainability in the construction industry: A review of recent developments based on LCA. Constr Build Mater 23:28–39. doi: 10.1016/j.conbuildmat.2007.11.012

Otsubo Y, Prud'homme R. (1994a) Effect of drop size distribuition on the flow behavior of oil-in-water emulsions. Rheol Acta 33 303-306 306:303–306. doi: 10.1007/BF00366956

Otsubo Y, Prud'homme RK (1994b) Rheology of oil-in-water emulsions. Rheol Acta 33:29–37. doi: 10.1007/BF00453461

Otsubo Y, Prud'homme RK (1992) Flow behavior of oil-in-water emulsions. J Soc Rheol Japan 20:125–131.

Ouellette RJ, Rawn JD, Ouellette RJ, Rawn JD (2015) 12 – Amines and Amides. In: Principles of Organic Chemistry. pp 315–342

Padmanabhan M, Bhattacharya M (1991) Flow Behavior and Exit Pressures of Corn Meal under High-Shear- High-Temperature Extrusion Conditions Using a Slit Die. J Rheol (N Y N Y) 35:315–343. doi: 10.1122/1.550217

Panda M, Mazumdar M (1999) Engineering Properties of EVA-modified bitumen binder for paving mixes. 11:131–137.

Pandey MP, Kim CS (2011) Lignin Depolymerization and Conversion : A Review of Thermochemical Methods. 29–41. doi: 10.1002/ceat.201000270

Partal P, Martínez-Boza FJ (2011) Modification of bitumen using polyurethanes. In: Polymer Modified Bitumen. pp 43–71

Partal P, Martınez Bosa F, Conde B, Gallegos C (1999) Rheological characterisation of synthetic binders and unmodified bitumens. Fuel 78:1–10.

Pérez-Jiménez F, Martínez AH, Miró R, et al (2014) Effect of compaction temperature and procedure on the design of asphalt mixtures using Marshall and gyratory compactors. Constr Build Mater 65:264–269. doi: 10.1016/j.conbuildmat.2014.04.135

Pérez-Lepe A, Martínez-Boza FJ, Attané P, Gallegos C (2006) Destabilization mechanism of polyethylene-modified bitumen. J Appl Polym Sci 100:260–267. doi: 10.1002/app.23091

Petersen JC, Robertson R. E, Branthaver JF, et al (1994) SHRP-A-367 : Binder Characterization and Evaluation Volume 1.

Pfeiffer JP, Saal RN. (1939) Asphaltic bitumen as colloid system. In: The sixteenth colloid symposium. pp 139–149

Polacco G, Berlincioni S, Biondi D, et al (2005) Asphalt modification with different polyethylene-based polymers. Eur Polym J 41:2831–2844. doi: 10.1016/j.eurpolymj.2005.05.034

Polacco G, Filippi S, Merusi F, Stastna G (2015) A review of the fundamentals of polymer-modified asphalts: Asphalt/polymer interactions and principles of compatibility. Adv Colloid Interface Sci 224:72–112. doi: 10.1016/j.cis.2015.07.010

Polacco G, Stastna J, Biondi D, Zanzotto L (2006) Relation between polymer architecture and nonlinear viscoelastic behavior of modified asphalts. Curr Opin Colloid Interface Sci 11:230–245. doi: 10.1016/j.cocis.2006.09.001

Qin Q, Farrar MJ, Pauli AT, Adams JJ (2014) Morphology, thermal analysis and rheology of Sasobit modified warm mix asphalt binders. Fuel 115:416–425. doi: 10.1016/j.fuel.2013.07.033

Quintero Q. CF, Momm L, Leite LFM, Bernucci LLB (2016) Effect of asphalt binder hardness and temperature on fatigue life and complex modulus of hot mixes. Constr Build Mater 114:755–762. doi: 10.1016/j.conbuildmat.2016.03.161

Radotić K, Mićić M (2016) Methods for Extraction and Purifi cation of Lignin and Cellulose from Plant Tissues. In: Sample Preparation Techniques for Soil, Plant, and Animal Samples, Springer Protocols Handbooks. pp 365–376

Ravve A (2012) Principles of Polymer Chemistry, 3rd edn. Springer

Read J, Whiteoak D (2003) The Shell Bitumen Handbook, 5th Edition.

Redelius P, Soenen H (2015) Relation between bitumen chemistry and performance. Fuel 140:34–43. doi: 10.1016/j.fuel.2014.09.044

Redelius PG (2004) Bitumen Solubility Model Using Hansen Solubility Parameter | Redelius, Per | digital library booksc. 1087–1092.

Robinson H (2004) Polymers in asphalt. Rapra Technology

Rodríguez-Valverde M., Cabrerizo-Vílchez M., Rosales-López P, et al (2002) Contact angle measurements on two (wood and stone) non-ideal surfaces. Colloids Surfaces A Physicochem Eng Asp 206:485–495. doi: 10.1016/S0927-7757(02)00054-7

Rodríguez-Valverde MA, Cabrerizo-Vílchez MA, Páez-Dueñas A, Hidalgo-Álvarez R (2003) Stability of highly charged particles: bitumen-in-water dispersions. Colloids Surfaces A Physicochem Eng Asp 222:233–251. doi: 10.1016/S0927-7757(03)00228-0

Ronald M, Luis FP (2016) Asphalt emulsions formulation: State-of-the-art and dependency of formulation on emulsions properties. Constr Build Mater 123:162–173. doi: 10.1016/j.conbuildmat.2016.06.129

Rossi D, Filippi S, Merusi F, et al (2013) Internal structure of bitumen/polymer/wax ternary mixtures for warm mix asphalts. J Appl Polym Sci 129:3341–3354. doi: 10.1002/app.39057

Rubio MC, Martínez G, Baena L, Moreno F (2012) Warm mix asphalt: an overview. J Clean Prod 24:76–84. doi: 10.1016/j.jclepro.2011.11.053

Saboo N (2015) Optimum Blending Requirements for EVA Modified Binder. Int J Pavement Res Technol 8:172–178. doi: 10.6135/ijprt.org.tw/2015.8(3).172

Salager J-L, Perez-Sanchez M, Garcia Y (1996) Physicochemical parameters influencing the emulsion drop size. Colloid Polym Sci 274:81–84. doi: 10.1007/BF00658913

Sengoz B, Topal A, Isikyakar G (2009) Morphology and image analysis of polymer modified bitumens. Constr Build Mater 23:1986–1992. doi:

10.1016/j.conbuildmat.2008.08.020

Shi XM, Zhang J, Jin J, Chen SJ (2008) Non-isothermal crystallization and melting of ethylene-vinyl acetate copolymers with different vinyl acetate contents. Express Polym Lett 2:623–629. doi: 10.3144/expresspolymlett.2008.75

Shirodkar P, Mehta Y, Nolan A, et al (2013) Development of blending chart for different degrees of blending of RAP binder and virgin binder. Resour Conserv Recycl 73:156–161. doi: 10.1016/j.resconrec.2013.01.018

Shirodkar P, Mehta Y, Nolan A, et al (2011) A study to determine the degree of partial blending of reclaimed asphalt pavement (RAP) binder for high RAP hot mix asphalt. Constr Build Mater 25:150–155. doi: 10.1016/j.conbuildmat.2010.06.045

Silva HMRD, Oliveira JRM, Peralta J, Zoorob SE (2010) Optimization of warm mix asphalts using different blends of binders and synthetic paraffin wax contents. Constr Build Mater 24:1621–1631. doi: 10.1016/j.conbuildmat.2010.02.030

Slaghek TM, Van VD, Giezen C, Haaksman IK (2015) Bitumen Composition.

Soenen H, Besamusca J, Fischer HR, et al (2013) Laboratory investigation of bitumen based on round robin DSC and AFM tests. Mater Struct 47:1205–1220. doi: 10.1617/s11527-013-0123-4

Soenen H, Redelius P (2014) The effect of aromatic interactions on the elasticity of bituminous binders. Rheol Acta 53:741–754. doi: 10.1007/s00397-014-0792-0

Somrang N, Nithitanakul M, Grady BP, Supaphol P (2004) Non-isothermal melt crystallization kinetics for ethylene-acrylic acid copolymers and ethylene-methyl acrylate-acrylic acid terpolymers. Eur Polym J 40:829–838. doi:

10.1016/j.eurpolymj.2003.11.021

Speight JG (1999) The Chemistry and Technology of Petroleum, 3rd editio. Marcel Dekker, New York

Stark W, Jaunich M (2011) Investigation of Ethylene/Vinyl Acetate Copolymer (EVA) by thermal analysis DSC and DMA. Polym Test 30:236–242. doi: 10.1016/j.polymertesting.2010.12.003

Starkweather HW (1965) The surface tension of polyethylene. Polym Eng Sci 5:5–6. doi: 10.1002/pen.760050102

Stauffer CE (1965) The Measurement of Surface Tension by the Pendant Drop Technique. J Phys Chem 69:1933–1938.

Sureshkumar MS, Filippi S, Polacco G, et al (2010) Internal structure and linear viscoelastic properties of EVA/asphalt nanocomposites. Eur Polym J 46:621–633. doi: 10.1016/j.eurpolymj.2009.12.024

Sybilski D, Vanelstraete A, Partl MN (2004) Recommendation of RILEM TC 182-PEB on bending beam and rheometer measurements of bituminous binders. Mater Struct 37:539–546. doi: 10.1617/14205

Tadros T (2011) Interparticle interactions in concentrated suspensions and their bulk (rheological) properties. Adv Colloid Interface Sci 168:263–77. doi: 10.1016/j.cis.2011.05.003

Tadros TF (2014) Formulation of Disperse System.

Tanner RI (2002) Engineering Rheology, 2nd edn. Oxford University Press

Thives LP, Ghisi E (2017) Asphalt mixtures emission and energy consumption: A

review. Renew Sustain Energy Rev 72:473–484. doi: 10.1016/j.rser.2017.01.087

Thomas KP (2005) Asphalt anti-aging apparatus and methods.

Vaitkus A, Čygas D, Laurinavičius A, et al (2016) Influence of warm mix asphalt technology on asphalt physical and mechanical properties. Constr Build Mater 112:800–806. doi: 10.1016/j.conbuildmat.2016.02.212

Van de Ven MFC, Jenkins KJ, Voskuilen JLM, Van den Beemt R (2007) Development of (half-) warm foamed bitumen mixes: state of the art. Int J Pavement Eng 8:163–175. doi: 10.1080/10298430601149635

Vidal R, Moliner E, Martínez G, Rubio MC (2013) Life cycle assessment of hot mix asphalt and zeolite-based warm mix asphalt with reclaimed asphalt pavement. Resour Conserv Recycl 74:101–114. doi: 10.1016/j.resconrec.2013.02.018

Walas SM (1997) Reaction Kinetics. In: Perry's Chemical Engineers' Handbook Seventh Edition.

Wen G, Zhang Y, Zhang Y, et al (2001) Vulcanization characteristics of asphalt/SBS blends in the presence of sulfur. J Appl Polym Sci 82:989–996.

West RC, Tran NH, Taylor AJ, Willis RJ (2015) Comparison of laboratory cracking test results with field performance of moderate and high RAP content surface mixtures on NCAT test track. In: 8th RILEM International Symposium on Testing and Characterization of Sustainable and Innovative Bituminous Materials. pp 979–992

Windeisen E, Wegener G (2016) Lignin as Building Unit for Polymers. In: Reference Module in Materials Science and Materials Engineering.

Wu S (1982) Polymer Interface and Adhesion. Marcel Dekker

Wunderlich B (1976) Macromolecular Physics. Academic Press

Yu X, Zaumanis M, dos Santos S, Poulikakos LD (2014) Rheological, microscopic, and chemical characterization of the rejuvenating effect on asphalt binders. Fuel 135:162–171. doi: 10.1016/j.fuel.2014.06.038

Yuliestyan A, Cuadri AA, García-Morales M, Partal P (2016a) Influence of polymer melting point and Melt Flow Index on the performance of ethylene-vinyl-acetate modified bitumen for reduced-temperature application. Mater Des 96:180–188. doi: 10.1016/j.matdes.2016.02.003

Yuliestyan A, Cuadri AA, García-Morales M, Partal P (2016b) Binder Design for Asphalt Mixes with Reduced Temperature: EVA Modified Bitumen and its Emulsions. Transp Res Procedia 14:3512–3518. doi: 10.1016/j.trpro.2016.05.319

Yuliestyan A, García-morales M, Moreno E, et al (2017) Assessment of modified lignin cationic emulsifier for bitumen emulsions used in road paving. Mater Des 131:242–251. doi: 10.1016/j.matdes.2017.06.024

Zanzotto L, Stastna J, Vacin O (2000) Thermomechanical Properties of several polymer modified asphalts. Appl Rheol 10:134–144.

Zaumanis M (2010) Warm mix asphalt investigation. A PhD thesis.

Zaumanis M, Mallick RB, Frank R (2014a) 100% recycled hot mix asphalt: A review and analysis. Resour Conserv Recycl 92:230–245. doi: http://dx.doi.org/10.1016/j.resconrec.2014.07.007

Zaumanis M, Mallick RB, Poulikakos L, Frank R (2014b) Influence of six rejuvenators

on the performance properties of Reclaimed Asphalt Pavement (RAP) binder and 100 % recycled asphalt mixtures. Constr Build Mater 71:538–550. doi: 10.1016/j.conbuildmat.2014.08.073

Zhao S, Huang B, Shu X, Woods ME (2016) Quantitative evaluation of blending and diffusion in high RAP and RAS mixtures. Mater Des 89:1161–1170. doi: 10.1016/j.matdes.2015.10.086

Zhu J, Birgisson B, Kringos N (2014) Polymer modification of bitumen: Advances and challenges. Eur Polym J 54:18–38. doi: 10.1016/j.eurpolymj.2014.02.005

Ziyani L, Gaudefroy V, Ferber V, Hammoum F (2016) A predictive and experimental method to assess bitumen emulsion wetting on mineral substrates. Colloids Surfaces A Physicochem Eng Asp 489:322–335. doi: 10.1016/j.colsurfa.2015.11.002

List of Figures

Chapter 4

Subchapter 4.1

Subchapter 4.2

Subchapter 4.3

Subchapter 4.4

Subchapter 4.5

Subchapter 4.6

List of Table

Chapter 2

Chapter 3

Chapter 4

Subchapter 4.1

Subchapter 4.2

Subchapter 4.3

Subchapter 4.4

Subchapter 4.5

Subchapter 4.6

List of Publications

Yuliestyan, A., Cuadri, A.A., García-Morales, M. and Partal, P., 2016. Influence of polymer melting point and Melt Flow Index on the performance of ethylene-vinyl-acetate modified bitumen for reduced-temperature application. *Materials & Design*, *96*, pp.180-188.

Yuliestyan, A., Cuadri, A.A., García-Morales, M. and Partal, P., 2016. Binder Design for Asphalt Mixes with Reduced Temperature: EVA Modified Bitumen and its Emulsions. *Transportation Research Procedia*, *14*, pp.3512-3518.

Yuliestyan, A., García-Morales, M., Moreno, E., Carrera, V., Partal, P., 2017. Assessment of modified lignin cationic emulsifier for bitumen emulsions used in road paving, *Materials & Design*, *131*, pp 242-251.

Yuliestyan, A., Cuadri, A.A., García-Morales, M. and Partal, P., Selection of Ethylene-Vinyl-Acetate properties for modified bitumen with enhanced end-performance. *Under review in Rheologica Acta*